CHALMERS

Strut-and-tie modelling of reinforced concrete pile caps

Master of Science Thesis in the Master's Programme Structural Engineering and Building Performance Design

GAUTIER CHANTELOT
ALEXANDRE MATHERN

Department of Civil and Environmental Engineering
Division of Structural Engineering
Concrete Structures
CHALMERS UNIVERSITY OF TECHNOLOGY
Göteborg, Sweden 2010
Master's Thesis 2010:51

MASTER'S THESIS 2010:51

Strut-and-tie modelling of reinforced concrete pile caps

Master of Science Thesis in the Master's Programme Structural Engineering and Building Performance Design

GAUTIER CHANTELOT

ALEXANDRE MATHERN

Department of Civil and Environmental Engineering
Division of Structural Engineering
Concrete Structures
CHALMERS UNIVERSITY OF TECHNOLOGY

Göteborg, Sweden 2010

Strut-and-tie modelling of reinforced concrete pile caps

Master of Science Thesis in the Master's Programme Structural Engineering and Building Performance Design
GAUTIER CHANTELOT
ALEXANDRE MATHERN

Department of Civil and Environmental Engineering
Division of Structural Engineering
Concrete Structures
Chalmers University of Technology
SE-412 96 Göteborg
Sweden
Telephone: + 46 (0)31-772 1000

Cover:
Force distribution in the strut-and-tie model of a ten-pile cap and geometry of the three-dimensional nodal zones above the piles

Department of Civil and Environmental Engineering
Göteborg, Sweden 2010

Strut-and-tie modelling of reinforced concrete pile caps

Master of Science Thesis in the Master's Programme Structural Engineering and Building Performance Design

GAUTIER CHANTELOT

ALEXANDRE MATHERN

Department of Civil and Environmental Engineering

Division of Structural Engineering

Concrete Structures

Chalmers University of Technology

ABSTRACT

Shear failure is an important failure mode for pile caps, civil engineering structures in reinforced concrete, often used as substructures for bridges. However, while relatively thin slabs, such as flat slabs for office buildings, have been subjected to intense research in the past, there is a lack of generic models for thicker structures today and building codes are still based on less appropriate empirical or semi-empirical models. For this reason, the design of pile caps for shear failures, and punching failure in particular, often results in dense reinforced structures. A rational approach to shear failures in three-dimensional structures is needed to provide a safe and efficient design of pile caps.

In order to comprehend the complex cracking and failure process in pile caps, the different shear transfer mechanisms of forces in structural concrete, as well as shear and punching failures of flexural elements are described in this thesis.

A review of the design procedures for shear and punching proposed by the Swedish design handbook (BBK04), the European standard (Eurocode 2) and the American building code (ACI 318-08) is conducted. The models of BBK and Eurocode are applied to the analysis of four-pile caps without shear reinforcement. The comparison with the experimental results indicates that the analysis with Eurocode predicts failure loads more accurately than with BBK, however both standards result in significant variations between similar cases, mainly because they accord too much importance to some parameters, while neglecting others.

In light of these facts, strut-and-tie models appear to represent a suitable alternative method to enhance the design of pile caps. Strut-and-tie models have been developed and used successfully in the last two decades, and present a rational and consistent approach for the design of discontinuity regions in reinforced concrete structures. Though, the guidelines for strut-and-tie modelling in the literature are mainly intended to study structures in plane, and it is questionable to apply them in the case of pile caps, structures with large proportions in the three dimensions. Adaptations seem required for the geometry and the strength of the components.

A strut-and-tie model adapted to the design and analysis of pile caps has been developed in this project. The model is based on consistent three-dimensional nodal zone geometry, which is suitable for all types of nodes. An iterative procedure is used to find the optimal position of the members by refining nodal zones dimensions with respect to

the strength of concrete under triaxial state of stress. Away from nodal regions, a strength criterion is formulated for combined splitting and crushing of struts confined by plain concrete. In addition, the specificities of shear transfer mechanisms in pile caps are considered and a combination of truss action and direct arch action for loads applied close to the supports is taken into account, hence reducing the required amount of shear reinforcement.

The method developed is compared to the design codes predictions for the analysis of four-pile caps. The results obtained by the strut-and-tie model are more reliable, both for assessing the failure loads and the failure modes. The iterative procedure is presented in some design examples and guidelines are given to apply the method to pile caps with large number of piles.

Modèle de bielles-et-tirants pour semelles sur pieux en béton armé

Thèse de Master du Programme Structural Engineering and Building Performance Design
GAUTIER CHANTELOT
ALEXANDRE MATHERN
Département de Génie Civil et Environnemental
Division de Génie des Structures
Structures en béton
Ecole Supérieure Polytechnique de Chalmers

RÉSUMÉ

Les ruptures par cisaillement constituent un mode de rupture important pour les semelles sur pieux, structures de génie civil en béton armé, utilisées couramment comme infrastructure de ponts. Néanmoins, alors que les dalles minces ont fait l'objet de recherches approfondies par le passé, il n'y a pas encore de modèle générique adapté aux structures plus épaisses, pour lesquelles les normes reposent toujours sur des modèles empiriques ou semi-empiriques. Pour cette raison, le dimensionnement des semelles sur pieux au cisaillement et au poinçonnement en particulier mène souvent à des structures densément renforcées. Une approche rationnelle des ruptures par cisaillement dans les structures à trois dimensions est nécessaire afin de permettre un dimensionnement des semelles sur pieux alliant sécurité et efficacité.

Afin de comprendre les processus complexes de fissuration et de rupture des semelles sur pieux, les différents mécanismes de transfert de forces dans le béton, ainsi que le cisaillement et poinçonnement des structures de flexion, sont présentés dans cette thèse.

Les procédures de dimensionnement au cisaillement et au poinçonnement sont décrites pour différentes normes : la norme suédoise (BBK), la norme européenne (Eurocode 2), et la norme américaine (ACI 318-08). Les modèles du BBK et de l'Eurocode sont appliqués à l'analyse de semelles sur quatre pieux sans renforcement transversal. La comparaison avec les valeurs expérimentales indique que les prédictions de la charge de rupture de l'Eurocode sont plus précises que celle du BBK, néanmoins les deux normes exhibent des variations importantes entre des cas analogues, principalement à cause de l'importance trop grande accordée à certains paramètres par rapport à d'autres.

Les modèles de bielles-et-tirants présentent une alternative appropriée à l'amélioration du dimensionnement des semelles sur pieux. Les modèles de bielles-et-tirants ont été développés et utilisés avec succès au cours des deux dernières décennies, ils proposent une approche rationnelle et consistante pour le design des régions discontinues dans les structures en béton armé. Cependant, les recommandations pour les modèles de bielles-et-tirants sont spécialement prévues pour l'étude de structures dans le plan, et leur application au cas des semelles sur pieux, structures avec de larges dimensions dans les trois directions, est discutable. Des adaptations semblent nécessaires concernant la géométrie et la résistance des éléments.

Un modèle de bielles-et-tirants adapté au dimensionnement et à l'analyse des semelles sur pieux est développé dans cette thèse. Le modèle repose sur une définition

consistante des régions nodales en trois-dimensions, qui peut être appliquée à tous les cas de nœuds. Un processus itératif est employé afin de déterminer la position optimale des éléments par rectification des dimensions des régions nodales en fonction de l'état de contrainte triaxial. Un critère de rupture tenant compte de l'influence du confinement dans l'écrasement et la séparation des bielles est également formulé. Les spécificités des semelles sur pieux quant aux mécanismes de transfert des contraintes de cisaillement sont considérées par la prise en compte de transferts par treillis ainsi que par arche directe pour les forces appliquées près des appuis, réduisant ainsi la quantité requise d'armatures de cisaillement.

La méthode développée est comparée aux prédictions des normes pour l'analyse de semelles sur quatre pieux. Les résultats obtenus par la méthode des bielles-et-tirants sont plus précis et fiables pour prédire la charge et le mode de rupture. La procédure itérative utilisée est détaillée par des exemples et des indications sont données pour l'application de la méthode à des semelles reposant sur un grand nombre de pieux.

Table of contents

Preface

This Master's thesis has been written within the Master's program Structural Engineering and Building Performance Design, in Chalmers University of Technology. The work was carried out at Skanska Teknik in Gothenburg between January and June 2010.

During our studies at Chalmers, we both attended two courses about concrete structures that were especially enriching and surely motivated us towards the choice of the subject.

We are grateful to Dr. Per-Ola Svahn, our supervisor at Skanska, who gave us the opportunity to undertake this thesis work in a good working environment at Skanska Teknik. We want to thank you sincerely for the time and for the relevant guidance you gave us all along the thesis.

We would like to present our most sincere acknowledgment to our supervisors at Chalmers, Dr. Rasmus Rempling and Dr. Björn Engström, who was also the examiner. Thank you for your interest in our work and for the support you gave us throughout the thesis period.

We also would like to deeply thank Dr. Per Kettil. The outcome of this thesis work would not have been the same without your daily support and the bright advice you gave us.

We also would like to thank our opponents Markus Härenstam and Rickard Augustsson for their feedback on our work.

We appreciated and would like to thank Dr. Rafael Souza and Dr. Karl-Heinz Reineck for the documents they let at our disposal.

Gautier Chantelot and Alexandre Mathern

Göteborg, June 2010

List of notations

Roman upper case letters

A_s	Cross sectional area of reinforcing steel
A_{sw}	Cross sectional area of shear reinforcement
$A_{sw,min}$	Minimum cross sectional area of shear reinforcement
$C_{Rd,c}$	Constant found in national annex (EC2, BBK)
CG	Center of gravity
F	Load
M_{Ed}	Applied moment (ACI, EC2)
V_n	Nominal shear resistance (ACI)
V_c	Concrete contribution to the shear resistance (ACI, BBK)
V_{Ed}	Applied shear force (ACI, EC2)
V_{Rd}	Design shear resistance (EC2)
$V_{Rd,c}$	Design shear resistance for members without shear reinforcement (EC2)
$V_{Rd,cs}$	Design shear resistance for members with shear reinforcement (EC2)
$V_{Rd,max}$	Design shear resistance in web shear compression failure (EC2)
$V_{Rd,s}$	Design shear resistance for members with shear reinforcement (EC2)
V_s	Steel contribution to the shear resistance (ACI, BBK)

Roman lower case letters

a, b	Width of the support respectively in x- and y-direction
a_c	Level of the axis of horizontal concrete struts
a_s	Level of the axis of flexural reinforcement (horizontal ties)
a_v	Distance between the face of the column and the face of the support
b_w	Beam width
c	Concrete cover
d	Effective depth
f_c	Specified concrete compressive strength
f_{cd}	Design value of concrete compressive strength
f_{cd1}	Concrete design strength for uniaxial compression
f_{cd2}	Concrete design strength of nodal zones with one tie
f_{cd3}	Concrete design strength of nodal zones with ties in more than one direction
f_{cd4}	Concrete design strength for triaxial compression
f_{ck}	Characteristic value of concrete compressive strength at 28 days
f_{ctd}	Design value of concrete tensile strength
f_{ctk}	Characteristic value of concrete tensile strength
f_{ctm}	Mean value of concrete tensile strength
f_{v1}	Design punching shear strength for inner and edge columns
f_{v2}	Design punching shear strength for corner columns
f_y	Specified yield strength of steel
f_{yd}	Design yield strength of steel
f_{yk}	Characteristic yield strength of steel
f_{ym}	Mean yield strength of steel
f_{ywd}	Design yield strength of shear reinforcement

X

$f_{ywd,ef}$	Effective design yield strength of shear reinforcement
k	Size effect factor
n	Iteration number n
n_l	Number of reinforcement layer
u	Length of the control perimeter (ACI, EC2, BBK)
u_c	Height of horizontal compressions struts
$u_{exterior}$	Length of control perimeter outside shear reinforcement (ACI)
u_i	Perimeter of the loaded area (EC2)
$u_{out,ef}$	Perimeter of the control perimeter with no required shear reinforcement
u_s	Height of flexural ties
s	Spacing between reinforcing bars
s_r	Radial spacing of shear reinforcement (EC2)
v_{min}	Constant found in national annex (EC2)
w_p	Width of the pile
v_i	Direction vector of the strut
$v_{Rd,max}$	Design shear strength in compressive failure(EC2)
w	Width
x	Direction, length coordinate
y	Direction, length coordinate
z	Lever arm of internal forces, direction, length coordinate

Greek letters

α_s	Constant (ACI)
β	Ratio of the vertical component of the load carried by the stirrups
β_c	Constant (ACI)
β_{ecc}	Constant accounting for eccentricity of the load applied (EC2)
γ	Partial safety factor
ΔV_{ed}	Net upward uplift force inside the control perimeter
ε	Strain
η	Eccentricity factor (BBK)
θ	Angle
θ_{xy}	Angle between between the inclined strut and a horizontal plane, e.g. (x,y)
θ_{yz}	Angle between the inclined strut and the vertical plane (x,z)
λ	Concrete density factor (ACI)
ξ	Size effect factor on the effective depth (BBK)
σ	Stress
σ_c	Compressive stress in the concrete
$\sigma_{Rd,max}$	Design strength for a concrete struts or node
τ_d	Design concrete shear strength (EC2)
τ_n	Nominal concrete shear strength (ACI)
υ	Reduction factor for the compressive strength of cracked strut (EC2)
Φ	Diameter of reinforcing bar
φ	Partial safety factor (ACI)

Subscripts

c	Concrete or compressive
d	Design
k	Characteristic
n	Nominal
s	Steel
t	Tensile
u	Ultimate
x	Direction
y	Direction
z	Direction

1 Introduction

In 1849, Joseph Monier, a Parisian gardener, first understood the potential of combining two materials, steel and concrete, in a single composite building material. Reinforced concrete was born and is by now the most used building material over the world. Concrete and steel complement each other in an efficient manner and provide a strong, workable and cost effective material.

However, the mechanical behaviour of structural concrete, a composite and anisotropic material, is a complex matter. Research on the subject is still very active and no generic theory is at the disposal of the designers. Therefore, in engineering practice, structures are mostly designed case-by-case based on empirical sectional approaches. These empirical approaches rely on many years of research and practice and provide simple and fine designs for most structures. Nevertheless, when the geometry of the studied element becomes peculiar, empirical sectional approaches show their limits; this is the case in pile caps.

Pile caps are construction elements that fulfill the function of transmitting the load from a column or a wall to a group of concrete piles; they constitute an interface between the superstructure and the substructure. Pile caps are subjected to concentrated loads and show large dimensions in the three directions resulting in highly non linear strain distributions. Pile caps mainly consist of disturbed regions; therefore the relevance of applying sectional approaches based on empirical formulas for flexural elements is questioned.

A design approach based on the lower bound theorem of the theory of plasticity called the strut-and-tie model was developed during the last decades to offer a consistent alternative for the design of disturbed regions. The strut-and-tie model is a design procedure already implemented and strongly recommended for the design of pile caps in, among others, the European and the American building codes.

This thesis work intends to answer the need expressed by designers at Skanska Teknik in Gothenburg, Sweden, to clarify and investigate the relevance of pile caps design using the national building code.

Therefore a generic study of shear failures, and especially punching shear failures, in structural concrete and in pile caps is carried out. Thereafter, the design approaches in the European, American and Swedish building codes are compared and the state of art of design based on three-dimensional strut-and-tie method is presented.

An innovative three-dimensional strut-and-tie method based on a consistent geometrical definition of the nodal regions is developed in this thesis. A sufficient amount of shear reinforcement is provided to control sliding shear failures and the web is checked against combined splitting and crushing failure of concrete.

The model is evaluated against experimental results and compared to current design practice. Design of pile caps based on the three-dimensional strut-and-tie model developed in this thesis is more cost effective and safer against shear failures than current sectional approaches of European and Swedish building codes.

In order to assist the practical design of pile caps, a semi-automated program is developed. This program can handle various load cases, pile cap shapes and piling layouts.

1.1   Aim

The main aims of this thesis work are:

- to investigate the shear and punching failures phenomenon,

- to provide a review of Swedish and international standards to the design for shear and punching in pile caps,

- to develop a 3-D strut-and-tie method adapted to the design of pile caps,

- to examine the possibility of automating the design procedure.

1.2   Limitations

The pile caps studied are here isolated from the structure and designed considering that they are subjected to a set of loads calculated by external means. However, including the infrastructure, the pile cap and the superstructure in one single design could lead to better considerations of uncertainties and partial safeties.

The position and inclination of the piles, the height of the pile cap as well as the size of the columns are found out in preliminary studies. The purpose of the strut-and-tie model developed is limited to the design of the flexural and shear reinforcement inside the pile cap.

1.3   Outline of the thesis

A literature study about shear and punching shear failure mechanisms in structural concrete is presented. In addition the European, American and Swedish design codes approaches to shear are described and compared.

A literature study on the two-dimensional strut-and-tie method and the state of art of three-dimensional strut-and-tie modelling are presented.

A generic three-dimensional strut-and-tie method based on a consistent geometrical definition of the nodal zone is developed. According to the authors' knowledge, the three-dimensional strut-and-tie method proposed in this thesis is the only existing one that:

- Defines consistent nodal regions and geometries for the nodal faces,

- Assures the concurrency between the centroids of the nodal region and the struts,

- Automatically optimizes the nodes position.

The model developed in this thesis accounts for the superposition of arch and truss actions in stocky elements and an innovative formulation is proposed to evaluate the strength of a web against combined splitting and crushing in three-dimensional structural concrete. Consequently, the design procedure proposed in this thesis guaranties that no unpredicted shear failure occurs before yielding of the flexural reinforcement.

The reliability of the model, for analysis and design purposes, is then evaluated against experimental results and compared to current design practice.

Eventually, the three-dimensional strut-and-tie model is implemented into a semi-automated program that handles designs for piles caps of various shapes, number and position of piles and columns and load cases.

1.4 Background

1.4.1 Pile caps

Pile caps are structural elements made of structural concrete that fulfill the function of transmitting the load from a column or a wall to a group of concrete piles. Pile caps are an interface between the superstructure and the substructure. The figures in this section are meant to illustrate the different building steps for pile caps.

Figure 1.1   Piles are driven into the ground

Piled foundations are routinely used in engineering works when the superficial layers of the soil do not assure a sufficient support. Piles can either be precast and driven into the ground, or cast in-situ directly into the ground. Piles transmit the loads to the ground either by friction with soils made of sandy materials, cohesion with soils that contains clay or by compression at the tip when the pile reaches bedrock or other resistant layer of soil. Usually a combination of upward friction or cohesion along the pile and vertical force at the tip of the pile are combined to calculate the bearing capacity of a pile.

When all the piles are in place, a thin layer of blinding concrete is cast. The purpose of this layer is to provide a rather smooth, dry and clean base for the pile cap.

Figure 1.2   Layer of blinding concrete cast over the piles

Afterwards, the formwork is set and reinforcement bars for the pile cap as well as projecting reinforcement for the superstructure are put in place.

Figure 1.3   Formwork and reinforcement of a pile cap

Eventually concrete is casted into the formwork.

Figure 1.4   Concrete is poured into the formwork

As can be seen in Figure 1.2 and in Figure 1.4 pile caps are usually buried in the ground level. Therefore, visual inspections are difficult and so is the assessment of the serviceability of the structure during lifetime.

Pile caps are usually cast at one time on top of the piles. Indeed, casting a thick slab all at once enables to avoid restraint between different layers of concrete due to differences of temperatures. The counterpart is that high temperatures can be reached in the core of the pile caps at setting due to the large volumes of concrete. Therefore, pile caps can be subjected to rather high thermal strains.

1.4.2   Design practice

The current design procedure for pile caps at Skanska is based on the prescriptions of the Swedish building code together with the Swedish handbook for concrete structures, BBK 04. The procedure is based on sectional approaches and is similar to the one for slabs: the flexural, shear and punching shear capacity have to be controlled for the design in the ultimate state. Provisions for minimum reinforcement amounts and spacing are considered in the service state.

Skanska's designers are unconvinced that the current design practice for pile caps is consistent and efficient. The superposition of empirical approaches and some provisions, especially for shear reinforcement, are regarded as doubtful. Skanska's designers expressed the need for a clarification on the subject and wanted to know more about the possibility to design pile caps using strut-and-tie models.

The strut-and-tie model is a design procedure already implemented and strongly recommended for the design of pile caps in, among others, the European and the American building codes.

This thesis project intends to answer these questions.

The Swedish design procedure for pile caps is confronted with foreign design codes as well as with experimental results. Thereafter the possibility to design pile caps using three-dimensional strut-and-tie models is studied.

1.5 Sectional approach and force flow approach

In the design of concrete structures, the distinction can be made between B-regions (standing for Bernoulli's regions or beam-like regions) and D-regions (standing for discontinuity-regions) (Schlaich 1987).

In B-regions, the linear strain distribution of flexure theory applies and thus a sectional analysis is appropriate to design these regions.

In D-regions, geometrical discontinuities or static discontinuities result in disturbances and the plane sections assumption is not valid anymore. According to St. Venant's principle, the D-regions are assumed to extend to a characteristic distance h away from the discontinuity, depending on the geometry as shown in Figure 1.5.
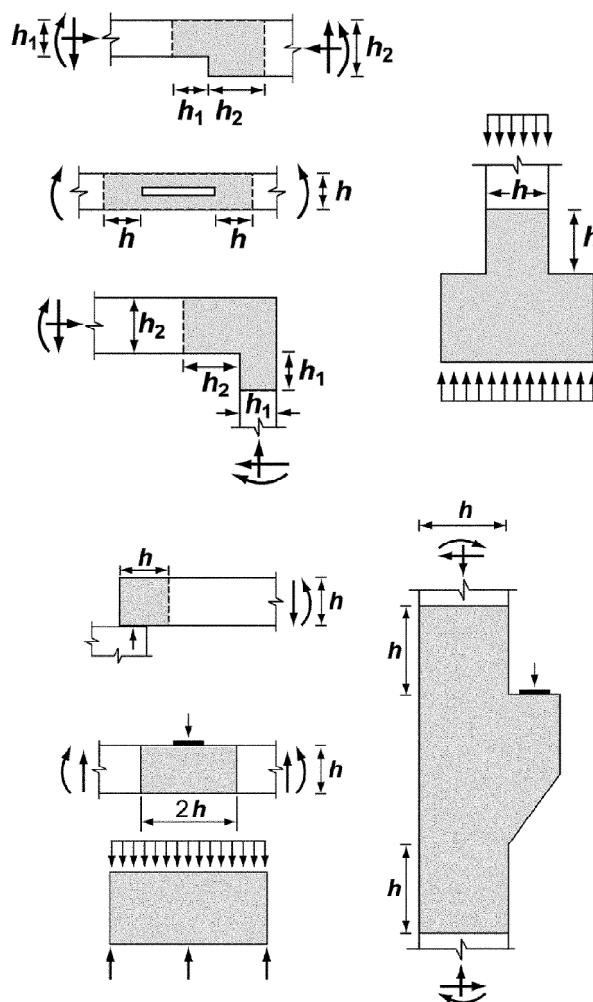
Figure 1.5   D-regions as described by Schlaich (1987), drawing adopted from (ACI 318-08)

According to this definition, pile cap are often in a range of dimension where the beam theory is not valid in any section and the whole pile cap constitutes a discontinuity region. Therefore design procedures based on sectional approach given by the codes for the design of pile caps are not appropriate.

A design approach based on the lower bound theorem of the theory of plasticity called the strut-and-tie method was developed during the last decades to offer a consistent alternative design to disturbed regions, as expressed by Adebar, Kuchma and Collins (1990, p. 81):

> *"Current design procedures for pile caps do not provide engineers with a clear understanding of the physical behaviour of these elements, Strut-and-tie models, on the other hand, can provide this understanding and hence offer the possibility of improving current design practice."*

Today, the strut-and-tie method is a design procedure implemented and strongly recommended for the design of pile caps in, among others, the European and the American building codes.

In the first part of this thesis work, shear and punching failures in structural concrete are described. Afterwards, the sectional approaches presented in different design codes are presented. The relative capacity of these different sectional approaches to assess the actual behaviour of pile caps is evaluated, in principle and against experiments.

2 Shear and punching shear in reinforced concrete elements

The aim of this chapter is to deliver a presentation of shear and punching shear actions in reinforced concrete structures. This presentation includes a general description of the phenomenon as well as specificities related to pile caps.

Shear failures are characterised by a local shattering of the shear links in the material that weakens the structure up to a point where it cannot transfer the load to the supports. Shear failure mechanisms in reinforced concrete usually consist of the unconstrained relative sliding of two parts of the structure.

Punching is a localised shear failure mode that occurs in structural elements with bending moments and shear transfer of forces in two directions, like in slabs or in pile caps. The punching failure mechanism consists of the separation of a concrete cone from the slab under a concentrated load or over a concentrated support reaction. The geometry of the punching cone is linked to the particular shear and moment distribution that occurs in the vicinity of a concentrated load.

An advanced comprehension of the shear transfer actions in reinforced concrete is required in order to understand the punching phenomenon. Therefore, in the first section: 2.1 Shear, the shear transfer actions and the shear failure mechanisms are presented. The second part, 2.2 Punching, deals with punching shear failures. In both parts, a comparison between three design codes is made, namely the Swedish BBK04, the American ACI 318-08 and the European Eurocode2.

2.1 Shear

2.1.1 Introductory remarks

The shear capacity assessment of a reinforced concrete element is one of the most misunderstood matters for most structural engineers. When it comes to the evaluation of the flexural capacity of a member, the difference in prediction between major design codes is barely greater than 10%. On the contrary, the predicted shear capacity of a reinforced concrete member can vary by a factor of more than 2 (Bentz et al. 2006). In 1985, an international competition took place in Toronto; 27 of the leading researchers in structural concrete were invited to predict the shear capacity of four reinforced concrete panels loaded in pure shear. Predictions of the resistance were usually higher than the experimental values and showed a coefficient of variation of 40%. On a single study case, ultimate capacity and strains predictions from different researchers may vary by more than 4 times (Collins et al. 1985).

The poor estimation of the mechanical behaviour of reinforced concrete loaded in shear comes from the lack of comprehensive analytical models. Three main reasons give rise to understanding obstacles:

In most situations, the concrete tensile capacity has to be taken into account in order to provide a good evaluation of the shear capacity.

The assessment of the relation between the tensile, compressive and shear stresses and their associated strains is highly non linear. Reinforced concrete is a composite material and shows non isotropic mechanical properties, which complicates the formulation of relationships between stresses and strains in the material.

An average formulation of the state of stresses and strains in the material is often not satisfying enough for cracked concrete as different and complex ways to transfer compressive, tensile and shear forces occur in plain concrete, in steel reinforcement, at the bond between steel and concrete and at crack interfaces. Hence, a general shear model has to embrace local phenomena.

2.1.2 Mechanical description of one-way shear force transfer in reinforced concrete structures – shear cracks, shear failures

2.1.2.1 Beam theory of elasticity

In an uncracked beam, the eccentricity between the load application point and the support induces shear forces transferred across the beam, resulting in inclined principal stresses in the web. For a load less than the cracking load, one can assume that steel reinforcement do not greatly affect the stiffness of the beam. Therefore; if the concrete cross section is constant, the stiffness is assumed to be constant along the length of the beam.

Under this assumption and for a given load case, Figure 2.1 shows the stress and strain distribution derived according to the linear elasticity theory.
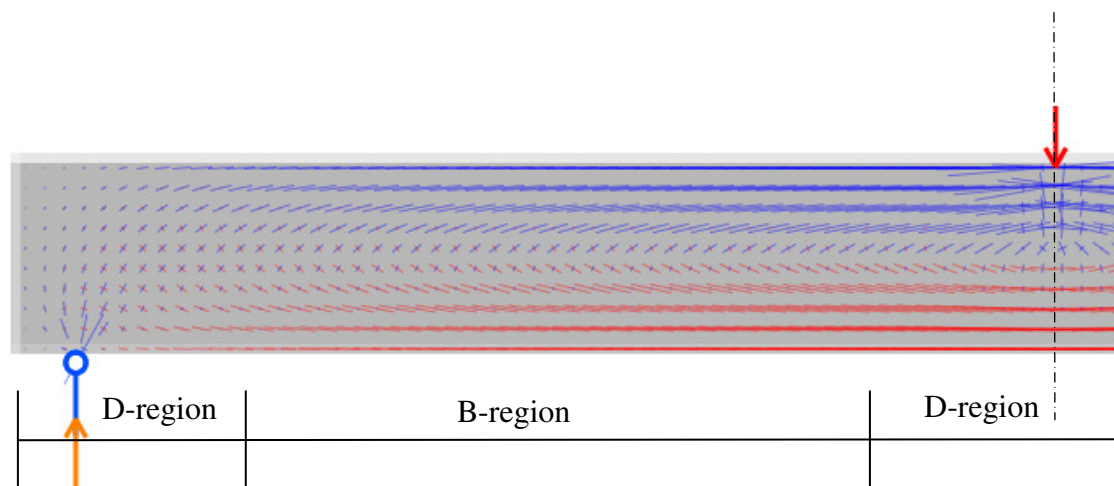
Figure 2.1   Principal stresses in an uncracked concrete beam found by linear elastic analysis

Different areas can be distinguished; D-regions (standing for discontinuity or disturbed) close to the support and the load application, and B-regions (standing for beam or Bernoulli) in between.

In the beam or Bernoulli regions, the direction of the principal compressive and tensile stresses at the neutral fibre is constantly inclined of 45 degrees in relation to the axis of the beam.

The shear diagram in Figure 2.2 shows that the maximum shear stress is reached at the neutral axis of the beam. For a rectangular cross section, the maximum shear stress is one and a half time higher than the mean shear stress in the section. At the top and bottom fibres of the section shear stresses are equal to zero, therefore there is no variation in normal stresses. Over the height of the cross section, a S-shaped normal stresses profile is derived.
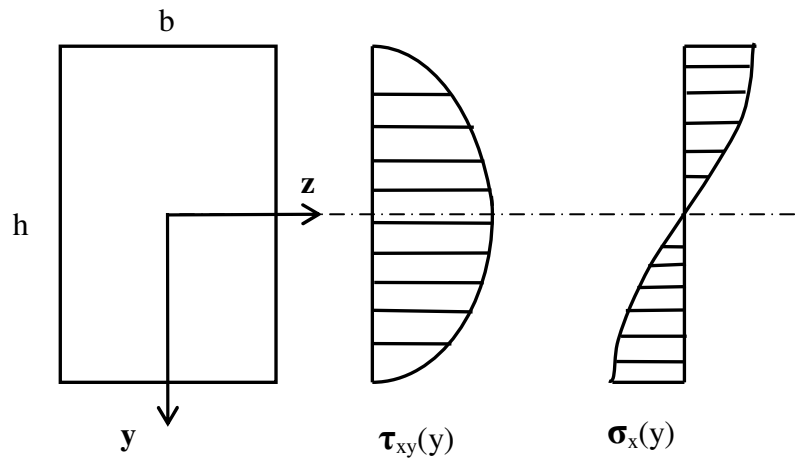
Figure 2.2   Shear and normal stress profiles in a B region according to the theory of elasticity, for a rectangular cross section

For many years, it has been accepted that the behaviour of the B-regions of flexural elements is sufficiently well represented by the so called beam theory. The beam theory is a simplification of the solution provided by elastic theory for B-regions. The main hypotheses are:

The Saint-Venant principle: the state of stress in a point far away from load application is only dependant on the general resultant moment and forces.

The Navier-Bernoulli hypothesis: sections remain plane when the beam deforms.

For a rectangular cross section, the simplified shear and normal stresses are found in Figure 2.3:
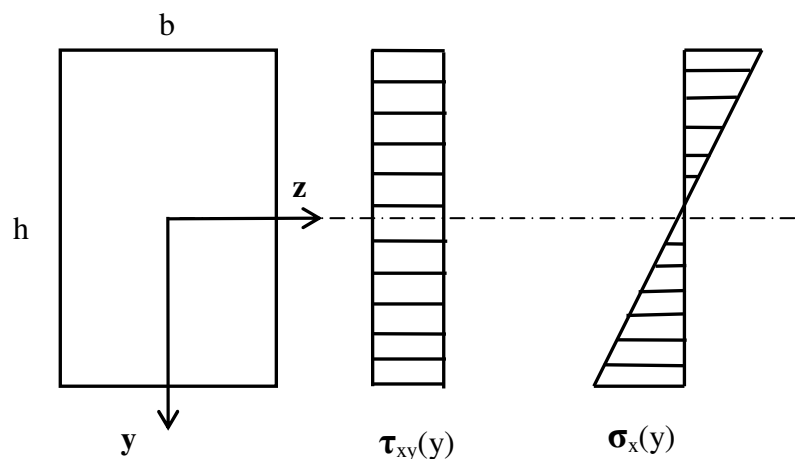
Figure 2.3   Section, shear and normal stresses according to the elastic beam theory, for a rectangular cross section

In the beam theory, the shear stress profile over the height of the beam needs to be constant to satisfy the plane deformation condition. This "mean" shear diagram approximation is quite different from the elastic solution. However, the shear induced deformations are usually considered as negligible compared to the flexural ones, therefore this deviation from the elastic shear profile is commonly accepted in calculation of deflections of beams.

2.1.2.2 Development of cracks in a beam

A combination of in plane shear and normal forces at a given point of the beam is assumed, derived according to the elastic solutions presented above. The theory of continuum mechanics allows the evaluation of the principal stress and strain direction and magnitude. The Mohr's circle is a useful tool to determine the principal directions.

In reference to Figure 2.4, ε_1 and ε_2 are respectively the principal tensile and compressive strains and θ is the direction of the principal compression at the considered point.

(a)   **(b)**
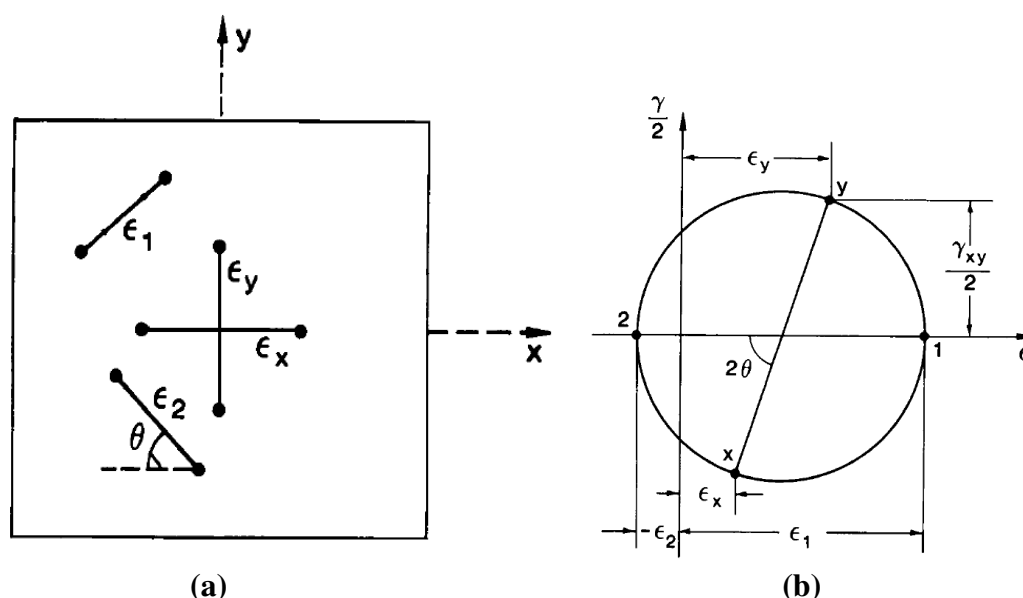
Figure 2.4   *(a) Principal stress and strain direction in a small membrane element in the web of a beam; (b) Mohr's circle of strains*

In Figure 2.1, the principal tensile stresses according to elastic analysis are represented with red crosses. For a non prestressed beam, the maximum tensile stresses occur in the tensile chord, in the maximum moment region.

When the principal tensile strain reaches the maximum deformation capacity of concrete, a local tensile failure occurs and a crack opens. This flexural crack propagates almost vertically, with θ close to 90 degrees, in the tensile region of the web, see Figure 2.5.
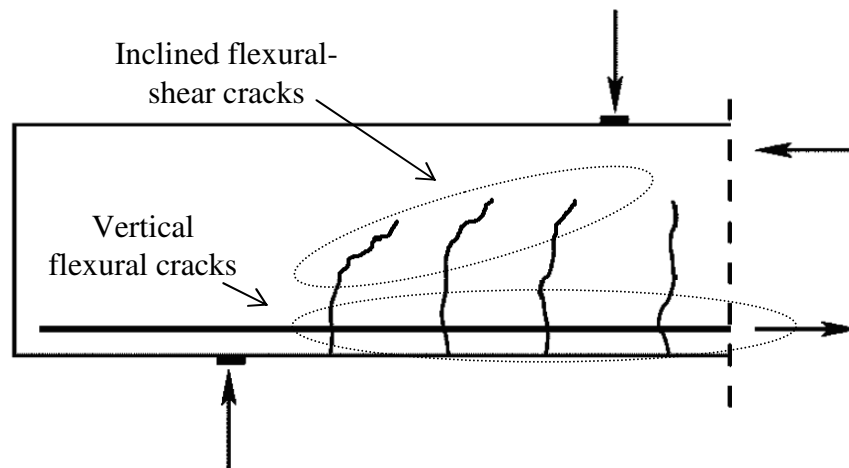
Figure 2.5   Development of cracks in a beam

With increasing load, the second classic cracks that occur are called the "inclined flexural-shear cracks", see Figure 2.5. These cracks initiate at the tip of the flexural cracks and propagate in the web with an inclined direction. They are caused by excessive principal tensile stress in the web. The direction of a crack depends on the direction θ of the principal stresses when the tensile capacity of concrete is reached. The direction of the principal stresses is dependent on the position of the point in the beam considered and the force distribution

As soon as cracks start to develop in reinforced concrete, the strains are not anymore equal in steel and concrete and drastic changes in stresses and strains in both materials are induced. Due to cracking, a redistribution of forces occurs in the whole element, for instance:

- Very small or no tensile stresses are transmitted by the concrete through the cracks. Steel carries almost the entire tensile stresses across a crack.

- Before cracking of the web, the planes where cracks are going to occur were subjected to the maximum tensile stresses and therefore were corresponding to principal strain directions. It is of importance to notice that, before cracking, no shear stresses were acting along these planes. After cracking, some shear stresses are transmitted by aggregate interlock and friction along the faces of the cracks. Consequently, the principal stress directions in the web in the vicinity of a crack are modified and the direction of the maximal tension changes at the tip of the cracks, see Figure 2.6. Hence, further cracks will not propagate in straight lines but in an inclined direction toward the load application point and are therefore called rotating cracks, see Figure 2.5.

- After cracking, the stiffness distribution is also dependant on the reinforcement arrangement along the beam.
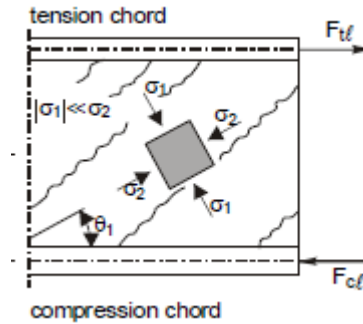
Figure 2.6   Principal average stresses in concrete in the web after cracking (Walraven 2002)

After some cracking has taken place, a sectional analysis using elastic and continuum mechanics theories is no longer adequate in order to account for local discontinuities. A refined study is needed to understand the development of the crack pattern and the redistribution of forces. Different models can be used:

- Non-linear finite element analysis is a powerful tool to study the development and influence of cracks in concrete structures up to failure. Compressive field approaches like

- The Modified Compression Field Theory developed by Vecchio and Collins (1986) proposed an analytical solution to evaluate the distribution of forces in cracked reinforced concrete. The Modified Compression Field Theory considers both stresses equilibrium and strains compatibility at the crack interface and in the uncracked material (between cracks).

2.1.2.3   Failure modes in beams

There are two classic types of failure in slender, non prestressed flexural elements that carry the load in one direction only:

The compression failure of the compressive chord or "ductile flexural failure":

After yielding of the reinforcement, if no redistribution of forces is possible, the deformations of the beam become important while the structure deflects in a ductile manner. The compressive flange of the beam softens and the centre of rotation of the sections goes down, reducing the internal level arm. Ductile flexural failure occurs when the ultimate capacity of the concrete compressive zone is reached.

The flexural failure is governed by concrete crushing after yielding of the steel. Indeed, the deformation capacity of the steel is normally not decisive.

The shear failure in the web of the beam or "shear flexure failure", see Figure 2.7(a):

Due to high local tensile stresses in the web the "inclined flexural shear cracks" propagate, see Figure 2.5, and reduces the capacity of the different possible shear transfer mechanisms described below in section 2.1.2.4.

When the shear transfer capacity between two neighbouring portions of the beam becomes too small, a static equilibrium cannot be found. A relative displacement between the two neighbouring portions takes place. The shear failure mechanism is characterised by shear sliding along a crack in beam without shear reinforcement and yielding of stirrups in a beam with shear reinforcement.

Figure 2.7   (a) Shear flexure, (b) Shear tension (Walraven 2002)

Three other modes of failure can be mentioned:

Brittle flexural failure:

In the case of a beam with huge amounts of reinforcements failure may occur by crushing of the concrete in the compressive zone before yielding of the flexural reinforcement.

Shear compression failure:

Compression failure of the web due to high principal compressive stresses in the region between induced shear cracks. This failure mode is normally associated with high amounts of shear reinforcement but may also be critical in sections with thin webs.

Shear tension failure, see Figure 2.7(b):

In the case of prestressed elements, a very brittle shear failure, starting at middle height of the web, may occur, without any prior flexural cracks. This failure mode is called "shear tension". Unlike non-prestressed flexural elements, the initiation of a web shear crack leads to an immediate and unstable crack propagation across the section. For a beam without stirrups if a "shear tension crack" initiates in the web it will therefore lead to the collapse of the element.

2.1.2.4   Mechanisms of shear transfer in cracked concrete

The presence of a crack in a beam induces a redistribution of stresses. Very few or no tension can be transferred through a crack, which is incompatible with the elastic stress distribution shown in Figure 2.1.

Some changes occur in the way the structure bears the bending moments. From now on, the tension in the bottom is transferred by the steel only through the cracks and by steel and concrete (tension stiffening) between two cracks. The compressive zone is slightly affected by the displacement of the neutral axis due to the change of stiffness of the beam at cracking.

However, the changes in shear transfer in the web are the most complicated. After cracking, six shear transfer mechanisms can be distinguished and are described below in Figure 2.8. In these drawings, local truss models inspired by Muttoni et al. (2008) are used. Through the understanding of these different shear transfer actions, conclusions were drown and have been applied in the design procedure developed in this thesis work.
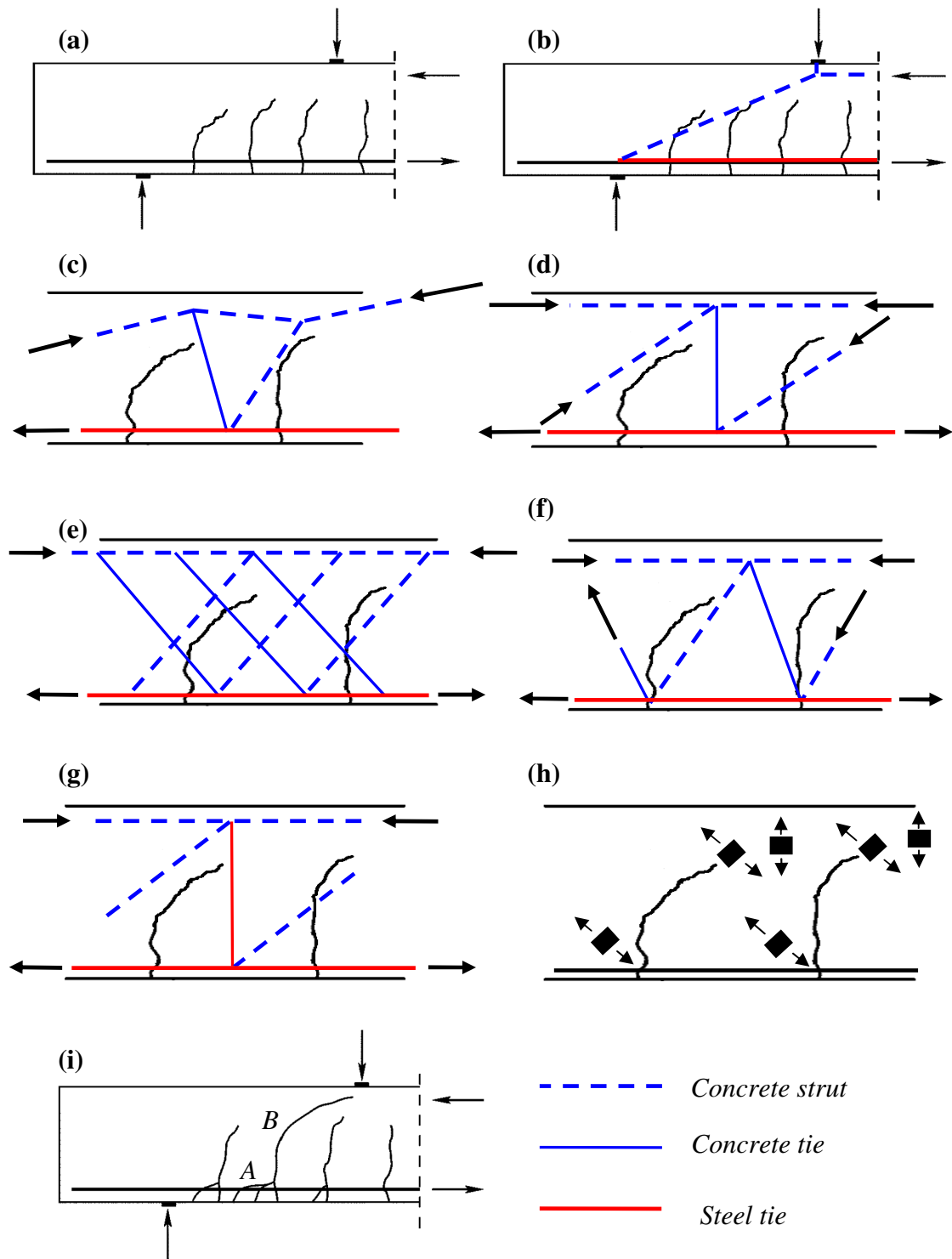
Figure 2.8   Shear transfer mechanisms in reinforced concrete (a) cracking pattern, (b) direct arch action, (c) shear forces in the uncracked concrete teeth, (d) interface shear transfer, (e) residual tensile stresses through the cracks, (f) dowel effect, (g) truss action: vertical stirrups and inclined struts, (h) tensile stresses due to (c), (d), (e) and (f), (i) final cracking pattern

(b) Direct arch action

The direct arch action is a process to transfer a load to a support without directly using the vertical tension or shear capacity of the material. The only transfer process is direct compression in the concrete struts and tension in the flexural reinforcement as shown in Figure 2.9.
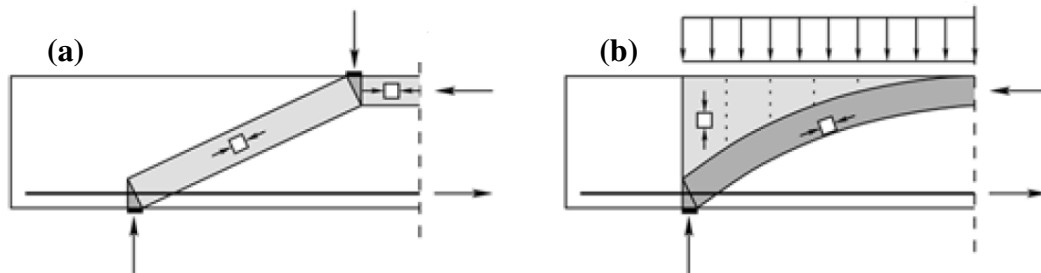
Figure 2.9   The unique static equilibrium in beams with flexural reinforcement only, according to plasticity theory, neglecting the tensile capacity of concrete, (a) point load, (b) distributed load (Muttoni et al. 2008)

The direct arch action is very attractive due to its apparent simplicity. However, the designer should not forget that the capacity of a structure to develop such a stress distribution is limited. Three reasons were distinguished:

- Close to the support in a slender beam, the directions of the compressive arch and the tension tie become very antagonists. Hence, strain incompatibilities may arise that the material is not able to scatter.

- The prismatic compressive strut drawn in Figure 2.9 is an idealised vision. Actually, the strut will transfer forces to its surrounding by shear action and thus will widen. In order to respect strain compatibilities, tensile stresses will appear perpendicular to the strut. These stresses can lead to cracks which reduce the capacity of the strut.

- A direct concrete arch cannot fully form if the beam is cracked. In the case of a cracked beam, more sophisticated way to transfer shear forces occur and are described below.

The shear transfer of forces by direct arch action is predominant in deep elements like pile caps. The magnitude of the shear transfer of forces by direct "arch action" was shown to be in good agreement with the geometry of the element. For example in Eurocode2, the ratio *a/d* as defined in the Figure 2.10, is used. It is usually considered that arch action contribution to the overall shear force transfer becomes low for *a/d>2.5*.
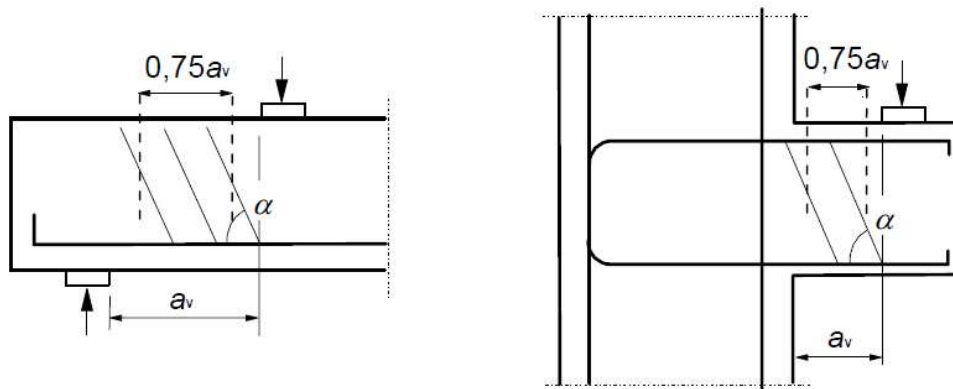
Figure 2.10   Examples were a significant part of the shear force is transferred by direct arch action, according to Eurocode 2

(c) Shear forces transferred in the uncracked concrete teeth

The uncracked zone of the beam between inclined shear cracks transfers vertical shear forces like in an uncracked beam, namely by orthogonal compressive and tensile stress fields in the web. This shear transfer action is often called cantilever action because the concrete teeth can be seen as bent between the compressive and tensile chords. The contribution of the cantilever action in the overall shear resistance is of increasing importance for beams with high uncracked web height, in prestressed beams and deep beams where crack control is assured for example.

(d) Interface shear transfer

A portion of the vertical shear capacity is provided by forces opposed to the slip direction along the cracks, v_{ci} in Figure 2.11.
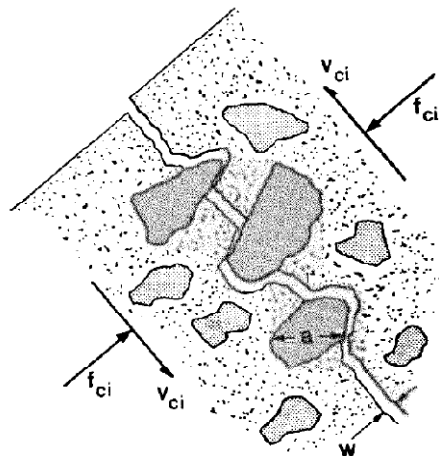
Figure 2.11   Forces at crack interface

Depending on the situation forces at crack interface can be called aggregate interlock or shear friction. Indeed, these two last expressions point out that the ability to transfer forces along the crack is not only dependant on the material properties, but on the crack geometry as well. Muttoni et al. (1996) distinguished "micro interlocking" and "macro interlocking" depending on the crack width. Therefore, the more general denomination: "interface shear transfer" is often used nowadays to name the transfer of forces that can occur at a crack interface.

The vertical component of the friction force contributes to the shear capacity of the member.

(e) Residual tensile stresses

It was shown recently that residual tensile forces can be transmitted through narrow cracks. Residual tension is significant for thin cracks 0.05 mm $< w < 0.15$ mm, these kind of cracks usually occur in thin beams with good crack control. It is not the case in deep members like pile caps, where cracks control is poor and cracks are wide due to size effects.

(f) Dowel action of the longitudinal reinforcement

Dowel action is the transfer of forces by shearing of the flexural steel. Dowel action requires relative displacement of two neighbouring concrete "teeth" in order to shear the flexural steel. This action generates compression and tension in the concrete around the bars. The dowel action of the longitudinal reinforcement is neglected in most compressive field approaches and in the strut-and-tie method. It is often considered that the displacements required to activate the capacity of the flexural bars in shear are too large to occur before failure of the beam. The CEB-FIP Model Code (CEB-FIP90, p115) suggests that a relative displacement between two neighbouring "concrete teeth" of 0,10 times Φ, the diameter of the steel bars, is required to fully activate the dowel action.

It is considered that dowel action will be negligible in pile caps because the displacements are limited and flexural bars with large diameters are used.

(g) Shear stresses carried by truss action in beams with transverse reinforcement

In a slender beam with vertical or inclined shear reinforcements, the main way to transfer shear forces is by combination of compression in inclined compressive struts and tension in the stirrups, the so-called truss action as illustrated in Figure 2.12.
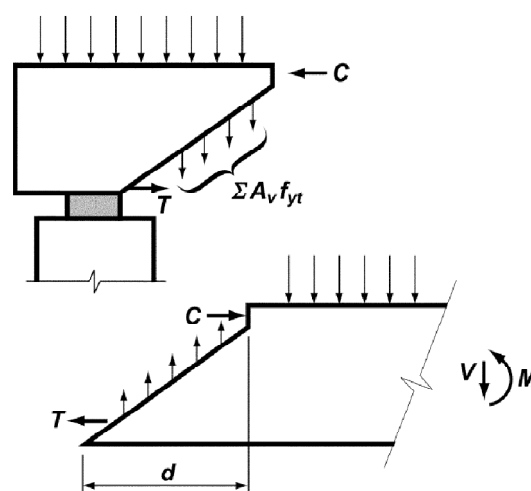
Figure 2.12   Free body diagram at the end of the beam (ACI 318-08)

For slender elements with stirrups, shear transfer of forces by combined tension in stirrups and compression in the web is overriding. For instance, this is the only shear transfer mechanism considered in the "variable inclination method" used in Eurocode.

2.1.2.5 Comments

These six different shear transfer mechanisms are important in order to understand the behaviour of cracked reinforced concrete structures. When the vertical flexural crack develops into an inclined shear crack in A (Figure 2.8(i)), shear transfer mechanisms (c), (d) and (f) cannot take place anymore. Assuming that residual tension through the crack (e) can only account for a negligible part of the load transfer, then the only way to transfer shear forces is by direct arch action (b) or by a combination of tension in the stirrups and inclined compression in the web (g). This assumption is commonly made in truss and strut-and-tie design approaches.

The calculation of the shear capacity of a beam is complicated to assess and depends greatly on the crack pattern and especially on the critical shear crack. Positions and shapes of cracks are difficult to predict as they depends on a lot of factors, among them the load history for example.

It should be pointed out that, if only direct arch action (b) takes place in the element, no direct tension occurs in the web since the tension in the bottom chord is constant from the middle of the beam to the support. Among the six shear transfer actions described in this chapter, the direct arch and truss actions are the only ones that do not require the "direct" use of the tensile strength of concrete (Figure 2.8 (h)). However, in the case of truss action, strain compatibility in the web between steel and concrete between cracks will induce tension in the concrete. In the case of arch action, some tensile stresses occur in the web due to the widening of the strut. These stresses can be classified as "secondary" as they emerge from strain compatibility with the surrounding of the strut. For instance, if the transverse stresses reach the concrete tensile strength, concrete will crack and the strut will become narrow providing a new equilibrium that does not need these "secondary" tensile stresses.

Except direct arch action, all the shear transfer mechanisms (namely: cantilever action (c), shear transfer at crack (d), residual tension through the cracks (e), dowel effect (f) and the stirrups contribution (g)) increase the tension in the web while they decrease the tensile forces in the flexural reinforcement. These actions are named "shear transfer of forces by truss action". They rely on the presence of a compressive and a tensile field crossing each other in the web. The compression field is carried by compression in the concrete while the tension field is taken either by tension in concrete (c, d, e and f) or tension in shear reinforcement (g). These effects are represented in a simplified manner by a "truss" model where compression is represented by dotted lines and tension by continuous lines in Figure 2.8. It is important to note that evaluating the tensile contribution of concrete is complex, mainly because of the uncertainty in the assessment of the cracking pattern of a reinforced concrete element. Therefore, in lots of design methods like the "variable inclination method" and most strut-and-tie models, the tensile contribution of concrete is neglected. This simplification leads to the fact that only two shear transfer mechanisms are considered: "direct arch action" and "shear transfer by combined tension in stirrups and compression in the web".

2.1.2.6 Conclusion

In the design method for pile caps using strut-and-tie models developed in this thesis work, a choice was made to focus on the duality of shear transfer mechanisms. On the one hand the transfer by "direct arch action", that does not directly rely on tension in the web, and thus does not require the use of stirrups. One the other hand the "shear transfer by truss action" that requires the presence of a tension field in the web (Figure 2.8 (h)). This tension field can be carried by concrete up to a certain limit, afterwards shear reinforcement must be provided. The strut-and-tie model developed in this thesis considers that no tension is carried by concrete, therefore, in the web, only shear reinforcement can carry tension. The model developed in this thesis work superimposes the "direct arch action" and the "shear transfer by truss action" in the same model. A static indeterminacy is raised and solved by choosing the amount of load that is transferred by each of these actions based on geometrical considerations and on the amount of shear reinforcement provided. A detailed quantitative explanation of this approach is presented in section 5.3.2: *Duality between shear transfer of forces by direct arch and by truss action in short span elements*.

2.1.3 Shear design according to building codes

2.1.3.1 Introduction

Three different design codes are presented: The Swedish handbook on concrete structures (BBK04), the Eurocode 2 (EC2) from Europe and the American Concrete Institute building code (ACI 318-08).

In order to be clearer for the reader, the variable names were harmonised on the basis of Eurocode 2 notations.

For each code, a presentation of the fundamental equations for shear, also called one-way shear, design is made. A comparison is then made between the different approaches. In section 7.2, the predictions of EC2 and BBK04 are compared with experimental failure loads of 4-pile caps without shear reinforcement. Some additional comments on the efficiency of the design codes are also made in that part.

2.1.3.2 ACI

Reference is made to ACI 318-08 (ACI318-08) in this part.

The design approach of the ACI building code is cross-sectional which means that the sectional capacity is compared to the sectional shear force.

The design approach of the ACI building code is based on the following three equations:

$$\varphi V_n \geq V_{Ed} \tag{2.1}$$

The design shear capacity should be higher than the actual shear force and is determined as a nominal shear capacity multiplied with φ, the strength reduction factor equal to 0.75 for shear. The nominal shear capacity can be expressed as:

$$V_n = \tau_n b_w d \tag{2.2}$$

The contribution of concrete and shear reinforcement are added to define the nominal shear capacity of the section.

$$V_n = V_c + V_s \tag{2.3}$$

Members not requiring design shear reinforcement

The contribution to the shear capacity of concrete, V_c, is set equal to the shear force required to cause significant inclined cracking and is, in the ACI code, considered to be the same for beams with and without shear reinforcement.

$$V_c = 2\sqrt{f_c}\, b_w d \tag{2.4}$$

Or, with a more detailed equation:

$$V_c = \left(1.9\lambda\sqrt{f_c} + 2500\rho\frac{V_{Ed}d}{M_{Ed}}\right)b_w d \leq 3.5\sqrt{f_c}\, b_w d \tag{2.5}$$

The maximum nominal shear stress is proportional to the tensile strength of concrete, which is defined as proportional to the square root of the concrete compressive strength. The shear capacity is also directly influenced by the amount of flexural reinforcement, the more the flexural steel ratio $\rho = A_s/b_w d$ is high, the more the propagation of a critical crack in the web is reduced. The term $V_{Ed}\,d/M_{Ed}$ limits the concrete shear capacity near inflexion points.

Another set of formulas also allows modifying the shear capacity of a member depending on with axial compression/tension. This case in encountered mainly in prestressed and post-tensioned members and is not relevant for pile caps.

Members requiring design shear reinforcement

According to the ACI code a minimum amount of shear reinforcement should be provided as soon as V_{Ed} exceeds $0.5\varphi V_c$.

$$V_{Ed} \leq 0.5\varphi V_c \tag{2.6}$$

This limitation reduces the risk of brittle failure in the web and allows crack width control.

A minimum area of shear reinforcement is required:

$$A_{sw,min} = 0.75\sqrt{f_c}\,\frac{b_w s}{f_y} \tag{2.7}$$

This area is chosen bigger for higher concrete strengths in order to prevent brittle failure.

Where shear reinforcement perpendicular to the axis of the beam are provided, the steel contribution to the shear capacity is:

$$V_s = \frac{A_w f_y d}{s} \tag{2.8}$$

Where A_w is the area of shear reinforcement within spacing s. V_s is calculated as the capacity provided by vertical stirrups in a 45 degrees truss model, see Figure 2.13. The ACI code considers a modified truss analogy including both the tensile capacity of the stirrups, V_s, and the tensile capacity provided by the concrete, V_c. The nominal shear capacity of the flexural element is then calculated using Equation 2.3.

Load applied close to a support
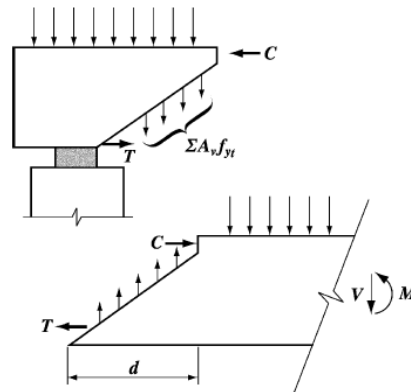
Figure 2.13   Free body diagrams of the end of a beam

The closest inclined crack at the support will extend in the web and meet the compression zone at approximately a distance *d* from the face of the support. The loads applied at a distance less than *d* from the column face are transferred directly by compression in the web above the crack; they do not enter in the calculation of the applied shear force *V* and do not increase the need for shear capacity. Accordingly, the ACI code states that sections located less than *d* from the support face are allowed to be designed for the applied shear force *V* at a distance *d* from the support face as well. However, this can only be applied if the shear force V_{Ed} at *d* is not *radically different* from the one applied at the support face. For instance, when a major part of the load is applied within *d* from the support face, the web might fail in a combination of splitting and crushing. This is the kind of failure that may occur in stocky pile caps and that are not well treated by design codes.

2.1.3.3   Eurocode 2

Reference is made to EN 1992-1-1:2004 (EN 1992-1-1:2004) in this part.

Members not requiring design shear reinforcement

The design shear capacity of a beam without shear reinforcement is:

$$V_{Rd,c} = \left[C_{Rd,c} k \left(100 \rho f_{ck} \right)^{\frac{1}{3}} \right] b_w d \tag{2.9}$$

In order to avoid the shear capacity of the beam to be null when the amount of flexural reinforcement goes to zero, the capacity of the beam should always be taken higher than:

$$V_{Rd,c} = v_{min} b_w d \tag{2.10}$$

This last expression is often preferred to the Equation 2.9 for the calculation of the shear capacity of a pile cap. Indeed, as pile caps often have low reinforcement ratios, Equation 3.10 gives a higher capacity.

The maximum nominal shear strength is proportional to the cubic root of the concrete compressive strength, f_{ck} and to the cubic root of the amount of flexural reinforcement, ρ. $C_{,Rd,c}$ and v_{min} are found in the respective national annex, the recommended values are $C_{,Rd,c}=0{,}18/\gamma_c$ and:

$$v_{min} = k^{\frac{3}{2}} f_{ck}^{\frac{1}{2}} \qquad\qquad (2.11)$$

The size effect factor, $k = 1+\sqrt{200/d}$, traduces the shear transfer capacity reduction occurring in deep flexural members.

The shear capacity of the section is the product of the nominal shear strength and the cross sectional area, $b_w d$

Members requiring design shear reinforcement

The design of members requiring shear reinforcement is based on a truss model with a variable inclination θ between the struts and the direction of the bea, see Figure 2.14.
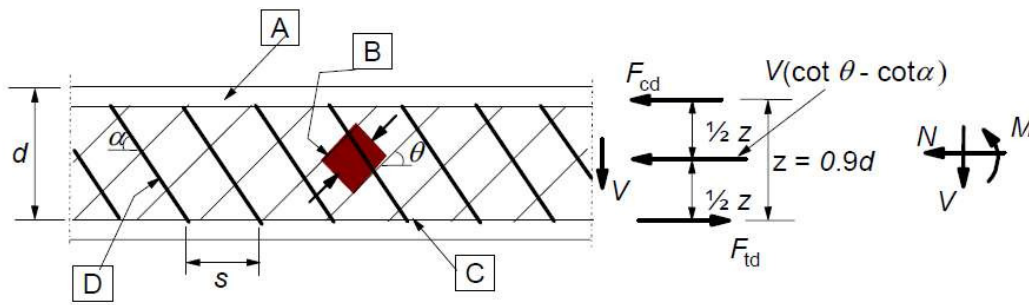
Figure 2.14   Truss model of the shear force transfer in a web (EN 1992-1-1:2004).

The variable inclination method assumes that the inclination θ of the average principal strains direction varies when the load increases and is finally (in the ultimate limit state) controlled by the reinforcement arrangement. Force redistribution results in an inclination smaller than 45 degrees, see Figure 2.15. Cracking and force redistribution processes are explained in section 2.1.2.4.
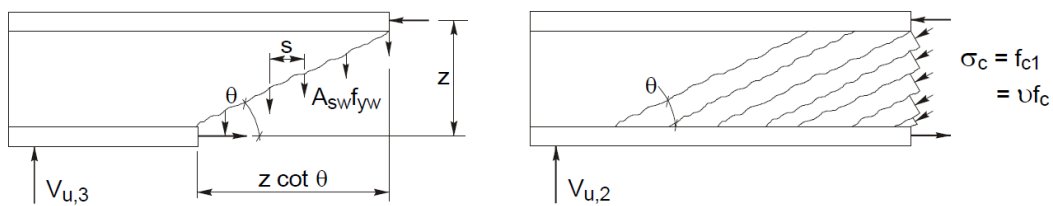
Figure 2.15   Variable inclination method (Walraven 2002)

The angle of inclination of the struts must be restricted due to the limited plastic strain redistribution capacity of concrete and steel. However the allowable value of θ is a national parameter stated in the respective national appendices. These are the recommended limits:

$$0.4 \ \leq \ \cot(\theta) \leq \ 2.5 \qquad\qquad (2.12)$$

This is to say that θ is chosen between 22° and 68°.

The shear resistance of a member with transverse reinforcement, V_{Rd}, is the smaller value of (2.13) and (2.14):

$$V_{Rd,s} = \frac{A_{sw}}{s} z f_{ywd} \cot\theta \qquad (2.13)$$

$$V_{Rd,\max} = \frac{b_w z \upsilon f_{cd}}{\cot\theta + \tan\theta} \qquad (2.14)$$

The factor υ into account the reduction of strength of a compressive strut cracked along its length: $\upsilon = 0,6(1 - f_{ck}/250)$.

Load applied close to a support

The direct arch action can be taken into account for a load applied close to the support both for members with and without shear reinforcement.
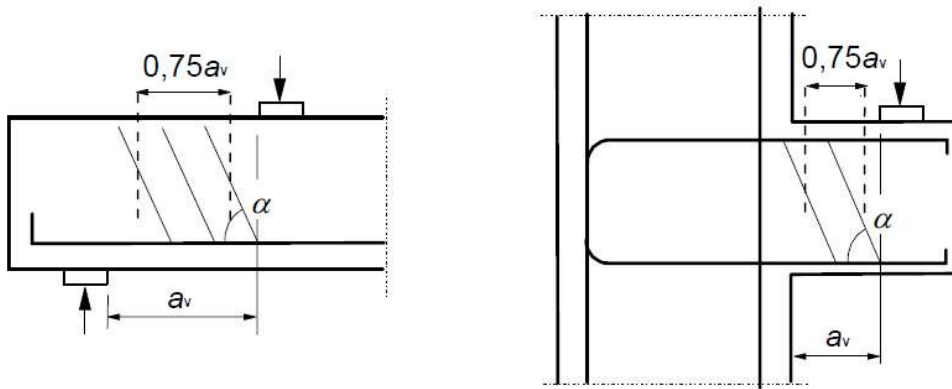
Figure 2.16   Load applied close to the support (EN 1992-1-1:2004)

For $0,5d < a_v < 2d$ as defined in Figure 2.16, the contribution to the shear force of this load, V_{Ed}, that needs to be resisted by the sectional capacity, should be reduced by $\beta = a_v/2d$, When evaluating this factor, a_v should not be taken smaller than *0.5d*. This reduction may be applied to check $V_{Rd,c}$ and V_{Rd} defined before.

However, the applied shear force $V_{Ed,}$ without reduction by the β factor, should always satisfy the following condition, both for members with and without shear reinforcement:

$$V_{Ed} \leq 0,5 b_w d \upsilon f_{cd} \qquad (2.15)$$

In addition, for members with shear reinforcement, the applied shear force V_{Ed}, without reduction from the β factor should satisfy:

$$V_{Ed} \leq A_{sw} f_{ywd} \qquad (2.16)$$

$A_{sw}f_{ywd}$ is the design resistance of the shear reinforcement crossing the inclined shear crack between the loaded areas (see Figure 2.16). Only the reinforcement within the $0,75a_v$ central region should be considered to contribute to the sectional shear capacity.

Eurocode 2 mentions that the strut-and-tie method is an alternative design procedure in such disturbed regions, with loads applied close to the supports. The comparative efficiency of the code design and the strut-and-tie method is a key question and is discussed in this thesis work.

CHALMERS, *Civil and Environmental Engineering*, Master's Thesis 2010:51

2.1.3.4 BBK

This part refers to the Swedish building code for concrete structures, BBK04 (BBK04)

Members not requiring design shear reinforcement

According to BBK04 there are two different ways to evaluate the shear capacity of flexural members not requiring shear reinforcement.

The approach that has been used for a long time in Sweden to calculate the shear capacity of a section, this method shall be called <u>former method</u> hereafter, is expressed as follow:

$$V_{Rd,c} = b_w d \tau_d \tag{2.17}$$

$$\tau_d = 0.30\xi(1+50\rho)f_{ctd} \tag{2.18}$$

With f_{ctd} the design tensile strength of concrete and ρ the ratio of flexural reinforcement $\rho = A_s/b_w d < 0.02$.

ξ is a size effect factor determined as follows:

$$\xi = \begin{cases} 1.4 & \text{for} \quad d < 0.2\text{m} \\ 1.6 - d & \text{for } 0.2\text{m} < d < 0.5\text{m} \\ 1.3 - 0.4d & \text{for } 0.5\text{m} < d < 1\text{m} \\ 0.9 & \text{for} \quad 1\text{m} < d \end{cases} \tag{2.19}$$

The other method to evaluate the shear capacity of the section is inspired by Eurocode, it shall be called <u>Eurocode inspired method</u>:

$$V_{Rd,c} = \max \begin{cases} \left(\dfrac{0.18k}{1.5\gamma_n} \sqrt[3]{100\rho f_{ck}} \right) b_w d \\ v_{min} b_w d \end{cases} \tag{2.20}$$

$$v_{min} = \frac{0.035}{\gamma_n} \sqrt{k^3 f_{ck}} \tag{2.21}$$

Where:

$$k = 1 + \sqrt{\frac{0.2}{d}} \leq 2.0 \tag{2.22}$$

k accounts for the strength reduction due to size effects.

$$\rho = \frac{A_s}{b_w d} \tag{2.23}$$

f_{ck} if the characteristic compressive strength of concrete, γ_n is a safety factor depending on the safety class γ_n equals 1,2 for bridges.

Members requiring design shear reinforcement

<u>Former method</u>

As long as the capacity of the concrete alone is not sufficient, stirrups should be provided. The shear capacity of the section is defined as the sum of the concrete and the steel capacities:

$$V_n = V_c + V_s \qquad (2.24)$$

Where V_c is defined as before and V_s, for shear reinforcement perpendicular to the flexural reinforcement, is defined as follows:

$$V_s = A_{sw} f_{sw} \frac{0.9d}{s} \qquad (2.25)$$

<u>Eurocode inspired method</u> Shear capacity, for stirrups perpendicular to the span of the flexural element, crushing of the concrete and yielding of the stirrups is controlled:

$$V_{Rd} = \min\{V_{Rd,s}, V_{Rd,\max}\} \qquad (2.26)$$

$$V_{Rd,s} = A_s f_{sd} \frac{z}{s} \cot\theta \qquad (2.27)$$

$$V_{Rd,\max} = \frac{b_w z v f_{cd}}{\cot\theta + \tan\theta} \qquad (2.28)$$

$$1 \leq \cot(\theta) \leq 2.5 \qquad (2.29)$$

z is the internal level arm and can be approximated to *0.9d*. The utilized portion of the concrete compressive strength, v, accounts for the reduced capacity of struts do to cracking.

Force applied close to support

When a load is applied close to a support, only a part of this load should be considered to create shear in the section. In the new version of BBK the approach from Eurocode is adopted and only a ratio $a_v/2d$ of the load should be considered, as defined in Figure 2.16. The former version of BBK is less conservative, a smaller part of the load (ratio = $a_v/3d$) was considered to create shear in the section, and for load applied up to a distance 3d from the support.

2.1.3.5 Comparison of codes

Similarities exist between the different codes (EC2, ACI318-08 and BBK04) presented above:

Sectional approaches are followed. Indeed, the actions on the structure are expressed in term of normal and shear stresses applied to vertical sections in the flexural element.

Truss models are used to represent the transfer of forces to the supports. Inclined compression in the web tends to spread part the flanges of the beam that are hold together by tension in the web.

For beams *without shear reinforcement* the codes propose quite similar formulation. These expressions state that the shear capacity of a section is dependent on the tensile strength of concrete mainly, but is also dependant on the amount of flexural reinforcement.

Dissimilarities exist between the different codes:

Two types of approaches are used to evaluate the shear capacity of beams with *shear reinforcement*. The first approach followed by the ACI Building Code and the former BBK, states that the shear capacity of a flexural element is the sum of a concrete and a steel contribution. On the other side, the Eurocode considers a "variable inclination method": a truss model using a variable direction for the compression field is used. In the variation inclination model, steel only provides vertical components to the shear force; there is no "concrete contribution". Afterwards, both the yielding of the stirrups and the crushing of the concrete in the web ought to be checked. It should be pointed out that the newer version of BBK includes this Eurocode approach to shear design.

The ACI Building Code and Eurocode approaches to the loads applied close to supports are quite different. Eurocode reduces the shear force applied to a section with a factor $\beta = a/2d$ for loads applied within a distance up to *2d* from the support but with a minimum of 25% of the load contributing to the shear stress anyway. On the other hand, the ACI Building Code considers that any load at a distance less than *d* from the support can be completely omitted with the restriction that, if a "major" part of the load is applied within a distance d from the column face, it then as to be taken into account. The choice of the section on which the shear should be checked has a big impact on the calculated shear capacity with the codes when load are applied close to supports. This aspect shows that the sectional approaches are not adapted to disturbed regions.

Eurocode does not impose any minimum amount of shear reinforcement for stresses lower than the capacity of the section. On the contrary the ACI Building Code imposes that, as long as the shear stress are half of the ultimate capacity of the section, minimum shear reinforcement have to be provided.

2.2   Punching shear

2.2.1   Introduction

Punching of reinforced concrete structures is a highly localised failure mechanism that arises only under *concentrated loads* and in structures that *convey shear forces in two directions*, like slabs.
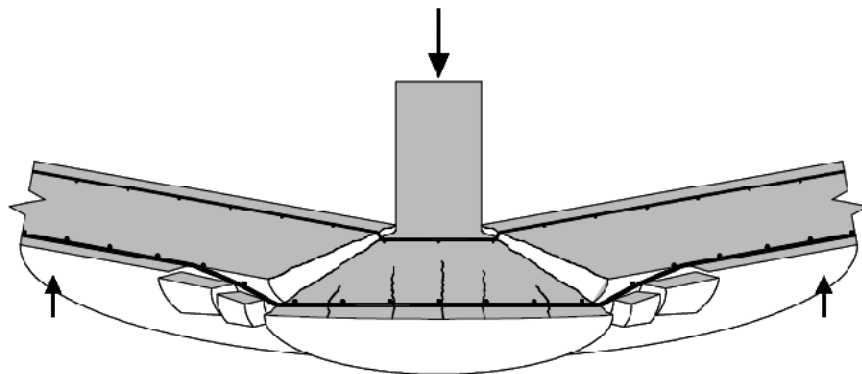
Figure 2.17   Punching shear failure of a reinforced concrete slab (Guandalini 2006)

At failure, a cone is separated from the rest of the slab along the punching shear cracks and penetrates through the slab, with an angle from the horizontal usually between 25 and 40 degrees (Guandalini 2006).

Punching failure occurs only in elements carrying bending moments and shear forces in two directions. For this reason, punching shear is often called two-way shear.

As a complex and brittle failure mechanism, punching failure needs special care in design.

2.2.2 Two-ways shear forces transfer in reinforced concrete structures – Punching shear cracks, punching shear failures

2.2.2.1 Definitions

Considering a polar coordinates system centred at the load application point, the following definitions are made, according to Figure 2.18:
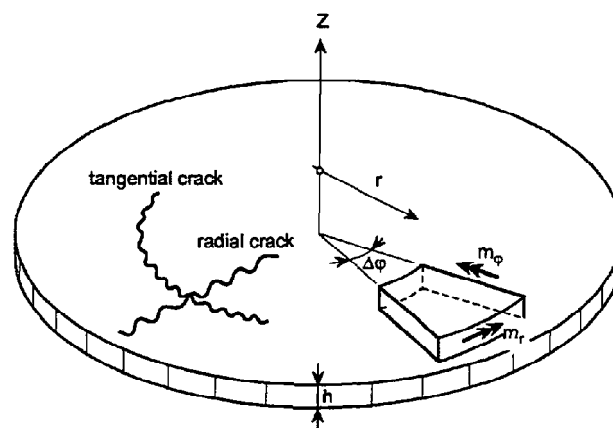
Figure 2.18   Circular slab with radial and tangential cracks and moments (Menétrey 1994)

Tangential cracks occur at a distance from the load application point and propagate more or less in the tangential direction. These cracks are induced by excessive radial moment, m_r. Tangential cracks are equivalent to flexural cracks in beams or one-way slabs.

Radial cracks start in the vicinity of the column face and propagate toward the edge of the slab. They are induced by the tangential moment, m_φ. Radial cracks and tangential moments are not found in one way structures.

Both radial and tangential cracks start on the tensile side of the slab.

2.2.2.2 Cracking processes

The response of a slab is strongly related to the cracking pattern. Cracking growth during loading is separated in seven different phases here:
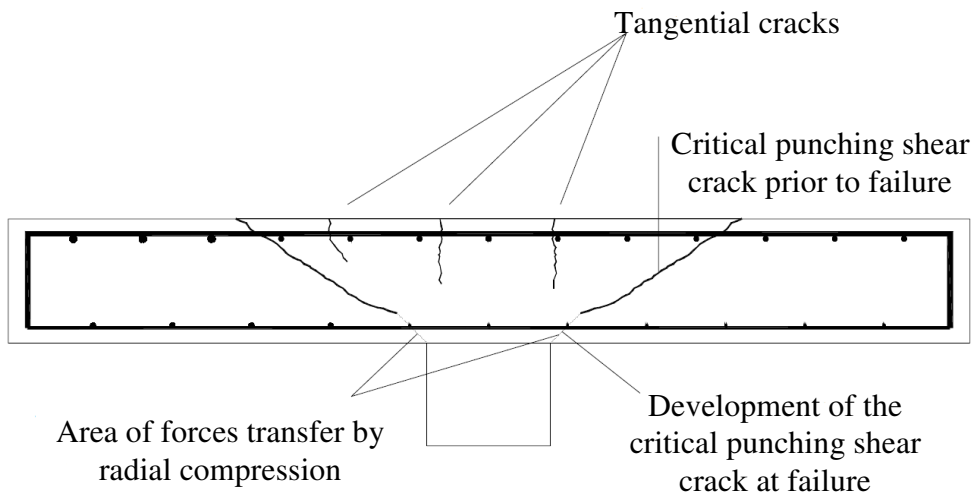
Figure 2.19   Cracking pattern of the slab at inner column before a punching failure occurs (Guandalini 2006)

$$F = F_{cr} \qquad F_{cr} < F < 0,9\ F_u \qquad F = F_u$$
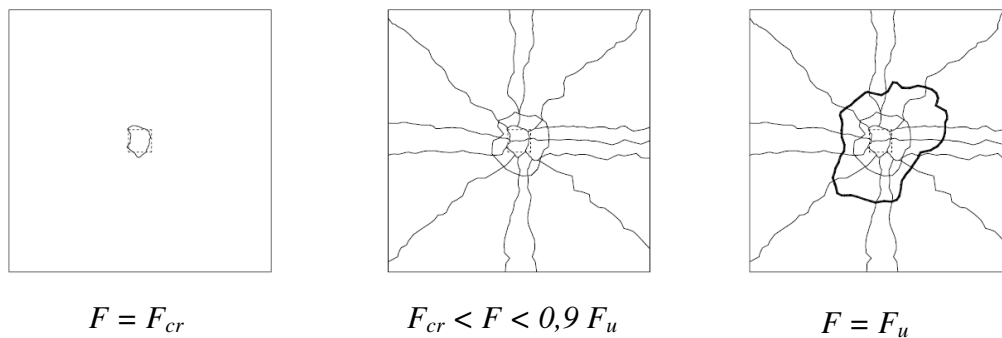
Figure 2.20   Cracking pattern of the slab at inner column, for different load levels, viewed from the tensile face (Guandalini 2006)

1. $F<F_{cr}$. Elastic uncracked deformation phase, detailed in 2.2.2.4

2. $F=F_{cr}$. First crack appears at the projection of the column perimeter on the tensile face of the slab (Figure 2.20, left). This crack is a tangential crack, induced by the high radial flexural moment (Figure 2.25). After the first cracking, the redistribution of forces between the radial and tangential direction starts.

3. $F_{cr} < F < F_u$. After a slight increase of the load, cracks start to form in the radial direction (Figure 2.20, centre). These cracks are induced by tangential moments (Figure 2.25).and spread in different directions, starting close from the column face.

4. $F_{cr} < F < F_u$. The number of radial cracks increases (Figure 2.20, centre).

5. $F_{cr} < F < F_u$. One or a few new tangential crack appears with diameter in the order of magnitude of two times the column diameter. These cracks have more or less "circular" shapes and are centred on the column (Figure 2.20, centre).

6. $F_{cr} < F < F_u$. After a certain load is reached, no new crack forms. However, with increasing load, the already existing radial and tangential cracks widen (Figure 2.20, centre).

7. $F = F_u$. Suddenly, a cone of reinforced concrete punches through the slab. This cone is delimited on the tensile face of the slab by a "circular" tangential crack, the dark line in Figure 2.20, right and Figure 2.21. This failure crack appears at the same time as failure occurs. Inside the depth of the slab the punching cone is delimited by inclined shear cracks (Figure 2.19), starting at the tip of the critical tangential crack.
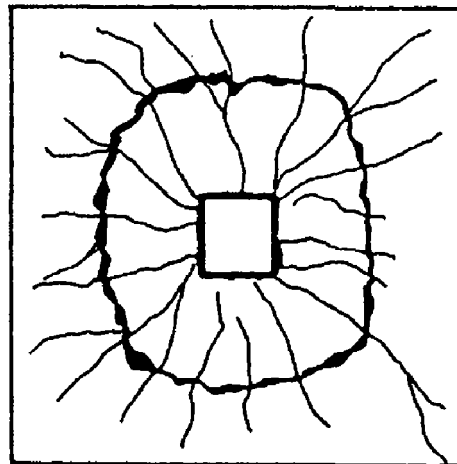
Figure 2.21   Critical tangential crack of the punching cone, viewed from the tensile face (Krüger 1999)

2.2.2.3 Failure mechanisms

Punching shear failure is characterised by the penetration of a cone of concrete through the slab. This punching cone can be seen in Figure 2.22 and in Figure 2.23 in a slab tested by Hallgren, Kinnunen and Nylander (1998).
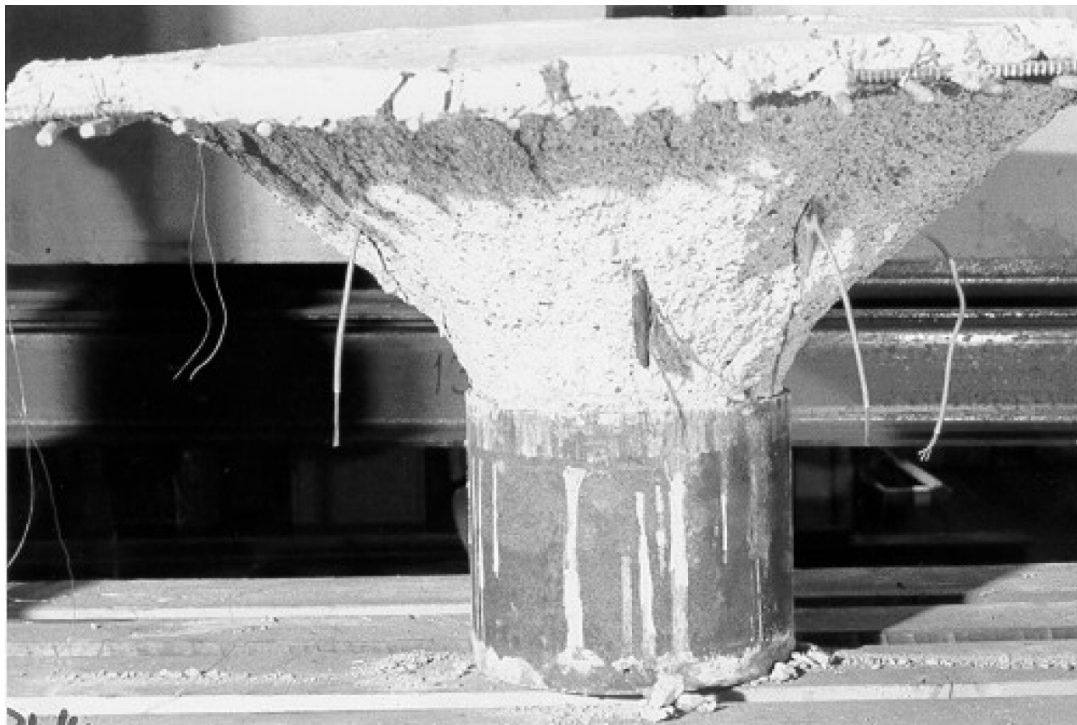
Figure 2.22   Punching cone in a slab, side view (Hallgren et al. 1998)
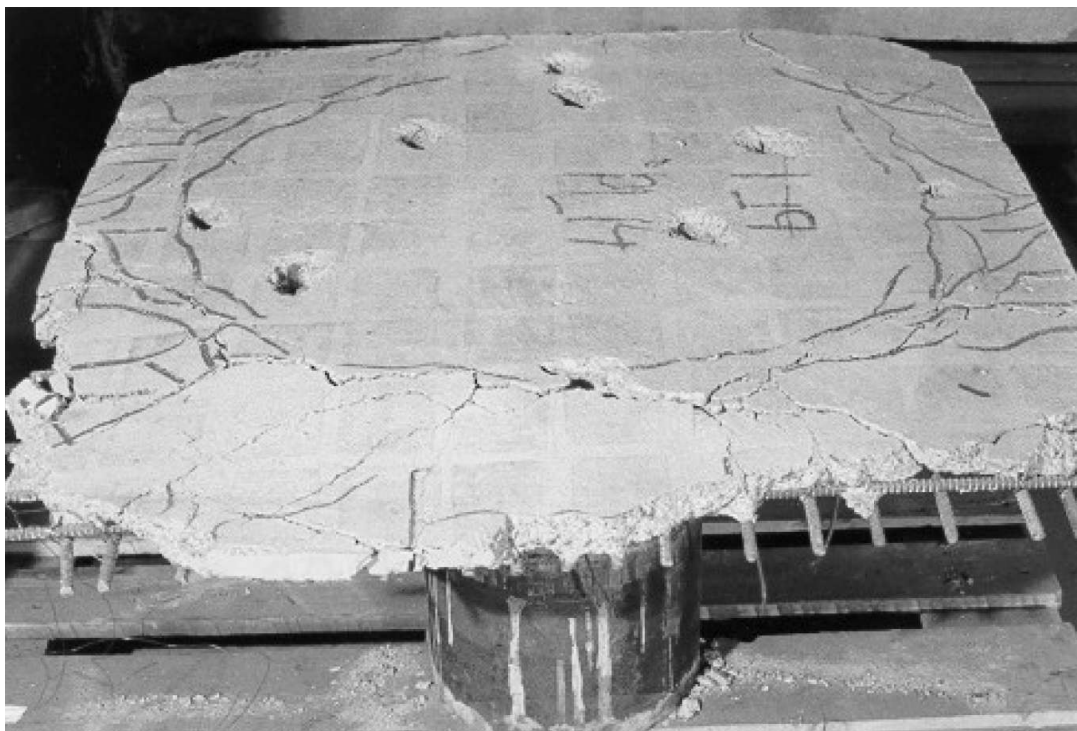
Figure 2.23   Punching cone in a slab, seen from above (Hallgren et al. 1998)

Three different types of punching failures can be distinguished in slabs with shear reinforcement:

     - Development of a punching cone inside the shear reinforced area. This failure mode occurs after yielding of the shear reinforcement.

- Development of a steep punching cone at the column face. This case occurs if the shear reinforcement against punching provided close to the column face was too weak or badly anchored.

- Development of a punching cone outside the shear reinforced area around the column. This failure mode happens when shear reinforcement was not provided at distances further away from the column.

2.2.2.4 Linear elastic analysis for circular slab

The linear elastic theory for circular slabs was developed by Poisson in 1829. The linear analysis performed here is valid as long as the stiffness is kept constant over the slab. This is very close to reality as long as the concrete remains uncracked. Thus a linear elastic analysis is a suitable theory in order to analyse the two first steps described in section 2.2.2.2 *Cracking processes,* namely elastic deformation and first tangential crack. After cracking the real moments and shear forces profiles will deviate from the elastic solution. However, the linear elastic solution can still be used in order to understand the overall behaviour of the slab and give qualitative explanations.
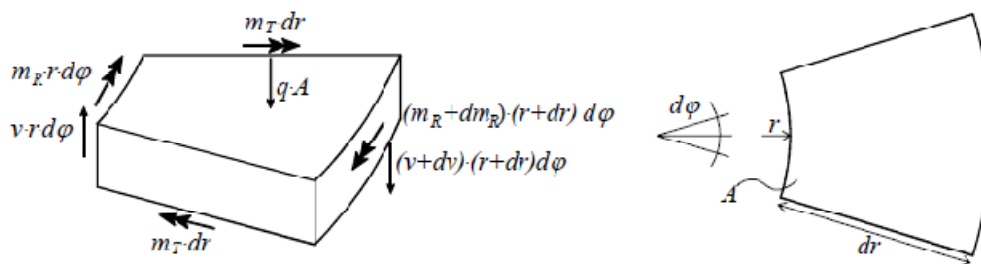
Figure 2.24   Actions on an elementary portion of the slab (Guandalini 2006)

The previous figure shows the equilibrium of a small elastic part of a circular slab. It can be noticed that tangential shear stresses are null. Indeed, at a given distance from the load application point, the tangential moment is constant independently of variations of φ due to the circular shape of the slab. This condition is not verified for slabs with non symmetric geometry and boundary conditions, as well as for slabs with eccentric loading. However, far from the load application point, the tangential shear can be considered as negligible.

Radial moment, tangential moment and shear stresses profile, are found in Figure 2.25.
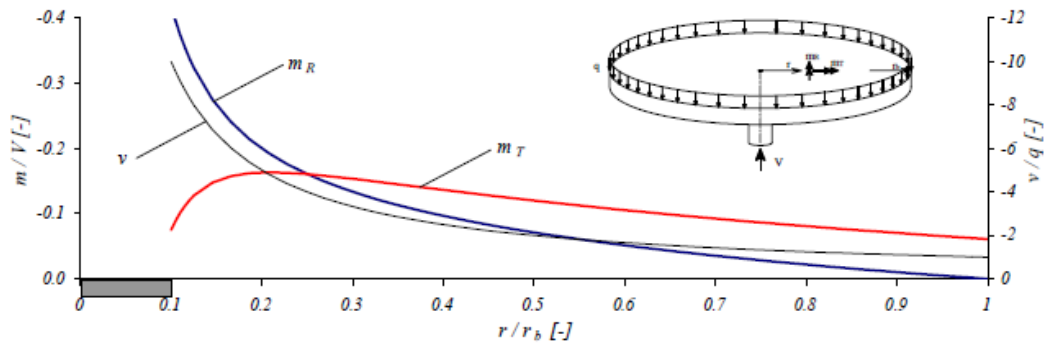
Figure 2.25 Linear elastic moment and shear profiles as a function of the distance from the centre in a circular slab (Guandalini 2006)

Some interesting observations can be made:

The shear stress, v, decreases with increasing distance from the load application point due to the fact that the cylindrical concrete cross section area that resists shear stresses increases with distance. The maximum shear stress is found at the column face.

The maximum moment is radial and is found at the column face. Therefore, the maximum tensile strain is found at the column face on the tensile membrane of the slab. This justifies the fact that the first crack is tangential and occurs at the column face.

The radial moment, m_r, goes down to a null value at the edge of the slab, while the tangential moment, m_t, keeps a value higher than 60% of its maximum all over the slab. This is in concordance with the observation that tangential cracks occur in the vicinity of the column while radial cracks propagate all over the slab.

At a distance approximately equal to one fourth of the slab radius, the tangential moment reaches its maximum and becomes higher than the radial moment. The combination of the two moments around that point gives rise to biaxial tension in the tensile membrane of the slab. The concrete is weakened by this state of stresses and is more prone to fail at lower load levels.

Some conclusions can be drawn from these remarks and from comparison between one way and two way shear element:

Unlike in beams, the shear stresses in slabs decrease with increasing distance to the concentrated load application point. When a beam is subjected to a point load, the shear stresses are constant over the length of the beam. In the case of a slab, the cylindrical cross section area that resists the shear forces increases with the distance from the load application. This means that the shear stresses are maximal at the column face and decreases with distance.

In beams, only radial flexural moments are present and the maximum moment is found at mid span. On the other hand, a combination of tangential moments and radial moments is found in slabs. The magnitude of these moments in the two directions is dependent on the distance from the load application. It is important to note that tangential moments are not maximal at the column face, but a little bit further away. In a slab, the presence of tangential moments induces radial cracking. This type of cracking does not exist for beams. Radial cracks, in combination with flexural tangential cracks separate the slab into segments. An idealised shape and force equilibrium of those segments was given by Kinnunen and Nylander, see Figure 3.8.

In this model, described in 2.2.2.5.a), the equilibrium of the compressed conical shell close to the load application point rules the punching capacity of the slab.
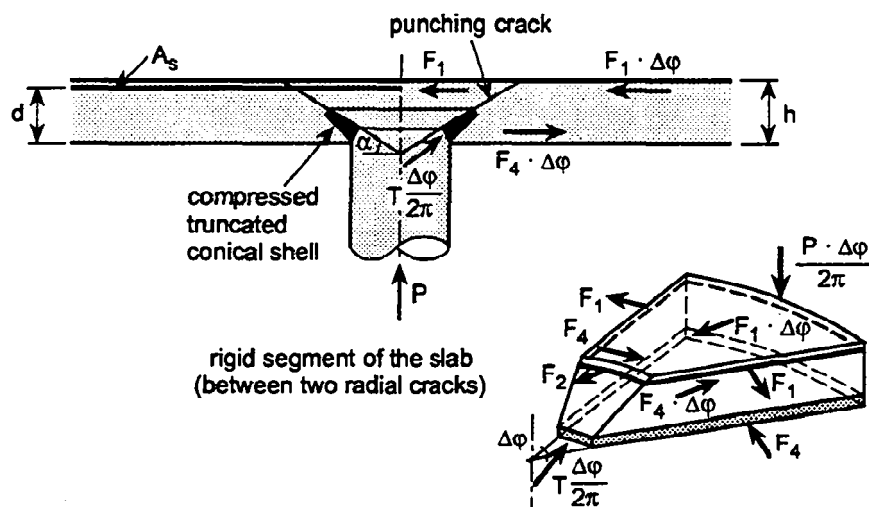
Figure 2.26   Punching shear mechanical model by Kinnunen and Nylander with the equilibrium of a rigid segment (Kinnunen et al. 1960)

In addition, with increasing load and modifications in the cracking pattern, redistribution of forces occurs between tangential and radial moments in the slab. On the contrary, in the case of isostatic beams, shear and moment profiles are independent of the load level.

These three statements point out that the force repartition is more complex in slabs than in beams. Hence it is more difficult to assess the cracking pattern, localise the critical sections or find the failure mechanisms. Nevertheless the maximum shear stresses and the worst moment combinations occur close to the column face, clearly showing that slabs subjected to point loads are subjected to highly localised failure modes. Therefore, models have been developed in order to account for these specificities.

2.2.2.5   Survey and classification of the different punching shear models

Different models, based on different assumptions and mechanical theories, have been developed during the last fifty years in order to describe punching failure in slabs. A survey and classification of these different approaches is proposed here.

Classifying different mechanical model approaches to punching shear is controversial. Indeed, some models combine different theories. The reference in this part is mainly made to Reineck (fib 2001) whose classification has been followed.

The model by Kinnunen and Nylander was early developed, in 1960. This model proposed a comprehensible force equilibrium of the punching cone and gave the basics to most research works carried out afterwards. Therefore, the Kinnunen and Nylander approach is extensively described in this part.

a)   The model proposed by Kinnunen and Nylander

The Kinnunen and Nylander (1960) approach is often considered as the first sound model proposed to represent punching shear.

The model developed by the Swedish researchers is based on a series of tests on slabs they carried out. During those tests, Kinnunen and Nylander noticed that the crack pattern of slabs over interior columns was always quite similar and that punching failure always happened after that cracking pattern had developed. The vertical tangential crack that propagates into an inclined shear crack at the column face combined to the vertical radial cracks at the side cut sectors from the slab, as shown in Figure 2.27 b.
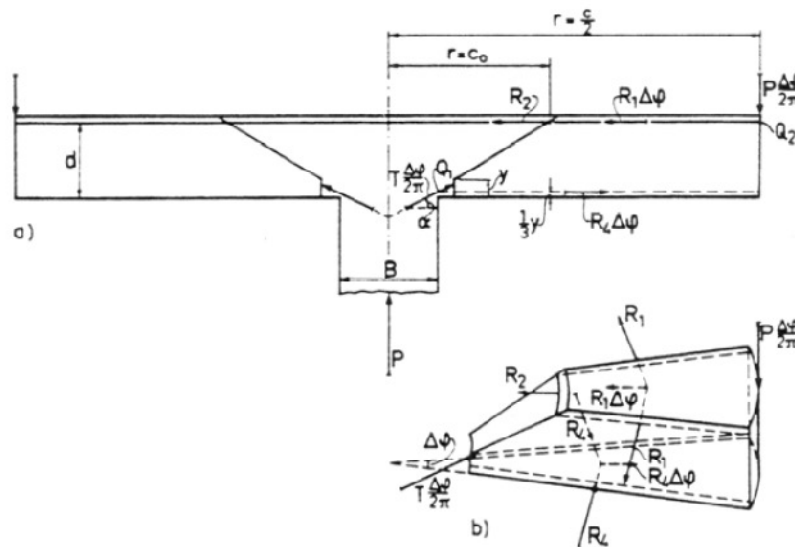
Figure 2.27 a) and b) Geometry and equilibrium of the model (Kinnunen et al. 1960).

In addition, they noticed that the curvature of the slab in the radial direction at some distance from the load was almost constant. Therefore, the sectors defined before could be considered as rigid. The displacement of the rigid sectors is then simplified to a rotation of an angle ψ around a centre of rotation located at the root of the shear crack. The centre of rotation is indicated as C.R. in Figure 2.27 d).
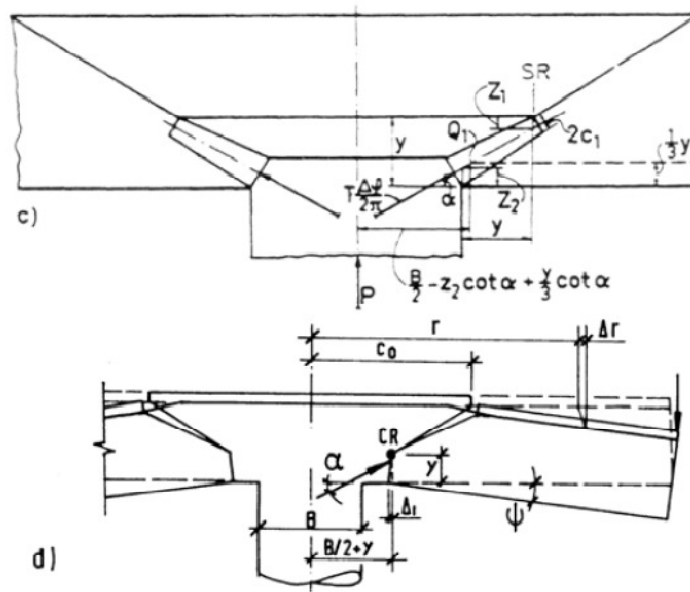
Figure 2.28 c) and d) Geometry and equilibrium of the model (Kinnunen et al. 1960).

Kinnunen and Nylander also considered the concrete expansion under loading in their analysis.

Based on these hypotheses and under some simplifying assumption based on their experiments, Kinnunen and Nylander established the equilibrium of the conical shape shown in Figure 2.27 c).

The solving process is a trial-and-error method: a compressive web height has to be found, that fulfils both the moment and force equilibrium equations formulated.

The failure criterion chosen is the ultimate compressive strain at the bottom of the slab, in the conical shape submitted to a triaxial state of stresses (ε_c = -1.96‰).

b)   Flexural capacity approach

Practice showed that, for many common slabs, the punching failure load was quite close to the flexural failure load. Based on that statement, different models have been developed. Although it is not the first one, the model developed by Moe (1961) is significant as it laid the basics for ACI design code in 1963.

Moe's empirical approach is based on the assumption that the ultimate capacity of a slab is linked to its flexural and one way shear capacities:

$$\frac{V_u}{V_{shear}} + A\frac{V_u}{V_{flex}} = 1 \tag{2.30}$$

Where *A* is derived and calibrated by tests results.

These kinds of empirical flexural capacity approaches have disappeared from most codes although it can still be found in section 6.9 of BBK04.

c)   Plasticity approach

The perfect plasticity theory, associated with limit theorems, is rather new and promising. Unlike elastic and elasto-plastic stress and strain equilibrium methods that require trial-and-error procedure, a direct evaluation of the bearing capacity of a structure is possible with the perfect plasticity theory. The theorems of limit analyses

(i.e. lower bound and upper bound) proposed by Drucker and Prager (1952) gave a simple and intuitive way to assess the ultimate strength of slabs.

It is important to note that, when using an upper bond method relying on the yield line theory, it is very convenient to know from the beginning either the yielding surface or the plastic flow displacement direction. In the case of punching, due to the symmetry of the problem, the displacement is orthogonal to the slab. The rate of internal work at failure is then dependant on the angle of the punching cone. In the case of direct strut action from the load to the support, the yield surface is known and the energy to develop a mechanism is dependent on the direction of the displacement at failure. Upper bound solutions were proposed by Braestrup (1976) and Marti and Thürlimann (1977). Lower bound solutions were suggested by Braestrup in 1985 (CEB 1985) and Pralong (1982). The latest involves the tension strength of concrete as well.

d) Failure mechanism approaches with concrete tensile stresses in failure surface

Failure mechanism approaches, for example the Kinunnen and Nylander model, assume the location of the critical cracks that will lead to the failure mechanism. The accuracy of a failure mechanism model relies on a good choice of critical cracks locations. For example, Kinnunen and Nylander defined the shape of the critical cracks by a comparison with experimental tests. Since, other methods have been developed, like non-linear finite element analyses.

The recent development of fracture mechanism also encouraged researchers to include additional shear transfer forces mechanism in their models (refer to Chapter *Mechanisms of shear transfer*). Accounting for the tensile strength of concrete was proved very promising and studied, among others, by Menétrey (1994).

e) Truss models or strut and tie model

Strut-and tie models used in design practice and in codes are smeared models. They do not define the exact location of cracks. These smeared strut-and-tie models account for cracking and the associated reduction of the different possible shear transfer mechanisms, by limiting some parameters:

Muttoni et al. (2008), among other authors, considered more local strut-and-ties models to explain the transfer of shear forces at a macro level. Truss models were developed to explain shear transfer mechanisms in cracked flexural elements. Local truss models shows how shear force are transferred above the cracks, in elements without shear reinforcement (direct arch action, shear transfer in the compression membrane), between cracks (cantilever effect, dowel effect) and at the crack interface (residual tensile stresses, interface shear transfer). These local truss models are described extensively in the chapter *Mechanisms of shear transfer*. These local models are relevant for understanding but still have not been rationalized and simplified enough to provide the basics of a design method.

Some authors proposed interesting smeared strut-and-tie model with concrete ties. The one way shear model by Reineck (2010) and the punching model by Pralong (1982) belong to the few propositions that were made on smeared truss models with concrete ties.

In this study, the issue of concrete tensile strength and its integration into a design procedure based on a strut-and-tie model has to be dealt with. Indeed, as explained in details previously, neglecting the tensile strength of concrete in pile caps is too

conservative when assessing the shear and local punching shear capacity to provide economically satisfying steel reinforcement quantities.

However, it was chosen not to specify concrete ties in the strut-and-tie model. Concrete tensile positive contribution is considered through the effect of confinement on the capacity of the strut to carry load by arch action. Details of the procedure are found in chapter 5: *Description of aspects specific to pile caps and implementation in the strut-and-tie model developed.*

f)   Fracture mechanics

Some recent models, like the one by Hallgren (2002), rely only on the fracture mechanics. They are usually coupled with heavy numerical analyses with a failure criterion derived from fracture mechanics.

2.2.3   Punching shear design according to building codes

2.2.3.1 Introduction

Similarly to the shear section, three different design codes are presented: The Swedish building code for concrete structures (BBK04) from Sweden, the Eurocode 2 (EC2) from Europe and the American Concrete Institute building code (ACI 318-08).

In order to be clearer for the reader, the variable names were harmonised on the basis of Eurocode 2 notations.

For each code, a presentation of the fundamental equations for punching shear design is made. A comparison is then made between the different approaches. In Chapter 7.2, the predictions of EC2 and BBK04 are compared with experimental failure loads of 4-pile caps without shear reinforcement. Some additional comments on the efficiency of the design codes are also made in that part.

2.2.3.2 ACI 318-08

Reference is made to ACI 318-08 in this part.

For slabs subjected to bending moments in two directions ACI building codes, like other building codes, requires a check of the punching capacity in addition to the check of the one-way shear capacity. The strength is evaluated along a pseudo-critical section and with a nominal shear capacity. The pseudo-critical section is defined by a control perimeter in the first dimension and by the effective shear depth d in the other dimension. The shear stresses on that surface depend on the size of the loading plate and on the ratio between the dimensions of the loading plate and the effective depth of the slab.

In order to simplify the calculation of the shear force applied, ACI code considers a pseudo-critical section located at $d/2$ from the periphery of the concentrated load. Hence a critical perimeter is defined as shown in Figure 2.29. The definition for the shape of the control perimeter depends on the geometry of the column and of the slab; details can be found in the code. Afterwards the shear strength is considered as almost independent of the ratio of column size to slab depth.
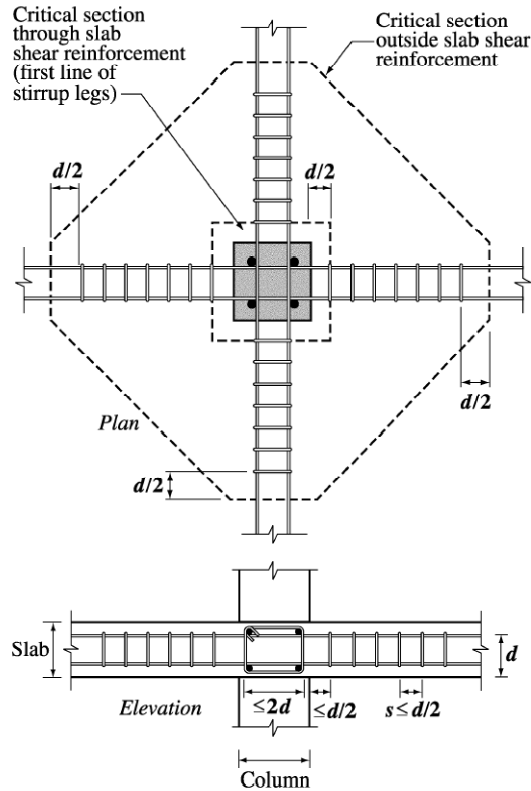
Figure 2.29   Control perimeters and arrangement of shear reinforcement for interior columns, ACI 318-08

Fundamental equations (2.1), (2.2) and (2.3) are still valid in this section. ACI building code consider that, in slab without shear reinforcement, the punching capacity is provided by the concrete (V_c) and that, in slabs with shear reinforcement, the punching capacity is calculated as the sum of a concrete and a steel componenet, as can be seen in (eq 2.31).

Inside the reinforced area, the ACI code adds the shear capacity of steel and concrete in the same way as for one-way shear:

$$V_n = V_c + V_s \tag{2.31}$$

The contribution of concrete to the shear resistance inside the control perimeter is the smallest value of equation (3.32), (3.33) and (3.34):

$$V_c \quad = \quad \left(2 + \frac{4}{\beta_c}\right)\lambda\sqrt{f'_c}\,ud \; \text{MPa} \tag{2.32}$$

$$V_c \quad = \quad \left(\frac{\alpha_s d}{b_0} + 2\right)\lambda\sqrt{f'_c}\,ud \; \text{MPa} \tag{2.33}$$

$$V_c \quad = \quad 4\lambda\sqrt{f'_c}\,ud \; \text{MPa} \tag{2.34}$$

With d is the effective depth and u the perimeter of the critical section, as defined in Figure 2.29.

α_s is chosen as 40 for interior, 30 for edge and 20 for corner columns. β_c is the ratio of the long to short side of the concentrated load or reaction area. λ is a factor accounting for concrete density.

If $V_u > \varphi \, V_c$ shear reinforcement must be used. Then, two critical sections have to be checked. A section situated within the reinforced area, with a control perimeter situated *d/2* from the column face and a section situated *d/2* from the outer shear reinforcement as shown in Figure 2.29.

With a limitation on the concrete contribution to the shear capacity:

$$V_c \quad \leq \quad 2\lambda\sqrt{f_{ck}}\,ud \tag{2.35}$$

And a limitation to the nominal shear capacity:

$$V_n \quad \leq \quad 6\sqrt{f_{ck}}\,ud \tag{2.36}$$

Inside the shear reinforced area, the contribution of stirrups to the shear capacity is:

$$V_s = \frac{A_{sw}f_{yt}d}{s} \tag{2.37}$$

A_{sw} is the cross sectional area of steel in one row around the column, *s* is the spacing of stirrups and f_y is the yield strength of steel that should not exceed 414MPa.

The set of formulas for shear studs in not presented here although extra shear capacity can be provided using shear studs.

Outside the shear reinforced zone, the shear stress resistance of the concrete is limited to the one way shear strength:

$$V_c \quad = \quad 0.17\lambda\sqrt{f_{ck}}\,u_{exterior}d \ \text{MPa} \tag{2.38}$$

Where $u_{exterior}$ is the perimeter of the critical section outside the shear reinforcement and is defined in Figure 2.29.

Force applied close to the support:

The loads applied inside the control perimeter are considered to be transferred directly by compression in the web above the crack. Refer to the shear design section 0.

2.2.3.3 Eurocode 2

In case of slabs that do not require shear reinforcement, different checks are required: One check for crushing at the column face and several checks at different control perimeters situated between the column face up to a distance *2d* (θ=26.6) from the column face. The most restrictive check is the design one.
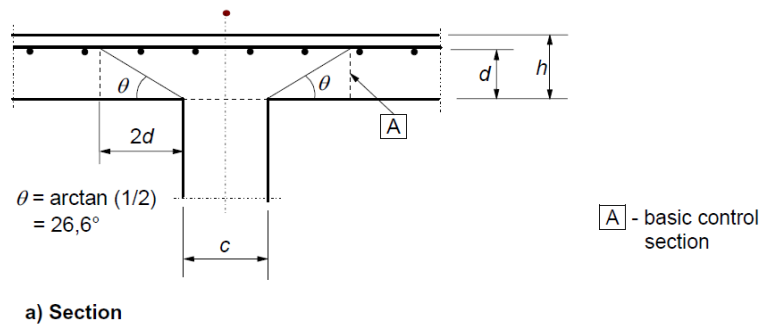
a) Section

Figure 2.30   Definition of the basic control perimeter – section view, from EC2

b) Plan
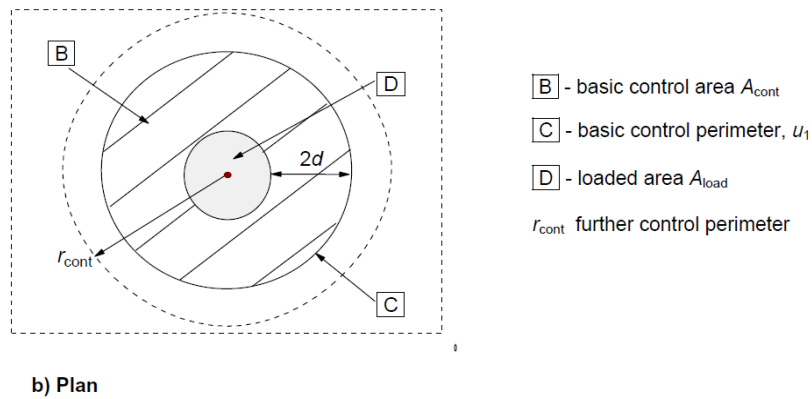
Figure 2.31   Definition of the basic control perimeter – plan view, from EC2

In this part, it is more convenient to work with shear stresses in order to account for the different control perimeters.

The allowable design shear stress at the column due to crushing of the concrete is:

$$v_{Rd,\max} = 0.5 \upsilon f_{cd}$$

$$V_{Rd,\max} = \frac{v_{Rd,\max} u_i d}{\beta_c} \tag{2.39}$$

With β_{ecc} a factor accounting for the eccentricity of the load compared to the control perimeter (Expression (6.36) to (6.48) in EC2), u_i the perimeter of the loaded area, d the effective depth.

In order to avoid risk of crushing of the concrete the previous restriction should always be verified. If not, the column to slab connection needs to be redesigned.

Thereafter, the stresses need to be checked along different control perimeters ranging from a distance *2d* down to the column face. With *u* the length of the control perimeter and *a* the distance the column face to the control perimeter considered The concrete punching shear capacity is defined as follows:

$$V_{Rd,c} = \frac{2d}{a}\left[\max\left\{ \begin{array}{c} C_{Rd,c} k \left(100 \rho f_{ck}\right)^{\frac{1}{3}} \\ v_{\min} \end{array} \right\} \right] ud \tag{2.40}$$

It should be checked that $V_{,Rd,c} < V_{,Ed,red}$ as defined below. Otherwise some shear reinforcement is required inside the control perimeter.

When shear reinforcement is provided, Eurocode considers that the punching shear capacity of the slab is the sum of a contribution from concrete and from steel:

$$V_{Rd,cs} = 0.75 V_{Rd,c} + 1.5 (d/s_r) A_{sw} f_{ywd,ef} (1/(ud)) \sin\alpha \qquad (2.41)$$

The punching shear capacity $V_{,Rd,c}$ or $V_{Rd,cs}$, should be compared to the reduced applied shear load $V_{Ed,red}$. $V_{Ed,red}$ is the applied shear force reduced by the vertical component of any load apply inside the control perimeter considered as defined in equation (2.45).

$$A_{sw} = \frac{\left(V_{Ed} - 0.75 V_{Rd,c}\right) s_r u}{1.5 f_{ywd,ef}} \qquad (2.42)$$

Where s_r is the radial spacing of shear reinforcement and:

$$f_{ywd,ef} = 250 + 0.25d \leq f_{ywd} \qquad (2.43)$$

The perimeter $u_{out,eff}$ where no shear reinforcement is required is:

$$u_{out,ef} = \frac{\beta V_{Ed}}{V_{Rd,c} d} \qquad (2.44)$$

The layout of the punching shear reinforcement should be done according to EC2 9.4.3.

Force applied close to the support:

$$V_{Ed,red} = V_{Ed} - \Delta V_{Ed} \qquad (2.45)$$

Where V_{Ed} is the column load and ΔV_{Ed} is the net upward force inside the control perimeter considered.

2.2.3.4 BBK

An alternative is possible for the design according to punching shear. The less demanding on calculations relates to chapter 6.9 in BBK04. If the following condition is verified:

$$\sqrt{\left(\frac{M_x}{V_x d}\right)^2 + \left(\frac{M_y}{V_y d}\right)^2} \leq 1.0 \qquad (2.46)$$

Then punching does need to be checked. Flexural and beam shear reinforcement can then be designed according to a sectional approach or a strut-and-tie method.

The second option is to follow recommendations from chapter 3.12 in BBK04. The punching shear capacity is checked along a control perimeter, *d/2* from the column face. The definition for the shape of the control perimeter depends on the geometry of the column and of the slab; details can be found below.

For inner and edge columns:

u is the length of the control perimeter defined in Figure 2.32and Figure 2.33.
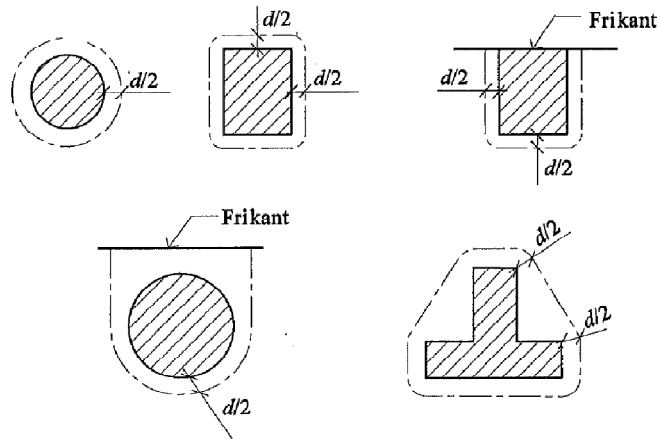
Figure 2.32   Control perimeter for inner and edge columns

$$V_u = \eta u d f_{v1} \tag{2.47}$$

$$f_{v1} = 0.45 \xi (1 + 50\rho) f_{ctd} \tag{2.48}$$

For corner columns:
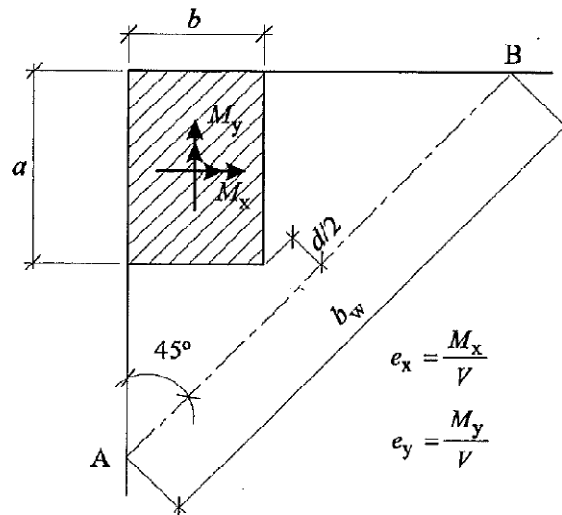
Figure 2.33   Control perimeter for corner columns

$$V_u = \eta b_w d f_{v2} \tag{2.49}$$

$$f_{v2} = 0.30 \xi (1 + 50\rho) f_{ctd} \tag{2.50}$$

ξ is defined in section 2.2.2.4, ρ is the amount of flexural reinforcement, limited to 1% in calculations and f_{ctd} is the tensile capacity of concrete. η is an eccentricity factor. d is the effective depth of the section.

The design procedure according to "betong handbook" is different and usually predicts a higher capacity regarding punching. However, for slabs with low reinforcement ratio like pile caps the difference is rather small.

If the capacity calculated V_u is below the shear force applied stirrups needs to be provided. One of the characteristics of design to punching using BBK is that, if shear reinforcement is used, the required amount of stirrups should be able to carry the entire vertical component of the load. This provision is restrictive compared to other design codes and is discussed in the next section.

2.2.3.5 Comparison

The design approaches to punching found in Eurocode (EC2), BBK04 and ACI 318-08 show some similarities and dissimilarities.

Unless some other approaches are possible, all the models propose a sectional approach based on the check of shear stresses on a pseudo-critical control perimeter at a given distance away from the concentrated load. ACI and BBK consider a control perimeter situated at a constant distance *d/2* from the column face while Eurocode approach consists in checking all the control perimeters situated between the column face up to a distance *2d* from the column face, taking the weakest perimeter as the designing one. Although Eurocode definition of control perimeters is more complicated and usually requires some calculation tools, it permits to get rid of strange variations in strength prediction occurring with a constant control perimeter when the geometry of the slab is slightly modified.

The three codes of practice consider that all the uplift loads applied inside the control perimeter can be subtracted to the shear force taken into account.

When shear reinforcement is required, Eurocode and ACI propose formulas that provide a reduced amount of shear reinforcement. Indeed, the overall punching capacity is calculated as the sum of a concrete and a steel contribution. On the other hand, BBK does not accept a reduction of the shear reinforcement. Therefore, as long as some transverse reinforcement is needed, it has to be able to carry the entire vertical component of the load.

The relative efficiency between EC2 and BBK for pile caps without shear reinforcement is illustrated by study cases and discussed in section 7.2.

A comparison between designs where stirrups are required is made in section 7.

3 The strut-and-tie method

3.1 Introductory remarks

The strut-and-tie method is a design method which uses a hypothetical equivalent truss to represent the stress field in structural concrete members in the ultimate limit state (ULS). The principle of the method is to simulate the flow of forces in cracked reinforced concrete, after plastic redistribution has occurred, by using struts, ties and connecting nodes. The struts are made of concrete and carry the compressive stresses while the ties are normally composed of reinforcement bars and carry the tensile stresses.

The strut-and-tie method is based on the lower bound theorem of the theory of plasticity. A stress field is assumed, which is in equilibrium with the external load and respects the yielding criterion at any point of the structure. Then according to the lower bound theorem, and assuming that the structure has enough ductility to satisfy any needed redistribution of forces, the failure load obtained by this method underestimates the theoretical failure load of the structure. In other words: "the structure will always find the same or a more efficient way to carry the load". Therefore the strut-and-tie method is well adapted to design discontinuity regions (D-regions, described in Section 1.5), and regions subjected to shear forces. It can be regarded as a "unified approach" as it takes every load effect (N, V, M and T) into consideration simultaneously, on the contrary of a sectional approach. Another major benefit of this method, compared to the empirical and semi-empirical formulas often used in codes, is that it provides a mechanical model as a basis for the design of a structure, which gives the designer a better understanding of the mechanical behaviour of D-regions.

In the representation of a strut-and-tie model, most often ties are indicated by continuous lines and struts by dashed lines. This convention is used hereafter to represent struts and ties in the models (not to confuse with 3-D drawings, where dashed lines indicate hidden edges).

3.2 Historical use of truss models

Since the beginning of the 20th century, designers started to use regular truss models in order to design structural concrete members by following the flow of forces. These models have been used to handle regions with high shear force or torsional moment, where the simple theories of flexure do not apply. An illustration of that is the use of truss models for shear design by Ritter in 1899 (Figure 3.1).
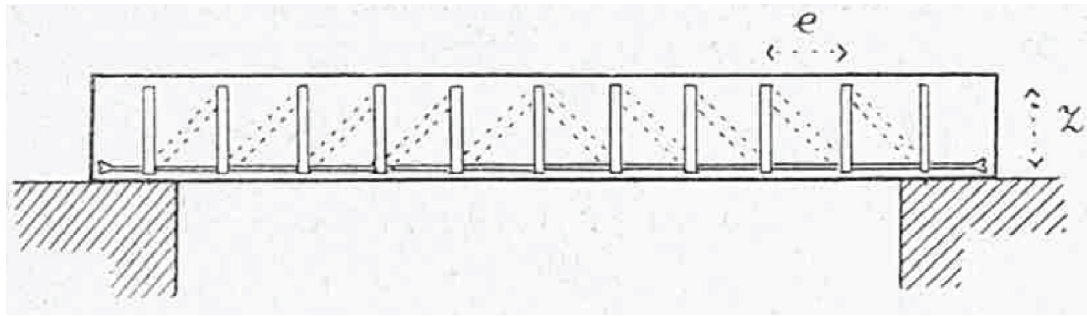
Figure 3.1   Truss model used by Ritter (1899)

However, it is only in the 80's, that the use of regular truss models has been systematised by the works of Marti (1985) and of Schlaich et al. (1987), who extended the method of regular truss models used previously mostly for beams, to general strut-and-tie models applicable to nearly all types of concrete structures.

Several studies have been conducted in the past two decades to study the reliability of strut-and-tie models. These studies underlined the suitability of design with strut-and-tie models for deep elements (with span to depth ratios below 2.5) for which codes appeared to be extremely conservative for most of the cases and unconservative for some other cases (Reineck 2002). However, in other cases it becomes more conservative as it does not take into account the concrete contribution (V_c) to the shear resistance in design with regard to shear. Concerning the design of pile caps, experimental studies have been conducted and concluded that the strut-and-tie model leads to safe predictions.

3.3   Strut-and-tie design in codes

Nowadays, most of the major codes of practice allow the use of strut-and-tie models. The Canadian Concrete Code was one of the first standards to include it, since 1984, as an alternative for shear design in regions including statical or geometrical discontinuities. The design according to stress fields using the strut-and-tie method became an alternative for the structural analysis of discontinuity regions in the CEB-FIP Model Code 1990. Strut-and-tie models were then introduced into the ACI Building Code in 2002. Then the Appendix A "Strut-and-tie models" was created and different parts of the codes were modified to allow the design with strut-and-tie models. In 2004, the strut-and-tie method was introduced to Eurocode 2, in Section 5.6.4 "Analysis with strut-and-tie models" and Section 6.5 "Design with strut-and-tie models".

3.4   Design procedure for the ultimate limit state

Several different design procedures can be followed for the design of a structural member using a strut-and-tie model. Figure 3.2 shows one example of an appropriate procedure.
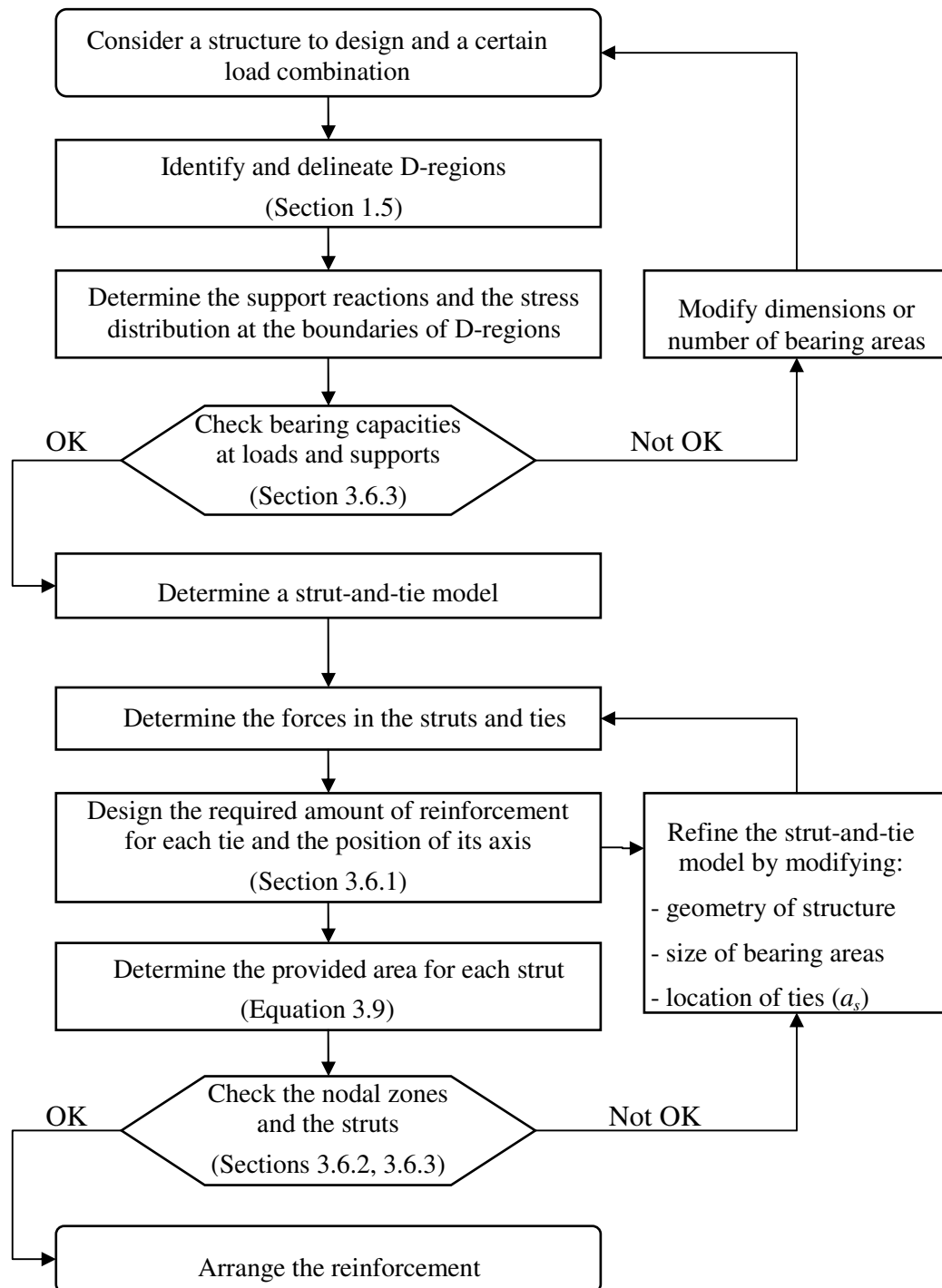
Figure 3.2   Flowchart detailing the design procedure when using the strut-and-tie method

3.5   Derivation of strut-and-tie models

As previously stated, a strut-and-tie model relies on a simulation of the stress field in a structure in the ultimate limit state, when the concrete is cracked and the structure is close to reach collapse. Then one can consider that plastic redistribution has occurred in the structural member and that the chosen force distribution is possible to happen,

which does not mean that it is not much on the safe side. However, it is still important that the strut-and-tie model remains rather close to the linear elastic stress field for two reasons:

- to take into account the limited plastic redistribution in reinforced concrete

- to provide acceptable performance in the service state

This is especially true in design of pile caps, which are reinforced concrete members with a low ability to plastic redistribution.

There are several ways to find an appropriate strut-and-tie model. A linear finite element analysis can be carried out to give an idea of the elastic stress field. The direction and intensity of principal stresses given by this analysis can provide good indications for the choice of the model. Some discretization methods using finite elements and optimisation criteria have also been developed in order to generate strut-and-tie models automatically, for instance by Kostic (2009) or for the software ForcePad. Besides, intuitive methods, such as the load path method (Schlaich et al. 1987) or the stress field method (Muttoni et al. 2008), can help the designer to position the struts and the ties by considering the resultants of the stress fields. These methods used together with the strut-and-tie method present the advantage to lead the designer to a better understanding of the mechanical behaviour of the structure.

Some other rules have to be followed when determining a strut-and-tie model for a structure, such as angle limitations (Section 3.5.1.1) and that the struts should not overlap or cross each other outside the node regions. Indeed, as struts are designed according to the concrete effective strength, it would lead to yielding in the overlapping area (Reineck 2002). On the other hand, ties can cross struts or other ties.

It is usually convenient to choose horizontal and vertical orthogonal ties, to obtain a need for reinforcement close to what is usually provided in practice. However, some other more advanced reinforcement layouts are sometimes used, and more efficient ways of reinforcing the member could be considered with the strut-and-tie models.

Another parameter affecting the choice of the model is the level of statical indeterminacy of the model. Indeterminate models increase the complexity of the procedure, as it is further discussed in Section 4.7.2. However, in some cases they can lead to more efficient models and a higher reliability in the service state. Indeed, in order to establish a statically determinate system the designer can be led to neglect solutions more complicated but closer to the elastic flow of forces. This could lead to severe cracking in some regions under service load.

3.5.1 Choice of the strut inclinations

3.5.1.1 Angle limitations

When building a strut-and-tie model, attention has to be paid to the choice of the inclination of the struts. Two kinds of problems could arise: on the one hand an inappropriate deviation angle at concentrated forces can lead to a too high need of plastic redistribution and strain compatibility problems between stressed and unstressed regions. On the other hand too small angles between struts and ties can also lead to strain compatibility problems. The recommendations of Schäfer in fib bulletin 3 (1999, cited in Engström 2009) are given hereafter, using the notations of Figure 3.3.
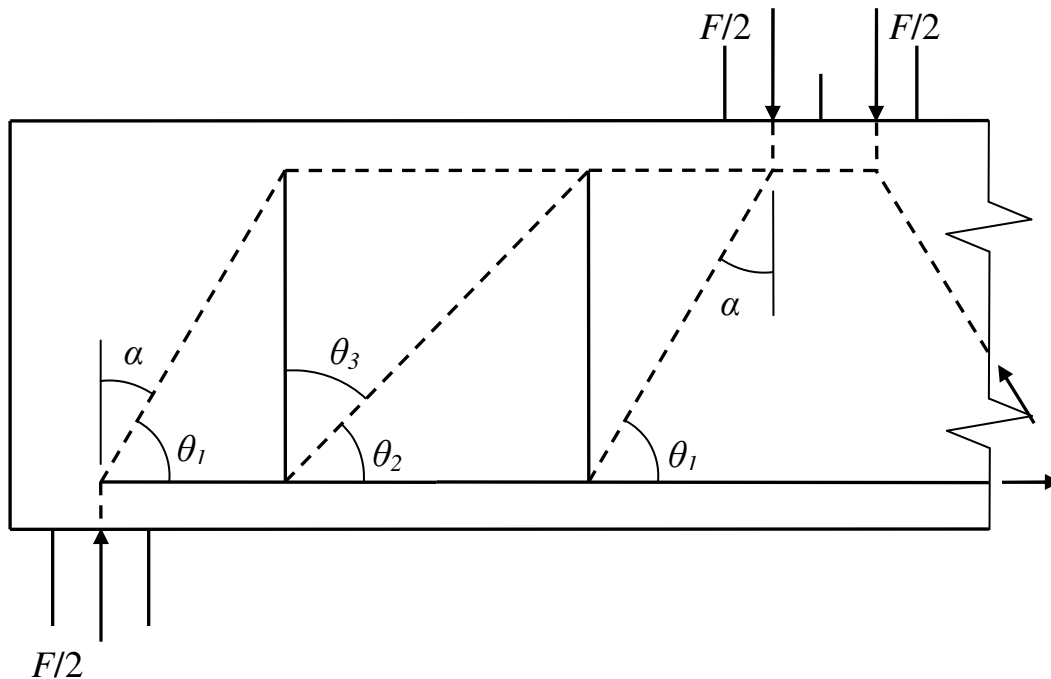
Figure 3.3   Angle recommendations in a deep beam with stirrups, for deviation of concentrated forces and between struts and ties

a)   Deviation of concentrated loads

$$\alpha \approx 30° \quad \text{and} \quad \alpha < 45° \tag{3.1}$$

Additionally, the stresses under concentrated loads should be directly spread out when entering the D-region.

b)   Angles between struts and ties

$$\theta_1 \approx 60° \quad \text{and} \quad \theta_1 > 45° \tag{3.2}$$

$$\theta_2 \approx 45° \quad \text{and} \quad \theta_2 > 30° \tag{3.3}$$

$$\theta_3 \approx 45° \quad \text{and} \quad \theta_3 > 30° \tag{3.4}$$

The recommendations on minimum angles to use in a strut-and-tie model differ between different authors and codes. For instance, in the ACI Building Code the minimum angle between a strut and a tie joining at a node is set to 25°.

It should be noticed in Figure 3.3 that the angle limitation for the deviation of the concentrated force of the column applies to the inclined strut; evidently the horizontal strut is not concerned as it does not directly derive from the spreading of the concentrated force but it is needed for the equilibrium of the model.

When the concentrated force is transferred in the model by several inclined struts, the limitation should apply to the angle of the resultant of the forces in the struts. However, this statement should go together with the appreciation of the designer, who should distinguish the cases where it can be accepted and where it could lead to any compatibility problem.

3.5.1.2 Optimal design

Several different strut-and-tie models can be chosen for a given problem. However some of them are more efficient than others. For instance, when the strut inclinations

θ_1 and θ_2 decrease in Figure 3.3, the forces in the struts and the forces in the horizontal reinforcement increase, while less vertical ties may be needed, hence reducing the amount of shear reinforcement required.

Schlaich et al. (1987) defined the optimal strut-and-tie model, for a certain load case, as being the one with the lowest need for reinforcement. This model would also be the one for which the strain energy is minimum, because the strains in the reinforcement are more important than the ones in the concrete.

3.6   Design of the components

When a strut-and-tie model is established, which respects the conditions of static equilibrium and the limitations of angles, the different components (ties, struts and nodal zones) have to be designed and checked, and if necessary the model has to be refined with respect to these checks.

3.6.1   Ties

The tensile forces in the member are normally carried by ties made of reinforcing bars. The position of the ties in the strut-and-tie model should correspond to the axis of the reinforcement. The required area of steel is given by:

$$A_s \geq \frac{T}{f_{yd}}$$ (3.5)

One of the main advantages of the strut-and-tie method is that it indicates the need for anchorage, however special attention has still to be paid to the anchorage, as it is required to make the design safe. The tie forces can be anchored by anchor plates or through bond resistance of straight or hooked bars. The design of anchorage lengths is not included directly in the models used as examples here, but some comments are made on anchorage in relation to pile caps and strut-and-tie models in Section 5.4.2.

If anchor plates or similar solutions are used the tensile forces in the ties can be assimilated to compressive forces acting from behind the node. Otherwise the force is also transferred within the node, which is less favourable. It is common however for the consideration of the nodal zones to assimilate ties to struts acting in compression on the other side.

3.6.2   Struts

The compressive forces in strut-and-tie models are carried by concrete struts. The design strength of a compressive strut depends on the state of transverse stress along the strut. If a transverse tensile stress field is taken through the compression stress field, the compressive strength decreases with the lateral tensile strain. The state of stress along the strut depends also on the shape of the compression stress field. If there is space for the stresses in the strut to expand between two singular nodes, the strut will have a "bottle shape" and the transverse tension induced will create cracking in the strut, which will reduce, in the same manner, the compressive strength of the strut. Otherwise, as for a strut located along the compression flange of a beam, the section of the strut will remain rather constant and the strut will be prismatic. One can also distinguish "fan-shape" struts between a singular node and a smeared node, and prismatic struts between two smeared nodes, for which the "bottle-shape" effect is negligible. Different types of concrete struts are represented in Figure 3.4.

| Fan-shape strut | Prismatic strut | Bottle-shape strut |
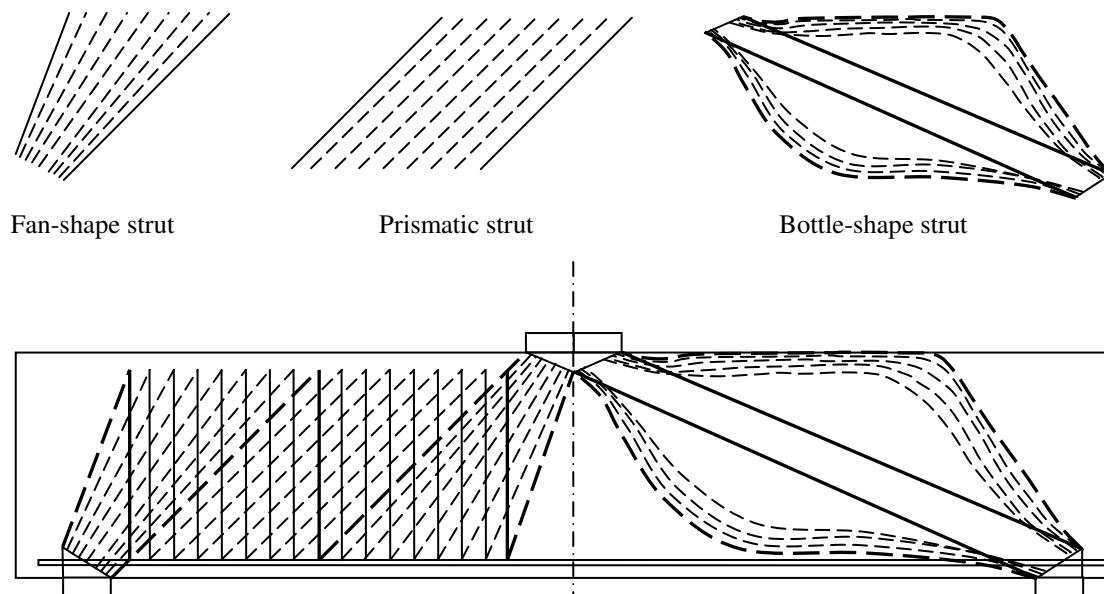
Figure 3.4   Different types of struts in a strut-and-tie model

a)   Strut with no transverse stress or with transverse compression (Figure 3.5 a)

This case corresponds to struts situated in uncracked zones, which have a constant cross section along their length. The recommended design strength according to EC2 is:

$$\sigma_{Rd,\max} = f_{cd} \tag{3.6}$$

Note that a higher compressive strength can be assumed in regions where multi-axial compression occurs.

b)   Strut with transverse tension (Figure 3.5 b)

This case corresponds either to "bottle-shape" struts or to struts crossed by a transverse tensile stress field, i.e. struts crossing cracked compression zones, for which the compressive strength decreases with the lateral tensile strain. If a more rigorous approach is not used to determine the loss of compressive strength, the recommended value in Eurocode 2 is:

$$\sigma_{Rd,\max} = 0.6\nu' f_{cd} \tag{3.7}$$

$$\nu' = 1 - \frac{f_{ck}}{250} \tag{3.8}$$

A major requirement of strut-and-tie models is that struts do not cross or overlap each other outside the node region. Indeed the struts are designed for a certain force so that the stress in the strut does not exceed the concrete compressive strength. In such cases the concrete strength could be exceeded in the overlapping or crossing region.

3.6.3   Nodes and nodal zones

3.6.3.1   Definitions of nodes and nodal zones

First of all, the distinction has to be stated between the terms: nodes and nodal zones, which are used hereafter. In a strut-and-tie model, the nodes correspond to the points of intersection between the axes of struts, ties and concentrated forces, where the forces in all the concurring members are usually calculated using equilibrium conditions. Indeed, the forces from the struts and ties connecting at the node must balance each other (Figure 3.6). On the other hand, the nodal zones (or node regions, node areas…) correspond to the concrete blocks around the nodes "in which forces acting in different directions, meet and balance" (Schäfer 1999); therefore it can be seen as the parts of the structure where stresses are deviated.

Two kinds of nodes can be distinguished in a strut-and-tie model: "singular" (or "concentrated") nodes and "smeared" (or "continuous") nodes. Most of the nodes are usually smeared nodes, where the struts represent wide concrete stress fields, which deviate each other over a large volume, or are deviated by ties made of many reinforcing bars spread over an extended nodal zone. Smeared nodes are not critical in a strut-and-tie model and hence do not need to be checked as long as the reinforcement is properly anchored and extend until the extremities of the stress field. The other type of nodes, the singular nodes, corresponds to the nodes close to statical or geometrical discontinuities, at concentrated loads or near openings for instance. In the case of a deep beam or a pile cap, singular nodes would be the nodes under the column and over the supports or piles; the other nodes being smeared over large regions. However, if shear reinforcement is not spread using many small stirrups, but designed with only large concentrated bars; the intersection between the struts and the stirrups should also be considered as a singular node. The singular nodes are often the critical points in a strut-and-tie model as the nodal zones correspond to the place of stress concentration in the concrete. Thus the check of singular nodes is particularly important in strut-and-tie models, and detailing of these zones has to be done accordingly, as it is usually the governing parameter in the design. Schlaich et al. (1987) affirmed that the stresses within a concrete D-region can be considered as safe if the bearing stresses in the nodal zones are below a certain limit.

The different nodes in a strut-and-tie model are usually referred to according to the members they are connecting, one C for every strut (Compression member) and one T for every tie (Tension member); the common nodes are presented in Figure 3.6.
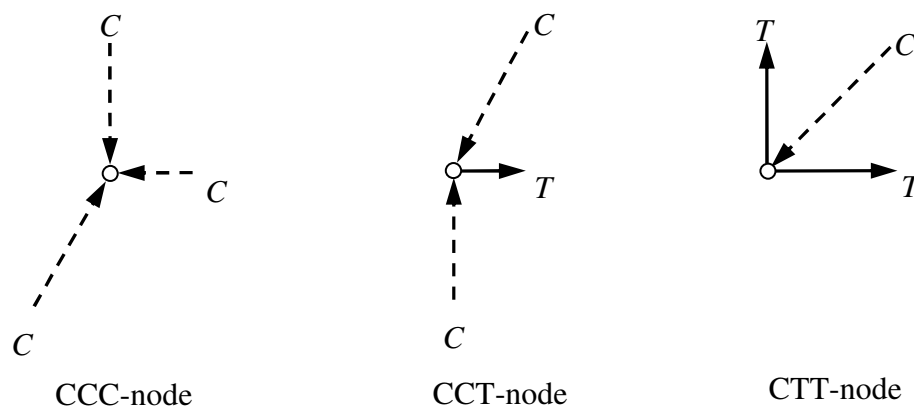
Figure 3.6   Denomination of nodes

3.6.3.2 Classification of nodal zones and description of their geometries

In the definition of the geometry of nodal zones ties are assimilated to struts acting on the other side of the node in compression. At the node, the strut acting on the other side of the nodal zone corresponds to the reinforcement

At the beginning of the development of strut-and-tie models, hydrostatic nodal zones were used. The faces of the nodal zones were perpendicular and proportional to the forces acting on the node, see Figure 3.7 (a). Therefore no shear stresses were created at the node (e). However it is almost impossible to manage to have geometries assuring hydrostatic nodes in a model. For this reason, all the major codes recognize non-hydrostatic nodes nowadays (Figure 3.8). Schlaich recommended to keep stress ratios on adjacent edges of a node above 0.5, otherwise the non-uniformity of stress distribution could make the check of the node unconservative (Schlaich et al. 1987).
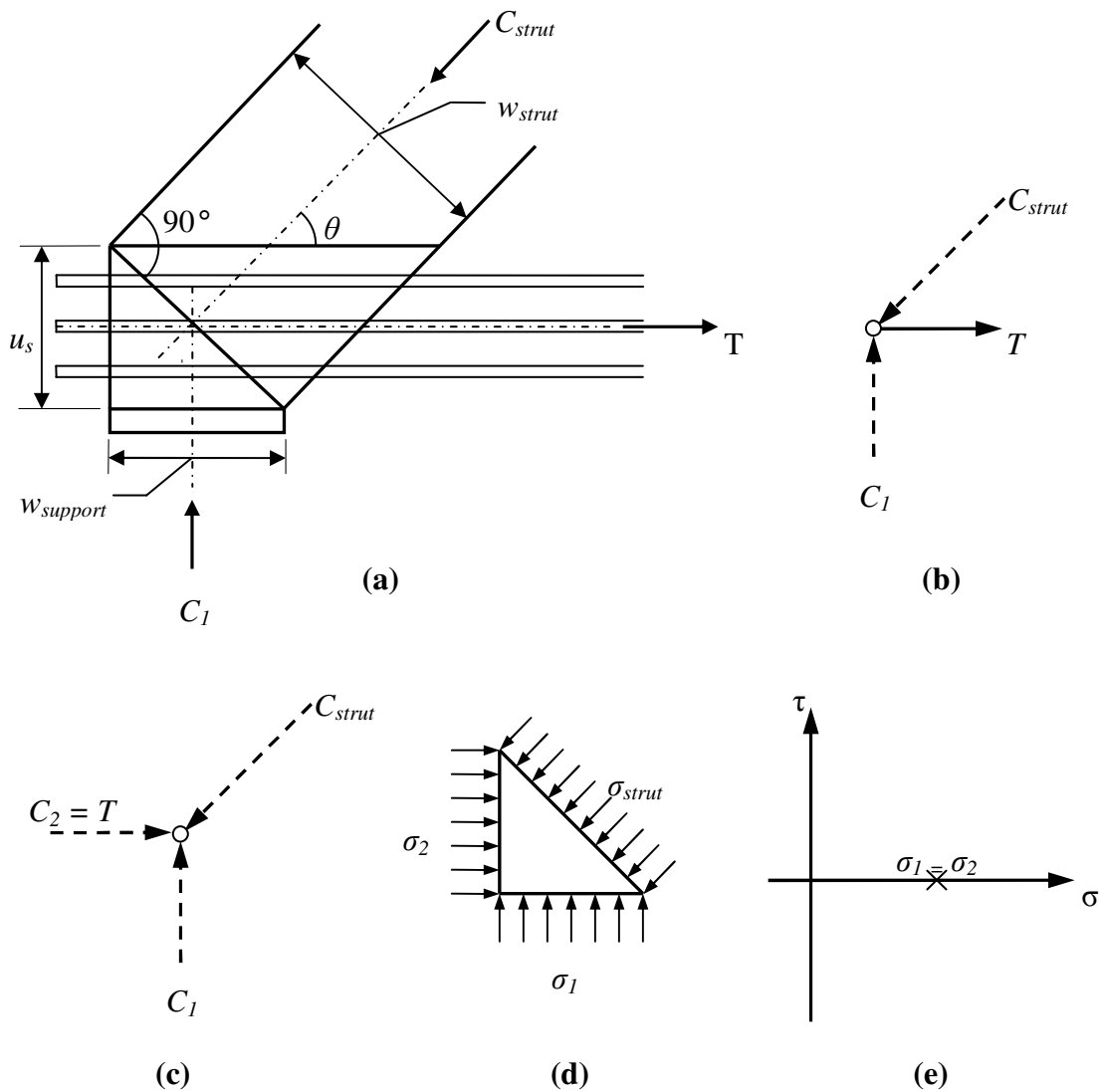
Figure 3.7   *Example of hydrostatic nodal zone (a) hydrostatic nodal zone and extended nodal zone for a CCT-node, (b) representation of the forces joining at the node, (c) equivalent representation of forces with tension considered as compression acting on the other side of the nodal zone (d) stresses acting on nodal zone, (e) Mohr's circle for the state of stress in the nodal zone, limited to a point in this case*
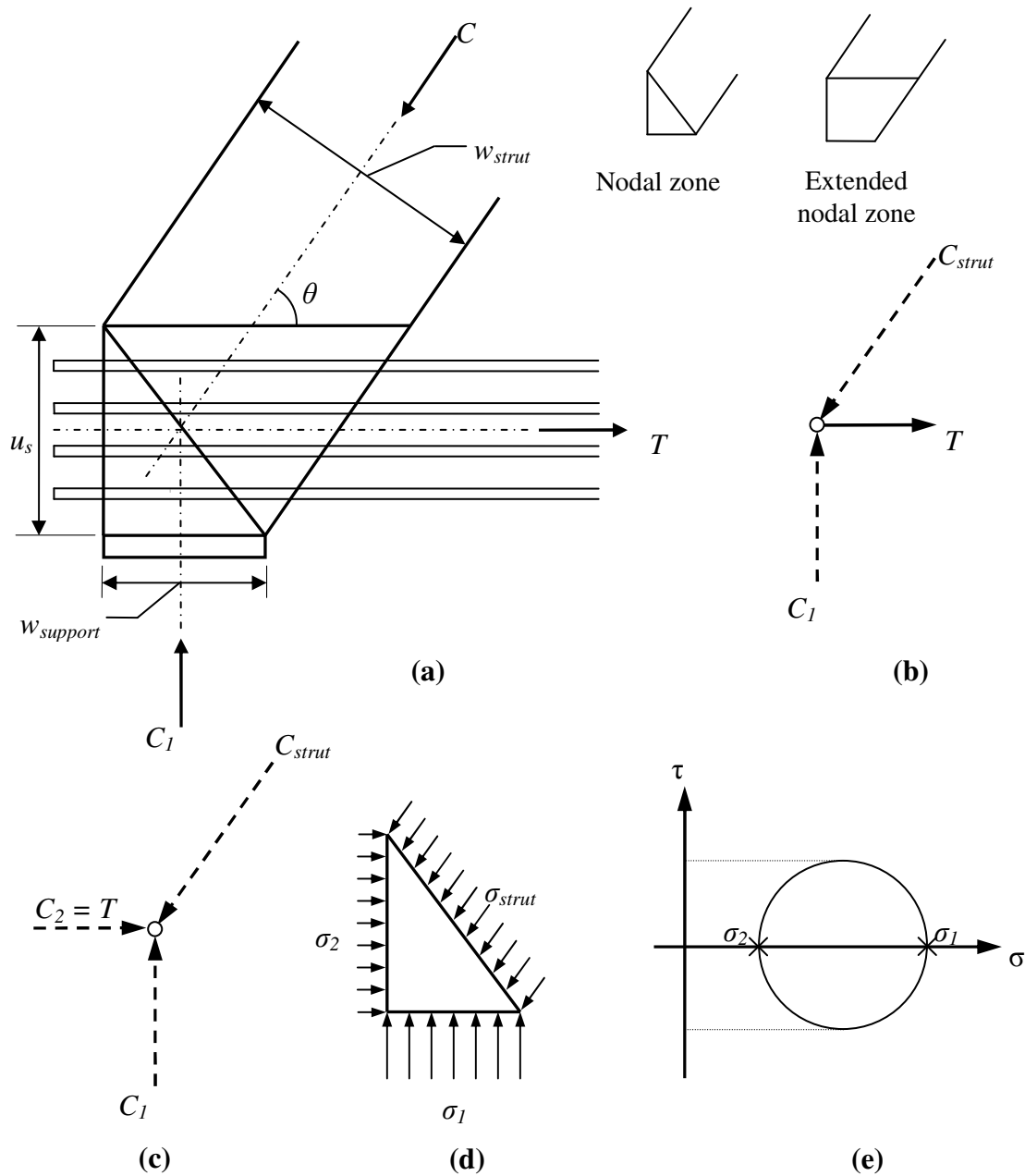
Figure 3.8   Example of non-hydrostatic nodal zone (a) non-hydrostatic nodal zone and extended nodal zone for a CCT-node, (b) representation of the forces joining at the node, (c) equivalent representation of forces with tension considered as compression acting on the other side of the nodal zone (d) stresses acting on nodal zone, (e) Mohr's circle for the state of stress in the nodal zone

Using the notations defined in Figure 3.7 and Figure 3.8, the width of the inclined strut is defined by:

$$w_{strut} = u_s \cdot \cos\theta + w_{support} \cdot \sin\theta \qquad (3.9)$$

The checks of hydrostatic and non-hydrostatic nodes are similar. Either the principal stresses are checked in the nodal area, or the stresses in the struts, defined by the force in the member divided by the cross sectional area, defined by Equation 3.9, are

checked against strength values defined for each type of node. Some recommendation of these strength values are given in Section 3.6.3.3.

While hydrostatic nodal zones are defined by the intersection of all the joining members, non-hydrostatic nodal zones are often defined by extended nodal zones, which correspond to the intersection between the two struts in balance at the node, located inside the structure. The difference between the nodal zone and the extended nodal zone is illustrated in Figure 3.8 and nodal zone geometries for different types of nodes are detailed hereafter.

Several types of nodal zones can be found in a strut-and-tie model depending on the forces acting on them. According to the denomination defined previously, the most common cases in a two-dimensional model are: CCC, CCT and CTT, illustrated below in Figure 3.9, Figure 3.10 and Figure 3.11.

A good way to explain the iterative choice of members' geometry and to introduce the problem of three-dimensional nodal zones treated in the next chapter (Section 4.3), is to look at how the geometry of different types of nodal zones is defined.
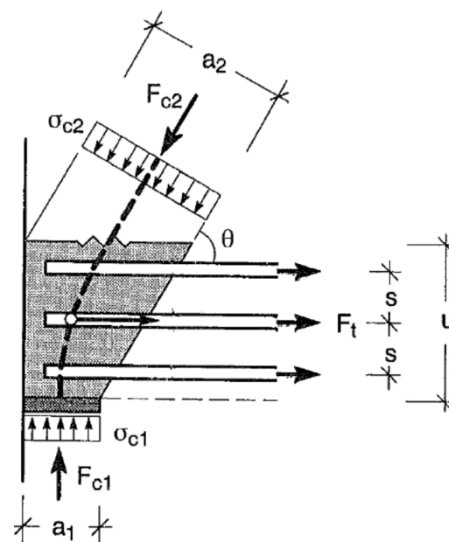
Figure 3.9   Example of compression-tension node with a tie in one direction (Schäfer 1999)

As it has been explained previously, to define the nodal zone, the ties are often represented as struts acting on the other side of the node. The definition of the CCT-nodal zone illustrated above in Figure 3.9 would therefore be equivalent to the one of a CCC-nodal zone with a horizontal strut acting on the left side of the node. It is quite clear in this case that the nodal zone is defined by the intersection of the struts inside the element, where the stresses from the tie deviate the stresses from the inclined strut in the nodal zone, to balance the external stresses. The width of the bearing plate and the vertical level of the node are sufficient to define the inclined strut and thus the nodal zone.
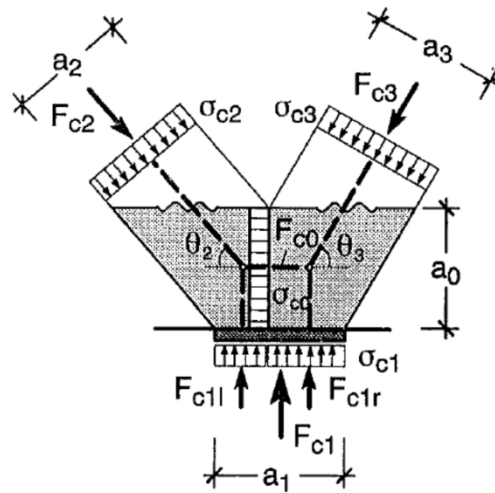
Figure 3.10   Example of compression node (Schäfer 1999)

For a CCC-node, the extended nodal zone, represented in Figure 3.10, actually includes two nodes, connected by a horizontal strut. Hence the nodal zone can be separated in two sub-areas, delimited by the vertical line passing through the intersection between the two inclined struts, and the border between the bearing areas influencing each of the struts. The horizontal strut, resulting from the action of each sub-nodal zone on the other can be considered to act at this border. Then each of the two sub-nodal zones corresponds to the elementary case of a CCC-node and the Equation 3.9 applies with $u_s=u_c$ in this case.

When the width of the struts has been chosen, the intersection of the struts defines the nodal zone. It is the same case for a CCT-node and a CTT-node with anchor plates, where the ties act as a strut working in compression from the other side of the node.
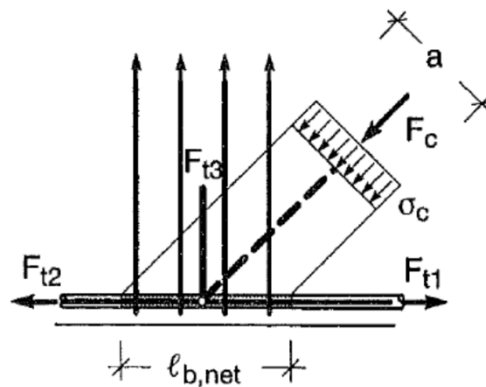
Figure 3.11   Example of compression-tension node with ties in more than one direction (Schäfer99)

For a CTT-node, the choice of the width of the strut, the width of the vertical tie and the bond length has to be consistent. If any one is chosen, the others have to follow, and the position of the corners of the nodal zone is determined.

In all cases the nodal zone can be defined as the intersection of all struts and ties intersecting at the node, the ties being considered as struts working in compression from the other side of the node.

3.6.3.3 Design strength values for the check of nodal zones

a)   Compression nodes

$$f_{cd1} = k_1\left(1 - \frac{f_{ck}}{250}\right)f_{cd} \qquad (3.10)$$

with k_1=1.0 (recommended value EC2)

k_1=0.85 (MC90)

Note that the design strength value of concrete can be increased for compression nodes subjected to secured biaxial or triaxial compression, the values which may be used are given in Section 4.3.6.

b)   Compression-tension nodes with ties in only one direction

$$f_{cd2} = k_2\left(1 - \frac{f_{ck}}{250}\right)f_{cd} \qquad (3.11)$$

with k_2=0.85 (recommended value EC2)

k_2=0.7 (MC90)

c)   Compression-tension nodes with ties in more than one direction

$$f_{cd3} = k_3\left(1 - \frac{f_{ck}}{250}\right)f_{cd} \qquad (3.12)$$

with k_3=0.75 (recommended value EC2)

k_3=0.6

Note that Eurocode 2 allows to increase these strengths by 10% when some favorable conditions are fulfilled, for instance if the reinforcement is placed in several layers, if the angles between struts and ties are more than 55°, or if the adequate confinement is provided at the nodes.

In the examples of design and analysis conducted in Chapter 6 and Chapter 7 this increase will be used because of the good confinement at the nodes provided in large three-dimensional structures such as pile caps.

4 Development of a strut-and-tie model adapted to the three-dimensional analysis of pile caps

4.1 State of the art in design of pile caps by strut-and-tie models

Several studies have been conducted on the design of pile caps by strut-and-tie models, in particular by Adebar (1990, 1996) and by Souza (2009). The results of these studies, and the conclusions drawn by the authors, show that the use of strut-and-tie models for the design of pile caps is promising. However, most of the time, the authors do not provide details on how to deal with three dimensional strut-and-tie models, for instance concerning the verification of nodes. The pile caps studied are also very simple in most of the cases; they consist often in pile caps supported by two to four piles, without shear reinforcement.

4.2 State of the art in 3D strut-and-tie models

"If the state of stress is not predominantly plane, as for example in the case with punching or concentrated loads, three-dimensional strut-and-tie models should be used." (Shlaich 1987, p. 8)

Even if some books and articles mention the case of 3-D strut-and-tie models, most of the 3-D problems found in the literature are solved as a combination of 2-D models following each plane of the member. For instance an I-beam could be analysed with two 2-D models in the planes of the flanges and another one in the plane of the web, with some nodes in common between the two in-plane models, as exemplified in Figure 4.1 (a). The analysis of a four-pile cap, similar to the one illustrated in Figure 4.1 (b), could be made by considering the diagonal plane in the pile cap including two opposite struts. Most of the articles about 3-D strut-and-tie models do not detail how to consider the intersection between struts and ties and how to check the nodal zones, thus it is likely that the authors used 2-D analogy in their models.
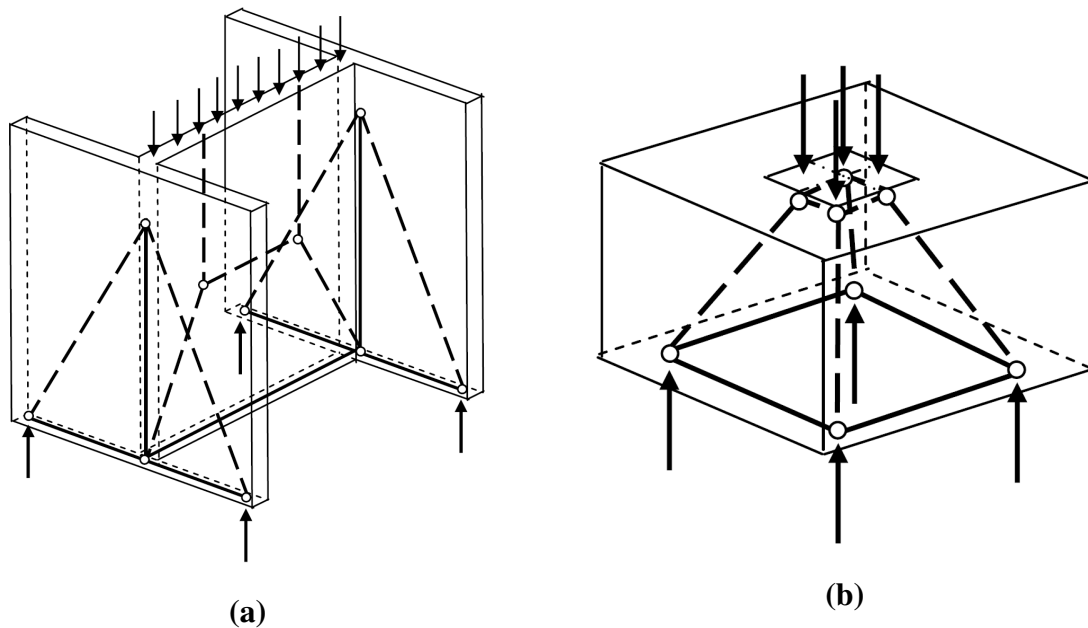
*Figure 4.1   Examples of 3-D strut-and-tie problems solved by 2-D analogy in the literature: **(a)** I-beam with a strut-and-tie model in each plate, **(b)** 3-D strut-and-tie model of four-pile cap requiring 2-D simplifications at nodal zones, adopted from Engström (2009)*

One such 3-D example is treated by Klein (2002). It consists in the study of a five-pile cap, similar to the four-pile cap of Figure 4.1 (b) with an additional pile at the centre, subjected to a vertical load and an overturning moment. The author of this example, made the following simplifying assumptions:

> *"- Assumption of square struts is needed to simplify complex geometry where struts intersect in three dimensions*
>
> *- Geometric dissimilarities between struts and nodes must be neglected (but checks should be made to assure the centroid is properly located and node area is sufficient)"*

However, despite these assumptions, the author concludes that the strut-and-tie model design is more rational and leads to more reliable performance compared to a traditional sectional design.

The geometry of nodal zones assumed by Klein (2002), and similar methods used in the literature, rely on simplifications based on the analogy with the 2-D definition of the nodal zone. For instance, in order to allow and facilitate the use of 3-D strut-and-tie models for the design of pile caps, revisions were made to the ACI Building Code where Section A.5.3 was added to simplify the detailing of nodal zones in 3-D, by not requiring an exact geometry compatibility between the struts and the faces of the nodal zone (Reineck 2002). The recommendation is formulated as follow:

> *"In a three-dimensional strut-and-tie model, the area of each face of a nodal zone shall not be less than that given in A.5.1 (Equation 3.9), and*

the shape of each face of the nodal zones shall be similar to the shape of the projection of the end of the struts onto the corresponding faces of the nodal zones." (ACI 318-08, p. 393)

The most logical procedure, using 2-D analogy, would be to consider the resultant of the forces in the struts and the ties in the same plane. Then the easiest way to proceed is to consider the resultant of the tie forces in the vertical plane of the strut, for instance in the case of the 4-pile cap in Figure 4.1 it would be the diagonal plane. Then the problem can be considered in two dimensions in this plane.

However, the limits of these methods arise when several struts are joining the same node, or when considering the detailing of the nodal zone which loses somehow geometrical consistency. In the case of the design of pile caps, which are elements with large dimensions in the three directions, the design using strut-and-tie model is governed by the nodal zones at the column and the piles. These nodal zones are subjected to complex three dimensional states of stress and using a method based on 2-D analogies and other simplification appear to be inadequate in this case. Therefore, a method was developed in this thesis work to define three-dimensional nodal zones in a consistent way.

A comparison between a simplified nodal zone geometry derived from 2-D and a more complex 3-D nodal zone geometry is presented in Section 4.3.3, Table 4.1, for a node corresponding to the one above a pile in a pile cap.

4.3   Three-dimensional nodal zones

In this study, a solution is proposed, to improve the design of nodal zones, when the struts and ties joining a node are not in the same plane. The aim of the method is to define consistent nodal zones, which fulfil static equilibrium and with compatibility between the faces of the nodal zone and the cross-sectional areas of the struts and ties meeting at the node. The improvements proposed are justified by the importance of the check of the strength of nodal zones in the design by strut-and-tie models, as expressed by Schäfer:

"Poor detailing of singular node regions is the most frequent cause for insufficient bearing capacity of reinforced concrete members." (Schäfer 1999)

It has been explained previously, in Section 3.6.3.2, that the dimensions of some struts at a node determine the dimension of some others. In this method, the loading and bearing areas are supposed to be known. The cross-sectional areas of the ties are determined according to the amount and position of the reinforcement. Then the aim of the method is to find the cross-sectional areas of the remaining inclined struts in order to obtain a node which fulfils equilibrium and compatibility.

Like in 2-D, many different nodes can be encountered and different ways of detailing them are possible. However, some typical nodes represent the most usual cases, especially as the study is limited to the case of pile caps.

The same denomination of nodes as in 2-D will be used, that is to say one C for every strut reaching the node and one T for every tie. In the definition of the nodal zones,

the tensile stresses from the ties will be represented as compression acting on the other side, as in the two-dimensional case (Section 3.6.3).

The criteria that should be fulfilled to define a consistent nodal zone are:

- All the faces of the nodal should be covered with stresses

- The centroids of the struts and ties should correspond to the axis used in the strut-and-tie model

- The struts should not overlap before the nodal zone

4.3.1 Geometry for consistent three-dimensional nodal zones

The three-dimensional method proposed in this work allows to define a consistent nodal geometry. The method consists in determining the shape of the undefined struts, using the known or assumed corners of the nodal zone and the direction vector parallel to the axis of the strut. Then the cross-sectional area of the strut can be calculated by the procedure described hereafter.

The parameters of the nodal zones that are supposed to be known in order to define the remaining struts are:

- the dimensions of the loading area (columns) and supporting areas (piles)

- the height of the node, which is defined by the height of horizontal struts or the height of influence areas of ties (two times the distance from the edge to the gravity centre of the bars)

Hereafter the dimensions of the supports are called a and b, respectively in the x- and y-direction. The height of the node is referred to as u_c for compression nodes under the column; u_c being equal to two times a_c, the distance from the edge to the axis of the horizontal strut used in the strut and tie model. The height of compression-tension nodes is defined by u_s, which is two times the distance from the edge to the axis of the reinforcement a_s, see Figure 4.2 for the illustration.
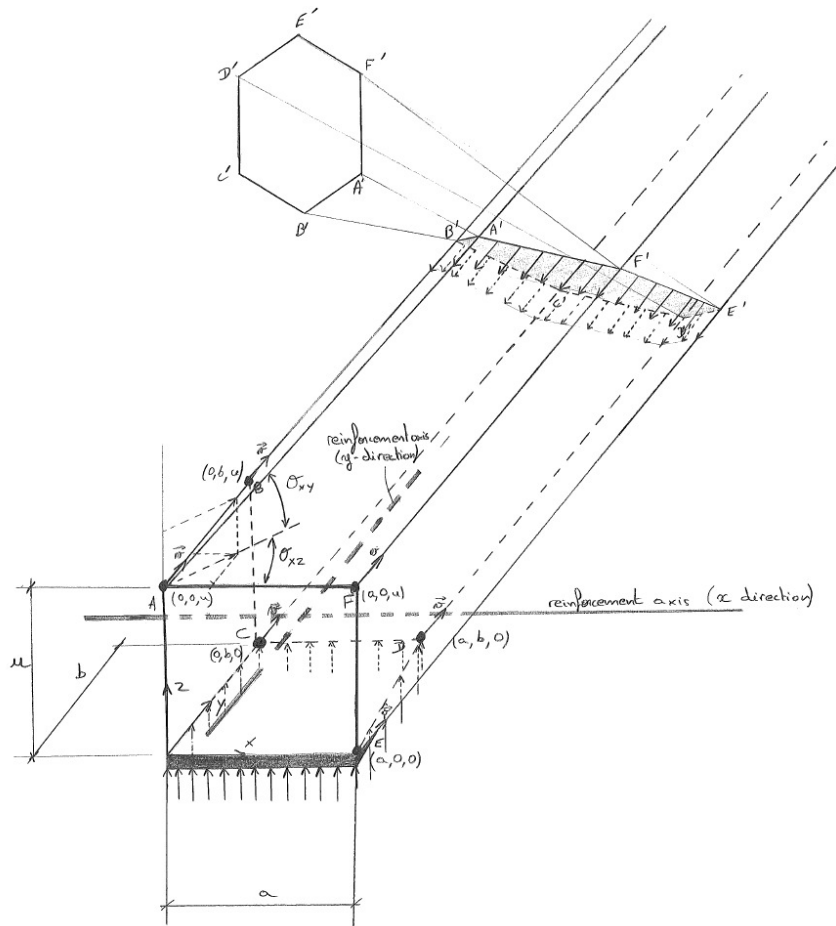
Figure 4.2   2C2T-node over a pile located at the corner of a pile cap (a 2C3T-node would be detailed similarly with a vertical tie passing through the centre of the lower face of the parallelepiped nodal zone)

The method consists in identifying the corners of the nodal zone. Knowing the dimensions of the bearing plate and the height of the node, some assumptions lead to the determination of the other corners. For instance, in Figure 4.3, some typical cases are presented, that can be found in the design of pile caps. These nodal zones correspond to the ones under columns, where concentrated compression stresses are spreading in the element. This is represented by several inclined struts leaving the node towards the piles. According to the geometry of the pile cap, a number of inclined struts is chosen. In a four-pile cap, there would be four inclined struts going to each pile, as shown in Figure 4.3 (b), while for the same pile cap with an additional pile under the column, there would be also a vertical strut, as shown in Figure 4.3 (a). Note that, in Figure 4.3 (a) and (b), four nodes would be used in the model, and therefore the general nodal zone under the column would be divided in four sub-nodal zones in Figure 4.3 (a) and (b), while eight nodes would be used in Figure 4.3 (c) corresponding to eight nodal zones. Each sub-nodal zone corresponds to the region of interaction between the external vertical stress, the stress in the inclined strut, and the stress in two perpendicular horizontal struts balancing the two first mentioned stresses. When the geometry of nodal zones is discussed hereafter it corresponds to the geometry of sub-nodal zones, also equivalent to the geometry of the 2C2T-nodal zone in Figure 4.2.

*Figure 4.3   Examples of nodal zones in pile caps **(a)** 6C-node under the column for a 5-pile cap (three of the struts are shown), **(b)** 5C-node under the column with triangular horizontal struts for a 4-pile cap (four inclined struts are shown), **(c)** 9C-node under a column for a 8-pile cap, combination of the two previous nodes (two struts are shown at each level)*

The geometry of the nodal zones in Figure 4.3 is consistent. However some problems arise to define the exact position of the nodes because of the complex geometries of the elementary nodal zones. As it has been explained previously, the position of a node should correspond to the point of intersection of the centroids of the struts balancing at the node. However, in such cases it is complicated to define the exact position of this point of intersection; moreover it is often unclear if the centroids of the four struts intersect at the same point. For this reason the use of rectangular parallelepiped nodal zones, as illustrated in Figure 4.4, seems to be an adequate solution. It will be shown hereafter that all types of nodes encountered in the design of a pile cap can be designed using this geometry, which is actually an extension of the two-dimensional geometry commonly used. The rectangular parallelepiped (or right

cuboid) shape of the nodal zone will be referred to later as "parallelepiped nodal zone" or "cuboid nodal zone".

As it has been explained in Section 3.6.3 for the two-dimensional case, in order to define the nodal zone, the ties can be considered as struts acting in compression from the opposite side of the nodal zone. Therefore in three-dimensions every nodal zone, or a partition of it, can be explained by the elementary 4C-nodal zone, which corresponds to one fourth of the parallelepiped nodal area defined in Figure 4.4.
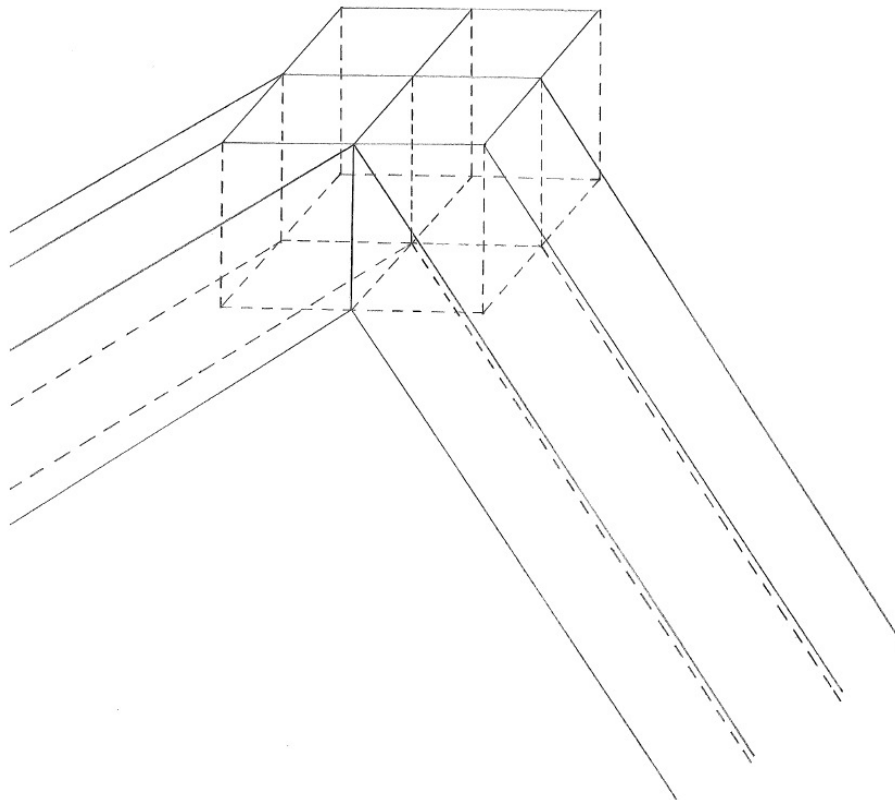
Figure 4.4   5C-node under the column, alternative with rectangular horizontal struts (only two of the inclined struts are shown). The inclined struts have a hexagonal cross-section as for the 2C2T-node in Figure 4.2

In this manner the parallelepiped geometry can be used as well for the 2C2T-node represented in Figure 4.2, as for its extension with a vertical tie (made for instance of stirrups), that is to say a 2C3T-node. Every type of three-dimensional concentrated nodal zone can be designed using the three-dimensional elementary 4C-node (Figure 4.4), and the two-dimensional elementary 3C-node (Figure 3.8), completed by the method for combining struts defined in Section 4.3.4. In more complex cases, the method presented could be adapted.

Demonstration: forces concurrent at the elementary 4C-node

In order to fulfil moment equilibrium of the node, the forces in the struts and the ties acting on the node should be concurrent. When drawing a strut-and-tie model, this assumption is considered to be true as the struts and ties are drawn such that they intersect at the node, and the unknown forces in the struts and the ties are calculated based on this assumption. However this assumption should also be fulfilled when designing the nodal zone. Then, if one considers the stresses acting on each face of the nodal zone, showing that the forces are concurrent is equivalent to showing that the

centroidal axes of the struts acting on the nodal zone are concurrent. As the elementary nodal zone is defined by the intersection of three orthogonal struts, it is obvious that the centroid of the resultant parallelepiped belongs to the centroidal axis of each of the strut. To demonstrate that it also belongs to the centroidal axis of the inclined hexagonal strut is not as straightforward. Note that it is obvious to show it in two dimensions, when the strut has a rectangular cross section (Figure 4.5). In three-dimensions, the demonstration can be done in several ways.
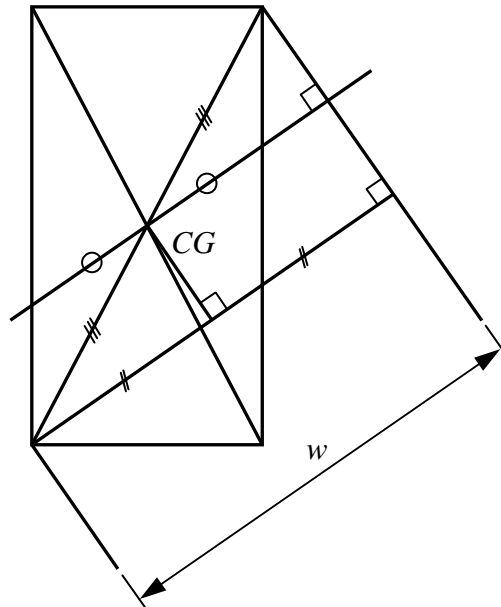
Figure 4.5   Concurrency between the centroidal axis of the inclined strut and the centroid of a two-dimensional 3C-nodal zone

It should be noticed that the strut is a prismatic geometrical object formed by the translation of the parallelepiped nodal zone in the direction of the direction vector $\vec{v}$ of the strut. Therefore any orthogonal cross-section of the strut corresponds to the projection of the parallelepiped, in the direction of $\vec{v}$, in the orthogonal plane to the strut. Then the hexagonal projection can be regarded as "the view of the cube from the orthogonal plane" (Figure 4.6) (not from a point or the centroid, as this would be a perspective view). The hexagon can be divided into a parallelogram and two triangles whose centre of symmetry is the centre of the parallelogram. The two triangles compensate each other and thus the centre of the parallelogram is the centre of the hexagonal cross section, and it corresponds also to the projection of the centre of gravity of the parallelepiped, as the parallelogram results from the projection of the diagonal face of the parallelepiped. Therefore the centroidal axis of the hexagonal strut goes through the centre of the parallelepiped, hence assuring the equilibrium of moments at the node.

Another way to demonstrate it would have been to show that the centre of gravity of the parallelepiped is the centre of symmetry of the orthogonal cross section of the strut passing at this point.
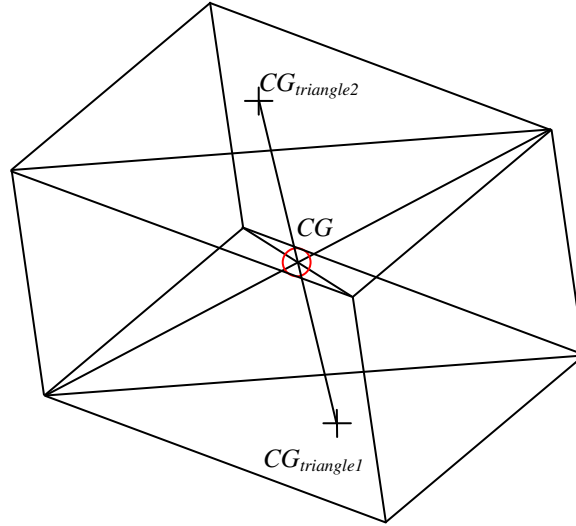
Figure 4.6   Centre of gravity of the cross-section of the inclined strut

4.3.2   Calculation of cross-sectional area of hexagonal struts

The following calculations are detailed in Appendix A, according to the notations defined in Figure 4.2. The direction vector of an inclined strut is defined by:

$$\vec{v} = (\cos\theta_{xy}\cos\theta_{xz}; \cos\theta_{xy}\sin\theta_{xz}; \sin\theta_{xy}) \tag{4.1}$$

The projection of the strut in an orthogonal plane corresponds to a hexagon. The sides of this hexagon and some diagonals are calculated in order to compute its cross-sectional area.

$$A'B' = \left\| \overrightarrow{AB} - (\overrightarrow{AB} \cdot \vec{v}) \cdot \vec{v} \right\| \tag{4.2}$$

Here A and B correspond to points at two adjacent vertex of the parallelepiped, used to define the edges of the inclined strut. $A'B'$ is equal to the distance between the projections of A and B in an orthogonal plane of the strut, as illustrated in Figure 4.2.

Therefore the cross-sectional area of the strut is a function of the truss and the nodal zone geometries.

$$Area(hexagon) = function\ (a; b; u; \theta_{xy}; \theta_{xz}) \tag{4.3}$$

$$Area(hexagon) = function(A'B'; B'C'; C'D'; D'E'; E'F'; A'C'; A'D'; A'E') \tag{4.4}$$

Then the cross-sectional area of the strut can be easily computed by calculating the area of the three triangles which compose the hexagon. Knowing the three sides a, b and c of a triangle, its area is (Heron's formula):

$$Area(triangle) = \frac{1}{4}\sqrt{(a^2 + b^2 + c^2)^2 - 2(a^4 + b^4 + c^4)} \tag{4.5}$$

4.3.3   Comparison between the common 2-D method and the 3-D method

The comparison conducted in this section shows the differences between the common 2-D method and the 3-D method developed in this thesis work and presented in the previous section, for the design of a 2C2T node (Figure 4.2), which corresponds to the

nodes above the piles in a pile cap. The 2-D method used corresponds to the one presented in Section 4.2 as the most logical one. It consists in considering the resultant of the two ties arriving at the node in the vertical plane passing through the inclined strut.

The common piles used by Skanska have the dimension: 0.275 x 0.275 m^2. Thus in this comparison: $w_{support} = a = b = 0.275$ m. The results of the comparison are presented in Table 4.1, for various directions of the inclined strut and different level of reinforcement u_s. The inclinations of the strut have been chosen to cover a wide range of cases that might be encountered in three-dimensional strut-and-tie models. The 2-D method and the 3-D method converge when the inclined strut is in the same vertical plane as one of the ties, e.g. $\theta_{xy} = 45°$ and $\theta_{xz} = 0°$, and the two methods diverge the most for $\theta_{xy} = 45°$ and $\theta_{xz} = 45°$. The values of the level of reinforcement u_s assigned correspond to rather common values in design of pile caps; one can notice that if u_s increases the difference between the two methods increases.

Table 4.1   Strut areas obtained by the 2-D and the 3-D methods for various strut inclinations in the case of a 2C2T node over a pile (Figure 4.2)

Pile width $w_{support}$ (m)	u_s (m)	θxy	θxz	Angle strut/x-tie	Angle strut/y-tie	Area strut 3-D (m^2)	Area strut 2-D (m^2)	$\dfrac{A_{3D} - A_{2D}}{A_{3D}}$
0.275	0.2	60°	45°	69°	69°	0.104	0.093	6 %
0.275	0.2	45°	45°	60°	60°	0.108	0.092	15 %
0.275	0.2	35°	45°	55°	55°	0.107	0.088	18 %
0.275	0.2	25°	45°	50°	50°	0.102	0.082	20 %
0.275	0.2	0°	45°	45°	45°	0.078	0.055	29 %
0.275	0.2	45°	30°	52°	69°	0.107	0.092	14 %
0.275	0.2	45°	15°	47°	80°	0.101	0.092	9 %
0.275	0.2	45°	→ 0°	45°	→ 90°	→ 0.092	0.092	→ 0 %
0.275	0.2	35°	35°	48°	62°	0.106	0.088	17 %
0.275	0.2	30°	30°	41° (<45°)	64°	0.103	0.085	17 %
0.275	0.3	60°	45°	69°	69°	0.124	0.107	14 %
0.275	0.3	45°	45°	60°	60°	0.136	0.112	18 %
0.275	0.1	45°	45°	60°	60°	0.081	0.073	10 %

The conclusion that can be drawn from this table is that the method proposed for the shape of the components for 3-D strut-an-tie models, besides from being more rational than the 2-D analogy method, leads to a more efficient design. The area obtained by the 3-D method is always greater or equal to the area in the 2-D method, which allows

in most of the cases a higher lever arm, therefore reducing the force in the horizontal struts and ties, hence the flexural reinforcement.

4.3.4 Nodes with more than one strut in the same quadrant

For common singular nodes in a pile cap, an orthogonal basis can be defined at the node by the vertical direction of the external load at the support, and the horizontal orthogonal directions of the main reinforcement in the structure. In three-dimensions, this orthogonal basis defines eight quadrants, of which four are located inside the structure; in two-dimensions it defines four quadrants with two inside the structure. If two struts meeting at the node are located in the same quadrant, the definition of the nodal region becomes more complex.

Some authors worked with this issue in the case of two-dimensional strut-and-tie models. The different methods proposed to solve this problem are illustrated in Figure 4.7.

| (a) | (b) | (c) |
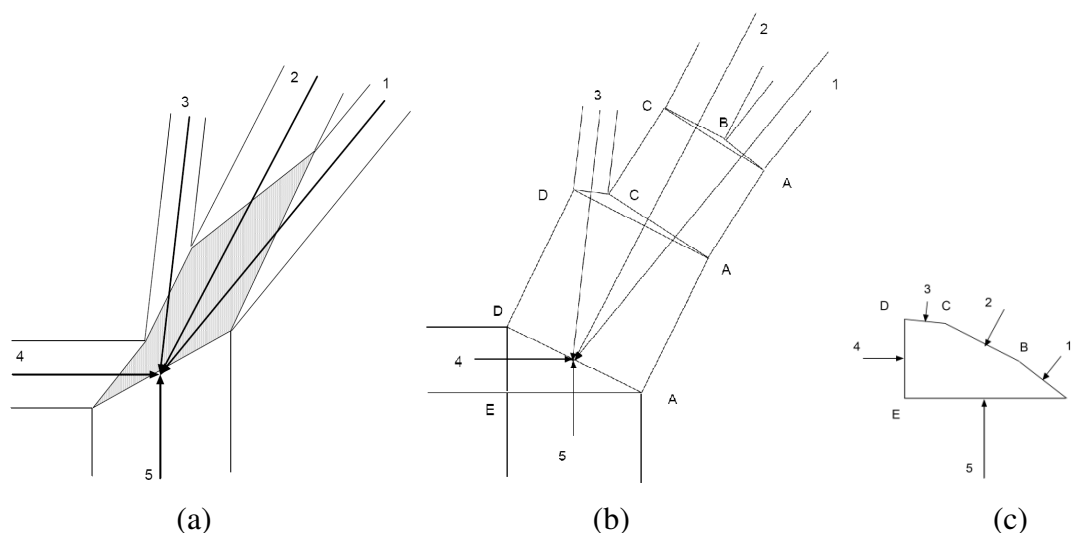
Figure 4.7   Nodes with overlapping struts (a) description of the problem, nodal zone geometry used by Kuchma in the software CAST, (b) solution proposed by Schlaich (1990), (c) solution proposed by Clyde (2008)

In his solution Schlaich (1990) systematically combines two adjacent struts, in order to obtain only simple nodes formed by the intersection of three struts, as illustrated in Figure 4.7 (b). The solution of Clyde (2008) is actually a variant of the solution proposed by Schlaich, without the intermediate struts between the triangular areas, as illustrated in Figure 4.7 (c). Consequently the main difference between the two solutions is that in Schlaich's solution the axes of all the struts intersect at the same point, while in Clyde's solution the resulting forces are not concurrent. However the moment equilibrium is still verified as all the triangle areas (ABC, ACD and ADE in Figure 4.7 (b) and (c)), which are common to both methods, are in equilibrium. This solution corresponds to what is usually done in practice, that is to say, to divide the support area in proportion to the incoming forces in the inclined struts and to divide the node in sub-nodes.

Nevertheless, these methods applicable quite easily in two-dimensions cannot be applied to three-dimensional cases, because the interface between the struts cannot be defined as easily as in 2-D and thus the consistency of the nodal zones would not be

preserved. An alternative method had to be found to conduct this work, which is suitable for three-dimensional nodal zones.

The method proposed here consists in checking the stress at the face of the node, from a hypothetical strut, resultant of all the converging struts located in the same quadrant. The axis of the resultant strut corresponds to the average between the directions of the converging struts, while the force in the resultant strut is equal to the projections of the forces in the different struts on this axis. Then the polygonal area of the resultant strut, on which the force is checked, is found as explained in the previous section.

The direction and the intensity of the force in the resultant strut are computed by:

$$\vec{F} = \sum_i F_i \frac{\vec{v}_i}{\left|\vec{v}_i\right|} \tag{4.6}$$

$$F = \left|\vec{F}\right| \tag{4.7}$$

Here $\vec{v}_i$ is a direction vector of the converging strut i.

For the construction and the analysis of the strut-and-tie model, all the converging struts located in the same quadrant should meet at the same point in the model.

If a model contains such kind of nodes, in many cases it also means that it is a statically indeterminate model. Then the designer has the possibility to rely on the stiffness of the struts and the ties or to make some choices to solve the indeterminacies. The different methods to deal with indeterminacy are further discussed in Section 4.7.2. The recommended method is to choose the proportion of the load carried by each strut. However, if the stiffness of the members should be used an iteration process could be used to define the areas of the converging struts as a proportion of the available area for the resultant strut.

It should be noticed that the method is applicable in the same manner to 2-D cases.

4.3.5 Position of nodes and refinement of nodal zones under concentrated loads

There are two types of nodes: the nodes located at external loads (columns or piles) and the intermediate nodes needed to build an appropriate strut-and-tie model for a structure.

The horizontal position of the nodes at load positions is often well defined except for cases where the centroids of the elements would not correspond. Concerning the intermediate nodes, chosen by the designer to build a strut-and-tie model which respect the limitations of angles, their position depends on the choice of geometry of the model.

The vertical position of nodes close to the edges of the structure (all nodes at loads and some intermediate nodes) depends on the choice of the height of horizontal struts and ties along the edges of the pile cap. In other words it depends on either a_s, the level of flexural reinforcement axis, or a_c, the level of horizontal concrete struts at the edges (under the columns in the case of a pile cap). It is convenient to choose the same height for the axis of flexural reinforcement in the two directions for the whole pile cap in order to simplify the design of the strut-and-tie model and the detailing of the nodal zones. Therefore, it is also recommended to consider that the reinforcement bars are alternated in the two directions if more than one layer is used, and then the

exact vertical position of the nodes can be chosen as the average between the heights in both directions. This alternation of flexural reinforcement layers in the two directions is also a better practice solution.

For other intermediate nodes located "within the pile cap", the vertical position depends on the choice of model geometry made by the designer.

According to the theory of plasticity, the horizontal position of the nodes at external loads may be chosen to minimise the inclination of the struts leaving the node. The method proposed consists in determining a sufficient bearing area with regard to the design bearing strength, and to choose the optimal arrangement of this area. Then the node is positioned on the axis of the resultant of the stresses acting on this bearing area. It is particularly favourable in the design of pile caps due to the usually large loading area and the influence of the strut inclinations on the forces in the members. The loaded areas should be chosen in order to minimise the distance to the connected piles. It should be noted however that this solution requires transverse tensile capacity of the column in its D-region.
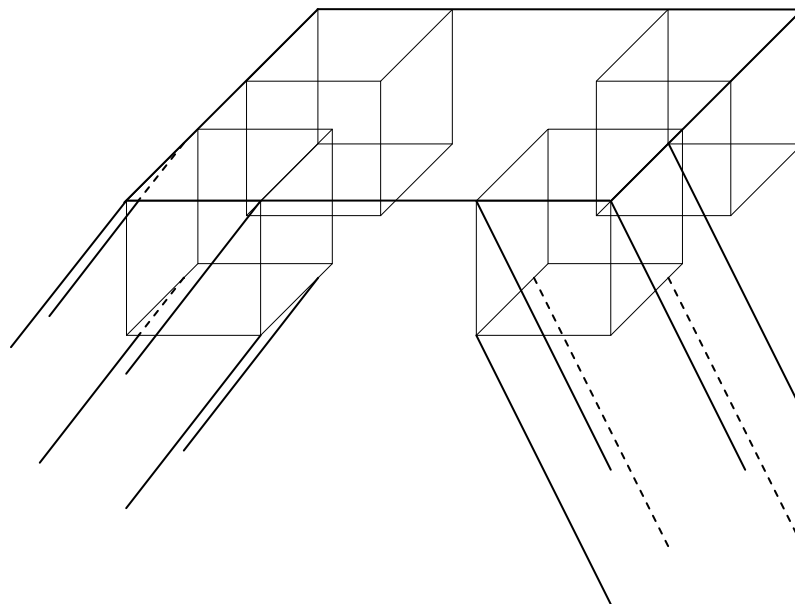
Figure 4.8   Refinement of nodal areas used in the strut-and-tie model for a 5C-node

The verification of the stresses in the struts acting on the nodal zones may require to modify the dimensions of the nodal zones. The choice of the horizontal and vertical dimensions of the parallelepiped nodal zones should be done iteratively in order to obtain the maximum admissible stresses and the most homogeneous stress distribution on the faces of the nodal zones, to assure a favourable triaxial compression state of stress in the nodal zones (Section 4.3.6).

The procedure is further explained in Section 6.2.3 for the simple case of a 4-pile cap and in Section 6.3.3, where the example of a 10-pile cap is treated, for which the bearing area at the column is divided into six smaller areas, with different optimal heights and sizes.

4.3.6   Strength values for 3-D nodal zones

In the case of nodes subjected to triaxial compression, the strength value of the concrete can be increased in the nodal zone. There must be only struts joining at these

nodes, and the magnitudes of the compression in the different directions have to ensure a secured triaxial state of stress in the nodal zone.

Some experimental results of tests conducted on cubes loaded by triaxial compression are presented in Figure 4.9. They show that rather low transversal stresses induce an important increase of the bearing strength. For instance, if the two transversal stresses are equal to 20% of the uniaxial cube strength, the strength in the third direction is in the order of two times the uniaxial strength. And if the two transversal stresses are equal to the uniaxial cube strength, the strength in the third direction is raised to approximately five times the uniaxial strength.

The method developed for the check of nodes with parallepiped nodal zones is particularly adapted to apply an enhancement of the strength due to triaxial compression, as it permits to check the stresses in the three-directions. In addition, the refinement of the nodal zone improves the three dimensional state of stress of the nodal zone, by assuring higher and more homogeneous stresses on all its faces.
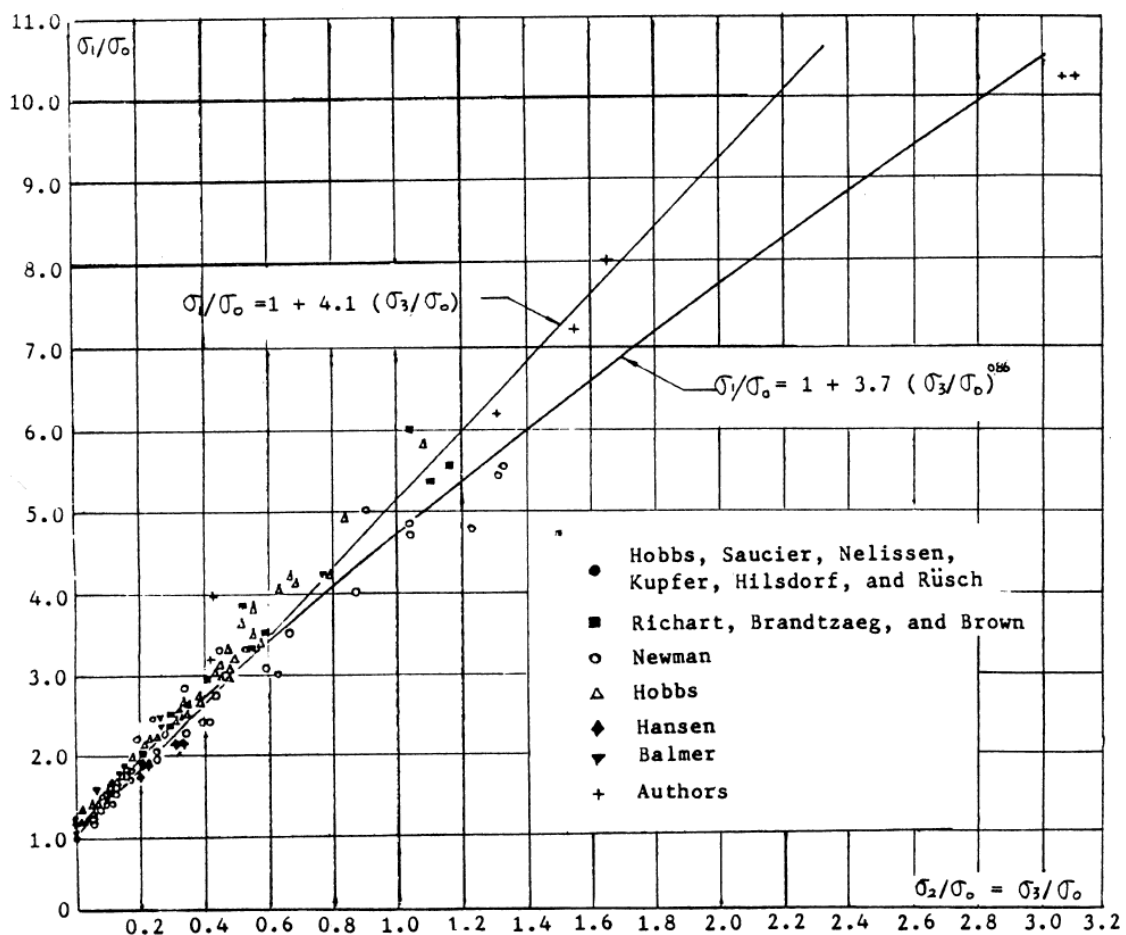
Figure 4.9   Results of triaxial compression tests conducted by Chuan-zhi (1987)

Several standards give recommendations for the triaxial compressive strength. Eurocode 2 gives the following upper limit for the strength, which may be used if the transverse stresses are known and bigger than $0.75 \cdot f_{ck}$:

$$f_{cd4} = k_4 \left(1 - \frac{f_{ck}}{250}\right) f_{cd} \qquad (4.8)$$

CHALMERS, *Civil and Environmental Engineering*, Master's Thesis 2010:51

with $k_4 = 3.0$ (recommended value EC2)

In the Recommendations of FIP (1999), the following value is recommended:

$$f_{cd4} = 3.88 f_{cd}$$ (4.9)

The choice has been made in this work to use the following strengths for design and analysis:

$$f_{cd4} = k_4 \left(1 - \frac{f_{ck}}{250}\right) f_{cd}$$ (4.10)

with $k_4 = 3$ in design (EC2 design value)

$k_4 = 3.88$ in analysis (FIP value with influence of the strength reduction factor depending on concrete strength)

4.4   Angle limitations in 3-D models

As for 2-D strut-and-tie models, some angle limitations have to be respected regarding the limited ductility of concrete and the need for strain compatibilities. The rules which applied for 2-D models (Section 3.5.1.1) can be adopted in 3-D. On the one hand, limitations impose for the spreading of a concentrated load, that the main inclined struts should be located in a cone, whose axis follows the direction of the load and makes an angle of about 30 degrees with the generatrix (aperture about 60 degrees, and not more than 90 degrees). On the other hand, the angle between struts and ties has to be above a certain limit. However in 3-D, the limitations should apply to the real angle between the tie and the strut, which is different form the angle between the tie and the projection of the strut in the vertical plane of the tie. Like in 2-D, this angle should be around 60 degrees, and not less than 45 degrees. This angle can easily be calculated by the following formula, using the scalar product between the direction vectors of the strut and the tie.

$$\theta = \mathrm{acos}\left(\frac{\vec{v}_{strut} \cdot \vec{v}_{tie}}{\left|\vec{v}_{strut}\right| \cdot \left|\vec{v}_{tie}\right|}\right)$$ (4.11)

4.5   Design load

A pile cap is designed for many load cases. The load cases concern the load from the superstructure which is applied on the pile cap usually by columns. The load effect can be separated, at the interface between the column and the pile cap, into a vertical force, horizontal forces, bending moments and a torsional moment. The other loads to take into consideration are the self weight of the pile cap and the weight of the soil overburden. In the case of a strut-and-tie model it is convenient to represent these two loads by forces at the column base, which is a safe side approximation. The design loads for which the pile cap has to be designed consist in combinations of the permanent load (self-weight of pile cap and superstructure) and different variable loads. How to deal with the different load cases in design with strut-and-tie models is further discussed in Section 5.2.3.

4.6   Forces in the piles

Several options can be chosen in order to define the reaction forces of the piles.

The first one consists in assigning these forces as external loads acting on the pile-cap. Then some choices have to be made by the designer. He or she can either assume the pile cap to be rigid and use simple statics to calculate the reactions. Note that in the case of a vertical force, it can be achieved directly in the strut-and-tie analysis by assigning a low stiffness to the piles (Figure 4.10 b). The designer can also use another more advanced method, like a finite element analysis. At Skanska, nowadays, a flexible-elastic behaviour is considered to calculate these forces for the design of the pile cap.

The second method consists in finding the forces in the pile by the FE-analysis of the strut-and-tie model, using the stiffness of the struts, the ties and the piles (Figure 4.10 a). This method will be further discussed in Section 4.7 for internal static indeterminacy.

It would be interesting to compare the forces in the piles obtained by the strut-and-tie analysis of a pile-cap using the real stiffness of the elements to those obtained with the flexible-elastic method, and to experimental values, in order to see if the reaction forces provided by a strut-and-tie analysis are reliable and if they could give more accurate values than the method used in design nowadays. Some explanations are given in Section 4.7.2 on how the stiffness of the elements in the strut-and-tie model can be assessed.
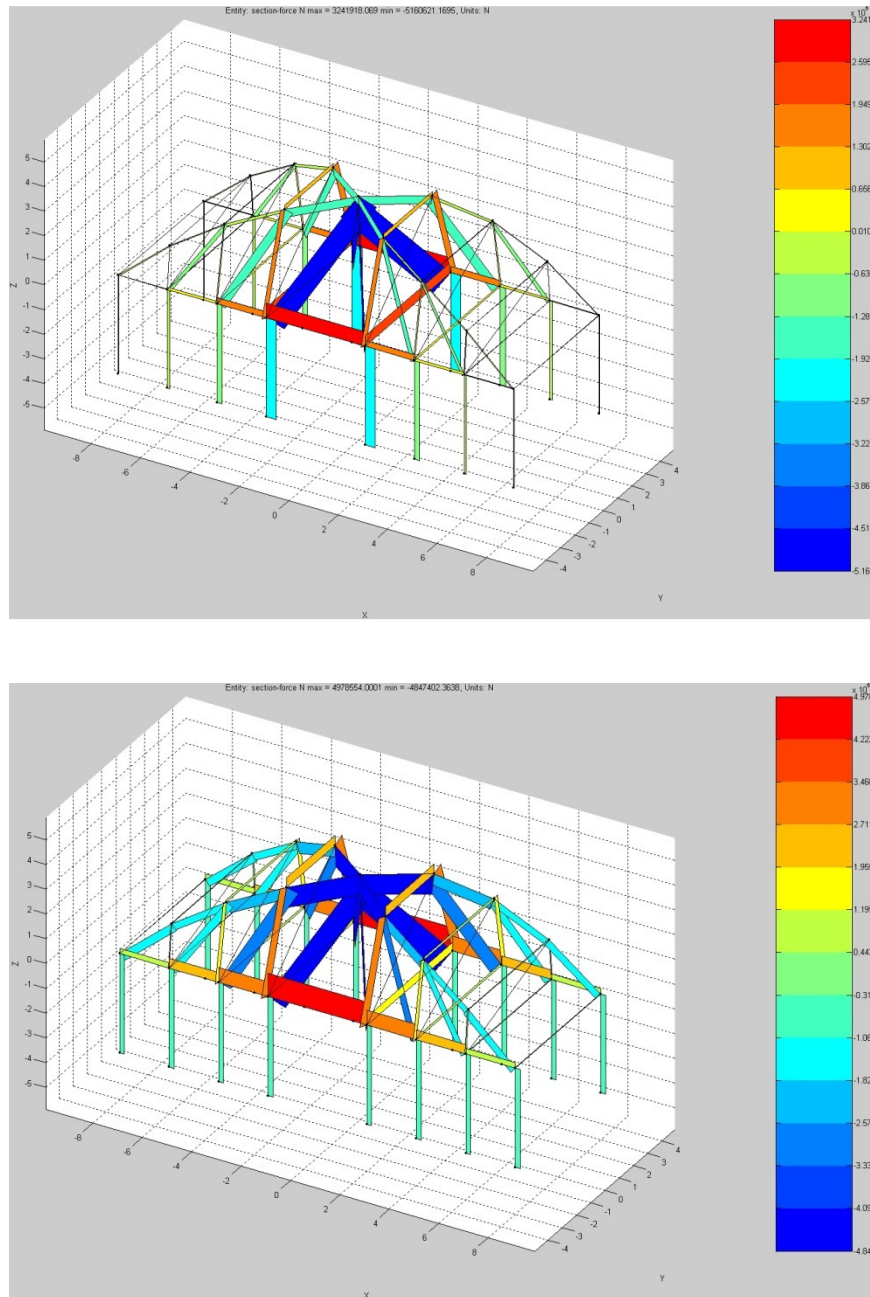
*Figure 4.10   Force distribution in a strut-and-tie model subjected to a vertical load obtained **(a)** with the real stiffness of the piles, **(b)** with a low stiffness of the piles. The stiffness of the struts and the ties are given and equal in both models.*

4.7   Discussion about the geometry of the models

4.7.1   Different approaches envisaged

The final aim of this project was to create a program for calculating easily the reinforcement of pile-caps, knowing the dimensions of the pile-cap, the pile coordinates and the load (the inputs). Therefore the final achievement would have been the development of a routine which can create a strut-and-tie model for any given combination of inputs.

During this thesis work, much thought concerned the geometry of strut-and-tie models for pile caps. Lots of models have been programmed and analysed to get ideas for the choice of the geometry and if possible to generate models automatically for various pile caps.

Two kinds of model were studied, which follow two different approaches of the strut-and-tie method. On the one hand singular models were considered (Figure 4.11) for which attention was paid to the load conditions and the elastic stress fields resulting. These models would require adaptations for specific load combinations. On the other hand, general models were considered that did not take into account the load case but only the geometry of the pile cap and the position of the piles (Figure 4.12). The purpose of these models was to obtain a strut-and-tie geometry that could easily be computed automatically and adapted to different load combinations.
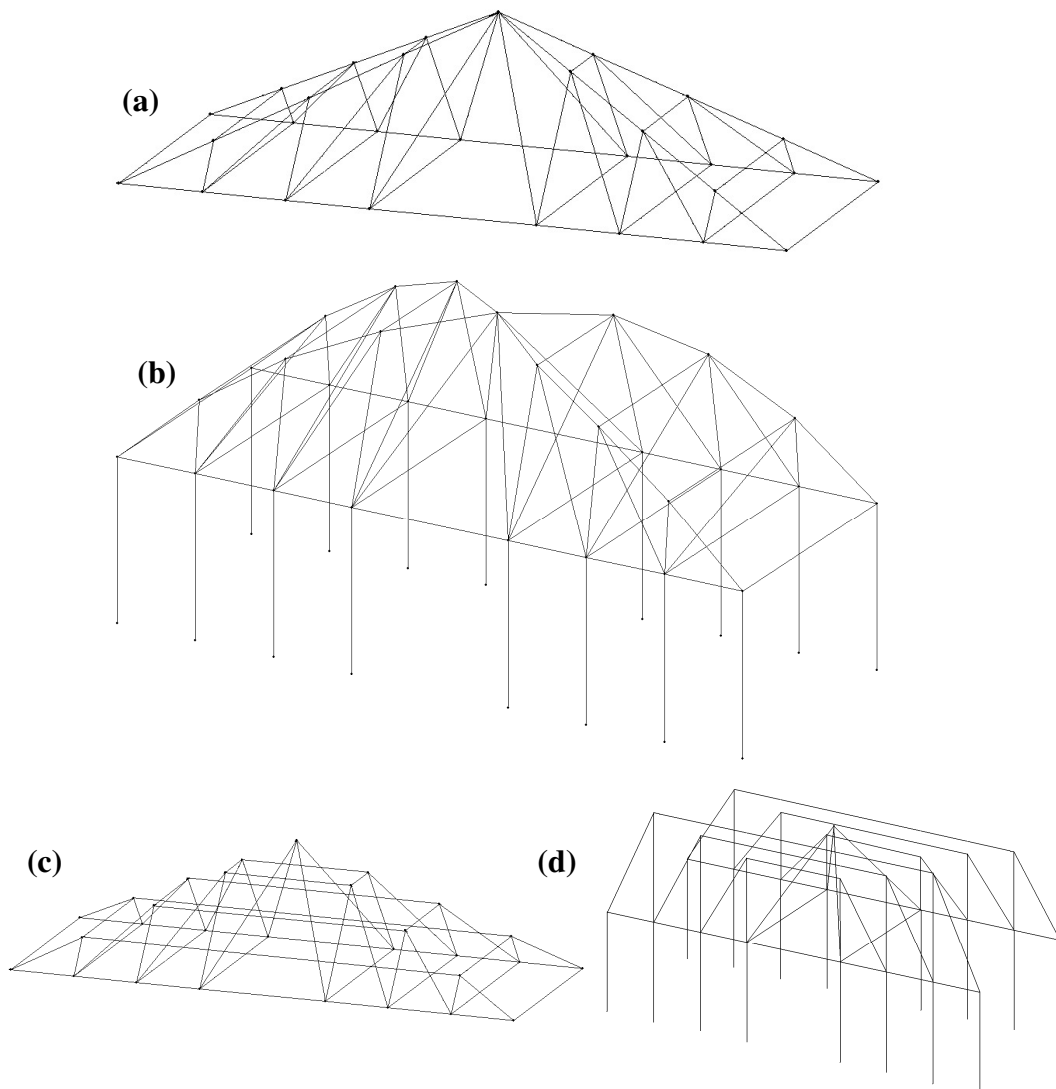
*Figure 4.11   Example of singular strut-and-tie models for a 16-pile cap subjected to a vertical load from a column **(a)** simple model with direct arch action and truss action using inclined stirrups, **(b)** enhancement of previous model using parabolic shape, **(c)** modification of elements in previous model to obtain a model statically determinate internally, **(d)** combination of 2-D and 3-D models to allow for vertical stirrups*
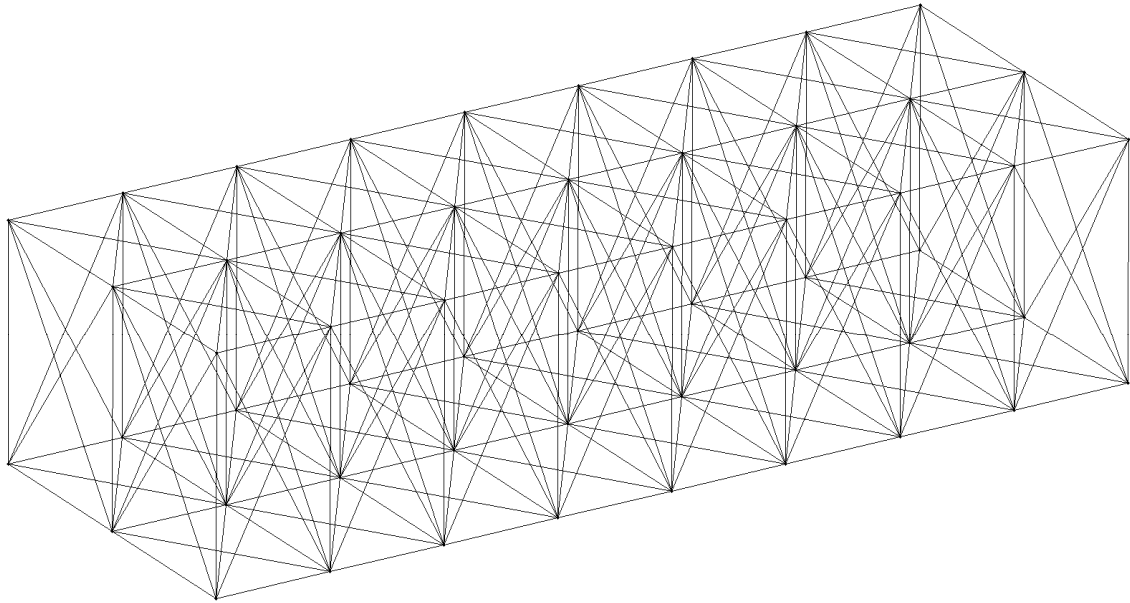
Figure 4.12   General strut-and-tie model for a 16-pile-cap

In general models the stiffness of the diagonal members working in tension is reduced by an iterative process, in order to keep only compression in the other diagonals and to keep only vertical and horizontal ties.

The singular model provides a force distribution close to the elastic stress field, while the general model requires a lot of plastic redistribution (Figure 4.13) and a higher amount of steel. Therefore the idea of general models does not seem to be appropriate without further refinement; it does not really comply with the strut-and-tie rules.
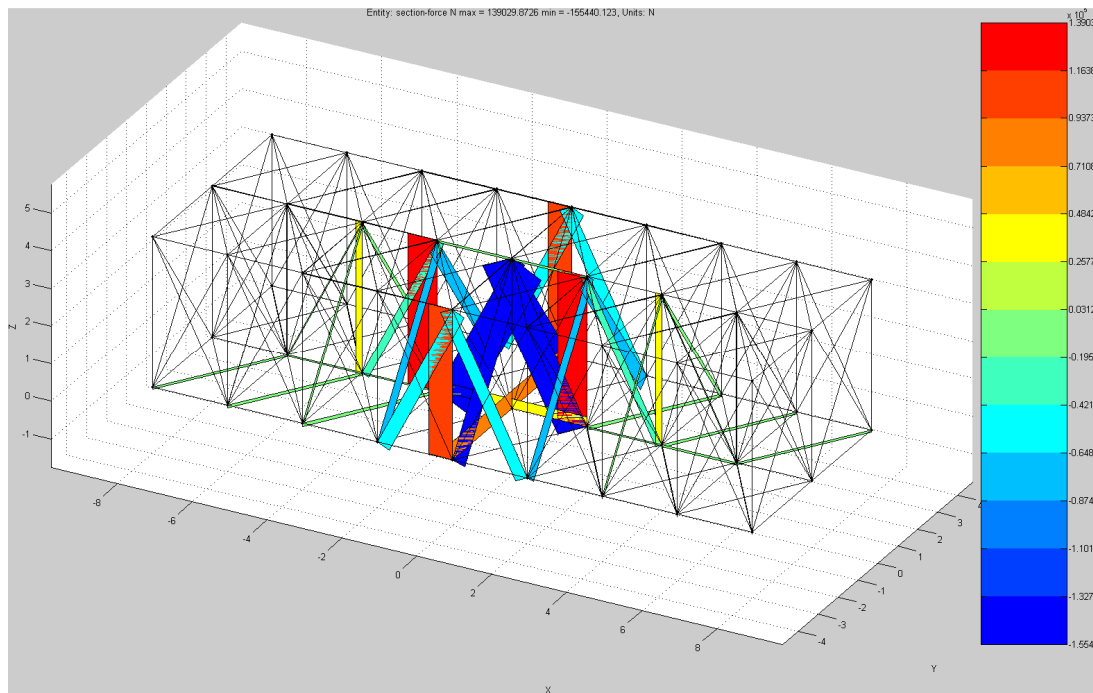
Figure 4.13   Force distribution in the general model under a vertical load applied at the middle, with given stiffnesses for struts and ties and after removal of the inclined ties (the picture illustrates the results after the 1st iteration, where some low loaded inclined ties appeared)

4.7.2   Procedures for statically indeterminate strut-and-tie models

In the case of a statically determinate model, the forces in the members will remain the same when the stiffness of these members changes for a given load. Therefore the forces in the strut-and-tie model are only dependant on the geometry of the model and not on the sectional properties of the members.

On the other hand, when a strut and tie model is internally indeterminate, the distribution of forces will depend on choices made by the designer, either on the stiffness of the elements or on the part of the load carried by each member. It is the same problem as for solving external indeterminacy for the loads in the piles, treated in Section 4.6.

4.7.2.1   Stiffness of the struts and the ties

The method to use the stiffness of the members of the strut-and-tie model was investigated at the beginning of this work. However, the results obtained were not compared to other methods. The investigation of the reliability of the stiffness of the struts and the ties to solve indeterminacy would constitute an interesting subject, which motivated the writing of these few comments.

The stiffness of the struts and the ties in an elastic analysis depends on the E-modulus of the material, and the length and area of the elements. The E-modulus, the length and the areas of the ties (area of steel) being clearly defined in a model, the uncertainty relies on the area of the struts. The struts' area should be equal to their area at the concentrated nodal zones, the nodal zones being considered as parallelepiped nodal zones whose dimensions are taken as the minimum according to the allowable bearing stress at the faces. The area of some struts obtained at concentrated nodal zones permits then to find the undetermined areas of other struts at

smeared nodal zones. The area of struts for which two different areas are defined at each end should be considered equal to the average between them. This assumption results in a lower stiffness of struts in the case of bottle shape struts.

This method requires to make preliminary assumptions, and then to use an iterative procedure to find the area and the position of the members until convergence. This method would be appropriate to analyse strut-and-tie models with plastic analysis.

4.7.2.2   Choices made by the designer

The other method consists in choosing a reasonable strut-and-tie model and to solve the remaining indeterminacies by rational choices. In this thesis work this method has been finally preferred. The strut-and-tie models used are based on two types of load transfers between the column and the piles (as explained in Section 5.3.2): truss action and direct arch action. The models based on one of these transfer are chosen as statically determinate, the combination of both leads then to one degree of indeterminacy at each interface, which is solved by assigning the proportion carried by each model.

5 Description of aspects specific to pile caps and implementation in the strut-and-tie model developed

5.1 Introductory remarks

The mechanical and detailing specificities associated to piles caps are treated in this chapter. Indeed, piles caps mechanical behavior is quite characteristic. In order to conceive efficiently a pile cap, the designer requires approaches to design of reinforced concrete structures that may differ from the ones he or she is used to. A classification of the specific aspects related to the design of pile caps is made. For each aspect treated, an effective implementation solution in the model developed, or design detailing for the pile cap is proposed.

Firstly, pile caps are designed for a precise structural function which is to carry concentrated load from the superstructure down to the foundation piles. In addition, pile caps are prone to be subjected to a wide range of load cases due to variable loads acting on the structure like wind, snow or earthquake actions. These aspects are discussed in section 5.2: *Structural function of pile caps*.

Secondly, measures were taken and implemented in the model in order to account for pile caps typical geometry, as explained in section 5.3: *Geometry of pile caps: deep three-dimensional structures*. Sections 5.3.2: *Duality between shear transfer of forces by direct arch and by truss action in short span elements* and 5.3.4: *Strength criterion for cracked inclined struts* are believed to be of particular interest as some innovative design approaches are proposed.

The last part, section 5.4: *Reinforcement arrangement and anchorage detailing*, inquires about different reinforcement layouts and anchorage solutions for pile caps and compares their comparative efficiency.

5.2 Structural function of pile caps

5.2.1 An interface between the superstructure and the substructure

Pile caps constitute the interface between the superstructure and the foundation piles. The purpose of pile caps is to transfer the load from the superstructure in a safe manner to the piles.

In order for the whole structure to be safe, each of these three elements, namely the superstructure, the pile cap (interface) and the foundation piles has to be safe. A major simplification comes from the fact that pile caps are very stiff structures which means that they can almost be considered as rigid. Therefore the load distribution between the piles is mainly dependant on the resulting force and moment applied at the column and on the stiffness of the piles themselves. The assumption of infinite rigidity of pile caps is sometimes used in design practice. However it is common at Skanska to consider the stiffness of the pile cap when determining the pile load distribution. For instance, linear elastic finite element models are sometimes used.

Nevertheless, uncertainties concerning the soil and pile stiffnesses make the pile loads difficult to predict. The difference between the loads applied on two different piles can be quite significant and is rather unpredictable, see Figure 5.1. In addition, when

piles are put into soil containing clay or moraine like in Västra Götaland, the load distribution between the piles becomes highly time dependant. For instance, at a young age a non negligible part of the load will be carried directly to the ground by the bottom of the slab. During some months, years or decades, the soil consolidates and settles under the pile cap, reducing the part of the load carried by the pile cap itself. This load is transferred to the piles, increasing greatly the compressive stresses in the top part of the piles.
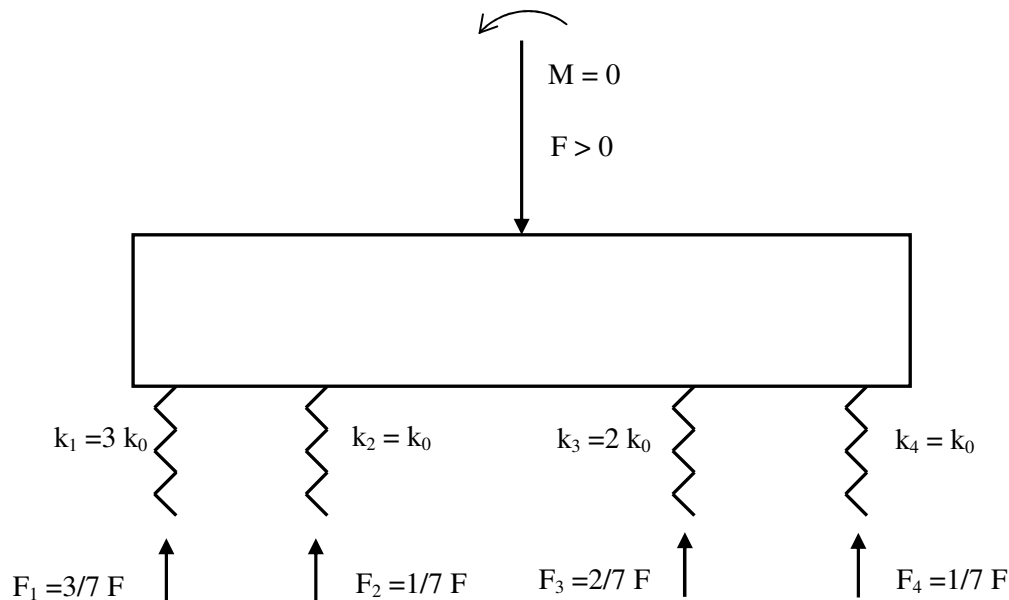
Figure 5.1   Possible load distribution between piles in a pile cap

In practice, piles are driven in soft soil with an inclined direction to the vertical (with a characteristic slope between 1:4 and 1:5), the piles slightly pointing toward the nearest column. As the piles point toward the load application point, a transverse component of the force can be carried by the piles, therefore reducing the necessary amount of flexural reinforcement in the piles. In addition, this inclination is interesting in order to carry possible transverse shear forces and moments in the piles. It should be pointed out that the piles direction and orientation of their profile, in the case of square piles, are prone to rather large uncertainties. However, it is not unusual at Skanska to measure the actual position and inclination of piles on site and take it into account for the design of the pile cap. In the 3D strut-and-tie model developed, all the examples were treated assuming vertical piles, which is on the safe side. However the program developed is able to take into account inclined piles if chosen by the designer.

The large uncertainties linked to soils mechanical behaviour is dealt with by geotechnical engineers by providing a statically indeterminate set of piles associated with large safety factors.

The geotechnical approach to uncertainty and safety in design can be troublesome for structural engineers. As an interface between the superstructure and the substructure, pile caps require a proper cooperation between the two fields in order to avoid misunderstandings and inappropriate designs.

CHALMERS, *Civil and Environmental Engineering*, Master's Thesis 2010:51

5.2.2   A structural element subjected to concentrated loads

Pile caps are often used in structures where high loads have to be carried on rather small areas. Therefore, piles associated to pile caps are often chosen as a foundation solution in the case of multi-storey buildings and in bridges for example. In the case of civil engineering works like the ones carried out at Skanska Teknik, pile caps are often loaded by columns, thus they are subjected to concentrated loads on both sides, by the piles and the columns. For this reason, pile caps are prone to fail locally by punching shear, close to the bearing areas. Therefore, the punching shear phenomenon is treated in section 2.2.

Nowadays, the Swedish concrete design handbook, BBK04, or the Concrete handbook – structural design are used by Skanska designers in order to evaluate the punching capacity of pile caps at the columns and at the piles. The impulse that gave birth to this thesis is that the designers, from their mechanical and practice experience, felt that the amount of reinforcement required by the Swedish design recommendations was not rational and probably too conservative for pile caps.

In the last decades, many of the main building design codes in the world were proved to be inappropriate and sometimes unsafe for the design of pile caps. Kani (1979) showed that sectional approaches were not rational and too conservative for deep and short elements, while strut-and-tie models manage to capture the real trend of the structures' shear capacity, see Figure 5.2.
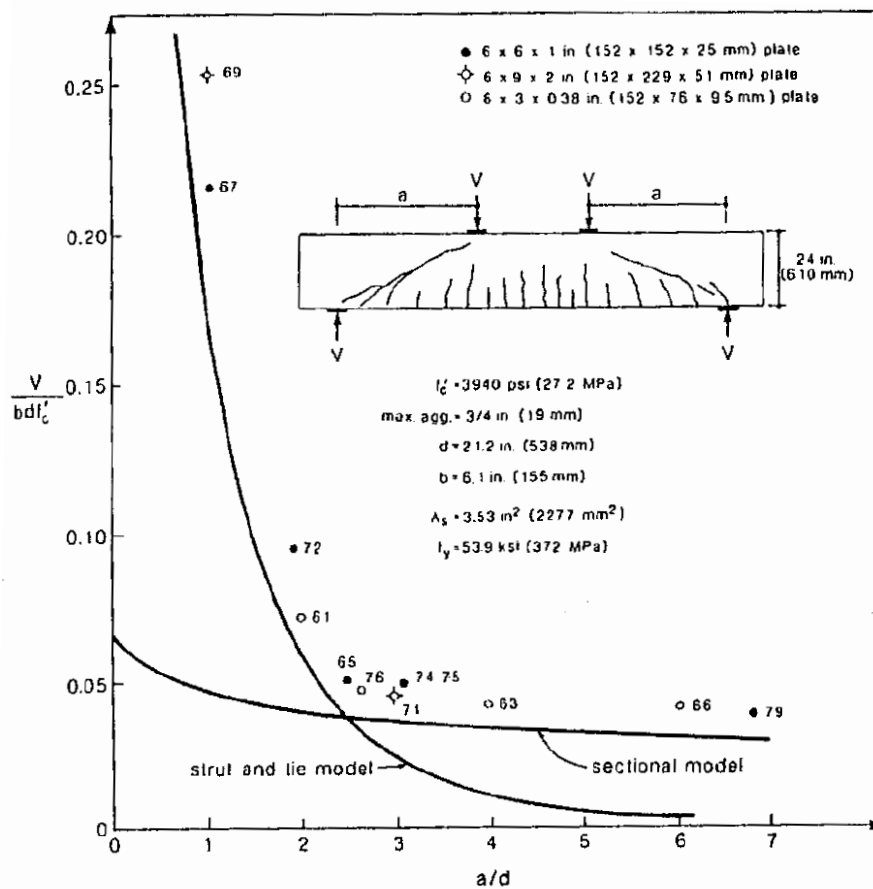
Figure 5.2   Predicted and observed nominal shear capacity of a series of beams depending on the aspect ratio, Kani (1979)

Therefore the strut-and-tie method was first implanted in the Canadian design code, which was then followed by the American and the European codes of design. Designers are now allowed and advised to use strut-and-tie approaches in the case of deep elements.

5.2.3 A structural element subjected to a wide range of load cases

Pile caps are prone to be subjected to a wide range of load cases due to several variable loads acting on the structure like wind, snow or earthquake actions. Therefore, pile caps must be designed to carry several load combinations.

Assuming that every pile has the same stiffness and that the pile cap is loaded by a single column, four types of design situations can be distinguished depending on the ratio between the vertical load and the moment applied at the column (M/N ratio). For each of these four cases, a simplified representation of a possible distribution of forces inside the pile caps is illustrated below. Note that the drawings refer to 2-D models like in beams; in pile caps, the choice of a strut-and-tie model can be more complicated.

(a) No moment resulting in a constant compressive normal stress in the column, equal compression in each pile, Figure 5.3.
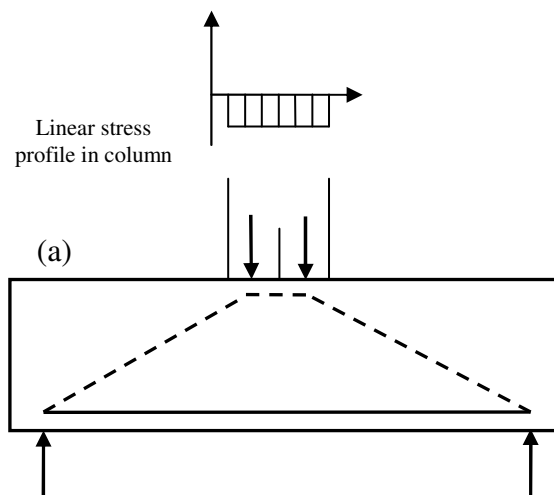
Figure 5.3   Strut-and-tie model for a case with no moment in the column

(b) Small moment resulting in variable normal compressive stresses in the column and variable compressive forces in the piles, Figure 5.4.
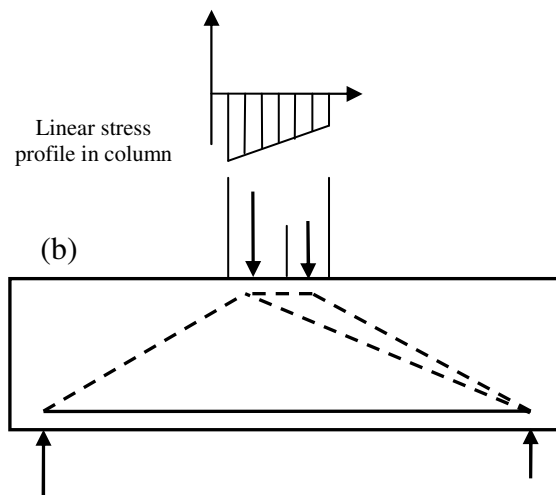
Figure 5.4   Strut-and-tie model for a case with small moment in the column

(c) Average moment resulting in both compressive and tensile normal stresses in the column but only compressive forces in the piles, Figure 5.5.
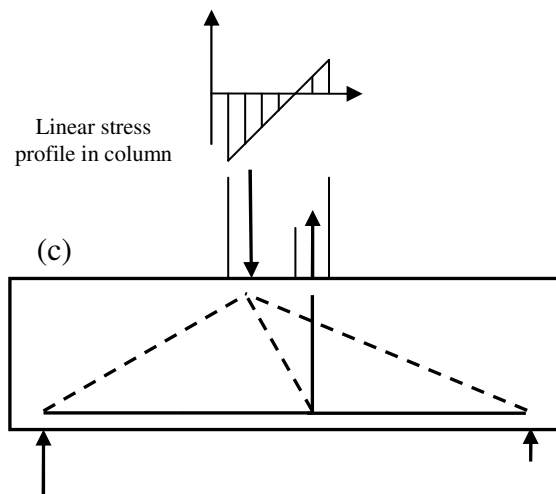
Figure 5.5   Strut-and-tie model for a case with moderate moment in the column

(d) High moment resulting in both compressive and tensile stresses in the column and a combination of piles loaded in compression and in tension, Figure 5.6.
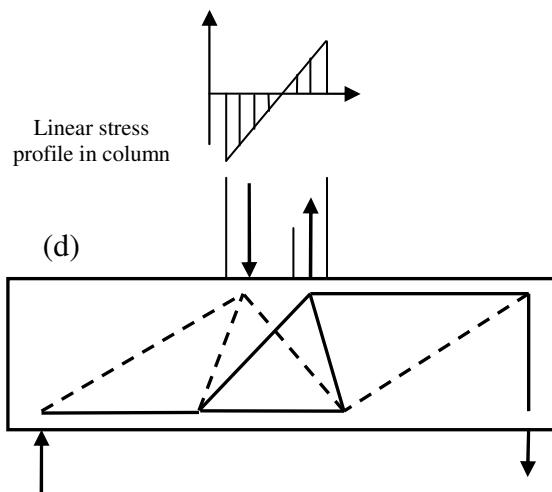
Figure 5.6   Strut-and-tie model for a case with high moment in the column

In practice at Skanska it is common to use some simplifications on the safe side for these different cases. For instance, in case (b) the most loaded pile is on the left and the left part of the pile cap is more critical than the right one. Assuming that no dominant direction is chosen for the moment induced by external loading, each quadrant of the pile cap should be designed for the most critical case. Case (b) can be treated by applying the load of the most loaded pile to the four piles, which means that case (b) can be treated with an equivalent strut-and-tie model similar to case (a).

The same kind of procedure can be applied for case (c). Indeed, it is possible to say that one of the quadrants (represented by the left part of the beam in Figure 5.5) is exposed to the highest compressive stresses. Therefore each of the quadrants should be designed to carry this possible load case and it is possible to refer to case (a) with increased load for all the piles. However, in case (c), some tension is found below the column and this should be considered in the design. Thus, if the designer considers that the magnitude of the tension is too high for concrete and minimum reinforcement alone to carry, then some extra reinforcement should be provided. For example a vertical stirrup like the one shown in Figure 5.5 is an acceptable solution. Of course, the same procedure applies for each direction and reinforcement should be provided equally in the four quadrants below the column.

In the particular case (d) it is not possible to refer to case (a) because of the tension in some of the piles. Therefore, the designer should consider an additional strut-and-tie model.

For the model developed in this thesis work, it is possible to calculate the needed reinforcement arrangement for a wide range of load cases with moments applied at the columns by referring to an equivalent strut-and-tie model similar to the one in Figure 5.3. However, when some piles work in tension, a different strut-and-tie model has to be provided; an example is given in Figure 5.6. In this case, if, for example, no dominant direction for the moment is given, each quadrant of the pile caps has to be designed for the case where maximum compression is found in the pile (the strut-and-tie model in the left part of Figure 5.6 could be used for example) and for the case where maximum tension is found in the pile (the strut-and-tie model in the right part of Figure 5.6 could used).

Pile caps are subjected to a wide range of load combinations. However, a limited number of strut-and-tie models are necessary in order to handle them.

5.3 Geometry of pile caps: deep three-dimensional structures with short spans

5.3.1 Design methodology adapted to three-dimensional structures

A pile cap typically shows large dimensions in all three directions as illustrated in Figure 5.7.
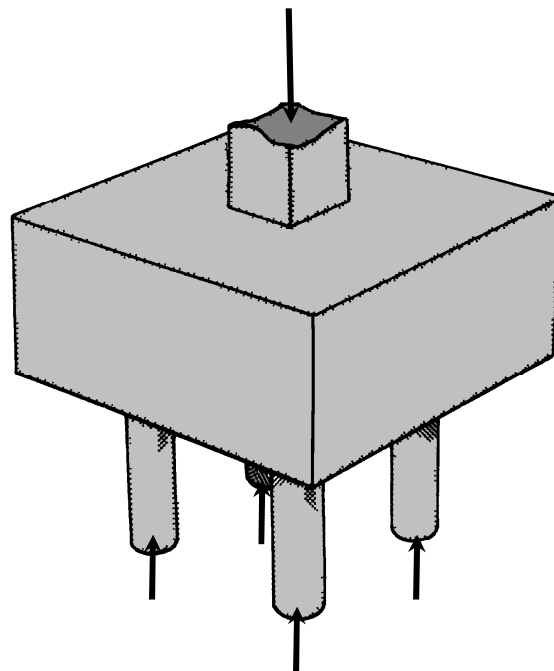
Figure 5.7   Stocky 4-pile caps

Because of this geometrical feature, pile caps do not strictly obey to simplified sectional approaches normally used to design most of reinforced structural elements. Pile caps cannot rigorously be considered as beams (design using beam or deep beam theory), neither as slabs (slab and flat slab design approach) and neither as walls (shear wall or plate theory). Two solutions are then possible for such three-dimensional elements:

On the one hand, the designer can keep using an empirical superposition of sectional approaches. These methods are explained in Chapter 2. In these methods a pile cap is alternatively considered as a beam for the bending capacity and for the one way shear strength, as a slab for the punching capacity and somehow as a shear plate when accounting for the size effects (i.e. shear capacity reduction due to the increase of crack widths with increasing height of the plate).

On the other hand, the designer can base the design on a study where the complete transfer of forces in the pile cap is considered at once. For instance, this could be done based on the theory of elasticity using fine mesh finite element analysis. This thesis work is based on another methodology, less demanding in powerful calculation tools:

the perfect theory of plasticity applied to reinforced concrete. A lower bond design approach called the strut-and-tie method is used.

5.3.2 Duality between shear transfer of forces by direct arch and by truss action in short span elements

In section 2.1.2.4: *Mechanisms of shear transfer in cracked concrete* the different shear transfer mechanisms that can occur in reinforced concrete structures were stated. Out of this discussion two families of reliable shear transfer mechanisms were distinguished: "direct arch action" and "truss action" as seen in Figure 5.8.
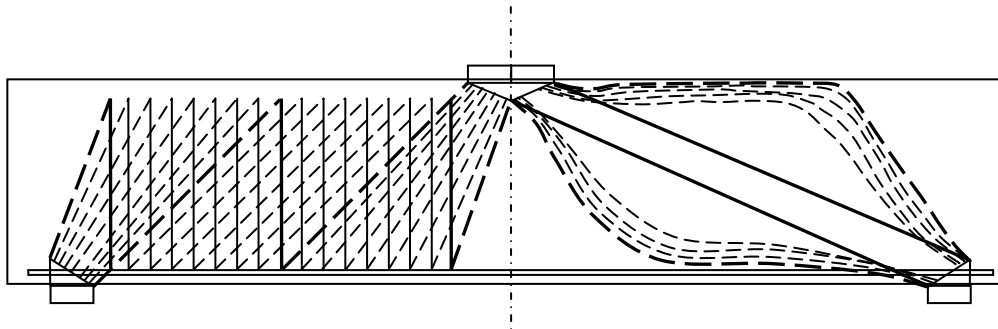
Figure 5.8   Shear transfer of forces by direct arch action with bottle-shaped strut and truss action with fan struts

There is a fundamental difference between these two families, as explained in section 2.1.2.4. The "truss action" directly relies on tension in the web, in concrete or in shear reinforcement, in order to transmit shear forces otherwise it cannot take place. On the other hand, the "direct arch action" can exist without an orthogonal tension field to the compressive strut in the web. However, due to strain compatibility, transverse tension develops (the so-called "bottle-shape" effect), that can lead to cracking that will reduce the capacity of the compressive strut. Nevertheless, if concrete cracks in the compressive struts, the need for transverse tension will decrease and a new equilibrium with narrow struts will occur. Note that this equilibrium does not rely on any tension in the web.

In the strut-and-tie model developed in this thesis the tensile strength of concrete is not considered in the "shear transfer of forces by truss action". Therefore, in a strut and tie model, where concrete is only used in compression, shear reinforcement will be needed every time a part of the load is transferred by "truss action", while they can be avoided if the load is only transmitted by "direct arch action"

Stating that 100% of the load is transferred by direct arch action, see Figure 5.9, will provide a design without vertical reinforcement. This kind of design is attractive due to its simplicity.
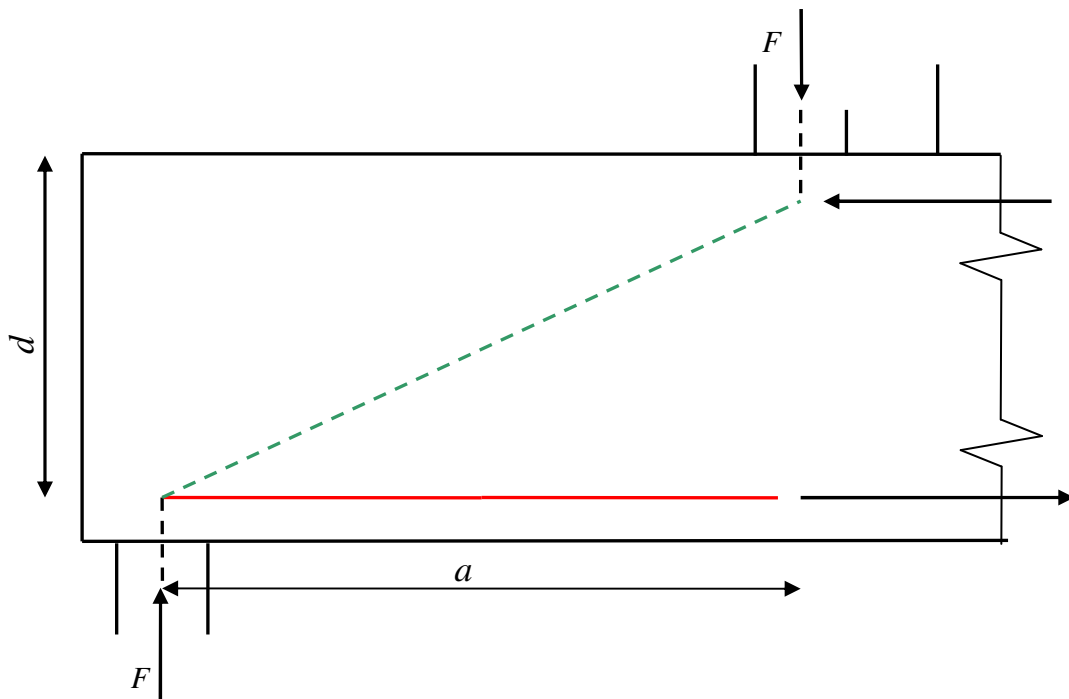
Figure 5.9   Force transfer by "direct arch action"

Note that *a* is defined as the distance between the resultant of the forces considered; *a* corresponds to the projection along a horizontal axis of the distance between the nodes in a strut-and-tie model. This definition differs from the simplified definitions of the level arm often considered in design (like the distance from the middle of the pile to the column face). *h* is the sectional depth of the pile cap, *d* is the effective depth and *F* is the magnitude of the applied load at the considered pile.

However the development of "direct arch action" alone can only occur for rather stocky pile caps. If a very slender pile cap is designed considering the strut-and-tie model showed in Figure 5.9 only, it will be given a huge amount of flexural reinforcement and no shear reinforcement at all. This pile cap will fail due to sliding shear for a load smaller than the intended failure load. Indeed, in the case of very slender pile caps the structure will develop a stress field in the ultimate state very different from the one presented in a simplified way in Figure 5.9. This ultimate state stress field is close to a pure "truss action" stress field, transverse tension in the web will cause critical cracking that will weaken the direct strut up to a shear failure. If the design was made considering that the structure was ductile enough to develop the stress field in Figure 5.9, it could lead to a *non conservative design* due to a sliding shear failure before yielding of the flexural reinforcement.

Stating that 100% of the load is transferred by beam action means that the *entire load* has to be pulled up by the shear reinforcement, see Figure 5.10.
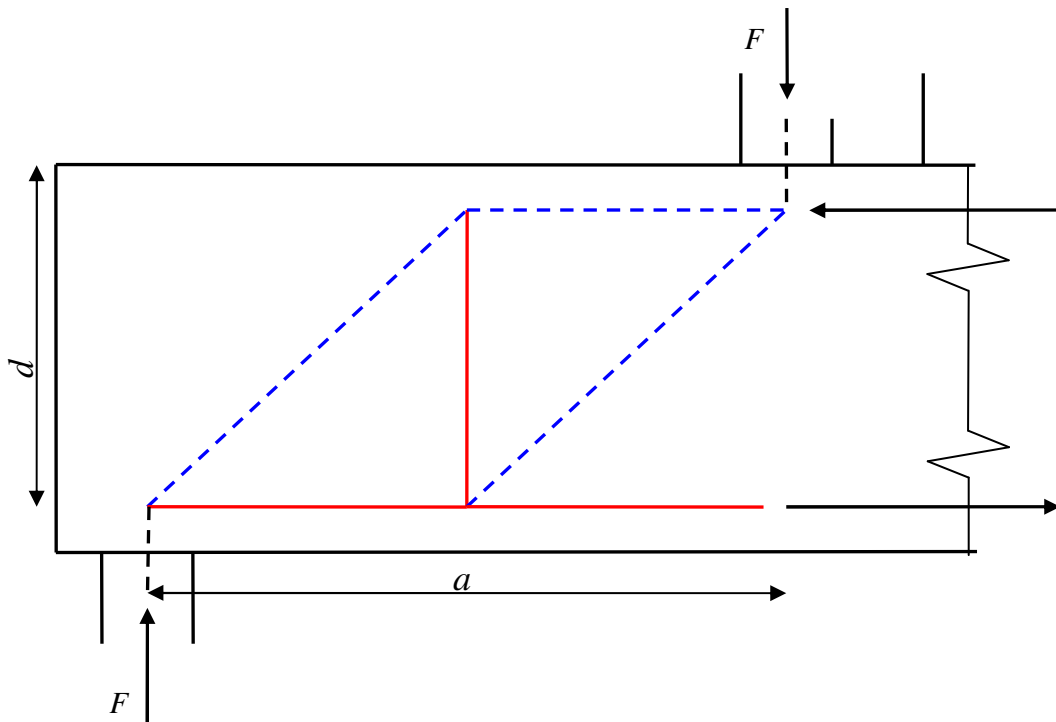
Figure 5.10   Force transfer by "truss action"

Pure truss action is the kind of model used for the design of slender flexural elements for example. However, this design would be *too conservative* in the case of stocky pile caps, where a major part of the load is transferred by direct compression struts.

In most of the strut-and-tie models used in design nowadays a concrete element is either considered as "stocky" and direct arch action only is taken into account or as "slender" in which case the entire load has to be pulled up by the shear reinforcement according to the truss model.

However, pile caps, like deep beams are often in a range of dimension where "direct arch action" and "truss action" both carry a significant part of the load, see Figure 5.11.

Based on this observation, a model for deep elements was developed in this thesis project where the load transfer to the support consists on the superposition of the shear transfer of forces by "direct arch action" and by "truss action"

The part of the load carried by each of these actions is statically indeterminate. As the strut-and-tie model relies on the lower bound theorem it is possible, in the frame of the plasticity theory, to choose this distribution. The choice of the distribution is the core issue in the model.
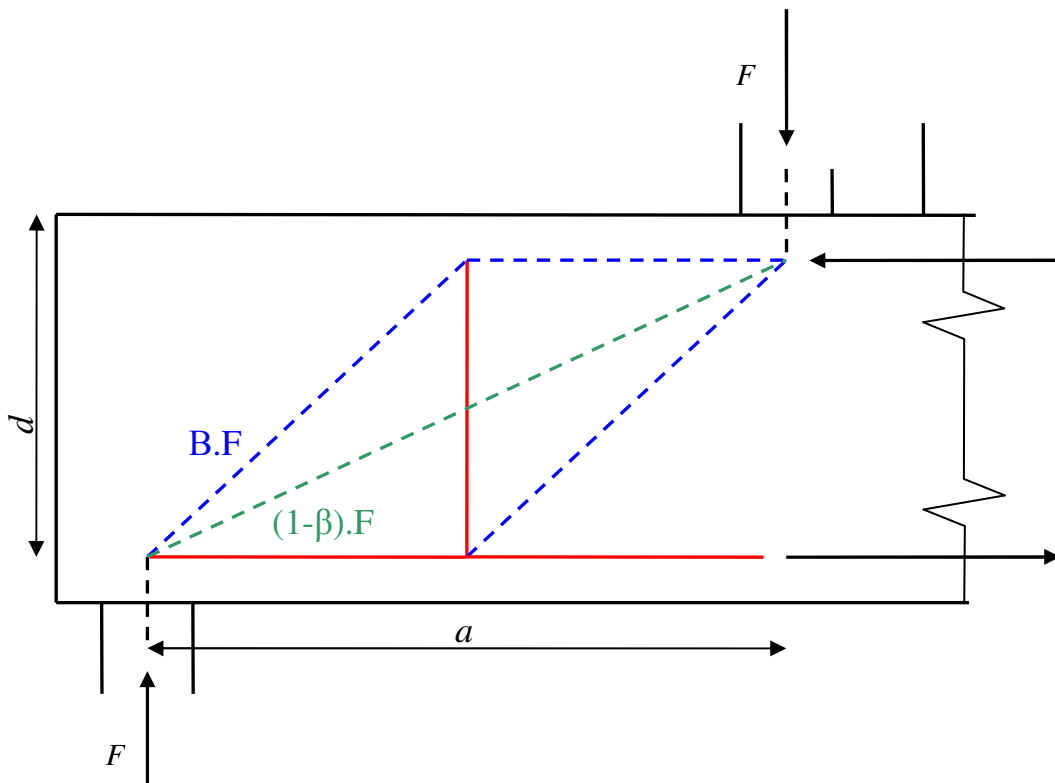
Figure 5.11   Transfer of forces by combined "direct arch action" and "truss action"

One idea developed in this thesis work, is too choose the ratio *β* of the shear force that the structure should carry by "truss action" in the ultimate limit state. The ratio *β* is defined as the actual shear force resisted by truss action divided by the actual total shear force in the ultimate limit state:

$$\beta = \frac{shear\ force\ resisted\ by\ truss\ action}{total\ shear\ force}$$

The design criterion selected in order to give a value to this distribution ratio *β* is expressed as follows:

The actual distribution ratio between the load transferred by "truss action" and the total load transferred in the structure in the ultimate limit state should be close to the one selected when designing the structure.

Once again, it should be pointed out that the ratio *β* is defined for the <u>actual</u> state of internal stresses in the ultimate limit state. The ratio *β* is dependent on several factors, the main parameters are: the geometry of the element, the concrete strength, the steel strength, the reinforcement arrangement and the loading history (related to the cracking pattern). Therefore, the ratio *β* cannot be exactly defined with an elastic analysis in a preliminary or design state.

However, the point here is to develop a design method and therefore the ratio *β* in the ultimate state should be evaluated in order to provide a safe and economical design. The core idea in this section is to define the ratio *β* depending on the geometry of the element only.

In other words, the influence of the reinforcement arrangement is considered to have less influence on the shear transfer mechanism than the geometry of the element. For

example, in the ultimate limit state, a very slender element will actually carry almost 100% of the load by truss action with or without flexural reinforcement, with or without shear reinforcement. In the same manner, a stocky element will carry a great part of the load by arch action before failure, whichever the reinforcement arrangement is.

In order to avoid misunderstandings, note that the failure mode and the type of internal stress field in the ULS (i.e. close to a direct arch action stress field or a truss action stress field, see Figure 5.8) is not directly link to the failure mode of the element. For example, in the case of a very slender element made of plain concrete, even if the internal stress field is close to a pure "truss action" stress field just before failure, the element will most probably fail in flexion as the tension in the bottom chord is the most critical.

Of course, the part of the load carried by "truss action" and by "direct arch action" respectively is influenced by the reinforcement arrangement and by the other factors (concrete strength, load history, etc…). Nevertheless, the assumption is made that, if the ratio β is calculated based on the geometry of the element only and if the amount of shear reinforcement provided is calculated in order to carry a load equal to $\beta x F$, then the proportion of the load carried by truss action just before failure will be close to β.

This assumption is wrong because a part of the stirrups capacity will be used in order to carry the tension induced by the bottle-shape effect. However in the rest of this thesis project, for the sake of simplicity, the β factor will be considered and referred to as the ratio between the actual shear force carried by stirrups and the total shear force in the ULS as well as the ratio between the shear force carried by truss action and the total shear force in the case of members with transverse reinforcement.

For the choice of β, a first proposition can be made inspired by the EC2 approach for loads applied close to the supports, as explained in section 2.1.3:

$$\beta = \frac{a}{2d}$$

With $0,5d < a < 2d$ (i.e.: $0,25 < \beta < 1$), d being the effective depth. When a, as defined in Figure 5.11, is smaller than $0,5d$, β is taken equal to $0,25$.

The second proposition is taken form "FIP recommendations (1999): Practical design of structural concrete" to:

$$\beta = \frac{1}{3}(\frac{2a}{z} - 1)$$

With z the internal level arm. When a is smaller than $0,5z$ no stirrups are provided.

This last proposition considers more transfer of forces by direct arch action than the one derived from Eurocode and was selected for the model developed in this thesis work. However, it is up to the designer to use the other definition of β if an agreement with Eurocode is preferred. The complete methodology for design of shear reinforcement and check of shear capacity of pile cap is found in section 5.3.6.

Figure 5.12 shows an example of a test on a pile cap carried out by Adebar, Kuchma and Collins (1990) where the steel strain was measured in the flexural reinforcement. The pile cap has outer dimensions D x d' x $H = 2360m$ x $1700mm$ x $600mm$ without stirrups. The design was based on an identical pile cap designed to resist 2000kN and

the amount of reinforcement was then doubled to study possible failure modes before yielding of the flexural reinforcement.
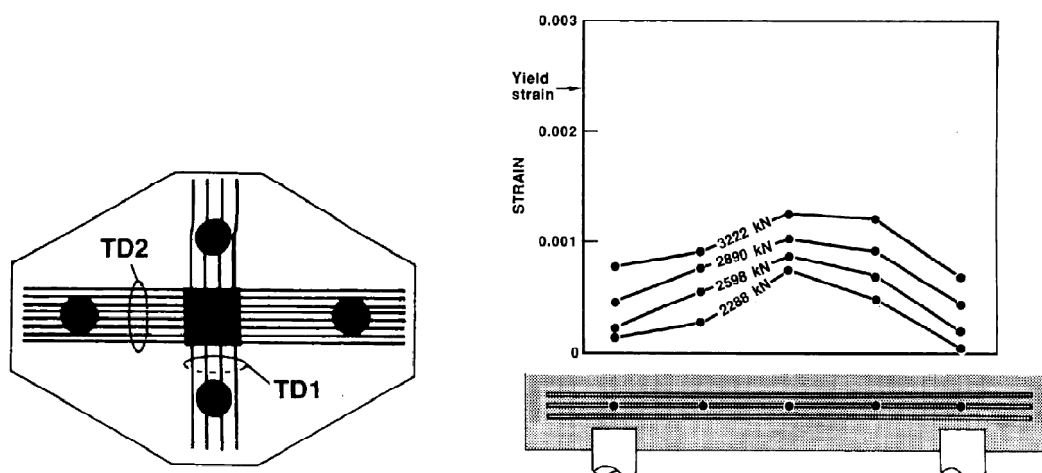
Figure 5.12   Distribution of tensile strain in the flexural reinforcement in the long span measured in a 4-pile cap without shear reinforcement (Adebar et al. 1990)

When designing this pile cap, the designers considered that 100% of the load was transferred by "direct arch action", using a strut-and-tie model following the Canadian design code recommendations. Therefore, as the pile cap does not contain stirrups and as the tension capacity of concrete was neglected, the only acceptable equilibrium model for the strut-and-tie model is the one shown in Figure 5.9. However, the real behaviour of the structure was different from what was supposed for design. For instance, for a load of 2288kN (i.e. 71% of the ultimate load) almost no tensile stresses are found in the flexural reinforcement over the piles which means that, for this load level almost all the load is carried by truss action using ties of concrete. Only a small part of the load is carried by direct arch action. The tension created at the node is taken by the concrete that is mostly uncracked as the strains are around $0,1x10^{-3}$, see Figure 5.12. A possible strut-and-tie model is shown in Figure 5.13.
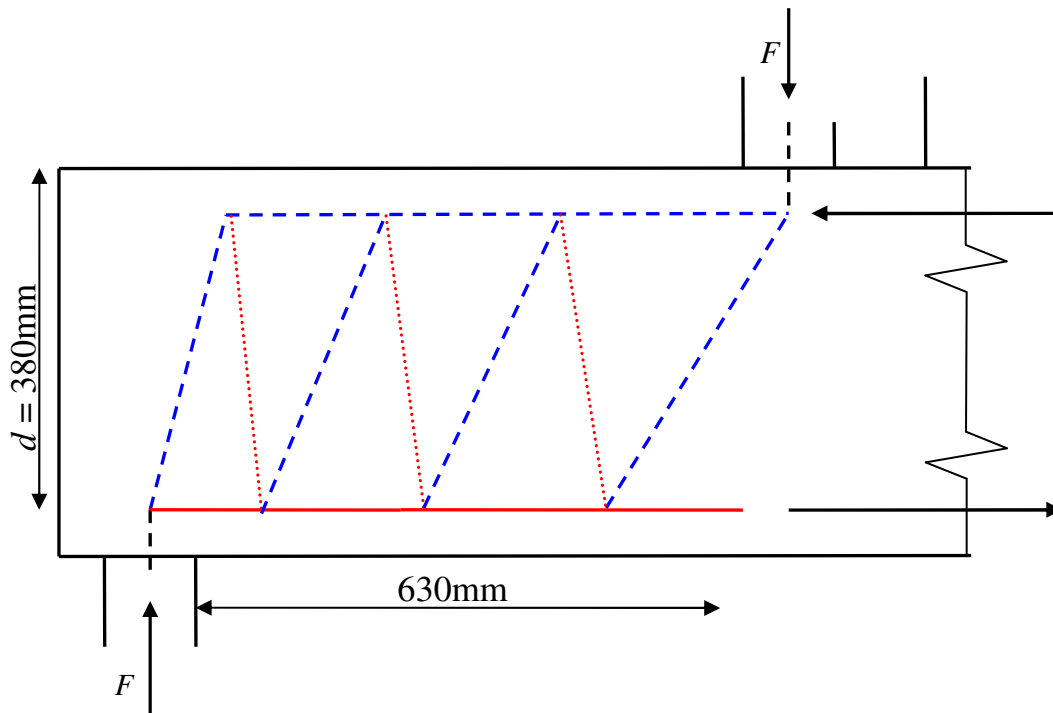
Figure 5.13   Transfer of forces by truss action without stirrups where no tension is found in the reinforcement over the piles

The red line represents the steel ties and the dotted lines represent the concrete ties. As the concrete is mostly uncracked close to the support, the bottom chord has a mechanical behaviour close to the one of plain concrete. For this reason a concrete tie is represented.

When the structure carried 71% of the ultimate load, the hypothesis that 100% of the load is transferred by direct arch action is completely wrong. However this remark does not challenge the design criterion proposed above which applies only for loads in the ultimate limit state (close to the actual failure load). Indeed, when the load in the test reached the actual failure, at 3222kN, the ratio between the part of the load carried by "direct arch" and "truss" actions is completely different. The tension at the anchorage level over the piles reached 75% of the tension in the middle of the pile cap (instead of almost 0% before). The model in Figure 5.14 can be chosen to model the actual state of equilibrium. The virtual concrete tie perpendicular to the direct strut is considered to be close to the actual direction of principal tensile stresses in the concrete in the web. This concrete tie is global and represents the average direction of the principal stresses. In order to understand all the different mechanisms that allow shear transfer in cracked concrete without stirrups, refer to section 2.1.2.4. Solving the static equilibrium leads to that 58,7% of the load is carried by direct arch action and 41,3% of the load is carried by truss action at failure.
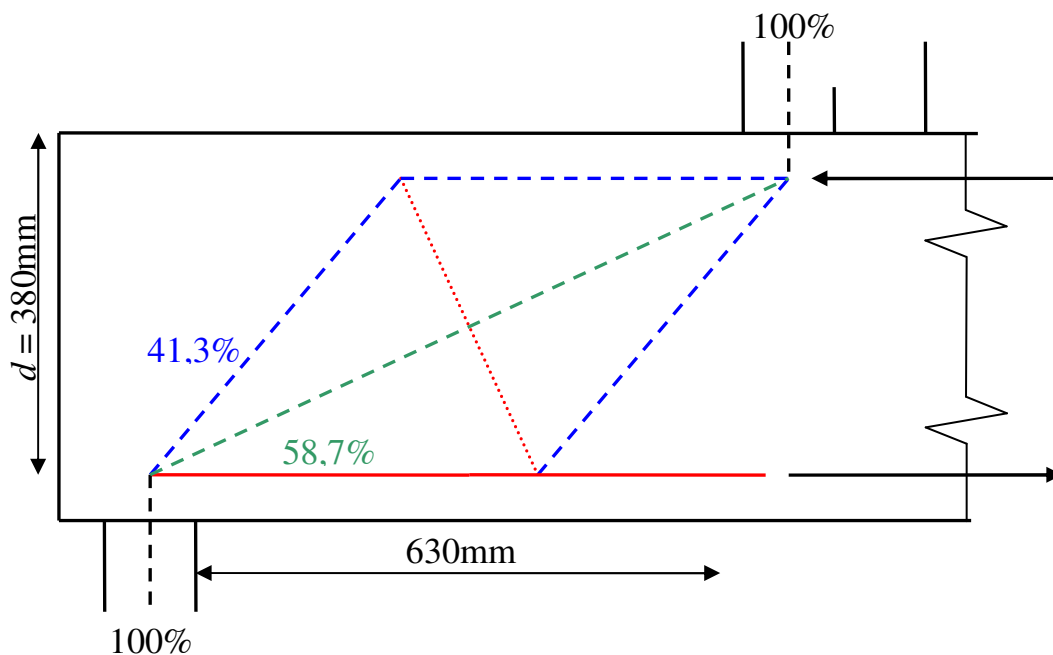
Figure 5.14   Simplified model with a concrete tie perpendicular to the compressive strut

This pile cap was originally designed considering the equilibrium model in Figure 5.9 that states that 100% of the load is transferred by direct arch action. However, at failure, only about 60% of the load was carried by arch action while the rest was carried by truss action making use of the concrete tensile capacity. The tension induced in the web by the truss action lead to the development of cracks that resulted in a shear failure of the structure before the flexural steel could be fully utilised. For instance, the strain in the flexural steel at failure was around half of the yield strain. From this point of view the design can be considered as non economical as the pile cap could have had almost the same bearing capacity with way less flexural reinforcement. It should be noted that this pile cap did not respect the criterion defined in this thesis work:

The actual distribution ratio between the load transferred by "truss action" and the total load transferred in the structure in the ultimate limit state should be close to the one selected when designing the structure.

The distribution of forces the pile cap was originally design for was rather different than the actual one at failure.

In the model proposed in this thesis the pile cap described in Figure 5.12 would have been designed differently. In fact stirrups would have been provided and designed to carry 88% of the vertical component of the load. By doing so a better control on the repartition of forces in the pile cap at failure is achieved.

5.3.3   Influence of confinement in three-dimensional structures

Confinement by inactive concrete is a feature of great interest in the model developed in this thesis project. Inactive concrete is defined as volumes of concrete that are subjected to low stresses. In well designed strut-and-tie models these volumes are the ones that are far from any strut or tie. It should be noticed that, due to the

characteristic geometry of pile caps, a very important amount of concrete is inactive. This feature is clearly pointed out in a strut-and-tie model, for example in Figure 4.1.

Important volumes of inactive concrete in a reinforced concrete structure give rise to important internal restraint when the element is loaded. These internal restraints can have a positive and a negative effect:

5.3.3.1 Deformation limitations due to internal restraint from inactive concrete

Deformation limitations due to internal restraint from inactive concrete have some *negative* effects on pile caps. Indeed, even for rather little deformation or load levels, a highly internally restrained structure can develop wide cracks that would deteriorate the bearing capacity of the structure. As a result, important redistribution of forces cannot take place in a pile caps because they require large deformations to develop. When the structure is loaded, the inactive concrete restrain For instance, steel reinforcement can hardly develop its ultimate strength because the need for deformation is not acceptable for the highly restrained structure. These facts are taken into account by drastic limitations on the choice of a strut-and-tie model for a pile cap:

Stress fields in pile caps cannot be chosen as antagonist as in flexural elements. As a result in the strut-and-tie model, the angle between two struts or a strut and a tie cannot be chosen as small in a pile cap as in a flexural element. For instance, in the model developed a very drastic choice was made to limit the admissible angle between the average strut inclination and the main horizontal tie to $\theta > 60$ degrees at the concentrated nodal regions and to $\theta' > 45$ degrees at smeared nodal regions, as shown in Figure 5.15.
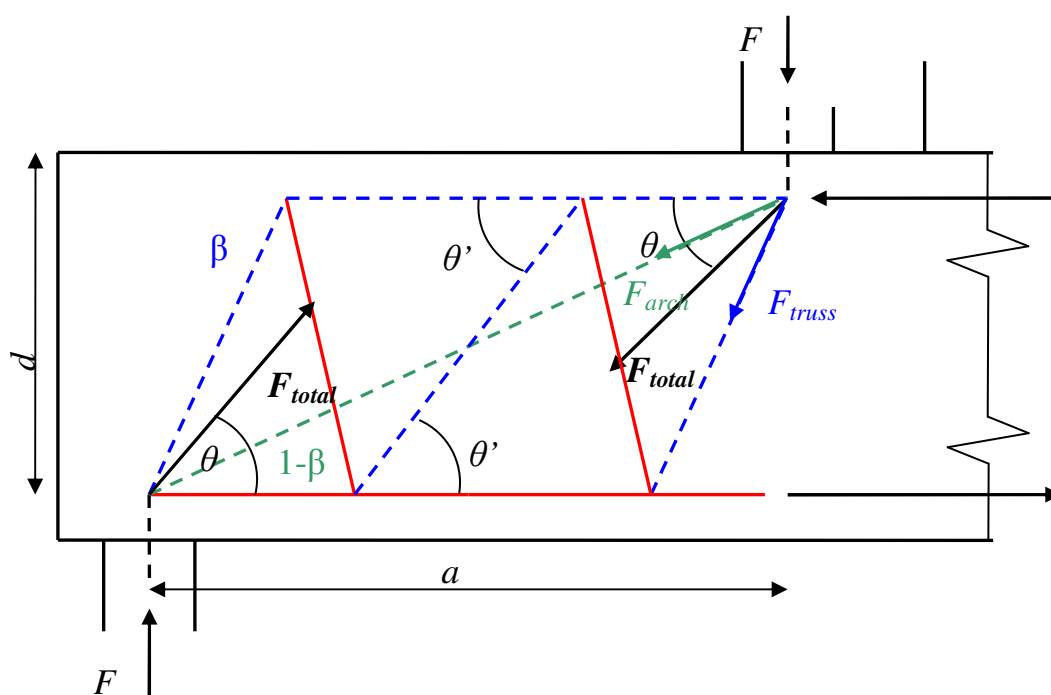
Figure 5.15   Limitations of angles between inclined compressive stress fields and the mean horizontal tie in the strut and tie model

F_{total} is the resultant of the forces transferred by arch action and truss action at the support; the vertical component of F_{total} is equal to the force F applied at the pile.

It should be noticed that deformations in the service state are never critical for pile caps due to the high deformation limitation induced by internal restraint from inactive concrete. Indeed, it is likely that a pile cap fails before unacceptable deformations are reached. Therefore deformations in the serviceability limit state are normally not checked in pile caps. It is interesting to see that these explanations about the deformation limitation of highly restrained structures can somehow be applied to prestressed and post-tensionned elements as well. The high restraint by inactive concrete is also the reason why pile caps can be considered as very rigid in comparison to the piles, leading to the fact that the load distribution between the piles is mainly dependant on their relative stiffness and on the load case, but not on the distribution of forces in the pile cap.

5.3.3.2 Compressive stresses induced by internal restraint from inactive concrete

Compressive stresses induced due to internal restraint from inactive concrete have a *positive* effect on pile caps. In this thesis work, this effect is called "confinement by inactive concrete"; it can be defined as the radial compression that develops around the compressive struts far from nodal regions.

Confinement by inactive concrete reduces greatly the tendency of compressive struts to develop transverse tensile stresses within the strut, hence increasing the compressive capacity of these struts. However, confinement by inactive concrete does not have an important effect on the capacity of the nodal areas below the columns, which are already subjected to a triaxial state of stress due to the loading conditions. The effect of confinement by plain concrete is also limited at the nodal areas above the piles where the support and incoming struts compressive pressures in the nodal region have an important magnitude.

Both triaxial compression due to the loading and to the confinement by plain inactive concrete lead to the choice of a failure criterion for concrete subjected to a multi-axial state of stress. In qualitative terms, the compressive capacity of a concrete strut is enhanced by compression in the other directions and decreased by tension in the other directions. A failure criterion depending on the triaxial state of stresses at the nodes is fundamental in a strut-and-tie model and is proposed in any design recommendation guide. A proposition for failure criterion of nodal zones is then presented in Section 3.6.3.3.

The procedure to evaluate the shear capacity of pile caps is not very relevant in design codes as pointed out in Chapter 7. The main reason is that the shear capacity of pile caps is evaluated in traditional sectional approaches as the lower value of the beam shear capacity and the punching shear capacity. However, stocky pile caps barely fail in a classic sliding failure mode as assumed by the equations of beam and punching shear. On the contrary shear failures in pile caps often have the form of a combination of splitting and crushing of the inclined struts in the web.

The shear capacity of a pile cap is better represented by the capacity of the inclined strut with regard to splitting and its ability to transmit compressive forces after cracking, than by traditional building code formulations for sectional design. The quality of the criterion for the strength with regard to splitting/crushing of the inclined struts going from the column to the pile is decisive for the reliability of the model. However failure criteria for inclined struts surrounded by inactive plain concrete are seldom. This comes from the fact that wide elements distributing loads in three dimensions like pile caps are rather complicated and not that often studied. The model

developed in this thesis considers that the shear capacity in rather stocky pile caps without stirrups should be expressed as the load carrying capacity of a cracked inclined strut crossed by a tension field and surrounded by large volumes of inactive concrete. The shape of the strut is taken into account with great attention. A design method is proposed and presented in the Section 5.3.4 which follows.

5.3.4   Strength criterion for cracked inclined struts

The purpose of this paragraph is to define a strength criterion for cracked inclined struts surrounded by large volume of inactive concrete and crossed by a perpendicular tension field.

Strut-and-tie models normally provide safe designs by considering the state of stresses in critical concentrated regions. However, sometimes the failure is dependent on what happens away from these concentrated regions. For example, in Figure 5.16 a crack will form at middle height first, reducing the capacity of the specimen to carry compression leading to an early failure of the cylinder. Therefore, considering that only the triaxial compressive state of stress under the bearings is decisive would lead to unconservative design. The geometry of the specimen far from the nodal regions has a great influence on its compressive capacity. Hence, when plain concrete without enough distributed transverse reinforcement is subjected to concentrated loads, the risk for splitting failure has to be taken into account.
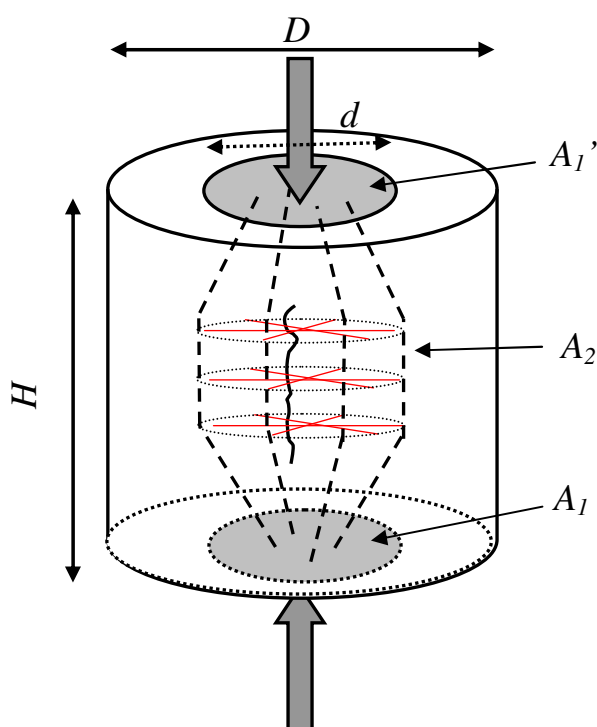
Figure 5.16   Splitting in a concrete cylinder, tension develops in radial directions

Figure 5.17 shows experimental results on the influence of transverse tension due to bottle shaped stress field when the tension is resisted only in one direction, like in walls or deep beams. In that case, the specimen cracked for bearing stresses between $0.9\,f_c$ down to $0.5\,f_c$ in the worst case (for D/d approximately equal to 2) and failed for a range of bearing stresses between $0.9\,f_c$ and $0.75\,f_c$. After more refined analysis, a

lower value of $0,6 f_c$ was derived and is commonly used as a bearing stress limitation in strut-and-tie models for deep beams subjected to concentrated loads for example.
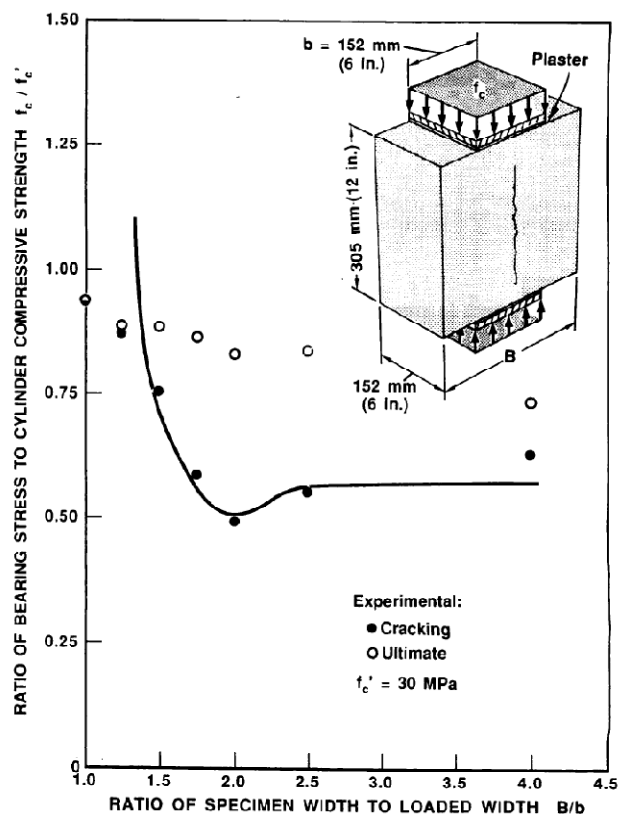
Figure 5.17   Influence of self generated transverse tension on the cracking load and ultimate load of a specimen of plain concrete (Adebar et al. 1990)

In the case of a double-punch test, as shown in Figure 5.16, the compressive stresses spread in all radial directions resulting in radial tension in the middle of the specimen also resisted in all radial directions. In a double-punch test the risk of splitting is less decisive than for the two-dimensional case because:

1. A rather low opening of the bottle shape results in a great increase of the bearing area at mid-height, meaning that less transverse tension is created for the same increase of bearing surface.

2. As the tension is resisted in all radial directions (see the red lines in Figure 5.16), the tensile stresses are reduced in each single direction.

3. The tension in the bottle shape is reduced thanks to the confinement provided by surrounded concrete, see Section 5.3.3.2.

The study of double punch tests carried out by Chen (1972) and Adebar and Zhou (1996) revealed that the maximum bearing stress allowed in cylinder splitting tests, like the one shown in Figure 5.16, was dependant on the geometry of the cylinder and the size of the loading plates. The maximum bearing stress at failure varied between $1,0 f_c$ (in the case when $D/d=1$, uniaxial compression) up to $3,5 f_c$ when both the ratios D/d and H/d were high. The approach developed in this thesis work was inspired by the formulation of Adebar and Zhou (1996) to evaluate the strength of inclined compressive struts in pile caps.

The principle of the method developed in this thesis is to evaluate the shear capacity of stocky structures by considering the splitting/crushing strength of the web far from the nodal zones. The web is idealised to an equivalent concrete cylinder with dimensions dependant on the geometry of the pile cap, as shown in Figure 5.18.
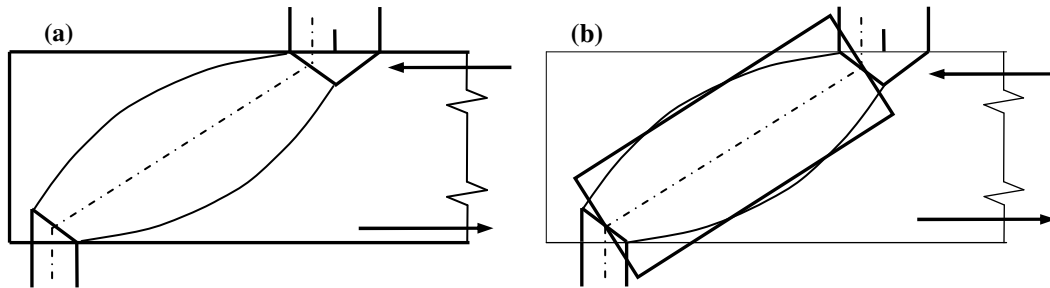
Figure 5.18   (a) Transfer of forces in a bottle-shape strut in the web of a deep element, (b) Idealised bottle-shape in an equivalent cylinder

The cylinder length, H, is equal to the distance between the nodes. The cylinder diameter, D, is equal to half the length of a segment perpendicular to the axis of the cylinder and limited at the ends by the resultants of concrete and steel forces in the flanges, this segment is represented by a short-dashed line in Figure 5.19. d, as defined in Figure 5.16, is the diameter of the supports. In this case the two supports do not have the same dimensions and they do not have a circular shape. An equivalent area and diameter for each support is defined by equation (5.2). The diameter d_{mean} as shown in Figure 5.19 is then defined as the average support diameter in equation (5.3).

$$D = \frac{z}{2\sin\theta} \tag{5.1}$$
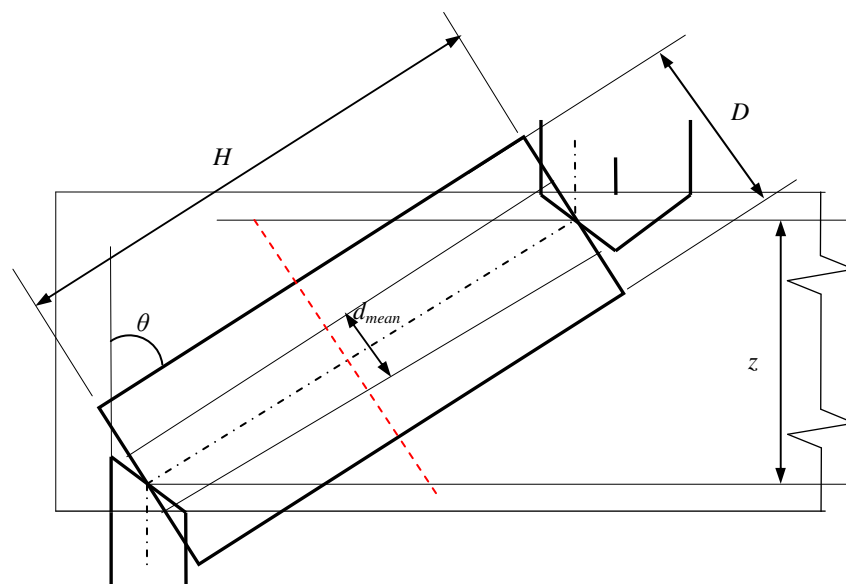
Figure 5.19   Geometry of the equivalent cylinder

The loading areas, on each side of the equivalent cylinder, are defined as the hexagonal faces of the inclined struts in the nodal regions as defined in Section 4.3.1.

The double-punch tests were done for loading plates of the same size at both ends; therefore it was chosen here to consider the average area, A_{mean}, of the two hexagons as loading area:

$$A_{mean} = \frac{\pi}{4}(\sqrt{\frac{A_1}{\pi}} + \sqrt{\frac{A_1'}{\pi}})^2 \qquad (5.2)$$

A_1 and A'_1 are the hexagonal areas as defined in Figure 5.16.

$$d_{mean} = 2\sqrt{\frac{A_{mean}}{\pi}} \qquad (5.3)$$

Afterwards, the shear capacity is related to the compressive capacity of the cylinder which is derived from experimental results of the double-punch tests. The compressin strength of the strut, $\sigma_{confinement}$ provided by the average prismatic cross sectional area, A_{mean} of the strut is expressed as:

$$\sigma_{confinement} = k_{confinement} f_c \qquad (5.4)$$

f_c is the compressive strength of concrete, chosen as the mean strength of concrete, f_{cm} is analysis at the ultimate state or as the design strength of concrete, f_{cd} in design cases. $k_{confinement}$ is defined following the formulation of Adebar and Zhou:

$$k_{confinement} = 1 + 2\alpha_1\beta_1 \qquad (5.5)$$

$$\alpha_1 = 0.33(\frac{D}{d_{mean}} - 1) \leq 1 \qquad (5.6)$$

$$\beta_1 = 0.33(\frac{H}{d_{mean}} - 1) \leq 1 \qquad (5.7)$$

As α_1 and β_1 varies between 0 and 1, $k_{confinement}$ varies between 1 and 3. The trend that the strength of a cylinder to resist double punching is enhanced both by D/d_{mean} and by H/d_{mean} can be seen in Figure 5.20. Note that, even if the cracking load is below 1 for some cases, the cylinders never fail for bearing load below the concrete compressive strength.
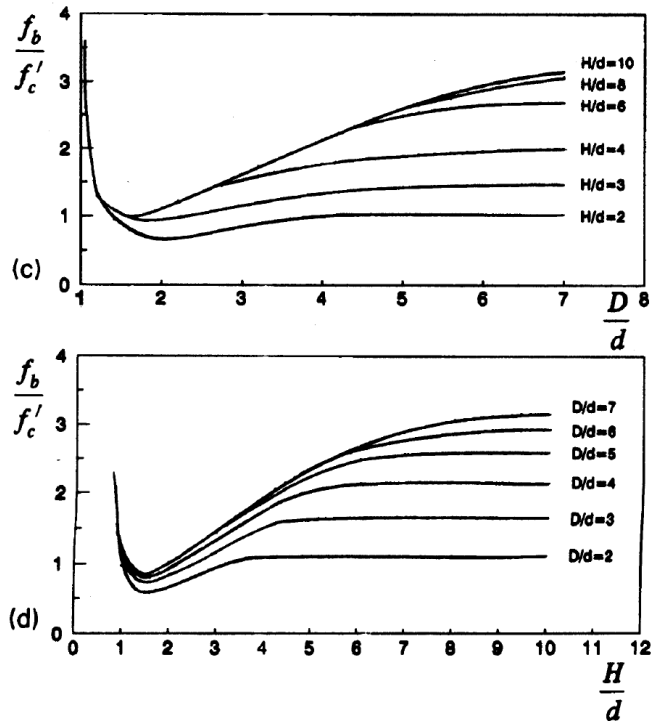
Figure 5.20   Analytical study of the ratio between bearing stress at cracking, f_b to concrete strength, f_c in double punch cylinder tests (Adebar et al. 1996)

The principle of the method is to estimate the splitting/crushing capacity of an equivalent concrete cylinder. However, the real shape of the compressive strut is quite different than a cylinder specimen. Indeed, the supports are not facing each other, see Figure 5.15, which means that shear transfer of forces by truss action occurs in the web. The fact that shear forces are transferred results in a tension field crossing the compressive field in the web. The magnitude of the tension field crossing the compressive strut in a non-reinforced web will be dependent on the aspect ratio β, as explained in the Section 5.3.2: *Duality between shear transfer of forces by direct arch and by truss action in short span elements*. The more slender the element is, the more important the part of the load transferred by truss action is important and the more the capacity of the strut is reduced. In strut-and-tie models, it is common to reduce the capacity of a strut crossed by a non negligible tensile field by a factor $k_{web}=0,6$.

The approach selected in the model developed in this thesis is to consider that, in rather stocky pile caps, the compressive capacity of the inclined is enhanced by confinement from inactive concrete ($k_{confinement}$) and is reduced by the tension field induced by shear transfer of forces by truss action in the web (k_{web}). A global reduction factor k_{arch}, taking both effects into account, is applied to the mean sectional area, A_{mean} of the prismatic strut defined in Figure 5.19 and in Figure 5.21.

$$k_{arch} = k_{confinement} \times k_{web} \quad \text{(reduction factor)} \tag{5.8}$$

$$\sigma_{arch} = k_{arch} f_c \qquad \text{(compressive strength of strut)} \tag{5.9}$$

$$F_{arch} = \sigma_{arch} A_{mean} \qquad \text{(compressive capacity of strut)} \tag{5.10}$$
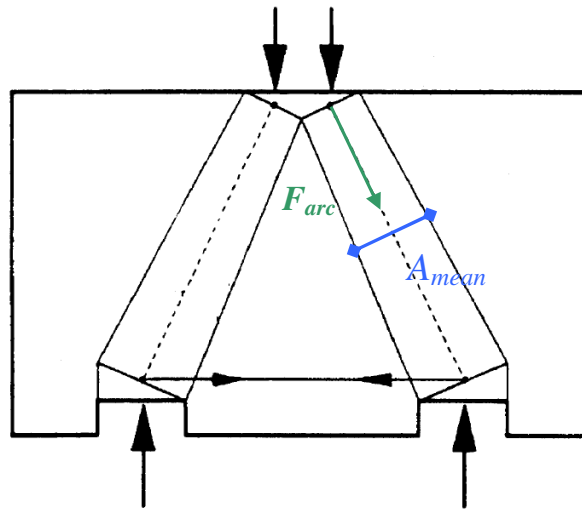
Figure 5.21   Prismatic struts between nodal zones in a pile cap

A summary of the different cases that have to be considered in pile caps and the associated checks of the inclined compressive strut is presented in Section 5.3.6.

5.3.5   Size effect in deep elements and in pile caps

"Size effect" is the common expression that refers to the decrease of the nominal shear strength of beams with increasing size.
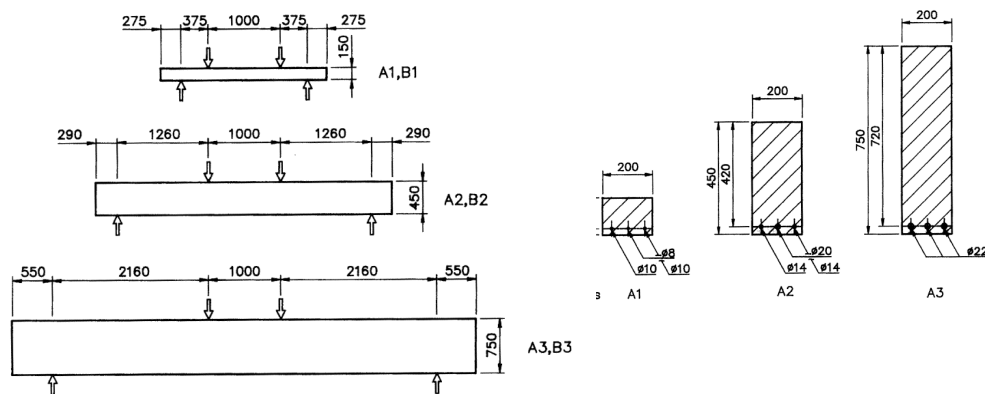
Figure 5.22   Dimension of slender beams loaded in shear (Walraven 1978)

The beams shown in Figure 5.22 all have the same aspect ratio $a/d=3$. Figure 5.23 (a) shows the variation of the relative shear capacity divided by the concrete tensile strength ($v_u = V_u/bdf_{ct}$) of the beams with increasing dimension. It can be seen that, the bigger the beams are the smaller the relative shear capacity is.
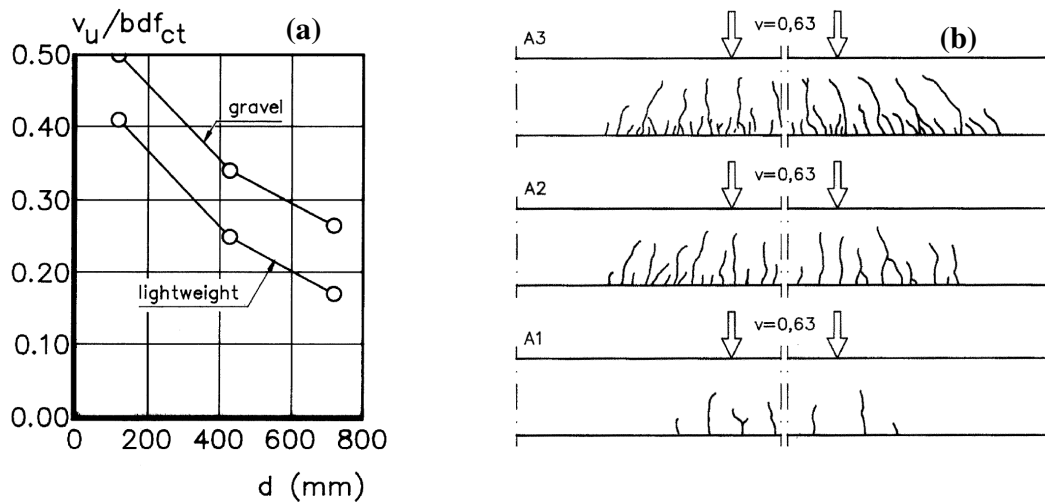
Figure 5.23 *(a) Relative shear capacity of gravel and lightweight concrete beams with constant aspect ratio and increasing effective depth, (b) Crack patterns of the beams, reduced to equal proportions, at the same relative shear force (Walraven 1978)*

Historically different hypotheses have been presented to justify this behaviour.

In 1939, Weibull (1939) argued that the size effect could be explained as the increased probability to find a weaker section with increasing size of the beams. Although interesting for members subjected to pure tension, this approach has been disregarded by researchers over time for shear.

In 1972, Taylor (1972) advanced that the reduction of shear strength could be explained by the increasing size of cracks in deep members. He considered that the interlock phenomenon contributed with about 35 up to 50 percent of the total shear capacity and argued that, if the aggregate size was kept constant, the interlock phenomenon would become less effective in deep members. However Taylor's proposition was proven wrong by Walraven (1978). Indeed, in lightweight aggregate, the cracks intersect the aggregate particles and do not form mainly in the cement paste like in gravel concrete. Therefore very little aggregate interlocking occurs. Nevertheless, as shown in Figure 5.23 (a), lightweight concrete is also prone to size effects.

The most accepted explanation up to now was proposed by Reinhardt (1981) and further developed by Bažant (1994) and is based on linear elastic fracture mechanics. As can be seen in Figure 5.23 (b), for the same relative shear force, a beam shows more critical crack pattern if its dimensions are bigger. Indeed, linear elastic fracture mechanics theory pointed out that the crack propagation was more important in larger members because of the greater energy-release rate. The comparison between strength predictions of deep members according to both static and fracture mechanics is shown in Figure 5.24.
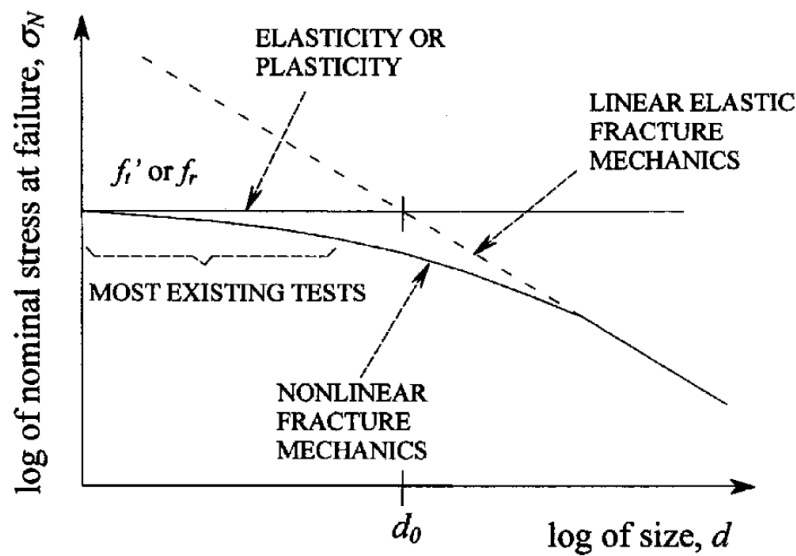
Figure 5.24 Size effect influence on shear strength prediction by static and fracture mechanics (Bažant 1994)

It is now accepted by most of the researchers that the more critical cracking pattern in larger members results in concrete softening. This fact was acknowledged in the Modified Compression Field Theory developed by Vecchio and Collins (1986), were the strength of cracked concrete in compression is dependent on the principal tensile strains in uncracked concrete, on the cracks width at crack interface and on the average tensile strain in cracked concrete.

However, the case of pile caps is different and no relevant information was found in current literature about the actual importance of size effects in pile caps. Indeed, the conclusions drawn above cannot be easily extended to pile caps. Stocky pile caps do not develop the same cracking pattern as deep beams. For instance, Adebar, Kuchma and Collins (1990) showed that pile caps without stirrups had very few cracks before failure compared to deep beams, which means that the softening of the concrete struts is less developed. This is due to the large importance of confinement by inactive concrete which allow highly loaded bottle-shaped concrete struts to carry high stresses without severe cracking. If the dimensions of a specimen are increased, the confinement is increased way more in a pile cap than in a deep beam where the width is kept constant. For these reasons, it was assumed in this thesis work that no correction factor for the size effect should be considered in the model. However it would be very interesting to carry out some experimental study on the subject in order to get a better understanding of the influence of size in three-dimensional structures.

It should be pointed out that ignoring size effect, as it is proposed in the model developed in this thesis, is in contradiction with the sectional approach according to design codes. For instance in Eurocode, and respectively in BBK, the factors k and ξ are used to take into account the strength reduction due to size effect. These factors are implemented in both the formulas to evaluate beam shear capacity and punching shear capacity.

5.3.6 Summary of the strength criteria for the inclined struts and for the amount of shear reinforcement.

In the model developed in this thesis work, truss action and direct arch action are distinguished as explained in Section 5.3.2: *Duality between shear transfer of forces by direct arch and by truss action in short span elements,* resulting in the definition of a *β* factor accounting for the part of the load carried by truss action and influencing the need for shear reinforcement.

In addition, a method to evaluate the capacity of the inclined struts to transfer compression was developed and is explained in Section 5.3.4: *Strength criterion for cracked inclined struts.*

Finally, the influence from the pile cap dimensions related to the so-called size effect is not considered as explained in Section 5.3.5: *Size effect in deep elements and in pile caps.*

The design method for the inclined struts is exposed in this part; in parallel checks of the nodal regions must be carried out. Checks at the nodes are presented in Section 3.6.3.3.

Three cases are distinguished depending on the aspect ratio *a/z* of the concrete volume between the pile and the column, *a* being the horizontal component of the distance between the nodes and *z* being the internal level arm; both of them can be efficiently evaluated in the model developed. Figure 5.25 shows the strut-and-tie model proposed for the transfer of forces in pile caps.
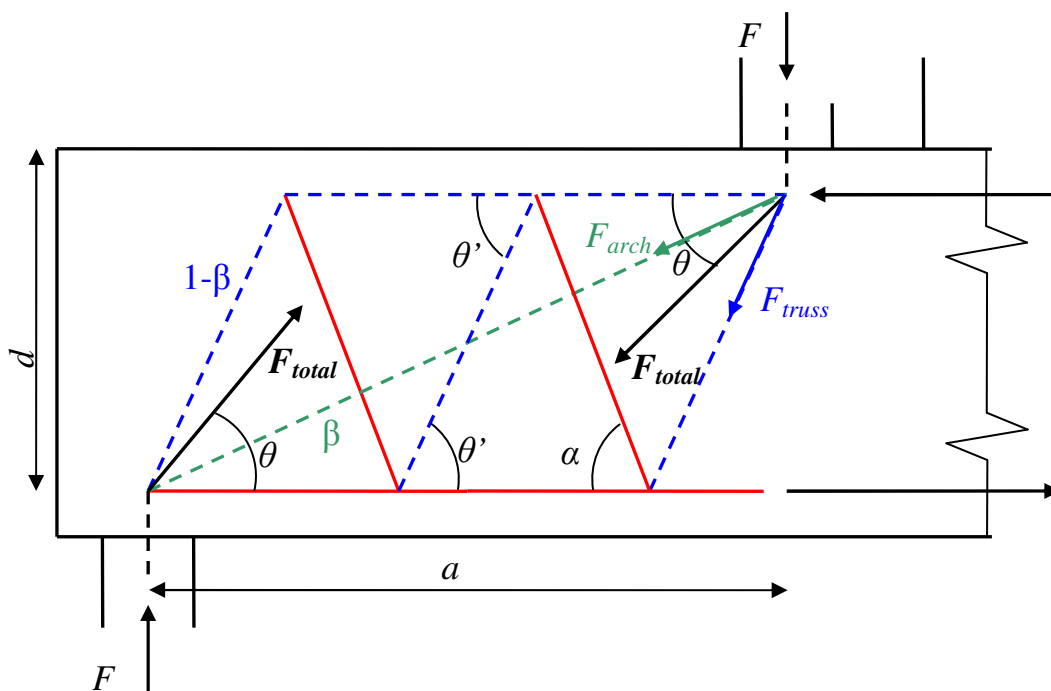
Figure 5.25   Model proposed for the transfer of forces in deep elements

a)   When $a < z/2$ ($\theta > 60$ degrees, $\beta=0$)

The entire load is considered to be transferred by direct arch action, $F_{total} = F_{arch}$ as defined in Figure 5.25. No stirrups need to be provided and no sliding shear failures need to be considered. However, the inclined strut is checked against

splitting/crushing with the method defined in Section 5.3.4. The compressive stresses in the equivalent cylinder are limited to a strength $k_{arch}f_c$ provided by the average prismatic area A_{mean}:

$$F_{arch} = \frac{F}{\sin \theta} \tag{5.11}$$

$$F_{arch} \leq F_{R,arch} = k_{arch} A_{mean} f_c \tag{5.12}$$

f_c is the compressive strength of concrete, chosen as the mean strength of concrete, f_{cm} in analyses at the ultimate state or as the design strength of concrete, f_{cd} in design cases.

b) When $z/2 < a < 2z$ (26 degrees $< \theta <$ 60 degrees, $0 < \beta < 1$)

The load is carried by arch and truss action in combination: $F_{total} = F_{arch} + F_{truss}$. Stirrups have to be provided. The needed amount of transverse reinforcement, A_{sd}, is provided to resist the part of the load transferred by truss action:

$$A_{sd} = \frac{\beta F}{f_{yd} \sin \alpha} \tag{5.13}$$

$$\beta = \frac{1}{3}(\frac{2a}{z} - 1) \tag{5.14}$$

f_{yd} is the design yield strength of steel, α is the angle between the horizontal and the direction of the stirrups.

The vertical resultant of F_{arch}, see Figure 5.15, is equal to *(1-β)* times the total load *F*. The corresponding force F_{arch} should be considered when checking the resistance of the inclined strut. The simplifying assumption made is that the amount of steel provided is used only to carry a part of the load by truss action after cracking, which means that the stirrups cannot be used to restrain the tension due to bottle-shaped stress field. However the stirrups have a positive effect on the shear capacity as they reduce the load transferred through direct arch action, thus making the check for splitting of the inclined strut less critical. This approach is of course simplified as the provided amount of steel will be used in reality both to keep cracks together and prevent splitting as well as to transmit forces by truss action.

Provided that enough anchorage is provided for the steel bars, designing pile caps with this method assures that no shear failure or punching shear failure can occur before the flexural reinforcement yields. Indeed, the amount of stirrups is designed to prevent a sliding shear failure (eq 5.13) and the web is checked against crushing of the concrete (eq 5.15).

$$F_{arch} = \frac{F}{\sin \theta}(1 - \beta) \leq F_{R,arch} = k_{arch} A_{mean} f_c \tag{5.15}$$

c) When $a > 2z$

The load is considered to be transmitted fully by truss action, $F_{truss} = F_{total}$, see Figure 5.25. The stirrups are designed in order to resist the whole shear force:

$$A_{sd} = \frac{F}{f_{yd} \sin \alpha} \tag{5.16}$$

In this case the structure contains some B-regions and the pile cap can be qualified as slender. The model is on the safe side but not effective to assess the shear capacity of the pile cap. Indeed, the concrete tensile strength, the amount of flexural reinforcement as well as size effect will have greater importance that are not implemented in the model developed in this thesis work. In this case, checks for beam shear and punching shear according to the desired design code or other methods could be used by the designer. However it is rather seldom to find pile caps that belong to this range of aspect ratios, for instance the pile caps studied in the frame of this work in actual structures built at Skanska showed aspects ratios where all or most of the piles were situated at a distance smaller than *2z* from the column.

5.4   Reinforcement arrangement and anchorage detailing

5.4.1   Reinforcement arrangement

5.4.1.1   Flexural reinforcement arrangement

The question of whether or not the flexural reinforcement should be smeared in pile caps is an uneasy question.

Blévot and Frémy (1967) conducted several tests on about 100 pile caps. They showed that spreading flexural reinforcement uniformly over the bottom of the pile cap, instead of using square bunched (concentrated) reinforcement over the supports, reduced in average the failure load by 20% for four pile cap and by 50% for three pile caps. In 1973, Clarke (1973) arrived to a similar conclusion with an average increase of the ultimate load by 15% when using square bunched reinforcement on four pile caps compared to smeared arrangement.

It was also shown by Blévot and Frémy (1967) that using square bunched reinforcement resulted in higher capacity than using cross bunched reinforcement, see Figure 5.26. They also showed that cross bunched reinforcement did not provide better ultimate capacity than grid reinforcement.

cross bunched reinforcement   *square bunched reinforcement*   *grid reinforcement*
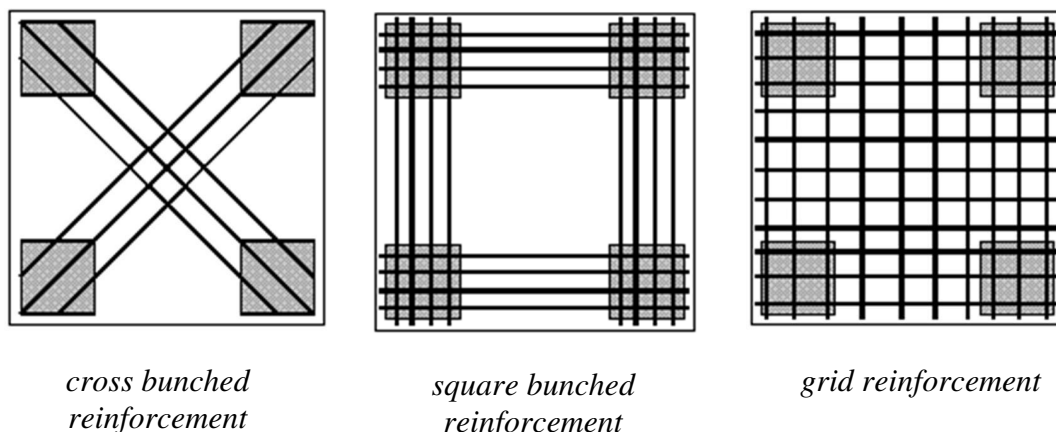
Figure 5.26   Some of the reinforcement layouts used in Blévot and Frémy (1967) experiments

The increase in ultimate capacity provided by square bunched reinforcement against grid reinforcement can be justified by two reasons:

First, as it is shown in a strut-and-tie model, the load needs to be carried from the column down to the pile. On the contrary, sectional approaches provide only reinforcement for the moment and shear forces across transverse sections without considering the actual geometry of the D-region and especially the location of the piles. In the case of a grid pattern, the flexural reinforcement in the middle of the pile cap will be less efficient than the flexural reinforcement over the piles resulting in a reduced ultimate capacity.

The second reason that gave rise to an increased capacity is the confinement provided by flexural reinforcement bars crossing each other at the pile. This can be seen by comparing bunched square and cross bunched reinforcement, the latter resulting in a lower capacity. Indeed, reinforcement in two directions other the supports will create better confinement, improving the triaxial state of stress in the nodal region. This results in an enhancement of the strength of incoming struts in the node as well as an improvement of the anchorage capacity as shown. On the over hand, cross bunched reinforcement layout is interesting because in total it demands less total bar length than the squared bunched layout.

These observations corroborate the idea that designs using strut-and-tie models give a better picture of the flow of forces and lead to a better design of disturbed regions *in the ultimate limit state*. However, the practical design of structures, and pile caps can sometimes benefit from spread reinforcement. For example, Blévot and Frémy (1967) concluded that using only square bunched reinforcement could lead to large cracking and advised to use a combination of square bunched and grid reinforcement. Indeed, special attention is needed for cracking in the service state and certain reinforcement for crack control may be needed between the main ties. In addition, providing a great amount of flexural steel over a support can lead to a layout requiring many layers. The internal level arm is reduced and the forces in the tensile and compressive chords are increased.

A practical approach is to spread the reinforcement in the neighbourhood of the nodal zone and provide transverse bars in U-bends that can secure equilibrium between the strut force and the bars outside the support area, as shown by the strut-and-tie model in Figure 5.27. This method possesses the valuable advantage to confine the nodal zone, on the other hand additional confining steel has to be provided.
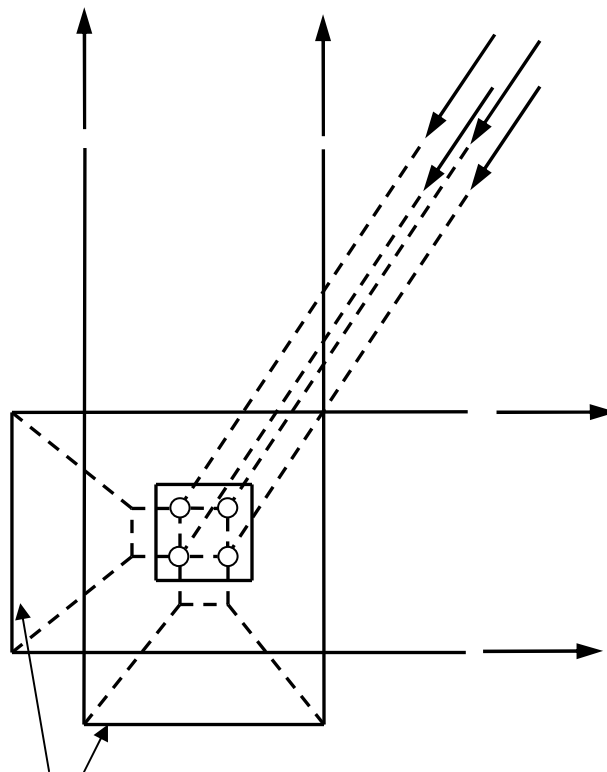
Figure 5.27   Strut-and-tie model that allows the use of spread reinforcement outside the support area

The confinement guaranties an enhancement of the capacity of the nodal zone to carry compressive stresses and to anchor bars. The compressive strut incoming in the node is still directed towards the pile, the shape of the node is not modified. Nevertheless, a part of the horizontal component of the load is resisted by confinement compression "from behind" the node instead of being carried by the flexural reinforcement situated over the pile only, see Figure 5.27. The possibility to develop such a state of stresses is very dependent on the geometry of the pile cap close to the piles, indeed a sufficient area behind the node is required to make the reinforcement layout shown in Figure 5.27 possible to realise.

Spreading the reinforcement in a limited area around the pile can be very interesting in order to reduce the number of steel layers required. The choice is let to the designer who then has to account for the tension induced in the confining bars.

5.4.1.2   Shear reinforcement arrangement

In beam design it is rather uncommon to use inclined stirrups instead of vertical stirrups. In this section it will be shown that using inclined shear reinforcement in deep elements, and especially in pile caps, is very advantageous.

Considering the "truss action" for the shear transfer of forces, using inclined stirrups allows pulling up the load in a shorter path to the support. The need for stirrups is then reduced. This effect can be easily seen in strut-and-tie models:

CHALMERS, *Civil and Environmental Engineering*, Master's Thesis 2010:51
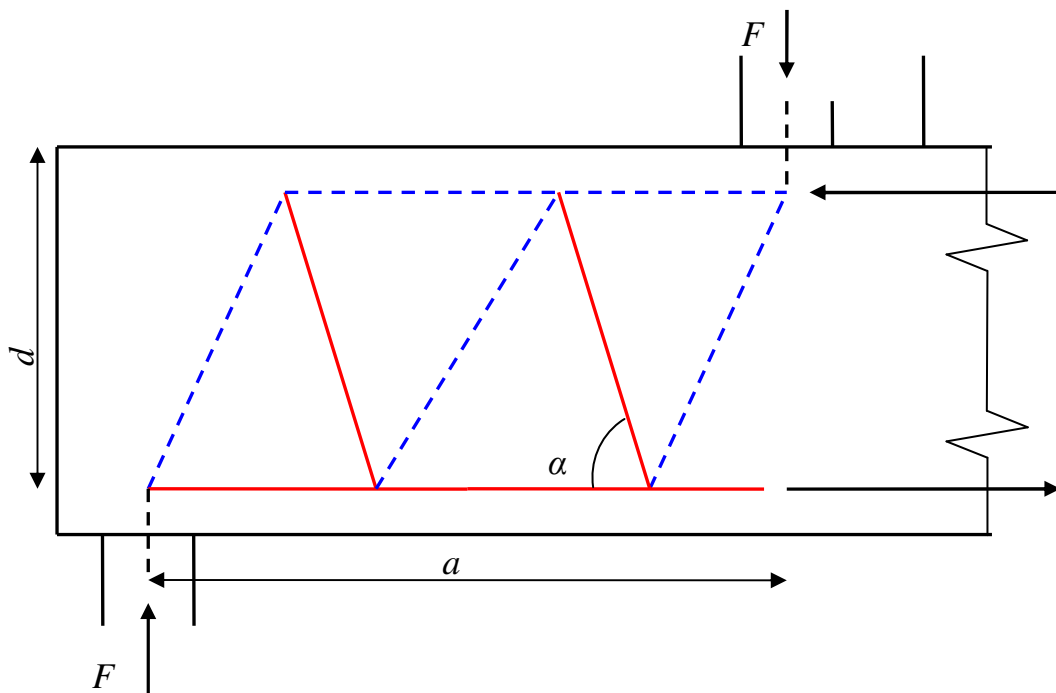
Figure 5.28   Shear transfer of forces by truss action using inclined stirrups
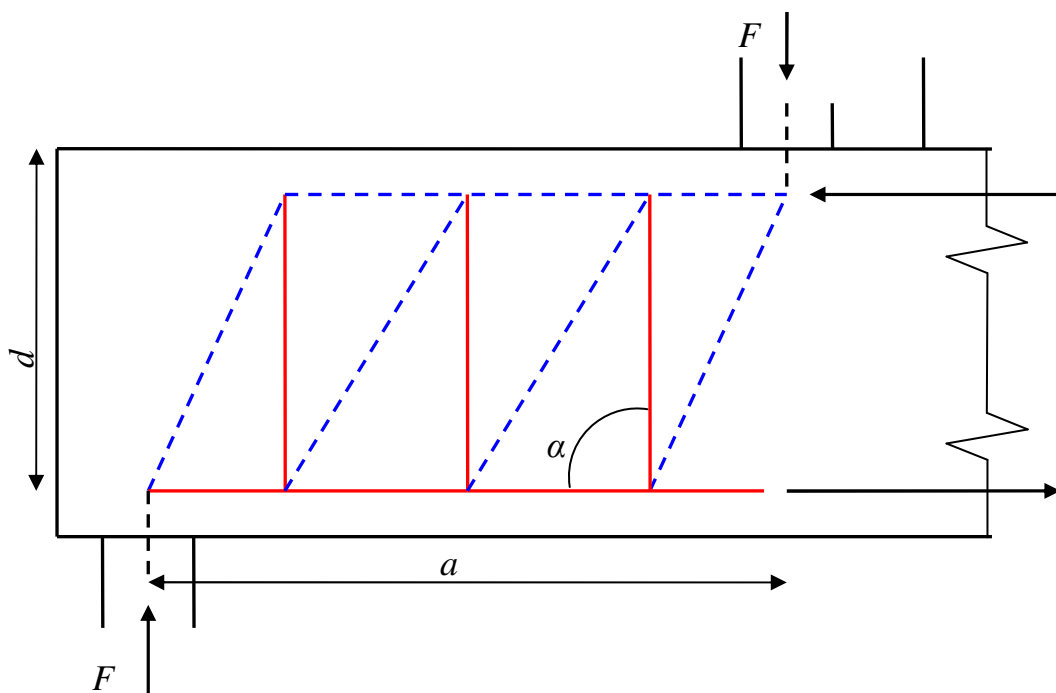
Figure 5.29   Shear transfer of forces by truss action using vertical stirrups

In both cases shown in the figures above, the change in direction of the compressive field at the support is turned by approximately 30 degrees. The first model, Figure 5.28, shows inclined stirrups and the second one, Figure 5.29, vertical stirrups.

The amount of stirrups required in the first case is smaller than in the second case:

$$A_{s,inclined} = 2\frac{F}{\sin\alpha} \leq A_{s,vertical} = 3F$$

Considering the "direct arch action", using inclined stirrups is also valuable, as seen in Figure 5.30:
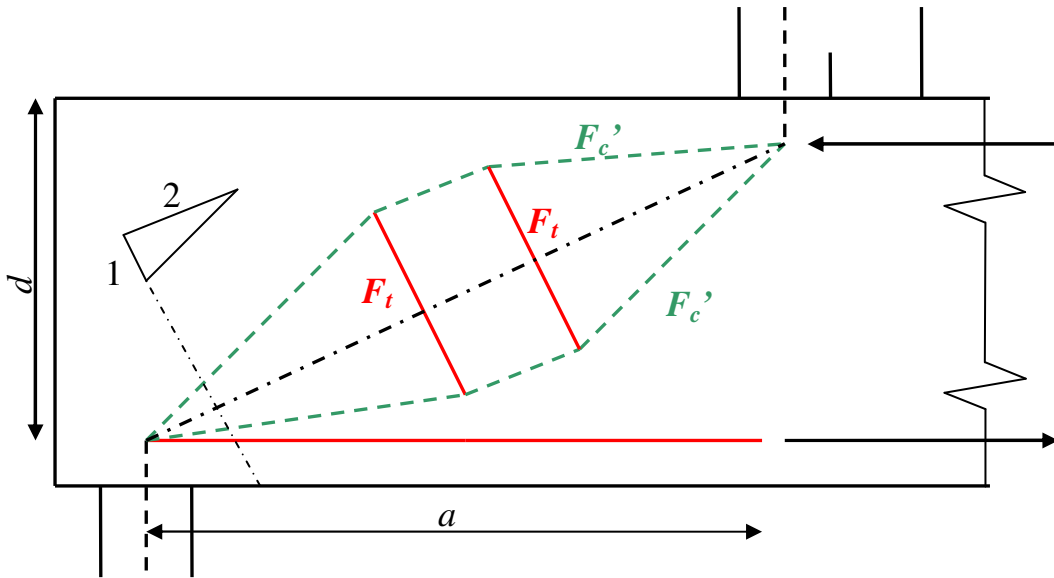
Figure 5.30   Shear transfer of forces by direct arch action and associated transverse tension.

The strut going directly to the support does not keep a prismatic shape but expands and creates tension near its middle. A common assumption is that the strut opens following a 2:1 slope as shown in the Figure 5.30.

The direction of the induced tensile stress field is perpendicular to the direction of the strut, in average. A reinforcement arrangement following the elastic tension field derived is considered appropriate. Therefore inclined stirrups can be used with less deformation demand from the structure and can be considered as more sound than vertical stirrups. Using stirrups perpendicular to the direction of the inclined strut will enhance tremendously its capacity as shown in Figure 5.31:

CHALMERS, *Civil and Environmental Engineering*, Master's Thesis 2010:51
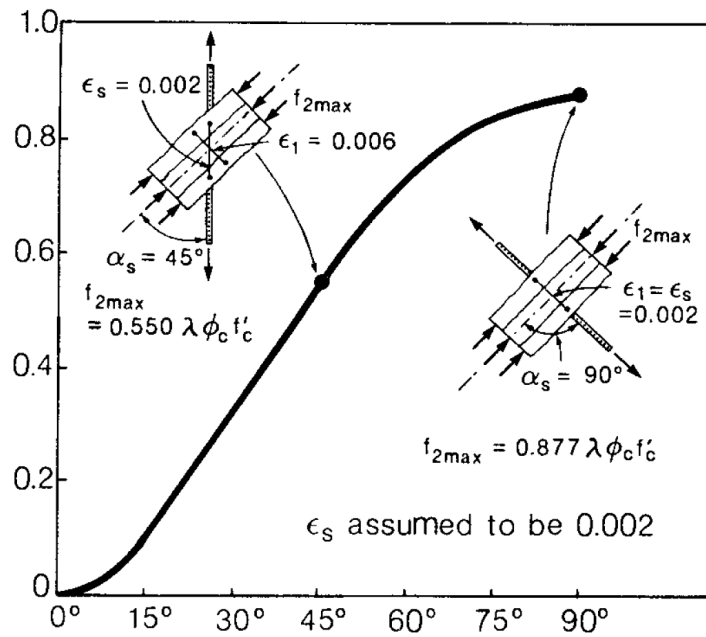
Figure 5.31   Crushing strength of compression struts depending on the inclination of the stirrups crossing the strut (1986)

Indeed, the tensile strain perpendicular to the strut is highly reduced when using perpendicular stirrups. The strength of the strut is changed from a factor 0,55 to a factor 0,87, which means an increase in capacity of almost 60%.

As explained before, in pile caps, strut action and not truss action is predominant, which means that the shear capacity of pile caps is often determined by the splitting/crushing strength of the inclined struts. Therefore, providing stirrups perpendicular to the average compression field direction in the web is extremely valuable.

The proposition made in this thesis work is to incline the stirrups at 90 degrees from the direction of the vector F_{total}, as shown in Figure 5.25, which can be considered as the average direction of the compressive stresses.

Another aspect that encourages the use of inclined stirrups is understood when studying the punching failure mode. Indeed, inclined stirrups in the vicinity of the supports will cross the possible critical cracks of a punching cone with a greater angle and be used with higher efficiency. Using bent reinforcement under concentrated load or above concentrated supports is considered as a practical way to reduce the risks of brittle punching failures. For example, Broms (2000) proposed a reinforcement arrangement for flat slabs including bent bars above the supports and showed that the behaviour of the structure was improved, especially its ductility.

As confirmed by designers at Skanska, the use of inclined stirrups instead of vertical stirrups in pile caps would not be problematic in practice and has already been adopted in some previous pile caps. As a conclusion, in stocky pile caps were *a<2z,* the authors strongly recommend the utilisation of inclined stirrups.

5.4.1.3 Minimum reinforcement

When designing a reinforced concrete structure according to codes, a minimum reinforcement amount and a maximum bar spacing have to be respected at the surfaces to control cracking at the serviceability limit state and provide ductility to the structure. This minimum reinforcement can also be used in the ultimate limit state for different load cases; in other words, if the reinforcement required by design is sufficient, there is no need of additional reinforcement to control cracking in those regions. The recommended minimum reinforcement ratio by Eurocode 2 is ρ_{min}=0.001, and the maximum spacing is 300mm. The amount of minimum reinforcement can be higher than the one of the code if it is required by the client, for instance, Trafikverket (the Swedish Transport Administration) requires higher ratios in case of bridge design (ρ_{min}=0.005 or 0.008 according to the geometry of the pile cap).

In the case of design with a strut-and-tie model, the minimum reinforcement has to be added between the main ties when the distance between them requires it, and on the other faces of the structure where no ties are provided. However detailing rules are given in Eurocode 2 concerning the design of pile caps which apply well to the design with strut-and-tie models. It says that the main reinforcement design for the action of the different load cases should be concentrated in the stress zones between the top of the piles (which can be interpreted in different ways). Furthermore if the area of this reinforcement is higher than the minimum reinforcement, then distributed bars at the bottom face of the pile cap are not required. Besides, the minimum reinforcement at the side and top faces may be omitted if no tension develops at these faces.

5.4.2 Bond and anchorage

5.4.2.1 Bond and anchorage of flexural reinforcement

When designing according to sectional approaches, a common mistake made by designers is to underestimate the need for anchorage of the flexural reinforcement at the supports. One of the main advantages of the strut-and-tie model is that it clearly indicates to the designer that tension is resisted in nodes, and thus the need of anchorage is obvious. A numerical value expressing the need of anchorage can be directly found by the calculated tensile force in the main reinforcement in the nodal regions. Different anchorage solutions can be provided depending mainly on the geometry of the pile cap and the state of stress close to the nodal zone. The designer should try to avoid cracking of concrete in nodal zones as well as cracking of the inclined strut when detailing the anchorage region.

> *"A smooth surface of the tie where it crosses the node is better than good bond quality because strain compatibility with the bonded bar will tend to crack the node's concrete."* (Schlaich 1987)

A good bond between concrete and steel is necessary in order to transmit the horizontal stresses over the piles from one material to the other. However, the strains induced by the steel in the concrete in the nodal region over the piles are enhanced by a good bond transfer, which can result in cracking that will severely reduce the strength of the nodal region. This is the kind of classic problematic that is found when dealing with friction, for example a vehicle cannot gain speed without friction to the ground but at the same time this friction create opposite force to the motion of the

vehicle, reducing its speed. The solution is to choose the distribution of friction along the reinforcement bars in order to control the cracking pattern.

Firstly, in order to reduce the cracking of the nodal zone due to the bond action, it is somehow possible to reduce the friction between the reinforcement and the concrete in the nodal zone without weakening the capacity of the nodal region to deviate the force flow towards the column. This can be done by providing lower bond quality steel in the nodal zone and anchor the node "from behind", the resulting state of stresses is better for the nodal zone's mechanical behaviour, see Figure 5.32. However this is only possible if some space is available behind the node and if the nodal region has quite small dimensions, which is usually the case in pile caps.
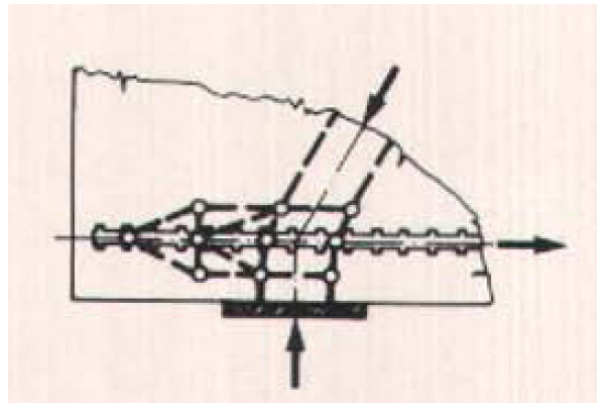
Figure 5.32   Main tie bar anchored in and behind the nodal region (Schlaich 1987)

Another way to reduce the cracking in the nodal zone is to spread the flexural reinforcement a bit around the node, thus confining the node and transferring a portion of the steel bars out of the nodal region as shown in Figure 5.27. The tensile strains and thus the tendency to crack are reduced in the nodal region. On the other hand, the designer has to consider that spreading the reinforcement will create extra transverse tensile stresses in the vicinity of the node for which additional U-bends have to be provided. The node region can also be confined using vertical stirrups, which is good for the anchorage.

The second important feature when designing a deep element like a pile cap is to assure that the compressive strut remains with no or little cracking as long as possible. Indeed, in stocky structures, most of the load is carried by direct arch action; if the compressive strut is badly cracked it will fail in a combination of splitting and crushing before the full capacity of the main reinforcement can be used, resulting in a shear failure.

In Figure 5.33 two beams without stirrups and with a shear span to effective depth ratio *a/d*=2,77 were tested (Muttoni et al. 2008). The only difference was that the beam EB1 used low bond steel while EA1 used good bond steel. Beam EA1 reached 50% of its capacity according to theory of plasticity while EB1 reached 86%. The reason is the cracking pattern. Thanks to low bond steel in EB1, flexural shear cracks developed mainly in the middle of the span and thus did not cross and weaken the compressive strut when they propagated into flexural shear cracks.
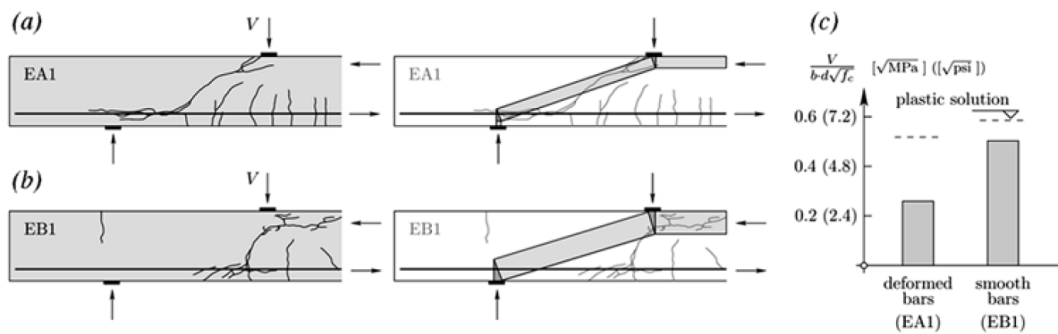
Figure 5.33 Influence of bond properties of flexural reinforcement on crack pattern and shear capacity of beams (Muttoni et al. 2008)

Providing rather low bond steel is only possible if sufficient anchorage length is provided within and behind the node. Hopefully this is usually the case in pile caps. The opportunity to use low bond steel and thus prevent the flexural shear cracks to develop through the compressive strut should be considered in pile caps.

5.4.2.2 Bond and anchorage of shear reinforcement

The rules for bond and anchorage of shear reinforcement follow the same trend as the one for main reinforcement. The main concerns are to provide enough reinforcement and anchorage to carry the load and to reduce the cracking of the direct compressive strut in the web.

Beam BP0 and BP2 (with shear span to effective depth ratio *a/d*=2,44) were identical except that an additional *ø6* spiral reinforcement was added in BP2 as shown in Figure 5.34. This reinforcement could not participate actively to the improvement of the shear transfer by truss action as it was not anchored to the flexural reinforcement. However, it provided some crack control of the inclined strut, preventing the development of early critical cracks and splitting/compressive failure of the strut. Beam BP0 reached half of the capacity according to plasticity theory while BP2 reached its full capacity, meaning that BP2 was more than two times stronger than BP0.
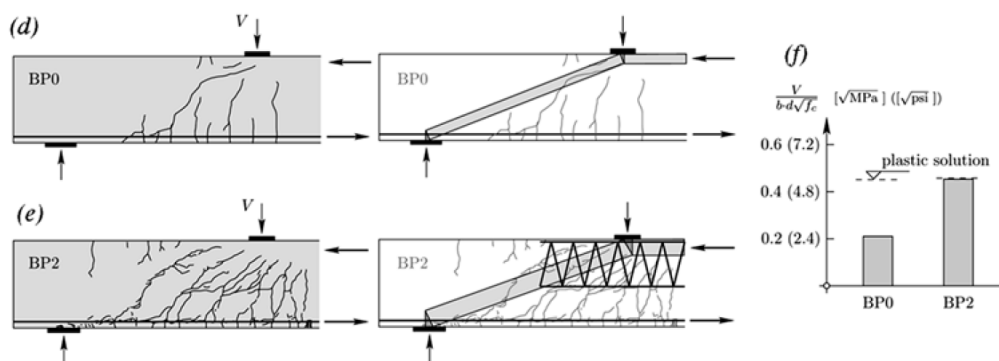
Figure 5.34 Influence of shear reinforcement on the cracking pattern and shear capacity of beams (Muttoni et al. 2008)

This experiment also shows that arch action was the predominant shear transfer mechanism in a beam with a span to effective depth ratio *a/d* close to 2,5. If crack control is provided by stirrups, as in the method developed in this thesis, the

possibility to develop direct arch action for rather slender members is possible. However, in this thesis work, for a span to depth ratio a/z higher than 2, the load is considered to be carried only by truss action and the stirrups are designed to carry the entire load. This experiment shows that the model is conservative for the design of shear reinforcement.

A way to reduce cracking of the inclined strut in the web is to use stirrups with low bond in the area were the stirrups cross the strut. This kind of reinforcement has a positive effect to reduce cracking in the web, but has a greater need for anchorage in both the compressive and tensile chords. However, space is usually not a problem in pile caps were a lot of volumes with good confinement can be used for anchorage. A detailing proposition for anchorage of low bond stirrups is shown in Figure 5.35:
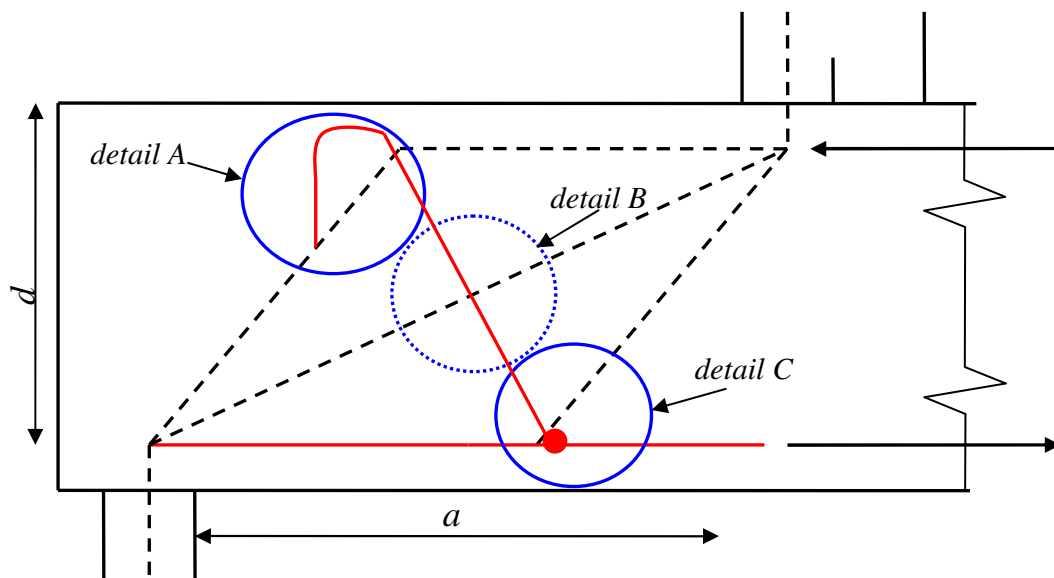
Figure 5.35   Proposition for arrangement and detailing of shear reinforcement

detail A: Can be a shear link or, as shown in Figure 5.35, a partially bent stirrup to provide anchorage in the compressive chord. As explained before, pile cap have great volumes of inactive concrete with good confinement properties, as in detail A area, for this reason using only a partially bent stirrup for detail A can be interesting in order to reduce the length of the stirrup.

detail B: Inside the web, the stirrups are made of low bond steel

detail C: The stirrups are anchored around the flexural steel reinforcement in the tension chord.

6 Examples of pile caps designed using the three-dimensional strut-and-tie model developed

6.1 Introductory remarks

The purpose of this section is to give guidelines on how to design pile caps with the three-dimensional model presented in Section 4. The design procedure is explained through an example of a 4-pile cap and one of a 10-pile cap.

A finite element program, FEM3DYN, developed and used at Skanska, has been used to solve the forces in the strut-and-tie models in the following examples. This program has been used because the purpose of this work was to develop a sub-program ready to be used together with FEM3DYN. Besides, it was convenient to obtain plots of the strut-and-tie models in order to check the geometry after programming, and the program also raised some issues regarding the stability of the models, which lead to interesting improvements. Finite element analyses were also needed to study the influence of the stiffness in statically indeterminate strut-and-tie models. However, the solution proposed at the end of this work is based on choices made by the designer to solve statically indeterminate models. Therefore a finite element analysis is not needed to use the models proposed and a simple program solving statically determinate truss models, could be developed to make the input of the model easier and the calculations faster.

FEM3DYN is a program based on Matlab; thus all programming was performed in this language. Many different cases have been programmed, which are not all referenced here; these cases rather contributed to a better understanding and the development of iterative solutions which are general enough to be applied to a wide range of different pile caps.

6.2 4-pile cap

6.2.1 Presentation of the design case

The design of a 4-pile cap is presented in this section. The first aim of this example is to describe the iterative procedure that has to be used in order to solve the three dimensional strut-and-tie model developed in this thesis work. This iterative procedure consists in modifying the model according to the need for reinforcement, the refinement of the nodal zones under the column, the check of singular parallelepiped nodal zones, and the check of diagonal struts to splitting and crushing. The second aim is to compare the amounts of reinforcement given by three different strut-and-tie models, which consider different modes of transfer of forces between the column and the piles: by direct arch action, by truss action and by a combination of direct arch action and truss action. The pile cap considered has a rectangular shape and is supported by square piles and loaded by a centrally placed rectangular column. The geometry of the pile cap is illustrated in Figure 6.1. The main program written on Matlab for this example, with the iterative procedure, can be found in Appendix B. Two alternative strut-and-tie models are shown in Figure 6.2.
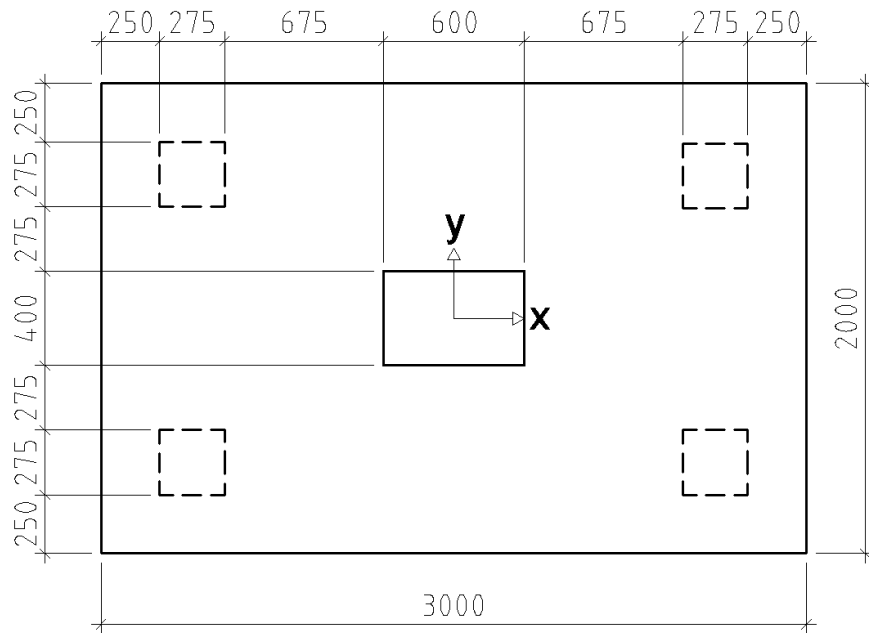
Figure 6.1   Geometry of the 4-pile cap
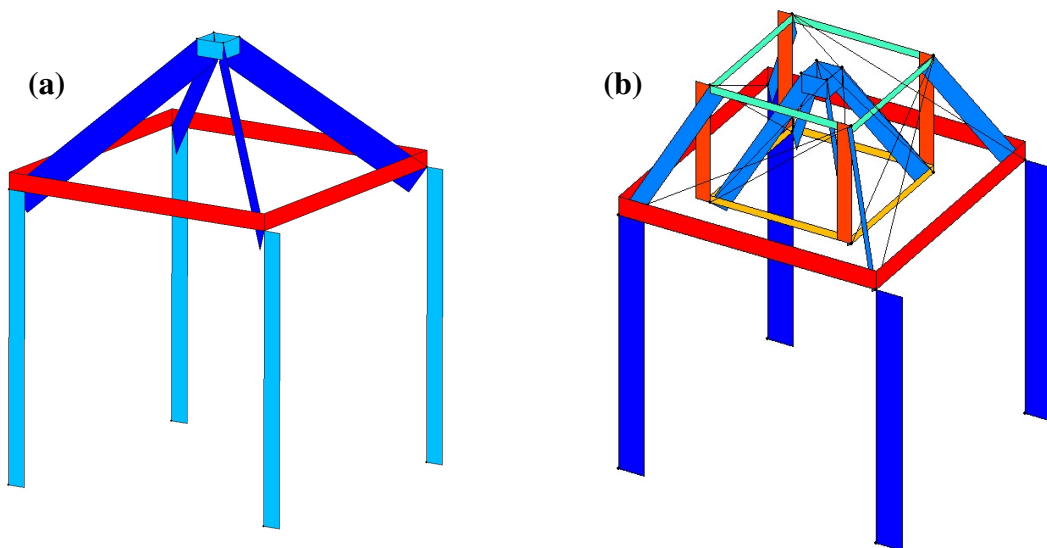
*Figure 6.2   Example of strut-and-tie models for 4-pile caps using **(a)** direct arch action, **(b)** combination of truss action and direct arch action*

The calculations conducted are:

- Amount of reinforcement in horizontal ties (along x and y-axis)

- Stress in the horizontal struts at the node under the column (along x and y-axis)

- Stress in the inclined strut at the node over the pile

- Stress in the inclined strut at the node under the column

- Stress at the middle of the diagonal bottle-shape strut (arch strut)

The concrete stresses mentioned above are checked with regard to strength criteria of nodes and struts.

The iterative process starts with an assumption of the heights $2.a_c$ of the horizontal struts and $2.a_s$ of the horizontal ties, which allows to define the provided areas for all the members. If the original assumption is not verified, the checks lead to a correction of a_s or a_c. Some of the checks mentioned above influence a_s, if they need correction, while the others influence a_c. The process is iterative, all parameters being checked in the same iteration, and small increases are made to a_s or a_c. For a better and faster convergence, the program is improved for the easier checks. The level of the main reinforcement a_s and the level of the horizontal struts a_c, are corrected directly by the values required for the stresses to be just lower than the design strength.

Notes:

Some difficulties were experienced for programming this example in FEM3DYN. If the bars are defined in the base [(1 0 0);(0 1 0);(0 0 1)], the model cannot be solved because the vertical bars cannot be defined. To solve this problem another base has to be used for the vertical bars, for instance: [(0 0 1);(0 1 0);(-1 0 0)]

Even if the strut-and-tie model is stable for this load case due to symmetry and can be solved, the model is not stable in general and the program returns an error message because of that. It happens often that strut-and-tie models are not stable, especially in the case of three-dimensional models and when the aim is to reach quite simple or even statically determinate models. However, in reality the stress field in the reinforced concrete structure is stable due to the restraint form the inactive concrete. Besides, it is natural that the program reacts when a model is a mechanism, which prevents from inconsistent results. A solution to overcome the problem is either to provide stabilizers to the model (Figure 6.2 b), which are members with a low stiffness, or to assign a certain low stiffness directly to all the nodes of the model.

6.2.2 Parameters used in the study

The coefficients used for the check of the nodes are the ones recommended by the Eurocode 2 and presented in Section 3.6.3.3 (k_3) and Section 4.3.6 (k_4).

- $k_4 = 3$ for the 5C-node under the column subjected to triaxial compression

- $k_3 = 0.75 \cdot 1.1$ for the 2C2T-nodes over the piles

6.2.3 Refinement of the nodal zones

The refinement of the nodal zones under the column, explained in Section 4.3.5 and illustrated in Figure 4.8, is used in this example in order to optimise the design. Indeed, the use of this method minimises the distance between the loads and the supports and ensures a secured triaxial compression state of stress in the nodal zone. In this example the aim is rather to explain the iterative procedure than to show the reduction of the amount of steel required.

The refinement is conducted in several steps. The first step consists of defining the reduced required area of the effective column section with regard to the bearing strength. As the nodal zones at the column are subjected to secured triaxial compression, the factor k_4 is used. The second step consists of changing the proportion between the sides of the nodal zones in order to have the same stress on

both faces on which the horizontal struts are acting. Another example of refinement of nodal zone is treated in the next example, Section 0, for a nodal zone divided in six.

6.2.4 Iterative procedure

Table 6.1   Algorithm for the strut-and-tie design procedure of a statically determinate pile cap

1. Enter the material properties

2. Enter the geometry of the pile cap (position and dimensions of piles and column)

3. Check the bearing stresses (outside iterative process as the pile and column dimensions are fixed, and the load is the same in every pile)

4. Reduce the column area to its required effective area

5. Enter initial values of a_s and a_c:

    a_s: corresponding to one layer of steel

    a_c: low value at the beginning

6. WHILE $a_s < 0.2d$ and $a_c < 0.3d$ (beginning of iterative process)

7. Compute the coordinates of the nodes of the strut-and-tie model (vertical coordinates changing in the loop as well as horizontal coordinates of nodes at column)

8. Calculate the provided cross-sectional area of each strut where it meets the nodal area according to the geometry of the nodal area (Section 4.3)

9. Building and analysis of the model using FEM3DYN

10. At 1st and 2nd iterations:

    Refine the proportion of the sides of the nodal zones under the column

11. From 3rd iteration:

    Calculate the tensile force in every tie

    Compute steel area required

    Compute number of layers required n_l

12. If $n_l(n) > n_l(n\text{-}1)$ (number of reinforcement layers n_l increases at iteration n)

    Compute new a_s

13. Check the stresses in the singular nodes at the faces of the nodal zones and in the middle of the diagonal strut (arch strut)

14. If $\sigma_c > \sigma_{Rd,max}$ at the faces of the singular nodes and at the middle of the diagonal strut (arch strut)

    Compute new a_c or change sides of nodal zones at column

15. If $a_s(n) = a_s(n\text{-}1)$ and $a_c(n) = a_c(n\text{-}1)$

    BREAK WHILE (end of iterative process)

16. END WHILE (next iteration: return to step 6)

17. Return:

    Level of axis of flexural reinforcement a_s (and a_c)

    Required steel areas of ties and number of bars

    Stresses in struts

6.2.5 Direct arch action

In one of the alternative models only the transfer of forces by direct arch action is considered, see Figure 6.2 (a). The results of the iterative design procedure are presented in Table 6.2.

Table 6.2   Design considering load transfer by direct arch action only

Direct arch action		1st iteration	2nd iteration	3rd iteration	4th iteration	10th iteration
Refinement of nodal zones at column	x-axis	166	98	104	104	104
	y-axis	110	187	176	176	176
Level of axes of horizontal struts and of reinforcement	a_c	20	20	20	25	55
	a_s	46	46	72	77	97
Total load per pile		1100	1100	1100	1100	1100
Load transfered by truss action		0	0	0	0	0
Load transfered by arch action		1100	1100	1100	1100	1100
Angle between strut of arch and horizontal plane		42.8°	43.1°	42.3°	42°	40.3°
Tie over piles x-axis	Force in the member	(1054)	1014	1047	1058	1121
	A_s	(2424)	2333	2408	2435	2578
	Number of bars (Ø16)	(13)	12 (2 layers)	12	13	13
Tie over piles y-axis	Force in the member	(551)	596	606	613	649
	A_s	(1267)	1370	1395	1410	1494
	Number of bars (Ø16)	(7)	7	7	8	8
Check of nodal zones						
Strut horizontal x-axis	Force in the member	-	-	1047	1059	1121
	Utilisation ratio	-	-	247%	199%	96%
Strut horizontal y-axis	Force in the member	-	-	607	613	649
	Utilisation ratio	-	-	243%	197%	95%
Diagonal strut	Force in the member	-	-	1635	1645	1700
	Utilisation ratio at column	-	-	148%	138%	97%
	Utilisation ratio at pile	-	-	109%	106%	98%
Check of diagonal strut to splitting/crushing						
Strut of arch at middle	Force in the member	-	-	1635	1645	1700
	Utilisation ratio	-	-	91%	87%	77%

The utilisation ratios used in the table correspond to the ratio of the compressive stress at a node face or in a strut to the design strength of the node or the strut. An utilisation ratio higher than one (100%) indicates that the stress is higher than the strength of the element. In this case, to assure a safe design, modifications of geometry are required in the strut-and-tie model to increase the area on which the stress is acting, hence reducing the stress. The iteration process ends when all the checks are verified, i.e. when all the utilisation ratios are smaller than one.

6.2.6 Truss action

In another alternative model, only the transfer of forces by truss action is considered, see the distribution of forces in Figure 6.3. The intermediate points determining both ends of the stirrups are positioned such so that the inner inclined struts and the outer inclined struts are identical and in the same plane. Therefore in this case with only truss action, the force in the corresponding inner and outer main ties are equal.
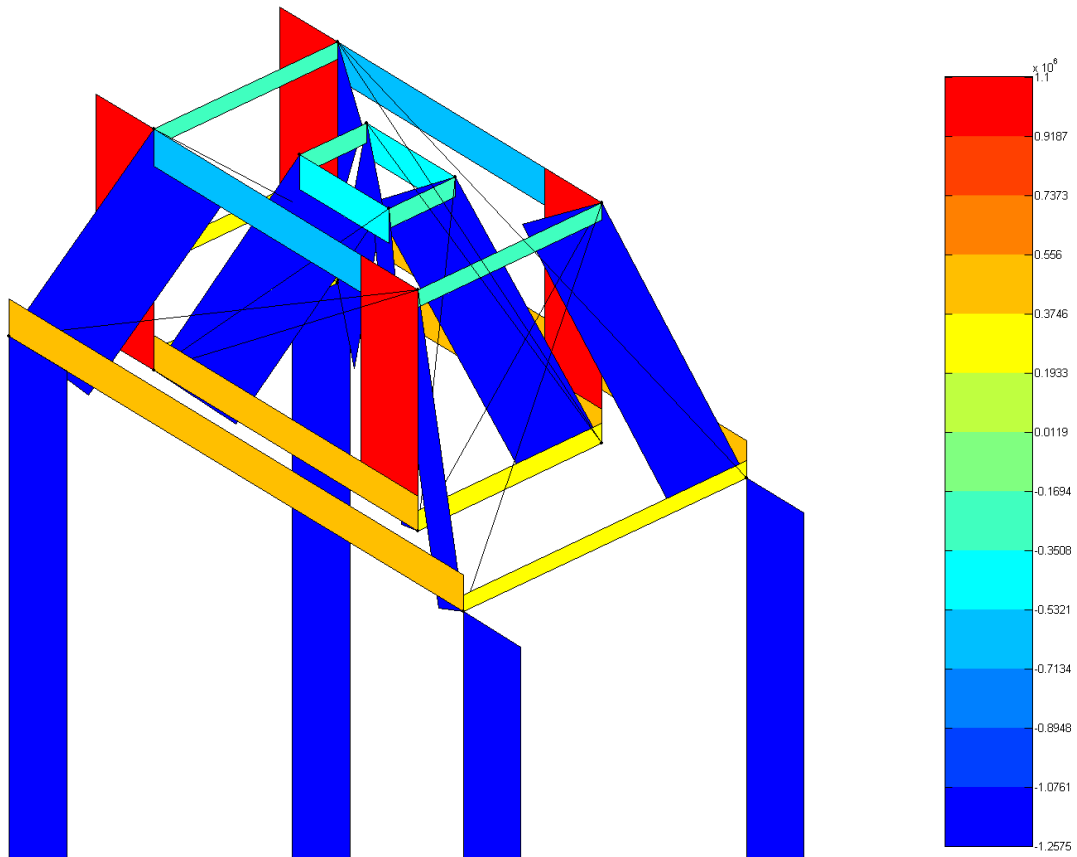
Figure 6.3   Force distribution in the strut-and-tie model of the 4-pile cap, considering only truss action (stabilisers and piles represented)

The results of the iterative design procedure are presented in Table 6.3.

Table 6.3   Design considering load transfer by truss action only

Truss action		1st iteration	2nd iteration	3rd iteration	4th iteration
Refinement of nodal zones at column	x-axis	166	98	104	104
	y-axis	110	187	176	176
Level of axes of horizontal struts and of reinforcement	a_c	20	20	20	25
	a_s	46	46	46	46
Total load per pile		1100	1100	1100	1100
Load transferred by truss action		1100	1100	1100	1100
Load transferred by arch action		0	0	0	0
Angle between strut of truss and horizontal plane		61.6°	61.9°	61.9°	61.7°
Ties x-axis (at each tie)	Force in the member	(527)	507	509	512
	A_s	(1213)	1167	1171	1177
	Number of bars (Ø16)	(7)	6	6	6
Ties y-axis (at each tie)	Force in the member	(275)	298	295	296
	A_s	(633)	685	678	682
	Number of bars (Ø16)	(4)	4	4	4
Stirrups (at each tie)	Force in the member	1100	1100	1100	1100
	A_s	2530	2530	2530	2530
	Number of bars (Ø12)	23	23	23	23
Check of nodal zones					
Strut horizontal x-axis	Force in the member	-	-	509	512
	Utilisation ratio	-	-	120%	96%
Strut horizontal y-axis	Force in the member	-	-	295	296
	Utilisation ratio	-	-	118%	95%
Inclined strut	Force in the member	-	-	1247	1249
	Utilisation ratio at column	-	-	104%	99%
	Utilisation ratio at pile	-	-	91%	91%

Note: The value of a_s used for the next iteration is the maximum value needed with regard to the different checks; here the increase of a_s required when adding a layer is more than the arbitrary increase of 20% between two iterations, assigned for insufficient areas at the nodes.

Since the inclination of the diagonal struts increases between two iterations, the stresses in the members become higher.

6.2.7   Combination of truss action and direct arch action

In the last alternative model, the load is transferred from the column to the support by combined truss action and direct beam action, as explained in Section 5.3.2. The proportion of the total load carried by truss action is defined by:

$$\beta = \frac{F_{truss}}{F_{total}} = \frac{2\dfrac{a}{z} - 1}{3} \tag{6.1}$$

The distribution of forces in the strut-and-tie model is presented in Figure 6.4.
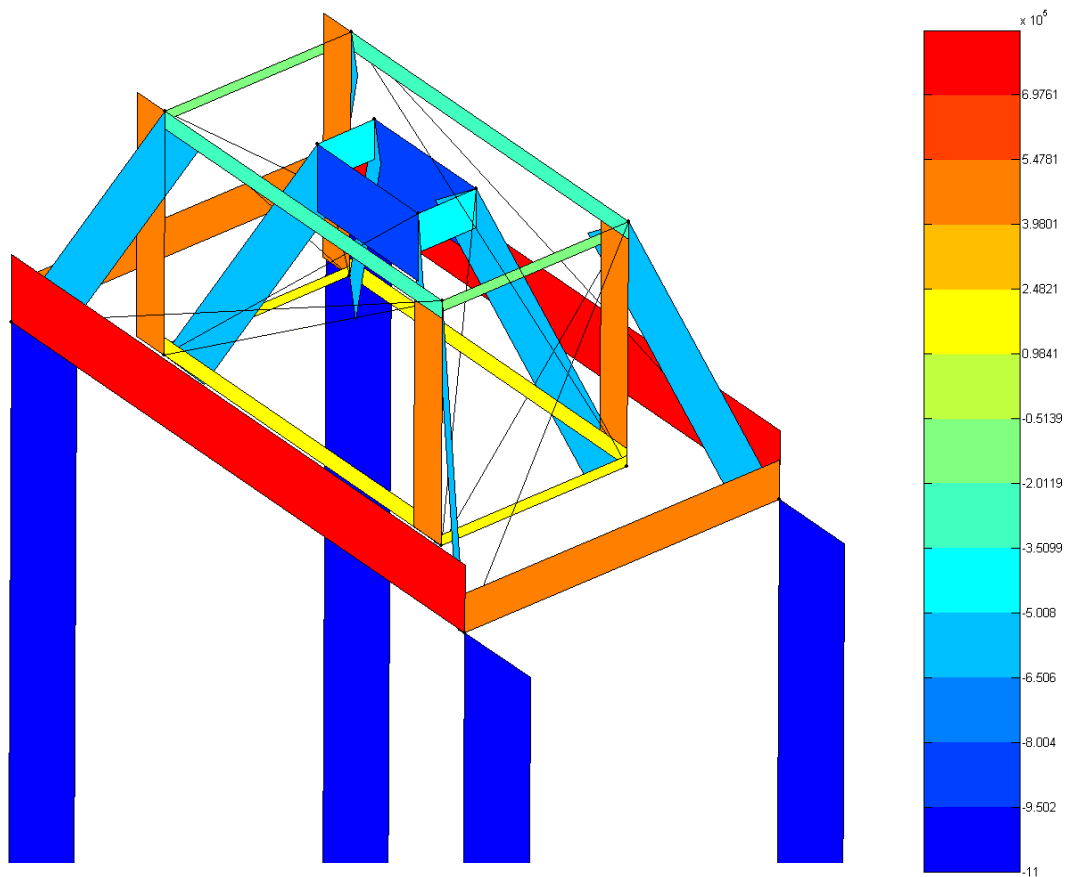
Figure 6.4   Force distribution in the strut-and-tie model of the 4-pile cap, considering a combination of truss action and direct arch action (stabilisers and piles represented)

The results of the iterative design procedure are presented in Table 6.4

Table 6.4   Design considering load transfer by a combination of truss action and direct arch action

Truss and direct arch actions		1st iteration	2nd iteration	3rd iteration	4th iteration	7th iteration
Refinement of nodal zones at column	x-direction	166	98	104	104	104
	y-direction	110	187	176	176	176
Level of axes of horizontal struts and of reinforcement	a_c	20	20	20	25	40
	a_s	46	46	72	72	72
Total load per pile		1100	1100	1100	1100	1100
Load transferred by truss action		426	418	440	445	458
Load transferred by arch action		674	682	660	655	642
Angle between strut of truss and horizontal plane		61.6°	61.9°	61.2°	61.1°	60.6°
Angle between strut of arch and horizontal plane		42.8°	43.1°	42.3°	42.1°	41.6°
Ties over piles x-axis	Force in the member	(850)	822	837	840	847
	A_s	(1954)	1889	1926	1932	1949
	Number of bars (Ø16)	(10)	10 (2 layers)	10	10	10
Ties over piles y-axis	Force in the member	(444)	483	485	487	491
	A_s	(1021)	1110	1116	1119	1129
	Number of bars (Ø16)	(6)	6	6	6	6
Ties intermediate x-axis	Force in the member	(204)	193	209	213	223
	A_s	(470)	443	482	489	513
	Number of bars (Ø16)	(3)	3	3	3	3
Ties intermediate y-axis	Force in the member	(107)	113	121	123	129
	A_s	(246)	260	279	283	195
	Number of bars (Ø16)	(2)	2	2	2	2
Stirrups	Force in the member	426	418	440	445	458
	A_s	980	961	1012	1022	1054
	Number of bars (Ø12)	9	9	9	10	10
Check of nodal zones						
Strut horizontal x-axis	Force in the member	-	-	838	840	848
	Utilisation ratio	-	-	197%	158%	100%
Strut horizontal y-axis	Force in the member	-	-	485	487	494
	Utilisation ratio	-	-	195%	156%	99%
Resultant diagonal strut	Force in the member	-	-	502	508	526
	Utilisation ratio at column	-	-	127%	119%	100%
	Utilisation ratio at pile	-	-	96%	96%	96%
	Angle / horizontal plane	-	-	48.7°	48.6°	48.3°
Check of diagonal strut to splitting/crushing						
Strut of arch at middle	Force in the member	-	-	981	977	966
	Utilisation ratio	-	-	56%	54%	51%

6.2.8 Concluding remarks

In this example, a 4-pile cap has been designed using three different strut-and-tie models, which correspond to three types of load transfer: by direct arch action, by truss action and by a combination of both. These strut-and-tie models follow the rules developed in this thesis work for three-dimensional strut-and-tie modelling and the iterative procedure used to solve the model has been explained. Besides, refinement of the nodal zones under the column has been used to improve the models.

The first type of load transfer studied, the load transfer by direct arch action, presents the advantage of not requiring shear reinforcement. However, the angle between the diagonal strut and the horizontal plane, about 40°, is lower than the recommendation for strut-and-tie modelling, which is 60° in this case (Section 3.5.1.1), and the design may be unsafe if the structure does not have enough ductility to satisfy the needed plastic redistribution. On the other hand, the second model, which considers a load transferred by truss action only, suppose that all the load is carried by shear reinforcement, hence requiring a lot of stirrups, while the main reinforcement is just reduced by one bar, due to a larger lever arm. The third model, where both direct arch action and truss action are used, seems a favourable and safe alternative; the amount of shear reinforcement is reduced compared to the previous model, as part of the load is carried by direct arch action.

6.3 10-pile cap

6.3.1 Presentation of the design case

The following example is based on a 10-pile cap built by Skanska for a bridge over E45 (the site Bohus, pile cap no. 27). Actually the original pile cap is a 20-pile cap loaded by two columns (see original drawing in Figure 6.5 and Figure 6.6), but it has been separated in two 10-pile caps in this example, which is possible as it is submitted to a vertical load only. The right part of the 20-pile cap is studied and the assumption is made that all the piles have the same orientation (Figure 6.7). The main purpose of this example is to give guidelines on how to apply the strut-and-tie model to the design of pile caps with a large number of piles, and to compare the design obtained to the one that has been worked out at Skanska Teknik using BBK and the "Concrete Handbook – Structural Design". Besides, the optimisation methods presented in this thesis work are evaluated through the comparison between four designs obtained using strut-and-tie models more or less optimised.

Several load combinations were used in the design with the codes. In order to simplify the procedure with the strut-and-tie model, with regard to the different load cases, it has been decided with the designer of the original pile cap that a load of 1100 kN at each pile would account for the load cases considered in the design according to the Swedish code. This load corresponds to the average load in the piles of the "worst" quadrant (most loaded quadrant) under the "worst" load case for this quadrant. This approach to simplify the consideration of the different load cases is further discussed in Section 5.2.3.
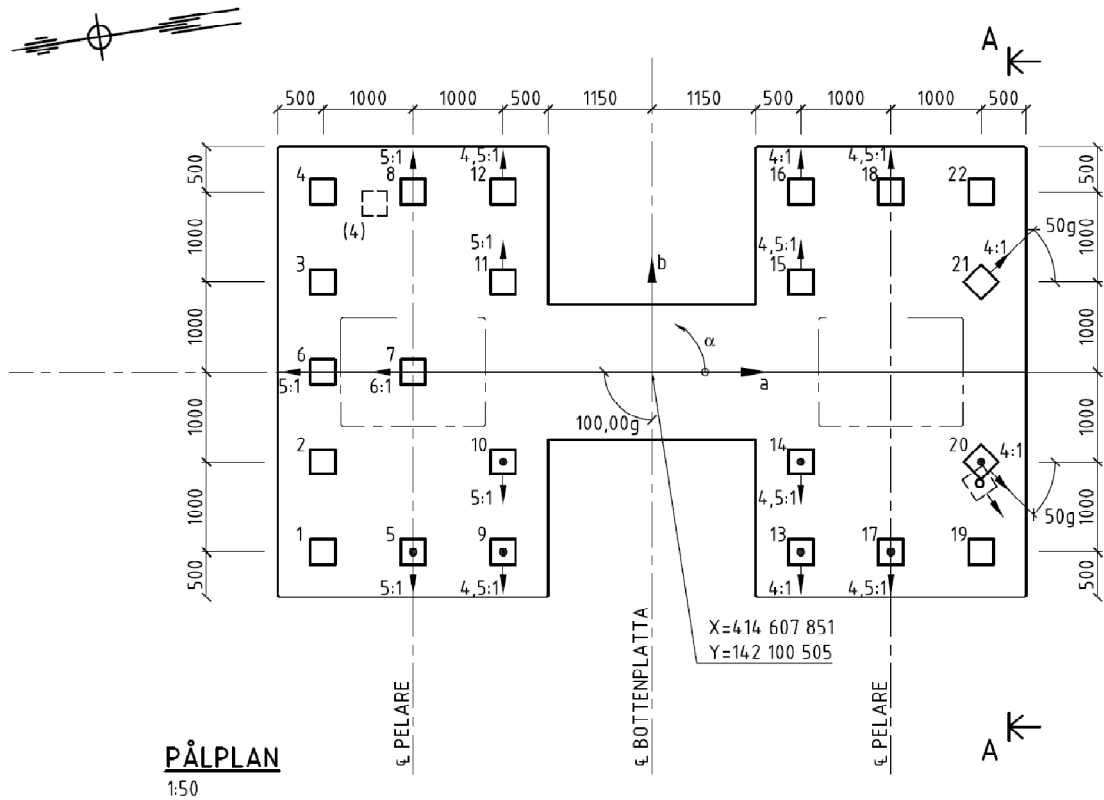
Figure 6.5   Original plan of the 20-pile cap
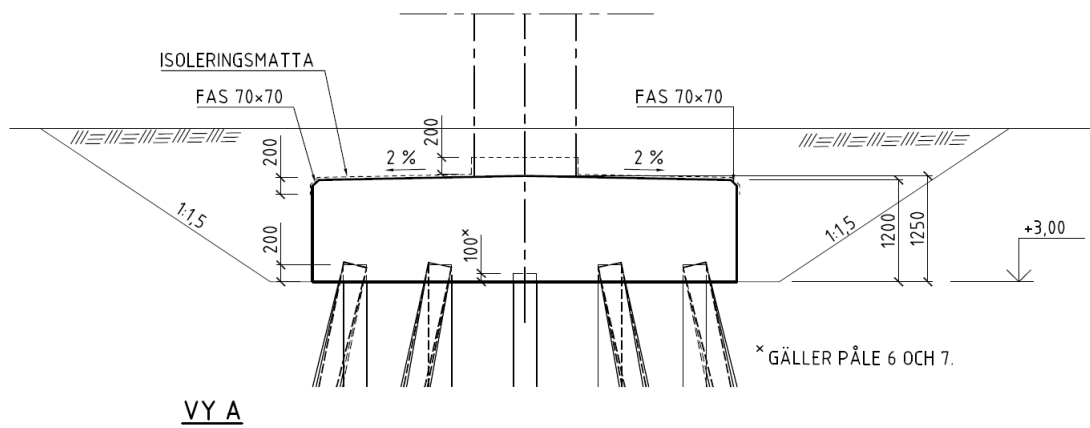
Figure 6.6   Section AA of the pile cap along the long side showing the pile inclinations
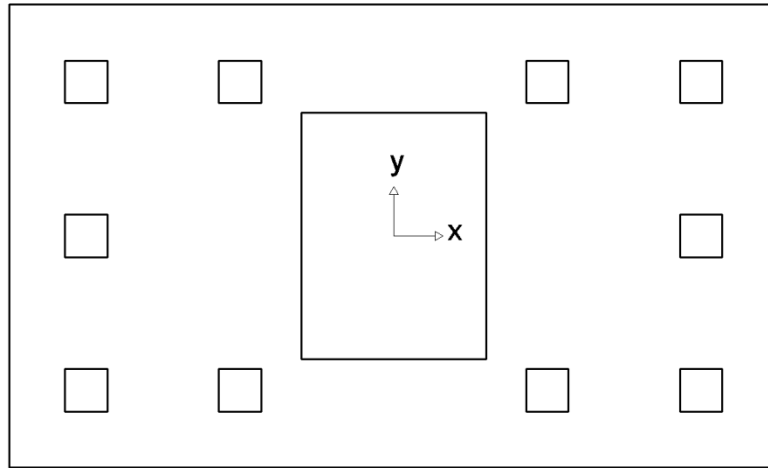
Figure 6.7   Geometry of the 10-pile cap considered for the design with strut-and-tie model

6.3.2 Strut-and-tie models

The four alternative strut-and-tie models used for this design case all include the following specificities of the strut-and-tie model developed in this thesis work, which have already been presented in the previous example (Section 6.2):

- an iterative procedure to find the required level of the singular nodes, that is to say the level of the main reinforcement a_s and the level of the horizontal struts a_c,

- the three-dimensional nodal zone geometry (described in Section 4.3),

- the check of the diagonal strut to splitting and crushing (see Section 5.3.4).

These three specificities assure that the design using the strut-and-tie model for the three-dimensional case of a pile cap is safe. One purpose of this example is to study the influence of the two other aspects of the strut-and-tie model developed in this thesis work, which aim at optimising the design by improving the performance of the structure:

- the combination of truss action and direct arch action,

- the refinement of the nodal zone geometry, already described in Section 4.3.5 and presented in the previous example Section 6.2.3.

In order to do so, the design of this 10-pile cap is conducted with four alternative strut-and-tie models. Model 1 and Model 2 carry the load from the column to the piles by truss action only, while in Model 3 and Model 4 a combination of truss action and direct arch action is used. Besides, a refinement of the geometry of the nodal zones under the column is used in Model 2 and Model 4. Consequently, Model 4 is the most optimised of the four models, as it includes both features, while Model 1 is the least optimised model.

Two different types of design are also conducted. In the first one the level of the main reinforcement a_s is modified according to the design with the strut-and-tie models, for instance, if the check of a node above a pile is not fulfilled or if several layers of reinforcement are needed to fit the bars above the piles, the level a_s of the main reinforcement is increased. On the other hand, in the second type of design, the level of the main reinforcement a_s is fixed equal to the value used in the original design

according to the code, where the main reinforcement has been placed in one layer, even if for this reason some checks of nodes could not be fulfilled. The reason for that is to provide a better comparison between the design with the strut-and-tie models and the design according to the code, by using the same lever arm in the two designs. Besides, the transverse forces induced by spreading the bars have not been taken into account in the original design.

The general geometry of the strut-and-tie models is illustrated in Figure 6.8, where the notations used hereafter for the nodes, the struts and the ties are explained.
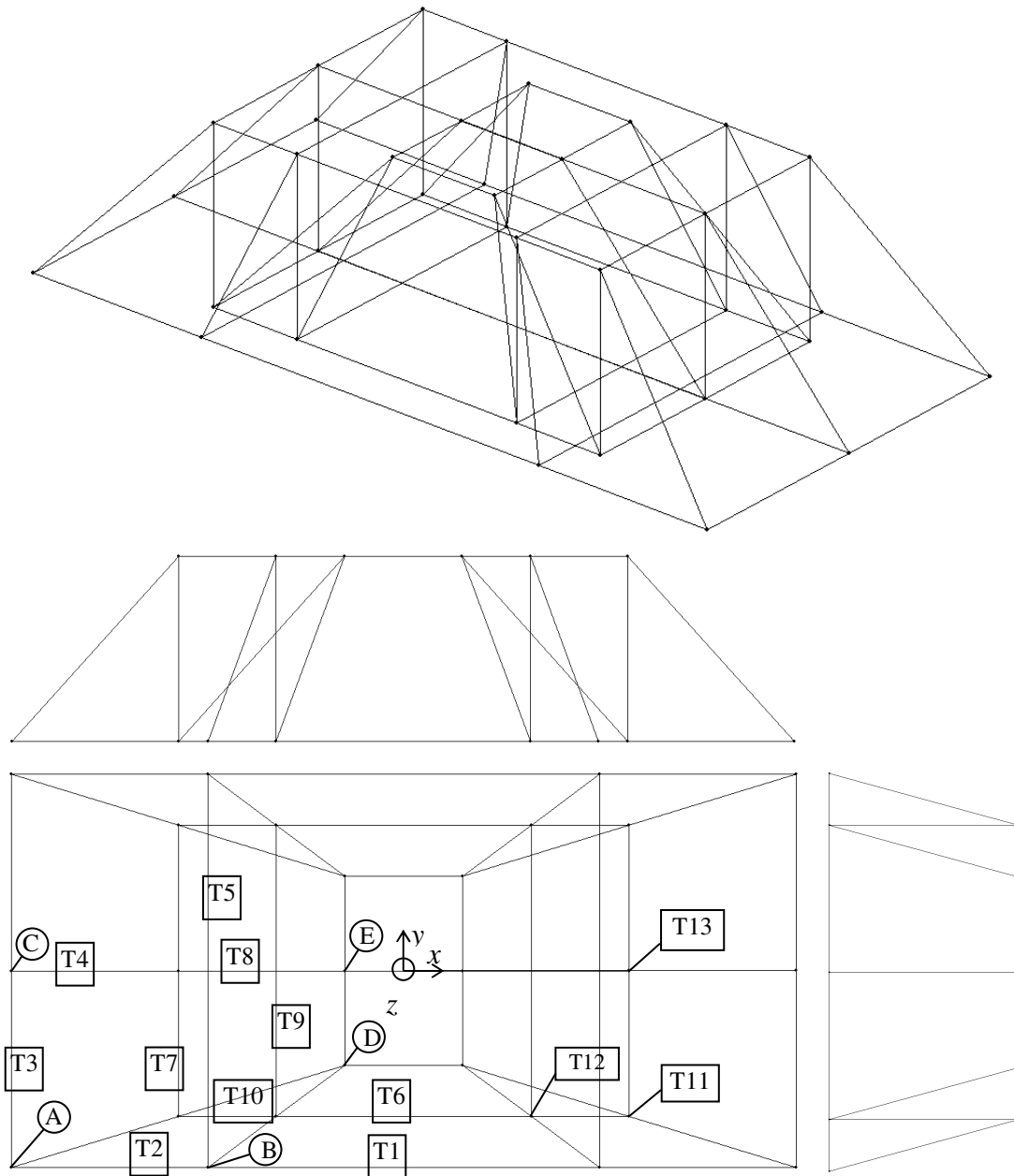
Figure 6.8   Strut-and-tie model geometry and denominations used in design: nodes A-E, main ties T1-10 (name corresponding to the bar crossed by the box), and shear ties T11-T13

6.3.3 Nodal zone geometry at the column

In this example, the choice has been made to have six nodes at the column, and therefore to divide the column area into six loaded areas, as illustrated in Figure 6.9 and Figure 6.10 (a). The reason for this choice is the small angle between the two inclined struts going from a corner of the column to the two piles along the longitudinal side of the pile cap. It is therefore appropriate in this case to combine these struts for the check of the node, by applying the method explained in Section 4.3.4 for nodes with more than one strut in the same quadrant. The horizontal struts in x-direction, joining the four nodes at the corners of the column, and the strut joining the two nodes in the middle cross each other perpendicularly, leading to favourable triaxial compression at the nodes in the middle. However, there is no interaction between these struts at the nodes in the middle (the stresses in the two transversal struts are not deviated in the nodal zone in the middle). For that reason, a different height can be chosen for these horizontal struts, as illustrated in Figure 6.10 (b). Then the strut-and-tie model for the 10-pile cap appears like superposition of a 3-D strut-and-tie model for the eight piles along the long sides of the pile cap (similar to a 4-pile cap strut-and-tie model due to the combination of pairs of struts) and a 2-D model for the two piles at the middle of the short sides.

Like in the previous example (Section 6.2.3), the nodal zone under the column are refined to optimise the strut-and-tie model. In this example, owing to the angle of the two inclined struts connected to the node at the corner of the column, it is obvious that the resultant of the forces in these struts will be bigger in y-direction than in x-direction. Therefore the horizontal struts in y-direction should have a bigger area than the horizontal struts in x-direction, which has been included in the algorithm. However, for a simplification of the algorithm, each area has been limited within the column influence areas which would have been used with no refinement. The areas at the corners being two times the ones at the middle as they are loaded by the load of two piles. For instance, in Figure 6.9, the dimension in x-direction of the nodal zone in the middle is the largest allowed, even it could be further increased by using some of the available influence area of the corner nodes.
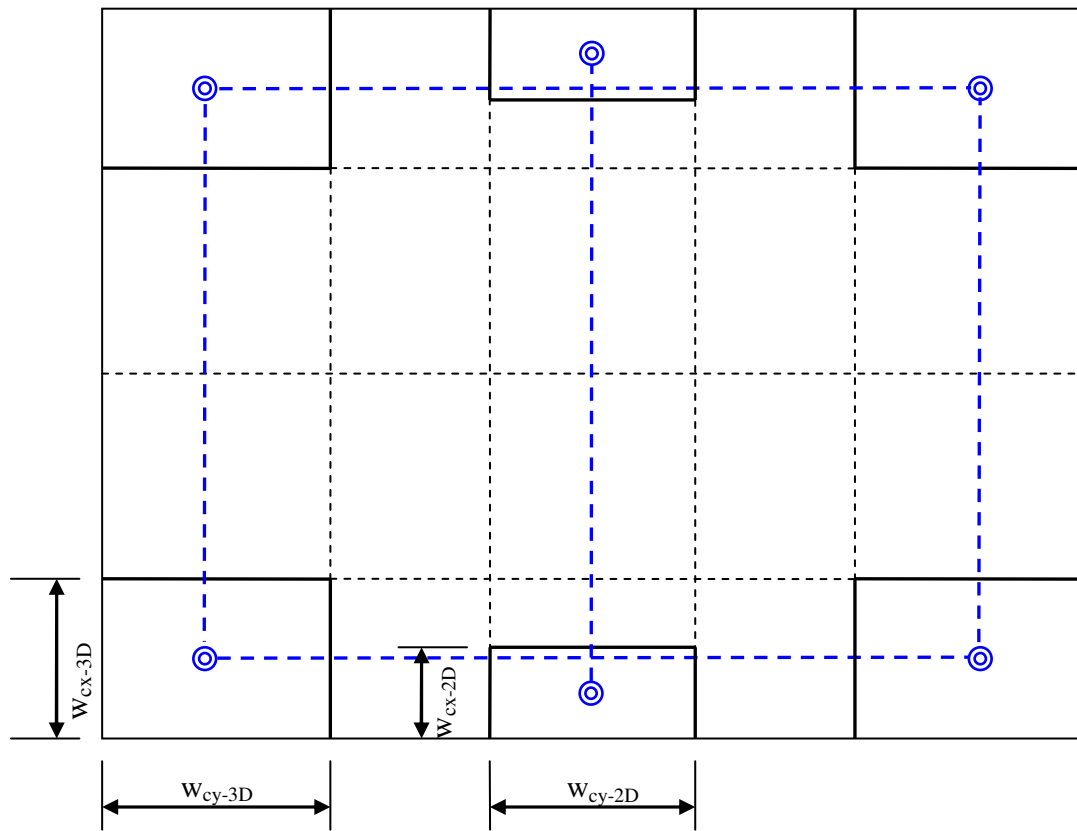
Figure 6.9   Configuration of the nodes and horizontal struts under the column (nodes and struts represented in blue)
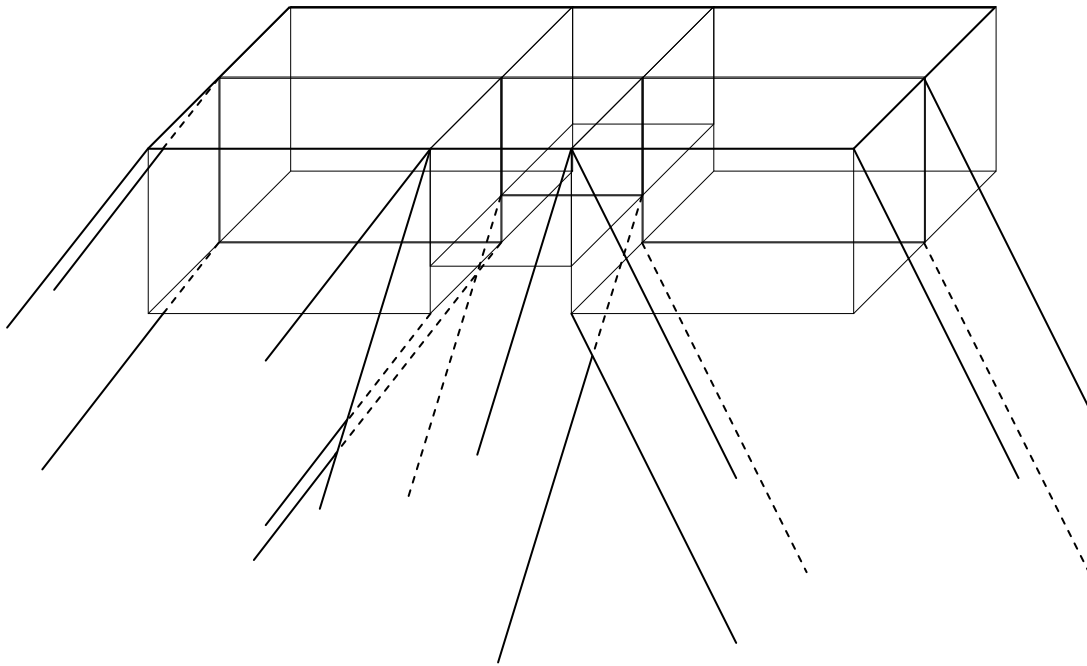
(a) Consideration of all the bearing area
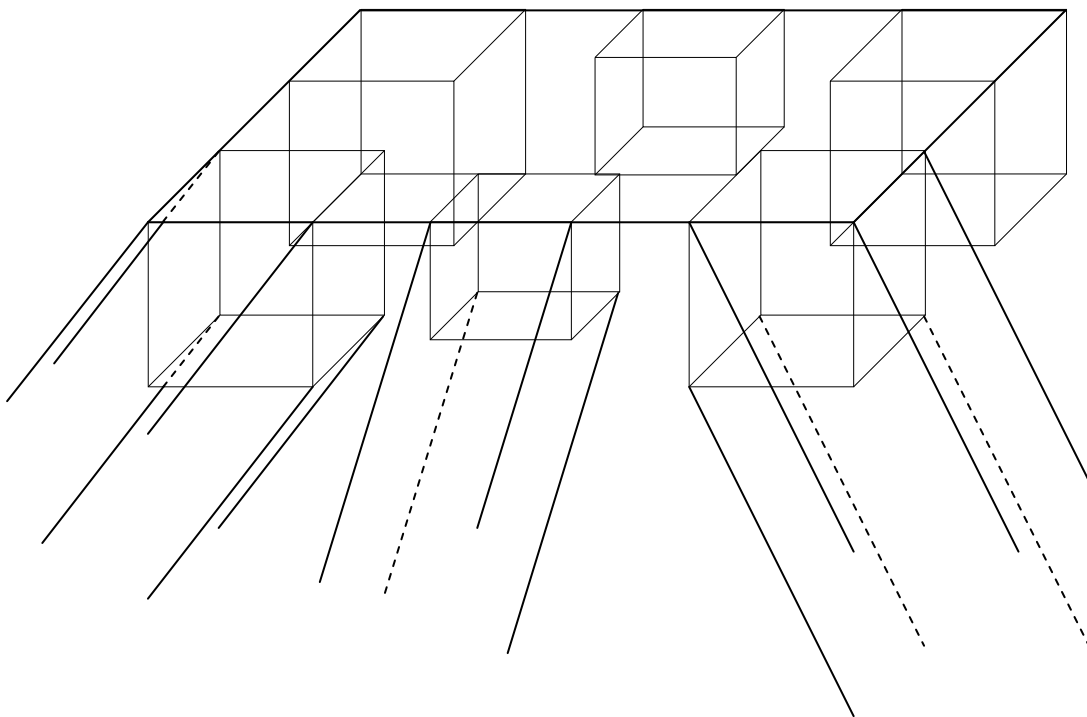
(b) Consideration of only the required portions of the bearing area

Figure 6.10   Idealisation of nodal zone geometry under the column (only the struts at the front nodes are shown)

It should be noted, when using the nodal zone geometries shown in Figure 6.10 (b), that the horizontal struts under the column are bottle-shape struts. The stresses in these struts spread between the nodes, inducing transverse tensile stresses. In some extreme cases, when the sum of the areas used for the nodal zones is small in

comparison to the total area of the column, it would be recommended to place reinforcement under the column to confine these stresses.

6.3.4 Design assumptions

The data used in the design with the strut-and-tie models correspond to the ones used in the original design. The concrete strength class is C35/45 and the reinforcing steel is of type B500B. The same diameter of bars is used as in the original design: 25 mm for the main bars and 16 mm for the stirrups. In order to compare the results of the original design with BBK with that obtained using the strut-and-tie models, the same partial coefficients are used, for safety class 3 (γ_n=1.2). In BBK these coefficients are applied to the strength of the materials. Therefore in this example the design strengths of concrete and steel are always determined as:

$$f_{cd} = \frac{35}{1.5 \cdot 1.2} = 19.4 \text{MPa} \qquad \text{and} \qquad f_{yd} = \frac{500}{1.15 \cdot 1.2} = 362.3 \text{MPa}$$

Like in the previous example of the design of a 4-pile cap, the coefficients used in the strut-and-tie model for the check of the nodes are the ones recommended by the Eurocode 2 and presented in Section 3.6.3.3 (k_2) and Section 4.3.6 (k_4). The coefficient k_2 is preferred to k_3 in this example, as k_3 seems too conservative for a pile cap with such a geometry, where the tensile stresses are much smaller in the transverse direction (x-direction) than in the longitudinal direction (y-direction).

- $k_4 = 3$ for the nodes under the column subjected to triaxial compression.

- $k_2 = 0.85 \cdot 1.1$ for the nodes over the piles

6.3.5 Results

6.3.5.1 Comparison between the alternative strut-and-tie models

In this Section; the results of the design with the four alternative strut-and-tie models are presented and commented. As it has been explained previously, in Section 6.3.2, two types of design are conducted. In the first one (Section a) below) the level of the main reinforcement a_s is free to be modified in order to satisfy the needs of the models. In the second type of design (Section b) below) a_s is fixed equal to the value used in the original design according to the code, where the main reinforcement has been placed in one layer

a) With the level of the main reinforcement as modified according to the design with the strut-and-tie model

The force distribution in two of the strut-and-tie models, at final iteration, is shown in Figure 6.11. The effect of the refinement of the nodal zones under the column on the geometry of the models is also illustrated in Figure 6.12. It should be noted, that the size of the column is fixed. In Figure 6.11 and in Figure 6.12, the dimensions of the column are the same in (a) and (b). It is the position of the nodes that is changed, the nodes being positioned closer to the edges of the column in (b), after refinement.
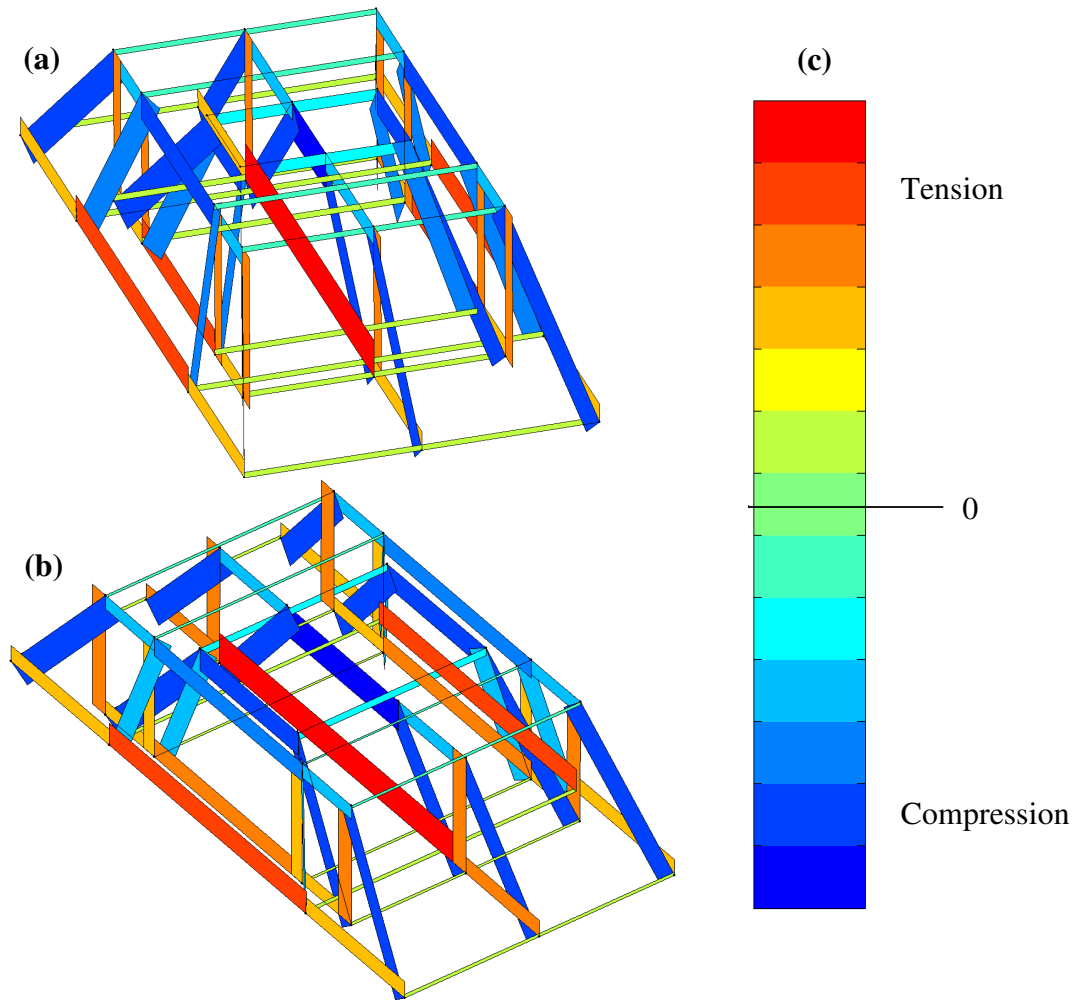
*Figure 6.11   Force distribution in alternative strut-and-tie models: **(a)** Model 1, with only truss action and without refinement of nodal zones under the column, **(b)** Model 4, with combination of truss action and direct arch ation and with refinement of nodal zones under the column, **(c)** indicative colour scale of stresses*

| (a) | (b) |
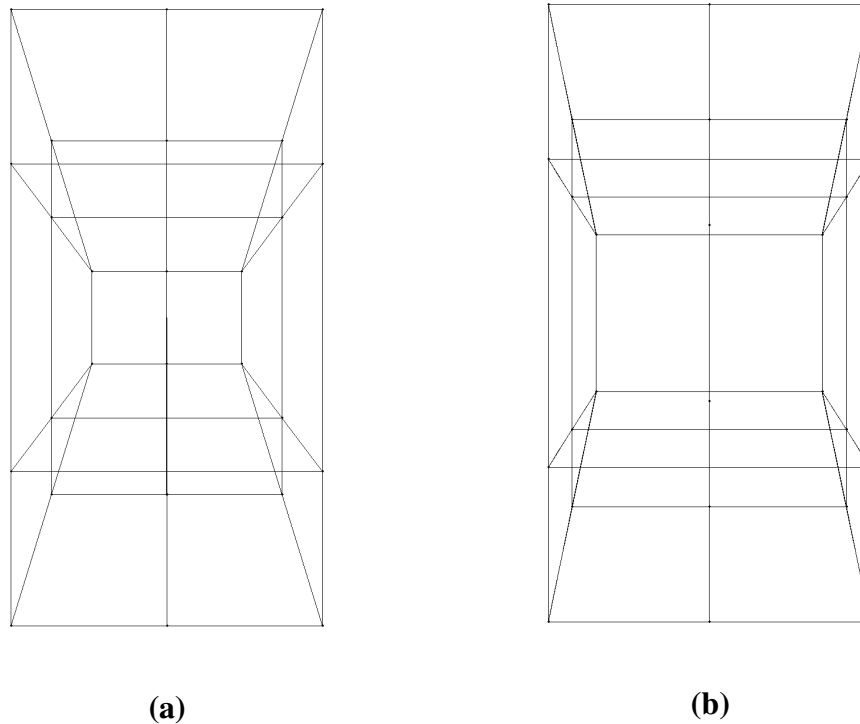
*Figure 6.12   Top view of the strut-and-tie model at the final iteration **(a)** without refinement of nodal zones under the column (Model 1 and Model 3), **(b)** after refinement of nodal zones under the column (Model 4)*

The results obtained at final iteration, for the four alternative strut-and-tie models, are given in Table 6.5 and the need for reinforcement in Table 6.6. The nomenclature of the struts and the ties used in these tables is described in Figure 6.8.

The first model is the reference one; no optimisation is done. The nodes are placed in the middle of their respective bearing areas and all the load is carried by truss action. In the second model, the node position is refined. As can be seen in Table 6.6, the needed reinforcement is reduced along with reduction of forces transmitted into the inclined and horizontal members of the model. Model 3 reduces the needed amount of stirrups by considering that a part of the load is transmitted by direct arch action. The effect, compared to Model 1 is beneficial. The combination of the refinement of node positions and transfer of a part of the load by arch action is applied in Model 4. This model is the most advanced and efficient one. The amount of reinforcement required is reduced by 22% compared to the reference model.

Table 6.5   *Geometry of the alternative strut-and-tie models at final iteration and utilisation ratios of nodes and struts, with a free level a_s of the main reinforcement*

			Model 1	Model 2	Model 3	Model 4
Description of model	Truss action		**X**	**X**	**X**	**X**
	Direct arch action				**X**	**X**
	Refinement of nodal zones			**X**		**X**
Total load per pile	(total load on pile cap: 11000kN)		1100	1100	1100	1100
Load transfered by truss action and load transfered by arch action	Truss AD	truss action	1100	1100	1081	918
		arch action	0	0	18	182
	Truss BD	truss action	1100	1100	344	127
		arch action	0	0	756	973
	Truss CE	truss action	1100	1100	1083	849
		arch action	0	0	17	251
Level of axes of reinforcement and of horizontal struts	a_s		120	100	120	125
	a_c 2D		70	55	70	60
	a_c 3D		25	35	30	50
Dimensions of the effective loading areas used under the column	wc-x 3D		600	116	600	123
	wc-y 3D		640	378	640	358
	wc-x 2D		600	69	600	69
	wc-y 2D		320	320	320	320
Check of nodal zones	Strut A		88%	92%	89%	91%
	Strut B		72%	78%	78%	73%
	Strut C		99%	98%	100%	100%
	Strut D		16%	98%	18%	98%
	Strut E		38%	85%	38%	81%
	Strut hor-x 3D		91%	91%	92%	94%
	Strut hor-y 3D		42%	91%	48%	96%
	Strut hor-x 2D		97%	100%	97%	95%
Check crushing/splitting of direct struts	Arch AD		0	0	1%	15%
	Arch BD		0	0	26%	57%
	Arch CE		0	0	1%	22%

In the most advanced strut-and-tie model (Model 4), it can be seen that the required level of the centroid of the main reinforcement, a_s, reaches a value of 120 mm (Table 6.5), as a_s is free to be modified according to the needs of the strut-and-tie model. However, when the same pile cap was designed using the "Concrete Handbook –

Structural Design", a_s was set to 75 mm. This difference has two reasons. In the model developed, the permissible region to spread the bars above the piles is very limited. According to the definition of the parallelepiped nodal zones and in order to respect a consistent deviation of stresses, the bars should be placed within the pile width above a pile, so that the influence width of the bars is equal to the pile width. For that reason, in some cases, the bars have to be placed in several layers, which increases the height of the nodes. The other reason, that is decisive in that case, is that the stresses in the inclined struts incoming in the nodal regions at the piles are too high. Therefore, the height of the nodes over the piles has to be increased in order to reduce the stresses.

Table 6.6   Reinforcement needed in the alternative strut-and-tie models, with a free level a_s of the main reinforcement

Description of model			Model 1	Model 2	Model 3	Model 4	Bars: number and length
Description of model	Truss action		X	X	X	X	number and length
	Direct arch action				X	X	
	Refinement of nodal			X		X	
Reinforcement required at each tie	T1	As	4024	3321	4905	4673	2 x 2000
		Number of bars	9 Ø25	7 Ø25	10 Ø25	10 Ø25	4000
	T2	As	2850	2490	2913	3035	4 x 1000
		Number of bars	6 Ø25	6 Ø25	6 Ø25	7 Ø25	4000
	T3	As	872	511	891	623	2 x 2000
		Number of bars	2 Ø25	2 Ø25	2 Ø25	2 Ø25	4000
	T4	As	2999	2545	3046	3180	2 x 750
		Number of bars	7 Ø25	6 Ø25	7 Ø25	7 Ø25	1500
	T5	As	872	511	1480	1008	2 x 2000
		Number of bars	2 Ø25	2 Ø25	4 Ø25	3 Ø25	4000
	T6	As	4026	3323	3189	2273	2 x 2500
		Number of bars	9 Ø25	7 Ø25	7 Ø25	5 Ø25	5000
	T7	As	872	511	863	446	2 x 1700
		Number of bars	2 Ø25	2 Ø25	2 Ø25	1 Ø25	3400
	T8	As	6000	4864	6000	5033	1 x 2500
		Number of bars	13 Ø25	10 Ø25	13 Ø25	11 Ø25	2500
	T9	As	872	511	274	62	2 x 1700
		Number of bars	2 Ø25	2 Ø25	1 Ø25	0 (Asmin)	3400
	T10	As	2851	2491	2820	2173	4 x 500
		Number of bars	6 Ø25	6 Ø25	6 Ø25	5 Ø25	2000
	T11	As	3036	3036	2986	2533	4 x 1000
		Number of bars	16 Ø16	16 Ø16	15 Ø16	13 Ø16	4000
	T12	As	3036	3036	949	349	4 x 1000
		Number of bars	16 Ø16	16 Ø16	5 Ø16	2 Ø16	4000
	T13	As	3036	3036	2989	2344	2 x 1000
		Number of bars	16 Ø16	16 Ø16	15 Ø16	12 Ø16	2000
Amount of reinforcement (without considering anchorage lengths)	Longitudinal (kg)		617	513	594	543	
	Transversal (kg)		114	114	132	90	
	Stirrups (kg)		252	252	174	133	
	Total (kg)		983	879	899	766	

A sketch of the layout of the main reinforcement according to the design with Model 4 is given in Figure 6.13. As can be seen on this figure, some ties require two layers. The height of the reinforcement, which is 75 mm above the piles for the first layer and 175 mm for the second layer, corresponds to the average between the two directions.

One could for instance place axis of the reinforcement along in x-direction at 62 mm and the one in y-direction at 88 mm. The reinforcement should be alternate in the two directions; it should be avoided to place two layers in one direction and two layers on top in the other direction, for the equilibrium at the node. The ties that are not over piles and do not connect singular nodes can be spread. However in this example it is only the case of Tie 8. Tie 6 could also be spread but as it has to be placed beside its exact position due to the conflict with the adjacent Tie 1, it is better to keep it concentrated, so that its axis is not too far from its position in the strut-and-tie model. The shear reinforcement is not represented. It has to be spread to cover the entire stress field at the smeared nodes. The recommendation of Eurocode 2 can be followed, that is to spread it along the strut over the "middle three-fourth" of the distance between the pile face and the column face, and over a certain distance laterally as well.

(a)   **(b)**
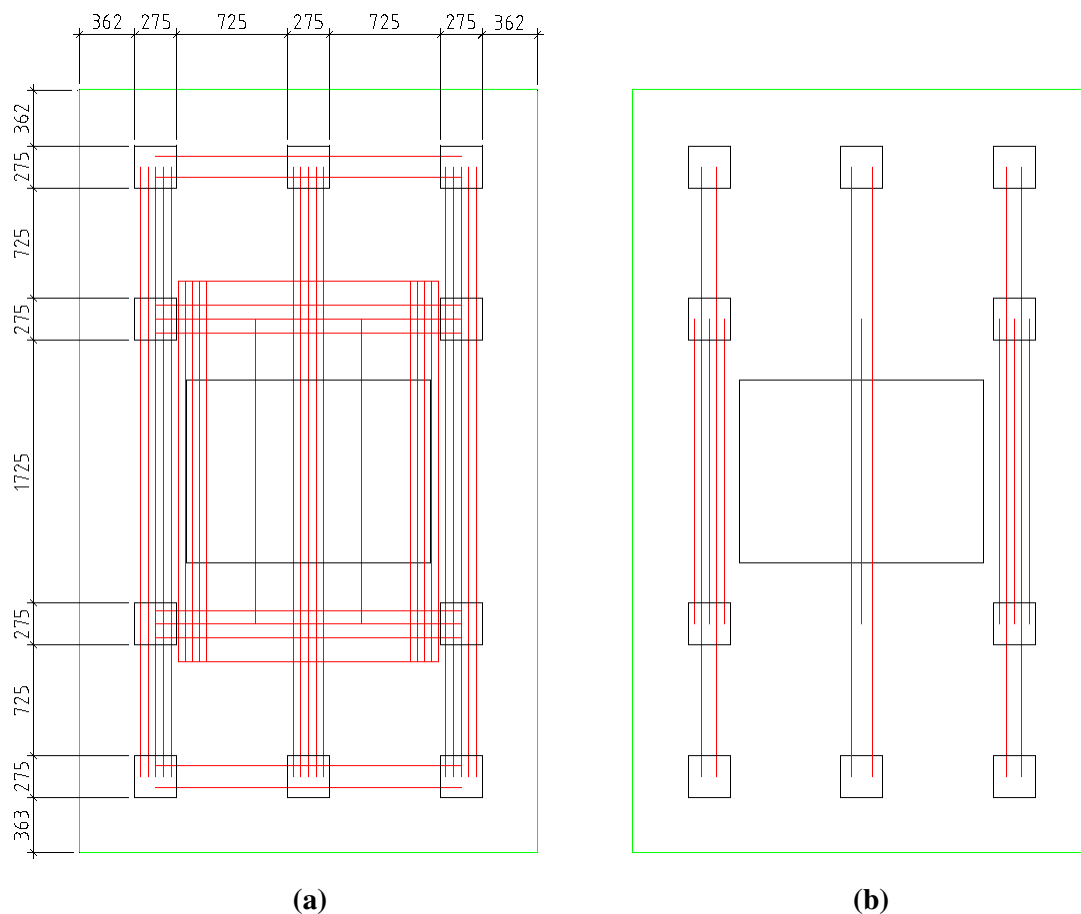
Figure 6.13   Layout of main reinforcement for the design with the strut-and-tie Model 4 (bars Ø25) (a) first layer 75mm above top of the piles, (b) second layer 175mm above top of the piles

b)   **With the level of the main reinforcement as fixed according to the design with the code**

The same example has been conducted with the height of main reinforcement a_s fixed to 75mm, which corresponds to the average between the two directions for one layer. The reason for that was to provide an additional comparison with the design using the codes where the reinforcement is spread in one layer. The results obtained at final iteration, for the four alternative strut-and-tie models, are given in Table 6.7 and the

need for reinforcement in Table 6.8. The nomenclature of the struts and the ties used in these tables is described in Figure 6.8. In the design with a_s fixed, the amount of steel required is reduced, from 766 kg (Table 6.6) to 724 kg (Table 6.8), with Model 4.

It should be noted that when spreading the main reinforcement, the transverse tension induced should be checked as described in Figure 5.27. Besides, some checks of compressive stresses from the inclined struts at nodal zones over the piles are not fulfilled anymore, and would require an increase of a_s. However the strength value used for these nodes, corresponding to two-dimensional CCT-nodes, seems a bit conservative in the three-dimensional case and as the increase in tension is not large, the results can still be considered for a comparison.

Table 6.7   *Geometry of the alternative strut-and-tie models at final iteration and utilisation ratios of nodes and struts, with a fixed level a_s of the main reinforcement*

			Model 1	Model 2	Model 3	Model 4
Description of model	Truss action		**X**	**X**	**X**	**X**
	Direct arch action				**X**	**X**
	Refinement of nodal zones			**X**		**X**
Total load per pile	(total load on pile cap: 11000kN)		1100	1100	1100	1100
Load transferred by truss action and load transferred by arch action	Truss AD	truss action	1100	1100	1013	848
		arch action	0	0	87	252
	Truss BD	truss action	1100	1100	310	100
		arch action	0	0	790	1000
	Truss CE	truss action	1100	1100	1003	777
		arch action	0	0	97	323
Level of axes of reinforcement and of horizontal struts	a_s		75	75	75	75
	a_c 2D		65	55	65	55
	a_c 3D		25	35	30	50
Dimensions of the loading areas used at the column	wc-x 3D		600	117	600	123
	wc-y 3D		640	378	640	358
	wc-x 2D		600	69	600	69
	wc-y 2D		320	320	320	320
Check of nodal zones	Strut A		107%	102%	112%	114%
	Strut B		83%	83%	94%	87%
	Strut C		115%	107%	122%	123%
	Strut D		16%	97%	18%	97%
	Strut E		37%	83%	37%	81%
	Strut hor-x 3D		87%	88%	92%	93%
	Strut hor-y 3D		40%	88%	47%	94%
	Strut hor-x 2D		98%	97%	98%	97%
Check of crushing/splitting of direct struts	Arch AD		-	-	4%	24%
	Arch BD		-	-	27%	59%
	Arch CE		-	-	7%	32%

Table 6.8   Reinforcement needed in the alternative strut-and-tie models, with a fixed level a_s of the main reinforcement

Description of model			Model 1	Model 2	Model 3	Model 4	Bars: number and length
	Truss action		**X**	**X**	**X**	**X**	
	Direct arch action				**X**	**X**	
	Refinement of nodal zones			**X**		**X**	
Reinforcement required at each tie	T1	As	3833	3233	4877	4596	2 x 2000
		Number of bars	8 Ø25	7 Ø25	10 Ø25	10 Ø25	4000
	T2	As	2715	2424	2946	3026	4 x 1000
		Number of bars	6 Ø25	5 Ø25	7 Ø25	7 Ø25	4000
	T3	As	831	498	901	621	2 x 2000
		Number of bars	2 Ø25	2 Ø25	2 Ø25	2 Ø25	4000
	T4	As	2834	2476	3084	3139	2 x 750
		Number of bars	6 Ø25	6 Ø25	7 Ø25	7 Ø25	1500
	T5	As	831	498	1435	965	2 x 2000
		Number of bars	2 Ø25	2 Ø25	3 Ø25	2 Ø25	4000
	T6	As	3835	3234	2831	1975	2 x 2500
		Number of bars	8 Ø25	7 Ø25	6 Ø25	5 Ø25	5000
	T7	As	831	498	769	390	2 x 1700
		Number of bars	2 Ø25	2 Ø25	2 Ø25	1 Ø25	3400
	T8	As	5670	4732	5670	4732	1 x 2500
		Number of bars	12 Ø25	10 Ø25	12 Ø25	10 Ø25	2500
	T9	As	831	498	235	46	2 x 1700
		Number of bars	2 Ø25	2 Ø25	1 Ø25	0 (Asmin)	3400
	T10	As	2716	2425	2515	1900	4 x 500
		Number of bars	6 Ø25	5 Ø25	6 Ø25	4 Ø25	2000
	T11	As	3036	3036	2796	2342	4 x 1000
		Number of bars	16 Ø16	16 Ø16	14 Ø16	12 Ø16	4000
	T12	As	3036	3036	856	276	4 x 1000
		Number of bars	16 Ø16	16 Ø16	5 Ø16	2 Ø16	4000
	T13	As	3036	3036	2769	2143	2 x 1000
		Number of bars	16 Ø16	16 Ø16	14 Ø16	11 Ø25	2000
Amount of reinforcement (without considering anchorage lengths)	Longitudinal (kg)		567	490	580	526	
	Transversal (kg)		114	114	116	75	
	Stirrups (kg)		252	252	164	123	
	Total (kg)		933	856	861	724	

6.3.5.2 Comparison between design with strut-and-tie models and design with sectional analysis according to BBK

One of the aims of this example is to compare the design with the strut-and-tie model to the design with sectional approach according to BBK and the "Concrete Handbook - Structural Design". As it has been said previously, the load of 1100 kN per pile, for which the pile cap is designed with the alternative strut-and-tie models, has been chosen with the designer of the existent pile cap in order to be able to compare the reinforcement amounts. The pile loads obtained in the worst quadrant when designing the pile cap with the code considering vertical load, bending moment and torque are applied to the entire model and the different load cases are thus considered simultaneously. It should be noticed that this way of dealing with the load cases is an approximation, which is quite common in practice and should be rather much on the safe side.

The plan of reinforcement obtained by Skanska with the sectional approach is shown in Figure 6.14. To simplify this comparison it was decided not to consider minimum reinforcement and anchorage lengths.
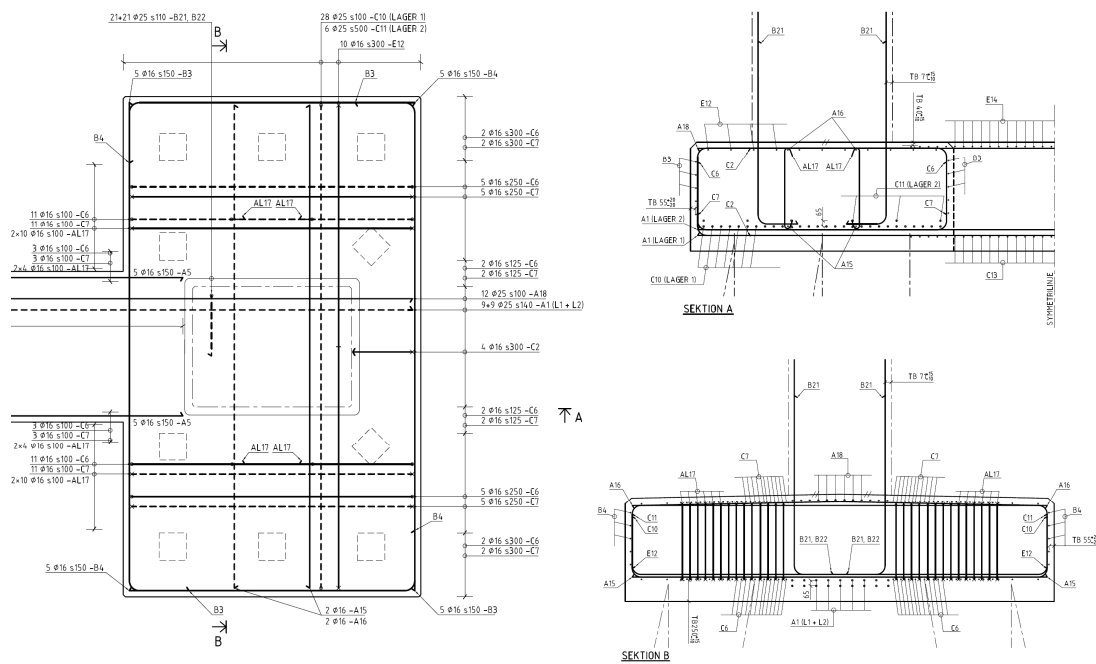
Figure 6.14   Reinforcement plan of the 10-pile cap designed by Skanska using a sectional approach with BBK

The minimum reinforcement ratio used in the original design is ρ_{min}=0.005 (bars of diameter 16 mm with a spacing of 300 mm), which corresponds to the requirements of Trafikverket (the Swedish Transport Administration) for bridge design. However this minimum reinforcement has been left out in the comparison.

The length of the bars was taken between the centre of the piles (equivalent to the position of the nodes over the piles in the strut-and-tie models), without considering any anchorage length. As the same bars were used, the anchorage lengths would have been approximately the same, thus increasing slightly the difference between the results. The considered length of bars corresponds to the length of ties in the model.

The total reinforcement required by the sectional approach with BBK has also been reduced, as limitation of crack widths has not been considered in the design using strut-and-tie models. Therefore the bars added with regard to crack control in the original design should not be included in the comparison, leading to reduction of the main reinforcement by 10% and of the shear reinforcement by 30%. The details of the required reinforcement amounts by the original design using the sectional approach with BBK are given in Table 6.9; these amounts are compared to the ones required by the four alternative strut-and-tie models for both types of design in Table 6.10.

Table 6.9   Needed reinforcement amounts according to sectional approach with BBK

Amount of reinforcement 10-pile cap	Diameter (mm)	Number of bars	Length (mm)	Amount (kg)
Main reinforcement along long side				
C10	25	28	4000	550
C11	25	6	4000	118
Total				668
Total -10% (crack control)				**601**
Main reinforcement along short side				
Total				**56**
Stirrups				
AL17	16	56	1000	113
C6	16	42	1000	84
Total				197
Total -30% (crack control)				**138**
Total reinforcement with BBK (reduced)				**795**

Table 6.10   Comparison of the required reinforcement amounts by sectional approach with BBK and by alternative strut-and-tie models

		Model 1	Model 2	Model 3	Model 4	BBK
Description of model	Truss action	**X**	**X**	**X**	**X**	**(X)**
	Direct arch action			**X**	**X**	**(X)**
	Refinement nodes position		**X**		**X**	**(X)**
With a free level a_s of the main reinforcement						
Amount of reinforcement	Longitundinal (kg)	617	513	594	543	601
	Transversal (kg)	114	114	132	90	56
	Stirrups (kg)	252	252	174	133	138
	Total (kg)	983	879	899	766	795
With a fixed level a_s of the main reinforcement						
Amount of reinforcement	Longitundinal (kg)	567	490	580	526	601
	Transversal (kg)	114	114	116	75	56
	Stirrups (kg)	252	252	164	123	138
	Total (kg)	933	856	861	724	795

The need for reinforcement calculated with the optimised strut-and-tie model (Model 4), both when a_s is fixed or free, is lower than the need for reinforcement obtained with the sectional approach using BBK. However the difference is small, the major difference between the two types of designs concerns the reinforcement layout. The main reinforcement layout proposed when designing with the strut-and-tie model is shown in Figure 6.13. Most of the main bars are concentrated over the piles and some of them, the ones that carry the load by truss action together with the stirrups, can be smeared. This design is rather different from the one with spread reinforcement over the bottom of the slab which is the result of the sectional approach. The proper flow of forces from the column to the piles is better taken into account with the strut-and-tie model. However, it results in a decrease of the internal level arm that leads to an increase of the required main reinforcement. Even so, the total amount of steel required by the design using the strut-and-tie model is still slightly lower than that needed when the design was made with BBK.

6.3.6   Concluding remarks

The total reinforcement amounts required by the sectional approach using BBK and by the optimised strut-and-tie models are very close. The reinforcement amount needed in Model 4, considering both transfer modes of the load (truss and arch actions) and the refinement of the nodal zone is a little bit lower than the one obtained with BBK, where the refinement of the nodes and the reduction of the load carried by truss action have also been taken into account. In light of these results, it can be seen

that it cannot be generalised that a design with a strut-and-tie model is more economical than a design with a sectional approach. The optimisation of the models improves the performance of the structure designed, which is a major concern when designing a structure.

7 Comparison of the model proposed with experimental results

7.1 Introduction

In this section the predictions from the European and Swedish building codes as well as the predictions from the three-dimensional model developed in this thesis work are compared to experimental results on pile caps without shear reinforcement found in the literature.

The design codes and the model developed are evaluated on their capacity to predict failure loads and failure modes as well as on their ability to provide safe and precise design capacity. The response of the three methods when some parameters are modified is investigated.

7.2 Analysis of 4-pile caps and comparison with experimental results

Several experimental studies conducted on 4-pile caps without shear reinforcement were found in the literature. The original reports of these experimental studies were not accessible for this thesis work, only summaries of these tests in other papers could be found (Souza 2009), (Park 2008), (Adebar 1996), (Cavers 2004) and (Zhou 1994). However, it was possible to constitute a solid and varied database of experiments carried out on twenty eight 4-pile caps without shear reinforcements.

7.2.1 Description of the experimental setup

The experiments reported here were originally carried out by of Blévot and Frémy (1967), Clarke (1973), Sabnis and Gogate (1984) and Suzuki (1998, 2000). As can be seen in Figure 7.1, different reinforcement layouts were used; 11 pile caps had grid reinforcement, 9 had bunched reinforcement placed in square over the piles, 8 had a combination of bunched and grid reinforcement. This last category is referred as combined in the following.

cross bunched
reinforcement

square bunched
reinforcement

grid reinforcement
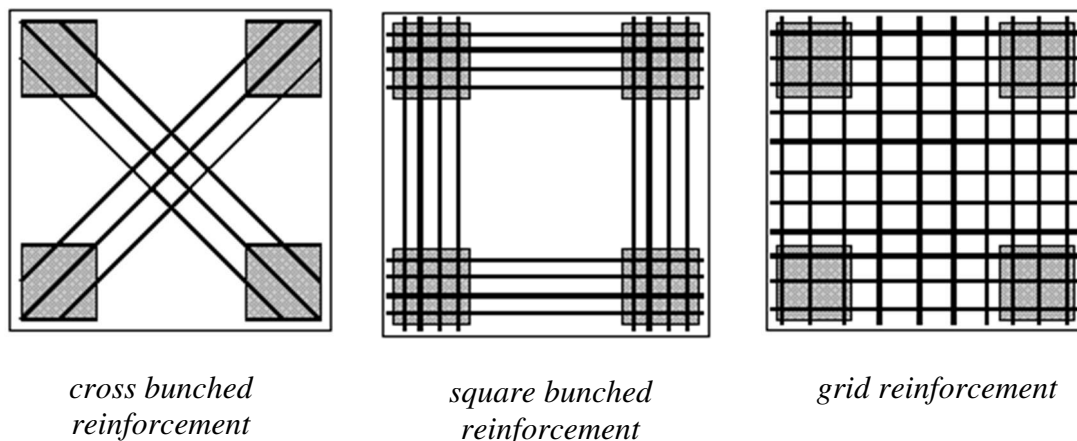
Figure 7.1   Some of the reinforcement layouts used in Blévot and Frémy experiments (Blévot 1967)

The pile caps tested by Clarke (1973), Sabnis and Gogate (1984) and Suzuki (1998, 2000) were square and had a constant height, as shown in Figure 7.2.
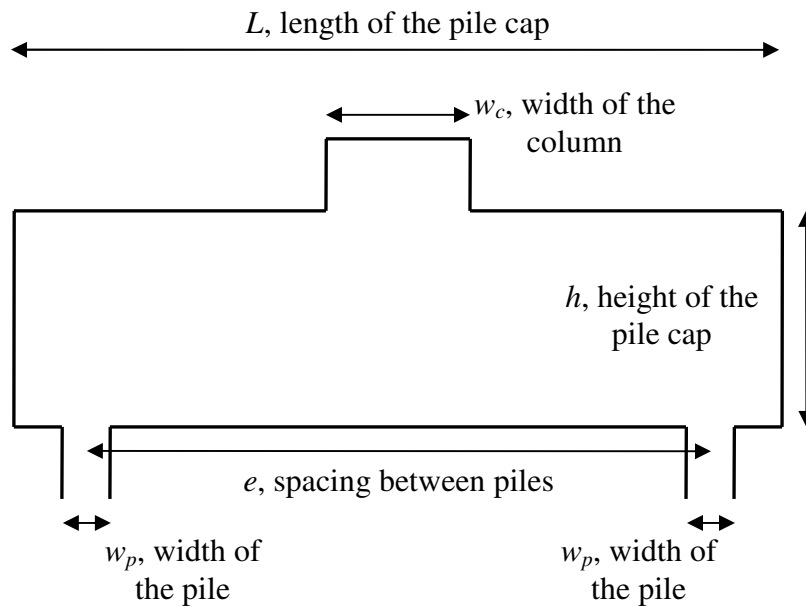
Figure 7.2   Definition of the characteristic dimensions of the pile caps in the test series from Clarke (1973), Sabnis and Gogate (1984) and Suzuki (1998, 2000)

The pile caps tested by Blévot and Frémy were deep with a height of 0,75m and 1m. In addition the top face was sloping so that the pile had a conical shape as can be seen in Figure 7.3 and Figure 7.4:
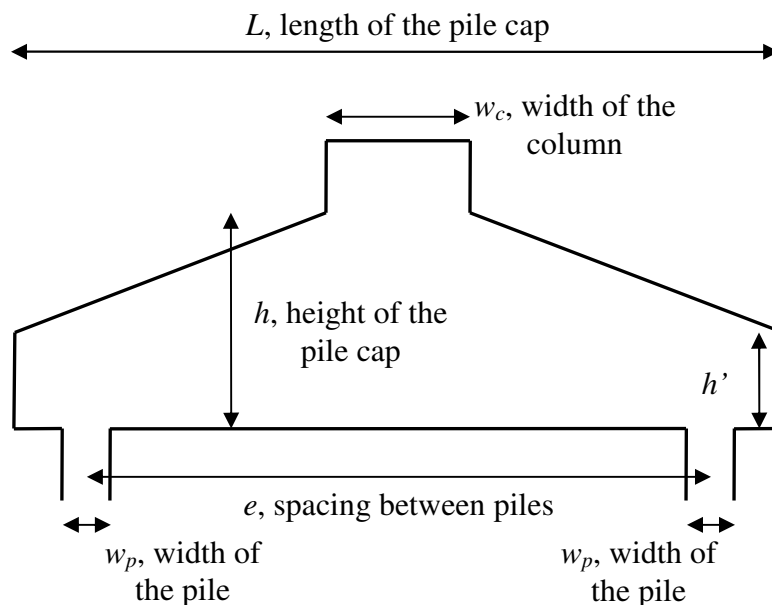
Figure 7.3   Definition of the characteristic dimensions of the pile caps from Blévot and Frémy (1967) experiments
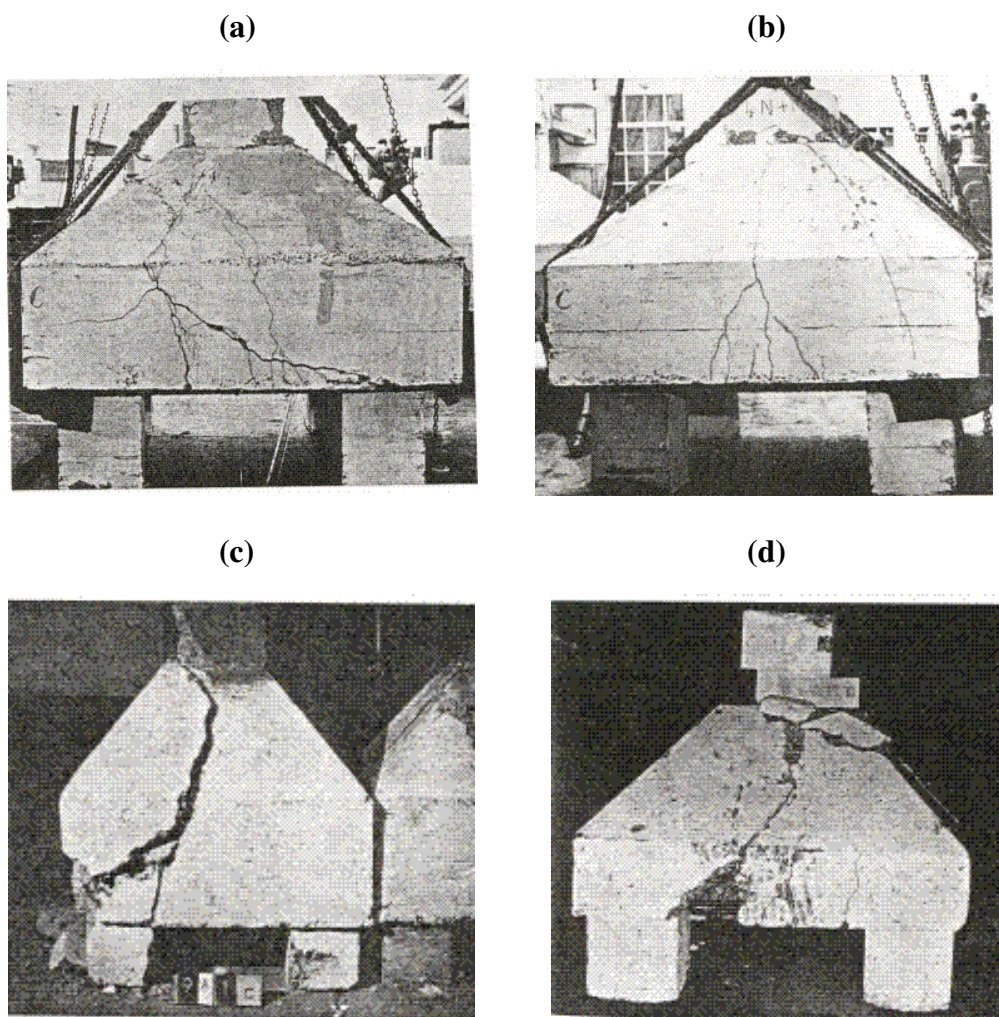
Figure 7.4   Deep pile caps tested by Blévot and Frémy, (a) diagonal cracking, (b) central cracking, (c) strut splitting, (d) complex failure.

No precise information could be found about the exact ratio between h and h' in the pile caps. Hence, it was assumed that h'/h= considering the pictures taken from the experiments, see Figure 7.4.

Some measures were taken to include the influence of the variable height of the pile caps in the predictions by building codes and the strut-and-tie models:

For the analysis using the codes, the variable height of the pile caps makes the assessment of the shear and punching shear capacities difficult. A simplification was made to consider a pyramidal shape. The shear capacity was calculated at the pile face, were the shear depth as defined in the codes is the smallest. The punching shear capacity was measured on control perimeters at various distances from the column and piles faces; depending on the position of the control perimeter an average shear depth was considered.

For the strut-and-tie model, the fact that the top face has a slope is considered by the reduction in confinement provided to the inclined struts. The assumption that the stresses are carried by direct arch action through a cylinder with dimensions shown in Figure 5.18 is not relevant in that case. Therefore, the width of the cylinder considered

was reduced to 60% of the width calculated for pile caps with constant height. This assumption almost always leads to $k_{confinement}$=1, meaning that there was very little positive effect from confinement on the splitting/crushing capacity of the main strut in the pile caps tested by Blévot and Frémy.

The complete data about the geometry and the materials used in different pile caps is found in Table 7.1. When the piles or the columns are circular they have been transformed to equivalent square assuming the same cross sectional area. The characteristic yield strength of steel and the characteristic compressive strength of concrete are given. Note that the concrete strength reported is the characteristic f_{ck}. Indeed, some authors reported the characteristic strength in their papers, others reported the mean strength. We decided to transform all the concrete's strength into characteristic strength. Calculations are found in Appendix D.

Table 7.1   Properties and failure load of the experiments specimens

28 Pile caps	L (m)	h (m)	Pitch between piles e(m)	Width of columns w_c(m)	Diameter of round piles (m)	Equivalent square width of piles w_p(m)	Reinforcement layout	A_s (one direction) (cm^2)	Steel yielding strength f_{yk} (Mpa)	Concrete cylinder strength f_{ck} (Mpa)	d (m)	Failure load (kN)
Clarke73												
A2	0,95	0,45	0,6	0,2	0,2	0.177	bunched square	7.85	410	27.2	0,4	1420
A8												1510
A5	0,95	0,45	0,6	0,2	0,2	0.177	bunched square	7.85	410	26.6	0,4	1400
A3	0,95	0,45	0,6	0 2	0,2	0.177	bunched square	5.50	410	30.4	0,4	1340
A6	0,95	0,45	0,6	0,2	0,2	0.177	bunched square	5.50	410	25.8	0,4	1230
B1	0,75	0,45	0,4	0,2	0,2	0,177	grid	6,28	410	26.7	0,4	2080
B3	0,75	0,45	0,4	0,2	0,2	0,177	grid	4,71	410	35	0,4	1770
Suzuki98												
BP-20-2-grid	0,9	0,2	0,54	0,3	0,15	0,133	grid	5,67	413	20.4	0,15	480
BP-30-25-2-grid	0,8	0,3	0,5	0,25	0,15	0,133	grid	5,67	413	26,3	0,25	725
BPC-20-30-1	0,8	0,2	0,5	0,3	0,15	0,133	bunched	4,25	405	29,8	0,15	495
BPC-20-30-2	0,8	0,2	0,5	0,3	0,15	0,133	bunched	4,25	405	29,8	0,15	500
BPC-20-1	0,9	0,2	0,54	0,3	0,15	0,133	bunched	5,67	413	21,9	0,15	519
BPC-20-2	0,9	0,2	0,54	0,3	0,15	0,133	bunched	5,67	413	19,9	0,15	529
Blévot & Frémy67												
4N1	1,59	0,75	1,2	0,5		0,35	combined	78,37	277,8	36,5	0,674	6865
4N1b	1,59	0,75	1,2	0,5		0,35	combined	47,16	479,6	40	0,681	6571
4N2	1,59	0,75	1,2	0,5		0,35	combined	67,86	289,4	36,4	0,66	6453
4N2b	1,59	0,75	1,2	0,5		0,35	combined	42	486,3	33,5	0,67	7247
4N3	1,59	1	1,2	0,5		0,35	combined	60,82	275	33,5	0,925	6375
4N3b	1,59	1	1,2	0,5		0,35	combined	38,47	453,3	48,3	0,931	8826
4N4	1,59	1	1,2	0,5		0,35	combined	58,88	291,4	34,7	0,92	7385
4N4b	1,59	1	1,2	0,5		0,35	combined	37,68	486,4	41,5	0,926	8581
Suzuki00												
BDA-40-25-70-1	0,7	0,4	0,45	0,25	0,15	0,133	grid	6,28	358	25,9	0,35	1019
BDA-40-25-70-2	0,7	0,4	0,45	0,25	0,15	0,133	grid	6,28	358	24,8	0,35	1068
BDA-20-25-90-1	0,9	0,2	0,45	0,25	0,15	0,133	grid	3,14	358	25,8	0,15	333
Sabnis and Gogate84												
SS1	0,325	0,15	0,2	0,0673 (equivalent)	0,076	0,067	grid	1,491	499,4	31,27	0,11	250
SS2	0,325	0,15	0,2	0,0673 (equivalent)	0,076	0,067	grid	0,974	743,2	31,27	0,11	245
SS3	0,325	0,15	0,2	0,0673 (equivalent)	0,076	0,067	grid	1,252	886	31,27	0,109	248
SS4	0,325	0,15	0,2	0,0673 (equivalent)	0,076	0,067	grid	1,819	599,8	31,27	0,11	226

For each pile cap, for both the design codes (EC2 and BBK) and the strut-and-tie model, predictions were made concerning both the mean and the design resistance:

The mean resistance prediction is based on the mean strength of materials. The mean concrete f_{cm} and steel f_{ym} strengths were used. It was assumed that the mean yield strength of steel was equal to $1.1f_{yk}$, indeed in deep elements like pile caps, large deformations cannot occur and it is very unlikely that steel will reach the ultimate strain. The mean resistance prediction considers no partial safety factor for the load and no partial safety factor for the materials. The design predictions are based on the design strength of materials, namely f_{cd} for concrete and f_{yd} for the steel. The design strength of materials was obtained by using γ_c and γ_s reduction factors that are stated in EC2 and BBK. The design strength prediction considers partial safety factor for material but here no partial safety factor for the load.

The procedure for determining the material strengths and the code predictions can be found in Appendix D.

The predictions for flexural capacity and one-way shear capacity are identical for Eurocode and BBK in sectional approaches, indeed, BBK recently adopted design approaches from Eurocode.

On the other hand, the methods for shear design differ between the two design codes. Predictions according to the Swedish design practice only concern BBK in the comparative tables presenting results hereafter, although it is common in Sweden to use the "Concrete handbook – structural design", which is said to predict higher punching capacities. However, in the case of pile caps, the flexural reinforcement ratio is usually very low, in which case BBK and the "Concrete handbook – structural design" predict almost the same punching capacity.

7.2.2 Analysis procedure with the three-dimensional strut-and-tie model

The procedure to evaluate the resistance of the pile caps analysed with the three-dimensional strut-and-tie model developed in this thesis work is based on a refinement of the node position. The maximum allowable strength at the column is aimed at without exceeding the allowable stresses in the components. An optimisation of the model is aimed at, based on the lower theorem of the theory of plasticity.

Five checks are made in the nodal zones. In the nodal region under the column, the bearing stresses, horizontal stresses, diagonal stresses on the faces of the node are evaluated. In the nodal region over the piles, the bearing stress and the diagonal stresses on the faces of the node are checked.

One check is made of steel stresses

One check is made of the strength of the web against crushing and splitting, far from the nodal regions.

The results of those seven checks are presented in Table 7.2. The second column ($Q_{f,e}/Q_{f,p}$) shows the ratio of the experimental failure load divided by the predicted failure load. The columns on the right show the rate of use of the materials for the different components. The two last columns on the right show the predicted and observed failure modes.

Table 7.2   Utilisation ratio of components and predicted failure modes

	Qfe/Qfp	Rate of steel used	Bearing stress at piles	Bearing stress column	Strut horizontal	Strut diagonal at column	Strut diagonal at middle	Strut diagonal at pile	Failure mode observed	Failure mode predicted
Clarke73										
A2	1,24	100%	36.3% (0,25fc)	91% (3,04fc)	41% (1,38fc)	60% (2 fc)	100% (0,57 fc)	38% (0,27 fc)	s	s
	1,32									
A8	1,63	100%	50% (0,38 fc)	39% (1,4 fc)	100% (3,6 fc)	53% (1,9 fc)	100% (0,75 fc)	52% (0,40 fc)	s	f+s
	1,73									
A5	1,16	100%	39%	93%	96%	95%	83%	39%	s	f
	1,62	99%	51%	33%	97%	48%	100%	54%		f+s
A3	1,54	100%	25%	100%	89%	95%	55%	25%	s	f
	2,06	100%	34%	45%	100%	58%	69%	35%		f
A6	1,43	100%	28%	100%	86%	93%	61%	29%	s	f
	1,93	100%	39%	41%	100%	55%	78%	40%		f
B1	1,24	100%	54%	100%	100%	100%	80%	48%	s	f
	1,77	100%	68%	48%	100%	54%	100%	61%		f+s
B3	1,32	100%	36%	100%	92%	99%	53%	32%	f	f
	1,73	100%	47%	100%	91%	99%	69%	41%		f
Suzuki98										
BP-20-2-grid	1,15	100%	29%	22%	40%	33%	100%	42%	f+s	s
	1,73	100%	36%	6%	35%	19%	100%	61%		s
BP-30-25-2-grid	0,94	100%	44	35%	80%	47%	100%	41%	s	s
	1,43	100%	53%	15%	33%	21%	100%	55%		s
BPC-20-30-1	1,10	100%	24%	100%	100%	100%	92%	25%	f	f
	1,54	100%	28%	30%	100%	51%	100%	34%		f+s
BPC-20-30-2	1,11	100%	24%	100%	100%	100%	92%	25%	f	f
	1,56	100%	28%	30%	100%	51%	100%	34%		f+s
BPC-20-1	1,05	100%	32%	9%	100%	29%	100%	46%	f+p	f+s
	1,81	100%	36%	6%	50%	20%	100%	57%		s
BPC-20-2	1,13	100%	33%	7%	99%	25%	100%	49%	f+p	f+s
	1,98	100%	36%	6%	32%	18%	100%	62%		s
Blévot & Frémy67										
4N1	1,07	100%	43%	18%	42%	26%	100%	55%	s	s
	1,65	100%	47%	20%	15%	16%	100%	69%		s
4N1b	1,03	100%	40	28%	20%	23%	100%	55%	s	s
	1,48	100%	46%	19%	14%	16%	100%	70%		s
4N2	1,07	100%	40%	26%	63%	37%	100%	47%	s	s
	1,59	100%	48%	20%	16%	17%	100%	67%		s
4N2b	1,19	100%	43%	18%	32%	23%	100%	24%	s	s
	1,84	100%	48%	20%	14%	16%	100%	72%		s
4N3	1,04	50%	43%	18%	100%	25%	100%	46%	s	s
	1,26	61%	25	10%	15%	40%	100%	73%		s
4N3b	1,16	100%	42%	22%	100%	30%	100%	46%	s	f+s
	1,59	100%	49%	20%	23%	21%	100%	55%		s
4N4	1,06	100%	48%	20%	32%	23%	100%	51%	s	s
	1,51	100%	58%	24%	13%	18%	100%	65%		s
4N4b	1,13	100%	47%	20%	40%	24%	100%	51%	s	s
	1,58	100%	54%	23%	15%	18%	100%	23%		s
Suzuki00										
BDA-40-25-70-1	0,77	100%	76%	100%	100%	100%	100%	63%	s	f+s
	1,24	100%	88%	21%	84%	27%	100%	74%		s
BDA-40-25-70-2	0,81	100%	78%	100%	100%	100%	100%	64%	f+s	f+s
	1,34	96%	89%	21%	90%	28%	100%	74%		s
BDA-20-25-90-1	1,09	100%	18%	100%	100%	100%	71%	18%	f	f
	1,44	100%	25%	100%	100%	100%	94%	26%		f+s
Sabnis and Gogate84										
SS1	1,10	100%	36%	87%	100%	93%	100%	29%	s	f+s
	1,59	100%	43%	37%	50%	43%	100%	37%		s
SS2	1,09	100%	35%	97%	100%	100%	100%	28%	s	f+s
	1,58	100%	43%	36%	55%	45%	100%	36%		s
SS3	1,00	100%	39%	57%	70%	63%	100%	32%	s	s
	1,46	90%	47%	40%	26%	29%	100%	45%		s
SS4	0,80	100%	44%	37%	40%	39%	100%	39%	s	s
	1,33	95%	47%	40%	23%	27%	100%	48%		s

When the check against crushing and splitting of the diagonal strut is limiting, the pile cap is defined as failed in shear.

When the checks in the nodal regions are limiting, the nodal regions are supposed to be softened, the internal level arm decreases and the pile cap is assume to fail in flexure.

The fact that the strut-and-tie model can predict the failure modes is dependant on the quality of the optimization of the node positions. If the state of stresses at failure is close than the one predicted by the strut-and-tie model, the chances to predict accurately the failure mode are increased.

7.2.3 Results

7.2.3.1 Comparison between the predictions from Eurocode and BBK

As the design methods for flexural capacity and one-way shear capacity are the same for both codes, differences arise only from the different punching approaches. In Table 7.3 the check that is limiting is highlighted in colors. It can be seen that, of the 28 piles caps reported, Eurocode, and respectively BBK, predicted failures in flexion (28%, 7%), one-way shear (43%, 29%) and punching at the column (29%, 64%) and none of them predicted failure due to punching at the piles. These differences are generated by the unequal predictions for punching capacity at the column and more precisely to the more restrictive check for punching with BBK. However, for some pile caps, the ratio between the predicted failure load (mean value) according to Eurocode and the experimental failure load was close to 1 and in one case even below 1, which is non conservative for a design resistance prediction.

BBK considers a control perimeter at a constant distance $d/2$ from the column face, while the Eurocode procedure implies checks at several control perimeters situated between the column face up to a distance $2d$ from the column face in the case of pile caps. Therefore, the BBK approach is more sensitive to the shape of the pile cap and a slight change in geometry can result in high variation of the resistance prediction. This can be seen in particular in the series of Sabnis and Gogate where BBK is too conservative for punching.

Table 7.3   Resistance predictions by Eurocode and BBK

		Flexural capacity (kN)	Shear capacity (kN)	EUROCODE2				BBK04			
				Punching capacity at column (kN)	Punching capacity at pile (kN)	Q_{EC2} (kN)	Q_{fe}/Q_{EC2}	Punching capacity at column (kN)	Punching capacity at pile (kN)	Q_{BBK} (kN)	Q_{fe}/Q_{BBK}
Clarke73											
A2	mean	1397	1414	1349	1948	1349	1,05	1600	2614	1397	1,02
	design	1096	1238	1287	1705	1096	1,30	747	1220	747	1,90
A8	mean	1397	1414	1349	1948	1349	1,12	1600	2618	1397	1,08
	design	1096	1238	1287	1705	1096	1,38	747	1220	747	2,02
A5	mean	1397	1402	1323	1932	1323	1,06	1577	2576	1397	1,00
	design	1096	1224	1272	1686	1096	1,28	736	1202	736	1,90
A3	mean	984	1476	1486	2034	984	1,36	1975	2737	984	1,36
	design	774	1308	1360	1803	774	1,73	781	1277	774	1,73
A6	mean	982	1386	1288	1909	982	1,25	1502	2453	982	1,25
	design	772	1205	1253	1661	772	1,59	701	1145	701	1,75
B1	mean	2234	1108	1327	3602	1108	1,88	4944	8089	1108	1,88
	design	1753	968	1327	3498	968	2,15	2307	3769	968	2,15
B3	mean	1685	1233	1675	4456	1233	1,44	5782	9445	1233	1,44
	design	1327	1108	1675	4004	1108	1,60	2698	4408	1108	1,60
Suzuki98											
BP-20-2-grid	mean	621	584	444	480	444	1,08	428	636	428	1,12
	design	480	530	403	436	403	1,19	199	297	199	2,41
BP-30-25-2-grid	mean	1263	859	1228	1466	859	0,84	1555	1982	859	0,84
	design	988	748	1228	1278	748	0,97	725	924	725	1,00
BPC-20-30-1	mean	556	587	606	601	556	0,89	628	841	556	0,89
	design	435	519	536	531	435	1,14	293	392	293	1,69
BPC-20-30-2	mean	556	587	606	601	556	0,90	628	841	556	0,90
	design	435	519	536	531	435	1,15	293	392	293	1,71
BPC-20-1	mean	623	605	460	497	460	1,13	449	667	449	1,16
	design	482	543	413	447	413	1,26	209	311	209	2,48
BPC-20-2	mean	620	581	442	478	442	1,20	421	626	420	1,26
	design	479	526	400	433	400	1,32	196	292	196	2,70
Blévot & Frémy67											
4N1	mean	8993	4108	3204	5423	3204	2,14	5636	5938	3204	2,14
	design	7025	3832	2989	5058	2989	2,30	2630	2771	2630	2,61
4N1b	mean	9353	3564	2780	4705	2780	2,36	5364	5651	2780	2,36
	design	7313	3335	2601	4403	2601	2,53	2503	2637	2503	2,63
4N2	mean	7960	3872	2958	5006	2958	2,18	5250	5518	2958	2,18
	design	6224	3611	2758	4668	2758	2,34	2450	2575	2450	2,63
4N2b	mean	8383	3247	2517	4261	2517	2,88	4627	4871	2517	2,88
	design	6545	3016	2338	3957	2338	3,10	2159	2273	2159	3,36
4N3	mean	16360	4315	4619	7817	4315	1,48	9147	10170	4315	1,48
	design	12770	4008	4290	7261	4008	1,59	4269	4746	4008	1,59
4N3b	mean	10090	4545	4896	8287	4545	1,94	11120	12390	4545	1,94
	design	7938	4149	4470	7565	4149	2,13	5191	5780	4149	2,13
4N4	mean	9772	4297	4575	7742	4297	1,72	9199	10021	4297	1,72
	design	7670	4000	4259	7208	4000	1,85	4293	4766	4000	1,85
4N4b	mean	10520	4224	4526	7660	4224	2,03	9902	11010	4224	2,03
	design	8268	3830	4104	6946	3830	2,24	4621	5139	3830	2,24
Suzuki00											
BDA-40-25-70-1	mean	1705	933	1413	1306	933	1,09	3809	4746	933	1,09
	design	1336	812	1413	2030	812	1,25	1778	2215	812	1,25
BDA-40-25-70-2	mean	1704	918	1360	2218	918	1,16	3701	4610	918	1,16
	design	1335	795	1360	1986	795	1,34	1727	2151	795	1,34
BDA-20-25-90-1	mean	366	624	509	985	366	0,91	476	926	366	0,91
	design	287	543	442	944	287	1,16	222	432	222	1,50
Sabnis and Gogate84											
SS1	mean	281	178	159	259	159	1,57	200	357	178	1,40
	design	219	161	159	236	159	1,57	94	167	94	2,66
SS2	mean	274	178	159	260	159	1,54	189	337	178	1,38
	design	213	158	159	260	158	1,55	88	157	88	2,78
SS3	mean	410	177	159	257	159	1,56	193	344	177	1,40
	design	317	157	158	228	157	1,58	90	161	90	2,76
SS4	mean	407	187	159	273	159	1,42	206	372	187	1,21
	design	314	173	159	252	159	1,42	97	173	97	2,33

It should also be pointed out that there are significant differences between the calculated mean and design punching capacities according to BBK that are not found with Eurocode. Indeed, Eurocode utilizes the characteristic compressive strength of concrete in the design resistance while BBK uses the design tensile strength which induces big strength reductions compared to mean strength prediction.

The predictions according to BBK, Eurocode and the 3-D strut-and-tie model for different flexural reinforcement layouts are compared in Table 7.4.

7.2.3.2 Comparison between design codes and the 3-D strut-and-tie model

It can be seen in Table 7.4 that BBK gives the most conservative predictions of the design resistance, with an average of 2.10 for the predicted to experimental failure loads compared to Eurocode and the 3-D strut-and-tie model that give respectively the value 1.64 and 1.61 of the corresponding ratio.

Table 7.4   *Comparison of mean and design resistance predictions to experimental failure loads with EC2, BBK04 and the strut-and-tie model.*

	bunched		combined		grid		general	
EC2	Average	Standard deviation	Average	Standard deviation	Average	standard deviation	Average	standard deviation
ULTIMATE CAPACITY	1,11	0,15	2,09	0,42	1,32	0,32	1,47	0,51
DESIGN CAPACITY	1,35	0,20	2,26	0,45	1,44	0,31	**1,64**	**0,51**
	bunched		combined		grid		general	
BBK04	Average	Standard deviation	Average	Standard deviation	Average	Standard deviation	Average	standard deviation
ULTIMATE CAPACITY	1,10	0,17	2,09	0,42	1,26	0,29	1,43	0,51
DESIGN CAPACITY	1,99	0,36	2,38	0,55	1,98	0,66	**2,10**	**0,56**
	bunched		combined		grid		general	
Strut-and-tie model	Average	Standard deviation	Average	Standard deviation	Average	Standard deviation	Average	standard deviation
ULTIMATE CAPACITY	1,23	0,17	1,09	0,06	1,03	0,18	1,11	0,17
DESIGN CAPACITY	1,76	0,19	1,56	0,16	1,51	0,18	**1,61**	**0,21**

The classification in bunched, combined and grid reinforcement layouts was made in order to evaluate the possible resistance variation induced by them. According to previous authors on the subject, grid reinforcement are said to be between 15% and 20% less resistant than bunched and composite ones, that are said to have somehow the same strength. It can be seen in Table 7.4 that only the strut-and-tie model predictions follow this trend. This is interpreted in two points:

Firstly it means that the codes were more sensitive to other parameters like the slenderness or the depth of the pile caps, than to the reinforcement layout, which

means that the number of experiments were not high enough to prevent the codes prediction to be distracted by those factors.

Secondly, it may mean that the 3-D strut-and-tie model is consistent enough not to be distracted by the non uniformity of the samples tested and still be able to capture the real trend.

Table 7.5 shows the ratios between experimental and design failure loads as well the ratios between experimental and mean predicted failure loads according to Eurocode, BBK and the strut-and-tie method. The predicted failure modes for each pile cap tested are also recalled.

Table 7.5   Observed failure load to predicted failure load ratios and failure modes for Eurocode, BBK and the strut-and-tie model

	Q_{fe} [Mpa]	Reported failure mode	EC2 Q_{fe}/Q_{fm}	Q_{fe}/Q_{fd}	Predicted failure mode	BBK04 Q_{fe}/Q_{fm}	Q_{fe}/Q_{fd}	Predicted failure mode	3-D strut-and-tie model Q_{fe}/Q_{fm}	Q_{fe}/Q_{fd}	Predicted failure mode
Bunched reinforcement layout											
[Clarke73]											
A2	1420	s	1,05	1,30	f	1,02	1,90	p	1,24	1,63	f+s
A8	1510	s	1,12	1,38	f	1,08	2,02	p	1,32	1,73	f+s
A5	1400	s	1,06	1,28	f	1,00	1,90	p	1,16	1,62	f+s
A3	1340	s	1,36	1,73	f	1,36	1,73	f	1,54	2,06	f
A6	1230	s	1,25	1,59	f	1,25	1,75	p	1,43	1,93	f
[Suzuki98]											
BPC-20-30-1	495	f	0,89	1,14	f	0,89	1,69	p	1,10	1,54	f+s
BPC-20-30-2	500	f	0,90	1,15	f	0,90	1,71	p	1,11	1,56	f+s
BPC-20-1	519	f+p	1,13	1,26	p	1,16	2,48	p	1,05	1,81	s
BPC-20-2	529	f+p	1,20	1,32	p	1,26	2,70	p	1,13	1,98	s
AVERAGE			1,11	**1,35**	44%	1,10	**1,99**	67%	1,23	**1,76**	75%
STANDARD DEVIATION			0,15	**0,20**		0,17	**0,36**		0,17	**0,19**	
Combined reinforcement layout											
[Blévot67]											
4N1	6865	s	2,14	2,30	p	2,14	2,61	p	1,07	1,65	s
4N1b	6571	s	2,36	2,53	p	2,36	2,63	p	1,03	1,48	s
4N2	6453	s	2,18	2,34	p	2,18	2,63	p	1,07	1,59	s
4N2b	7247	s	2,88	3,10	p	2,88	3,36	p	1,19	1,84	s
4N3	6375	s	1,48	1,59	s	1,48	1,59	s	1,04	1,26	s
4N3b	8826	s	1,94	2,13	s	1,94	2,13	s	1,16	1,59	s
4N4	7385	s	1,72	1,85	s	1,72	1,85	s	1,06	1,51	s
4N4b	8581	s	2,03	2,24	s	2,03	2,24	s	1,13	1,58	s
AVERAGE			2,09	**2,26**	100%	2,09	**2,38**	100%	1,09	**1,56**	100%
STANDARD. DEVIATION			0,42	**0,45**		0,42	**0,55**		0,06	**0,16**	
Grid Reinforcement Layout											
[Clarke73]											
B1	2080	s	1,88	2,15	s	1,88	2,15	s	1,24	1,77	f+s
B3	1770	f	1,44	1,60	s	1,44	1,60	s	1,32	1,73	f
[Suzuki98]											
BP-20-2-grid	480	f+s	1,08	1,19	p	1,12	2,41	p	1,15	1,73	s
BP-30-25-2-grid	725	s	0,84	0,97	s	0,84	1,00	p	0,94	1,43	s
[Suzuki00]											
BDA-40-25-70-1	1019	s	1,09	1,25	s	1,09	1,25	s	0,77	1,24	s
BDA-40-25-70-2	1068	f+s	1,16	1,34	s	1,16	1,34	s	0,81	1,34	s
BDA-20-25-90-1	333	f	0,91	1,16	f	0,91	1,50	p	1,09	1,44	f+s
[Sabnis84]											
SS1	250	s	1,57	1,57	s	1,40	2,66	p	1,10	1,59	s
SS2	245	s	1,54	1,55	s	1,38	2,78	p	1,09	1,58	s
SS3	248	s	1,56	1,58	s	1,40	2,76	p	1,00	1,46	s
SS4	226	s	1,42	1,42	s	1,21	2,33	p	0,80	1,33	s
AVERAGE			1,32	**1,44**	91%	1,26	**1,98**	82%	1,03	**1,51**	100%
STANDARD DEVIATION			0,32	**0,31**		0,29	**0,66**		0,18	**0,18**	
OVERALL											
FAILURE MODE					79%			82%			93%
AVERAGE			1,47	**1,64**		1,43	**2,10**		1,11	**1,61**	
STANDARD DEVIATION			0,51	**0,51**		0,51	**0,56**		0,17	**0,21**	

Concerning the specificities of the series tested:

In the test series of Suzuki (1998) with the most slender pile caps it can be seen that both codes are rather unreliable. Indeed, Eurocode is rather non conservative with design predictions close to 1.2 and even one prediction below 1. BBK is too

conservative regarding the punching capacity with an average prediction around 2 and rather large variations. The predictions of the 3-D strut-and-tie model are good.

In the test series of Blévot and Frémy (1967) pile caps have an average slenderness which corresponds to the average slenderness of the samples tested. They have two major characteristics: they are way deeper (and carry more load) than the rest of the experiments and they have a conical shape. All these pile caps are predicted to fail by shear or punching by the standard models and actually failed in shear. The predictions from the codes are too conservative while the predictions of the model are very good. This wrong resistance evaluation from the codes is believed to be linked to a combination of the two characteristics of the pile caps: depth and conical shape.

Indeed codes of practice assume that, for deep members loaded in shear, the relative capacity should be reduced in large elements due to size effects. However, size effects were proven to be linked to the concrete softening associated to the more critical cracking pattern in deep elements as explained in Section 5.3.5: *Size effect in deep elements and in pile caps*. Therefore, knowing that the web of stocky pile caps is rather uncracked before failure, accounting for size effects is not consistent and not done in the 3-D strut-and-tie model.

The conical shape of the pile caps, as can be seen in Figure 7.4, is taken into account both in the code and the 3-D strut-and-tie model approaches:

In the strut-and-tie model, the conical shape is considered to have no influence on the node region but reduces the splitting crushing capacity of the web due to the reduction of confinement of the strut. The simplified approach with an equivalent cylinder, as shown in Figure 5.18, is still relevant but the width of the cylinder needs to be reduced. The width of the cylinder was actually reduced by 60% which ended up in a ratio between the cylinder width and the size of the hexagonal node faces size to be equal or less than 1 (except one where the ratio was slightly over 1). This resulted in confinement factors equal to one (i.e. no positive confinement).

The effect of the conical shape in the codes was the consideration of a reduced effective depth for the calculation of the shear and punching capacities (the procedure is briefly explained at the beginning of this chapter and the calculations are found in Appendix D). The corresponding decrease of the nominal shear capacity induced is believed to be too conservative and reveals the inconsistency of a sectional approach for stocky pile caps. Indeed, a slight change in the shape of the element resulted in a wrong assessment of the resistance associated to an incorrect mechanical approach that might lead the designer to mistakes.

Table 7.5 shows that the 3D strut-and-tie model is able to predict correctly 93% of the failure modes, against 79% and 82% for Eurocode and BBK. However, failure mode prediction is a bit tricky as it is not always easy to specify the nature of a failure in pile caps. In fact, a combination of flexural, shear and punching failure is often occurring without a possibility to clearly separate them, for example some complex cracking patterns at failure are shown in Figure 7.4 For instance the model developed only predicts two types of failure: flexural and shear failures. Indeed punching failures are very seldom in stocky pile caps where a combination of splitting and cracking of the compressive strut seems to be the most common shear failure mechanism. Shear and punching failures were both considered as shear failure types for the counting in order to keep equity between the models.

The most important information in Table 7.4 and in Table 7.5 is the standard deviation. Indeed, the model developed has, out of a base of 28 experiments, showed a standard deviation in the design resistance predictions of 0.21 compared to 0.51 and 0.56 for Eurocode and BBK respectively. If a 4 pile cap without shear reinforcement was to be designed using the 3D strut-and-tie model, it would, in average, resist 1.61 times the load it was designed for and there is 5% chance that is fails below 1.26 times this load and less than 1% chance that it fails below 1.12 times this load. On the other hand, if the pile cap was designed, aiming at the same resistance, by the Eurocode, it would have resisted, in average, 1.64 times the design load but the 5% and 1% failure safety proof are reached for loads equal to 0.8 times and 0.45 times the design load (respectively 2.10, 1.18, 0.8 with BBK) Therefore, if a designer is conscious of these variations and wants to guarantee a 1% failure safety for the structure (without taking into account partial safety factors on loads, which will greatly improve the safety) it means that he would have to aim at a load 2.5 times higher when designing with Eurocode compared to using the 3D strut-and-tie model. Another way to express this is that, if a pile cap is designed, aiming at resisting a given load there is a risk of 10,5% that is fails before this load if designed with EC2, 2,5% if designed with BBK and 0,18% if it is designed with the strut-and-tie model.

If the average resistance and standard deviations evaluated from the 28 pile caps reported are considered as true, it means that tremendous improvement in design can be made using the 3-D strut-and-tie model. Although the database tested is too small to guarantee these conclusions, the trend is clearly shown that design with the 3D strut-and-tie model is more consistent, and thus more effective than sectional approaches.

The feeling of Skanska's designers that design according to BBK for punching was very drastic is confirmed by the high numbers of too conservative predictions of punching to EC2. Indeed, in some cases where the geometry is specific the BBK control perimeter definition is not good and slightly better results can be obtained applying the Eurocode procedure.

However, it should be pointed out that both design methods are of poor quality as shown by the high standard deviations. Indeed, even if the definition of control perimeters in EC2 is more advanced than the one in BBK, it remains a sectional approach, a method that is questionable for the analysis of pile caps and disturbed regions in general.

Swedish pile caps designers have to be aware of that the forthcoming change from BBK to EC2 design code will not solve their pile caps design issues. The improvement of the pile cap design relies on the acceptance that design procedures based on sectional approaches are not adapted to pile caps. The use of a design approach based on the well established strut-and-tie method, like the model presented in this thesis, is the most accessible way to greatly improve the design of pile caps.

7.3 Comparison with a 6-pile cap tested by Adebar, Kuchma and Collins

Adebar, Kuchma and Collins tested a large 6- pile cap (Adebar et al. 1990) and compared the failure load with the predictions using a sectional approach from the ACI Building Code and a strut-and-tie analysis in accordance with the Canadian Concrete Code. The layout of the tested pile cap is shown in Figure 7.5.
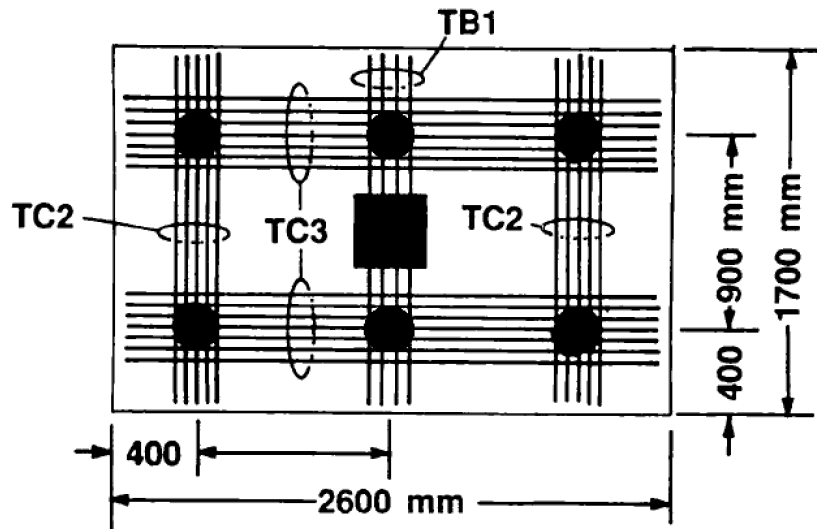
Figure 7.5   6-pile cap analysed
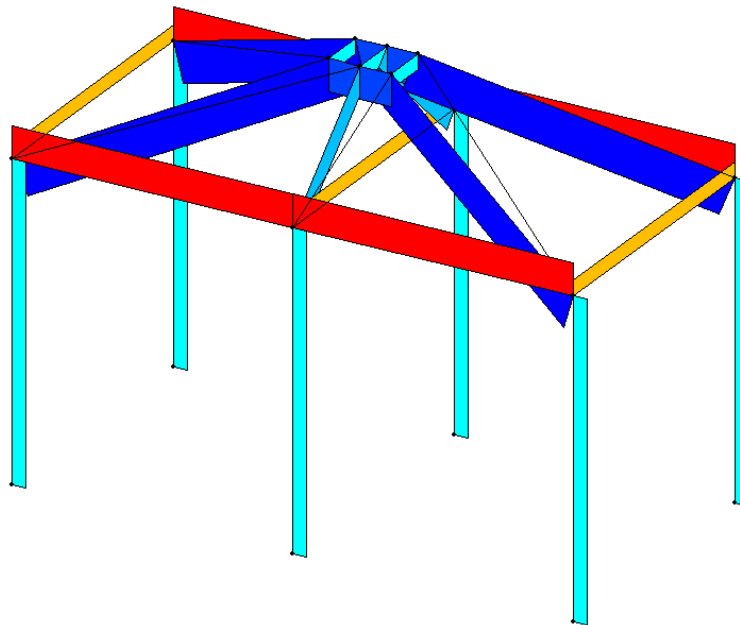
*Figure 7.6   Force distribution in the strut-and-tie model, assuming the same load in
each pile*

The authors obtained an experimental failure load of 2892 kN. The main transverse reinforcement between the two piles in the centre reached yielding before the failure, which was a shear failure characterised by a punching cone between the column's faces and the piles' faces.

The authors initially designed the pile cap using a strut-and-tie model for a load of 3000 kN, assuming the same load in the 6 piles (500 kN per pile). The corresponding strut-and-tie model is shown in Figure 7.6. The actual loads measured in the piles at failure were 1152 kN in each of the two closest piles and 147 kN in each of the four other piles; that is to say that 80% of the load was going to the two closest piles. Then using a strut-and-tie method in accordance with the Canadian Concrete Code, they calculated a predicted load of 2073 kN.

When analysing this pile cap using the strut-and-tie method, a column load of 3250 kN was obtained for the case of an equal share of the force between the piles (Figure 7.6) and 1735 kN for the same distribution as in the experiments, i.e. 0.8-0.2 (Figure 7.7).
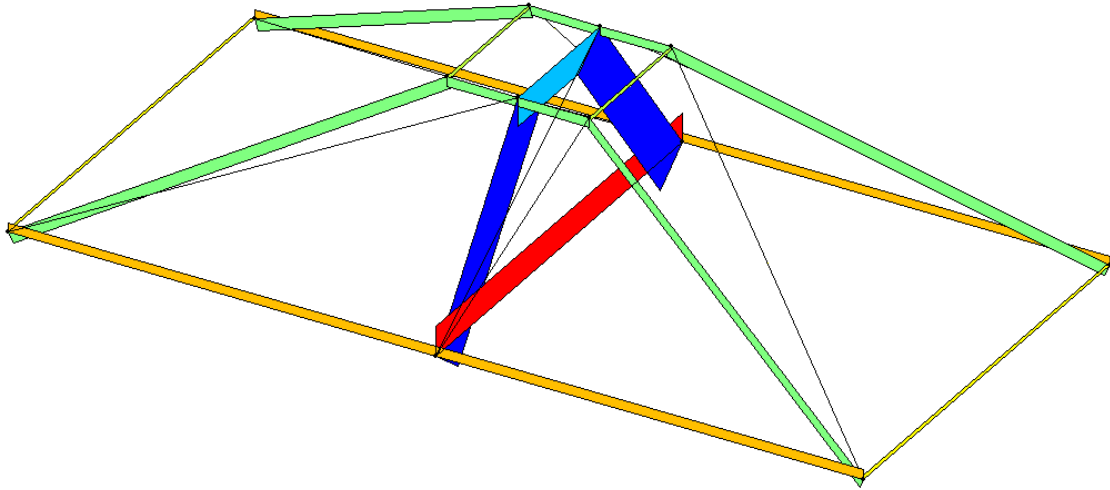
Figure 7.7   *Force distribution in the strut-and-tie model obtained with the pile load distribution set equal to the experimental one*

8 Conclusion

8.1 Recall of the framework

The current Swedish design provisions for pile caps are questionable and designers at Skanska Teknik expressed a need for clarification. This thesis work was commissioned in order to investigate the design of pile caps according to different standards and to study the possibility to design pile caps using strut-and-tie models.

This thesis work includes a generic description of shear failures in structural concrete, and punching shear failures in particular. Thereafter the design procedures for shear and punching in the Swedish, European and American codes are presented and compared. In addition predictions from the European and the Swedish codes are evaluated against experimental results.

The strut-and-tie method is presented for two-dimensional structures and the lack of development in three-dimensional models is pointed out. A three-dimensional strut-and-tie model, based on a consistent geometrical definition of the nodal zones and check of bottle-shape struts between concentrated nodes, is developed in this thesis work and its performance is evaluated against experimental results. Some design examples are conducted on pile caps, to provide guidelines for the application of the model and the iterative process required.

8.2 Concluding remarks

Out of the analysis of a series of 4-pile caps, the design procedure according to a sectional approach using the Swedish building code was shown to be slightly more conservative than the sectional approach using the Eurocode 2, due to differences in the evaluation of the punching capacity. However the predictions of the sectional approaches from these two building codes are both of rather poor quality.

Out of the literature study made during this thesis work, many features of pile caps were depicted. Some practical solutions to improve the design of pile caps are suggested.

In the strut-and-tie model developed in this thesis, a consistent geometry of the three-dimensional nodal zones is defined, which assures geometrical compatibility between the elements and the concurrency between the centroids of the nodal regions and the axes of the struts and ties. With this method, nodal zones, the critical parts of reinforced concrete structures, are defined in a reliable way. Furthermore, a strength criterion for combined splitting and crushing of bottle-shape struts far from nodal regions was defined in this thesis.

The model developed was confronted to experimental results and was proven to predict failures by splitting and crushing of the web in pile caps more accurately and with less scatter than sectional approaches from the European and the Swedish building codes. In addition, based on geometrical considerations, a sufficient amount of shear reinforcement is provided to ensure that no sliding shear failure can occur before yielding of the flexural reinforcement.

Therefore, the three-dimensional model developed in this thesis was proven to provide safe design against shear and punching shear failures.

A design example of a 4-pile cap is conducted to detail the characteristics of the model and the iterative procedure. The Swedish building code and the three-dimensional model developed in this thesis have been compared in the example of a ten-pile cap designed by Skanska. For this example, the design with the strut-and-tie model requires slightly less reinforcing steel.

The model was implemented into a semi-automated program based on Matlab, which can be used to design pile caps with various shapes, number and position of piles as well as external loads. The program uses an iterative process to assure optimisation of nodal zones geometry and calculates the required amount of main reinforcement and shear reinforcement.

This thesis work showed that, according to the opinion of designers at Skanska, the design procedure for pile caps according to a sectional approach using the Swedish building code is not consistent and often very conservative. Designers have to be aware that Eurocode's sectional approach for the design of pile caps is barely better than the one in BBK. The improvement of pile caps design relies on the acceptance that design procedures based on sectional approaches are not appropriate for such discontinuity regions. Fortunately, the use of a design approach based on three-dimensional strut-and-tie model models is allowed by the Eurocode. This opportunity should be taken to improve the design of pile caps.

8.3   Suggestions for further study

This thesis work does not have the pretention to develop an optimal strut-and-tie model for pile caps, which represents a long-winded task. This study has been conducted from the state of art of two-dimensional models and with the limited experimental database at disposal, thus the result of this work is rather to raise the lack of development of this topic and the need for further studies regarding many aspects of shear failures and strut-and-tie models for three-dimensional structures.

In comparison with the numerous experimental studies conducted on beams and deep beams, pile caps are missing some relevant tests. Furthermore, most of the studies on the subject concern four pile caps without shear reinforcement. Some studies have been conducted on four-pile caps with shear reinforcement by Suzuki (1997, 1998), but all the data required where not accessible during this thesis work. Nevertheless experiments would be needed for pile caps with more piles and with more complex geometries.

Several other possibilities of development for the models and cases to study were intended but were finally not performed because of the limited time. Some of the studies omitted are specified thereafter.

As it has been pointed out in this work, the cracking process of deep pile caps is different from the one of beams and slabs. Therefore it would be interesting to study the reliability of strut-and-tie models for the design of pile caps at the serviceability limit state. In this domain as well, relevant experiments would be needed to compare the cracking predictions obtained with strut-and-tie models.

The influence of the concrete tensile strength in shear transfer mechanisms is underestimated in sectional approaches and in strut-and-tie models in particular where it is not considered at all. Strut-and-tie models could be adapted to take into account the contribution of concrete in tension by means of concrete ties.

The definition of the failure criterion for splitting and crushing of the web was based on qualitative considerations and was not calibrated. A refinement and calibration of this failure criterion would lead to better results and safety regarding shear failures. In the same manner the ratio between the load carried by truss action and by direct arch action has been adapted from rules for beam design in building codes and could be improved to be less conservative.

In this study, the statically indeterminate strut-and-tie models were solved by making choices on the part of the load carried by each of the members. The study of the reliability of the stiffness of the struts and the ties to find the force distribution in the model, and the influence of inactive plain concrete, would constitute an interesting subject of study for models statically indeterminate internally, as well as for assessing the distribution of forces in the piles.

Finally, the strut-and-tie models were only used in this study to find the main reinforcement and the shear reinforcement; determining the number and position of the piles and the size of the pile cap was beyond the scope of this work. However, it could be added in the algorithm. Moreover another advantage of strut-and-tie model consists in the possibilities of optimisation that they offer. Some interesting parametrical studies could be performed on pile caps to improve the geometry of the common design, as the influence of depth or the use of capitals.

9 References

AASHTO LRFD, "Bridge Design Specifications and Commentary," 3rd Edition, *American Association of State Highway Transportation Officials*, Washington D.C., 2004, 1264 pp.

ACI 318-08, American Concrete Institute, January 2008.

Adebar, P., Kuchma, D., and Collins M.P. (1990) "Strut-and-Tie Models for the Design of Pile Caps: An Experimental Study," *ACI Structural Journal,* V. 87, No. 1, January-February 1990, pp. 81-92.

Adebar, P., and Zhou, Z (1993) "Bearing Strength of Compressive Struts Confined by Plain Concrete," *ACI Structural Journal*, V. 90, No. 5, September-October 1993, pp. 534-541

Adebar,P., and Zhou, Z. (1996) "Design of Deep Pile Caps By Strut-and-Tie Models," *ACI Structural Journal*, V. 93, No. 4, July-August 1996, pp.1-12.

Bazant, Z.P., Ozbolt, J., and Eligehausen, R. (1994) "Fracture Size Effect: Review of Evidence for Concrete Structures," *Journal of Structural Engineering*, V. 120, No. 8, 1994, pp. 2377–2398.

Bentz, E.C., Vecchio, F.J., and Collins, M.P. (2006) "Simplified Modified Compression Field Theory for Calculating Shear Strength of Reinforced Concrete Elements," *ACI Structural Journal*, V. 103, No. 4, July-August 2006, pp. 614-624.

Blévot, J. L., and Frémy, R. (1967) "Semelles sur Pieux," *Institute Technique du Bâtiment et des Travaux Publics*, V. 20, No. 230, 1967, pp. 223-295.

Betonghandbok - Konstruktion, utgåva 2 (1990): (Concrete Handbook - Construction, edition 2) (In Swedish).

BBK 04, Boverkets Handbok om Betongkonstruktioner, 2004. (The Swedish Building Administration's Handbook on Concrete Structures). Stockholm, Sweden: The Swedish Building Administration, Division of Buildings. (In Swedish).

Braestrup, M.W., Nielsen, M.P., Jensen, B.C., and Bach, F. (1976) "Axisymmetric Punching of Plain and Reinforced Concrete," Report R75, Struct. Research Laboratory, Technical Univ. of Denmark, Copenhagen 1976.

Broms, C. E. (1967) "A Method to Avoid the Punching Failure Mode,"*International workshop on Punching Shear Capacity of RC Slab,* Proceedings, Stockholm, 2000, pp. 117-124.

Cavers, W., and Fenton, G.A. (2004) "An Evaluation of Pile Cap Design Methods in accordance with the Canadian Design Standard", *Canadian Journal of Civil Engineering*, V. 31, No. 1, 2004, pp. 109-119.

CEB (1985) "Cracking and Deformations," Ecole Polytechnique Fédérale de Lausanne, *CEB Manual,* Lausanne, 1985.

Chen, W.F., and Trumbauer, B.E. (1972) "Double Punch Test and Tensile Strength of Concrete," *Journal of Materials*, JMLSA, V. 7, No. 2, June 1972, pp. 148-154.

Chuan-zhi, W., Zhen-hai, G., and Xiu-qin, Z. (1985) "Experimental Investigation of Biaxial and Triaxial Compressive Concrete Strength," *ACI materials Journal*, March-April 1987, pp. 92-100.

Clarke, J. L. (1973) "Behavior and Design of Pile Caps with Four Piles," *Technical Report No. 42.489*, Cement and Concrete Association, Wexham Springs, 1973.

Clyde, D. (2008) "Affinity Properties of Truss Model Nodes," *Magazine of Concrete Research*, (Morley Symposium on Concrete Plasticity and its Application), V. 60, No. 9, November 2008, pp. 651-655.

Collins, M.P., Vecchio F.J., Mehlhorn, G. (1985) "An International Competition to Predict the Response of Reinforced Concrete Panels," Institut für Massivban, Technische Hochschule Darmstadt, West Germany, May 1985, pp. 624-644.

Collins, M.P., and Mitchell, D (1986) "A Rational Approach to Shear Design – the 1984 Canadian Code Provisions," ACI Journal, V. 83, No. 6, November 1986, pp. 925-933.

Drucker, D. C., and Prager, W. (1952) "Soil Mechanics and Plastic Analysis for Limit Design," Quarterly of Applied Mathematics, V. 10, No. 2, pp. 157–165.

EN 1992-1-1:2004, Eurocode 2: Design of Concrete Structures – Part 1-1: General rules and rules for buildings, December 2004.

Engström, B. (2009) "Design and Analysis of Deep Beams, Plates and other Discontinuity Regions," Chalmers University of Technology, Gothenburg, Sweden, 2009, 50 pp.

Fip (1999) "Practical Design of Structural Concrete," fédération internationale de la précontrainte, September 1999, 113 pp.

Fib (2001) "Punching of Structural Concrete Slabs," *fib bulletin 12*, fédération internationale du béton, Lausanne, Suisse, Avril 2001, 307 pp.

Guandalini, S. (2006) "Poinçonnement Symétrique des Dalles en Béton Armé," Thèse no. 3380, Ecole Polytechnique Fédérale de Lausanne, 179 pp.

Hallgren, M., Kinnunen, S., and Nylander, B. (1998) "Punching Shear Tests on Column Footings," Technical report 1998:3, 1998, pp. 23.

Hallgren, M., and Bjerke, M. (2002) " Non-Linear Finite Element Analyses of Punching Shear Failure of Column Footings," *Cement & Concrete Composites 24,* 2006, pp. 491–496.

Hegger, J., Ricker, M., and Sherif, G. (2009) "Punching Strength of Reinforced Concrete Footings," *ACI Structural Journal*, V. 106, No. 5, September-October 2009, pp. 706-716.

Klein G. J. (2002) "Example 9: Pile Cap". In Reineck, K.-H., ed., "Examples for the Design of Structural Concrete with Strut-and-Tie Models," *SP*-208, American Concrete Institute, Farmington Hills, MI, 242 pp.

Kani, M.W., Huggins, M.W., and Wittkopp, R.R. (1979) "Kani on Shear in Reinforced Concrete," Departement of civil engineering, University of Toronto, 1979, pp. 225.

Kinnunen, S., Nylander H. (1960) "Punching of Concrete Slabs Without Shear Reinforcement," Transactions of the Royal Institute of Technology, No. 158, Stockholm, Sweden, 112 pp.

Kostic, N. (2009) "Topologie des Champs de Contraintes pour le Dimensionnement des Structures en Béton Armé," Thèse no. 4414, Ecole Polytechnique Fédérale de Lausanne, 235 pp.

Krüger, G. (1999) "Résistance au Poinçonnement Excentré des Planchers-Dalles," Thèse no. 2064, Ecole Polytechnique Fédérale de Lausanne, 174 pp.

Kuchma, D.A., and Collins, M.P. (1998) "Advances in Understanding Shear Performance of Concrete Structures," *Progress in Structural Engineering and Materials*, V. 1, No. 4, 1998, pp. 360-369.

Marti, P., and Thürlimann, B. (1977) "Fließbedingung für Stahlbeton mit Berücksichtigung der Betonzugfestigkeit," *Beton- und Stahlbetonbau*, V. 72, No. 1, January 1977, pp. 7-12.

Marti, P. (1980) "Zur Plastischen Berechnung von Stahlbeton," (Limit Analysis of Structural Concrete), Institut für Baustatik und Konstruktion, ETH Zürich, *IBK Bericht,* No. 104, Birkhäuser Verlag, Basel, Switzerland, October 1980, 176 pp.

Marti, P. (1985) "Basic Tools of Reinforced Concrete Beam Design," ACI Journal, *Proceedings* V. 82, No. 1, January-February 1985, pp. 45-56.

Marti, P. (1989) "Size Effect in Double-Punch Tests on Concrete Cylinders," *ACI Structural Journal,* V. 86, No 6, November/December 1989, pp. 597-601.

Marti, P. (1999) "Tragverhalten von Stahlbeton", Institut für Baustatik und Konstruktion, ETH Zürich, *IBK Bericht*, SP-008, September 1999, 301 pp.

Martin, B., Sanders, D. (2007) "Verification and Implementation of Strut-and-Tie Model in LRFD Bridge Design Specifications," *American Association of State Highway and Transportation Officials (AASHTO)*, November 2007, pp. 276.

Menétrey, P. (1994) "Numerical Analysis of Punching Failure in Reinforced Concrete Structures," Thèse no. 1279, Ecole Polytechnique Fédérale de Lausanne, 178 pp.

Menétrey, P., Walther, R., Zimmermann, T., Willam K.J., and Regan P.E. (1997) "Simulation of Punching Failure in Reinforced-Concrete Structures," *Journal of structural engineering*, May 1997, pp. 652-659.

Moe, J. (1961) "Shearing Strength of Reinforced Concrete Slabs and Footings under Concentrated Loads," Portland Cement Association, Bull. D47, Skokie, Illinois, April 1961.

Moe, J. (1962) discussion of "Shear and Diagonal Tension," by Joint ACI-ASCI Committee 326, *ACI Journal*, Proceedings V. 59, No. 9, September 1962, pp. 1334-1339.

Muttoni, A., and Schwartz, J. (1991) "Behaviour of Beams and Punching in Slabs without Shear Reinforcement," *IABSE reports*, V. 62, 1991, pp. 703-708.

Muttoni, A., Schwartz, J., and Thürlimann, B. (1997) "Design of Concrete Structures with Stress Fields," Birkhäuser Verlag, Basel, Boston and Berlin, Switzerland, 1997, 145 pp.

Muttoni, A., and Ruiz M.F. (2008) "Shear Strength of Members without Transverse Reinforcement as Function of Critical Shear Crack Width," *ACI Structural Journal*, V. 105, No 2, March-April 2008, pp. 163-172.

Park, J., Kuchma, D., and Souza, R. (2008) "Strength Predictions of Pile Caps by a Strut-and-Tie Model Approach," *Canadian Journal of Civil Engineering*, 35, 2008, pp. 1399-1413.

Pralong, J. (1982) "Poinconnement Symetrique des Planchers-Dalles," No. 131, Basel ; Birkhauser Verlag,, Bericht / Institut fur Baustatik und Konstruktion ETH Zurich, 1982, 118 pp.

Reineck, K.-H. (2002) ed., "Examples for the Design of Structural Concrete with Strut-and-Tie Models," *SP*-208, American Concrete Institute, Farmington Hills, MI, 242 pp.

Reineck, K.-H. (2010) "Strut-and-Tie Models using Concrete Tension Fields," 3rd fib International Congress, Washington, June 2010, 12 pp.

Reinhardt, H.W. (1981) "Similitude of Brittle Fracture of Structural Concrete," *Proc. Advanced Mechanics of Reinforced Concrete, IABSE Colloquium*, Delft, The Netherlands, 1981, pp. 175–184.

Ritter, W. (1899) Die Bauweise Hennebique, Schweizerische Bauzeitung, Bd, XXXIII, No. 7, January 1899.

Ruiz, M.F., and Muttoni, A. (2009) "Aplicaciones de los Campos de Esfuerzos Cortantes en el Análsis y Dimensionamiento de Losas de Hormigón Armado," (Applications of Shear Fields for Analysis and Design of Reinforced Concrete Slabs), *Hormigón y acero*, V. 60, No. 252, April-June 2009, pp. 73-88.

Schlaich, J., Schäfer, K., and Jennewein, M. (1987) "Toward a Consistent Design of Structural Concrete," *Journal of Prestressed Concrete Institute*, V. 32, No. 3, May-June 1987, pp. 74-150.

Schlaich, M., and Anagnostou, G. (1990) "Stress Fields for Nodes of Strut-and-Tie Models," *ASCE Journal of Structural Engineering*, V. 116, No. 1, January 1990, pp. 13-23.

Sherwood, E.G., Lubell, A.S., Bentz, E.C., and Collins, M.P. (2006) "One-Way Shear Strength of Thick Slabs and Wide Beams," *ACI Structural Journal*, V. 103, No. 6, November-December 2006, pp. 794-802.

Souza, R., Kuchma, D., Park, J., and Bittencourt, T. (2009) "Adaptable Strut-and-Tie Model for Design and Verification of Four-Pile caps," *ACI Structural Journal*, V. 106, No. 2, March-April 2009, pp. 142-150.

Schäfer, K. (1999) "Nodes," Section 4.4.4 in Structural Concrete, Vol. 2, fédération internationale du béton (fib), Bulletin 2, Lausanne, Suisse, pp. 257-275.

Su, R. K. L., and Chandler, A.M. (2001) "Design Criteria for Unified Strut and Tie Models," *Progress in Structural Engineering and Materials*, V. 3, No. 3, 2001, pp. 288-298

Taylor, H.P.J. (1972) "Shear Strength of Large Beams," *Journal of the Structural Division ASCE*, V. 98, No. 11, 1972, pp. 2473–2490.

Vecchio, F.J., and Collins, M.P. (1986) "The Modified Compression-Field Theory for Reinforced Concrete Elements Subjected to Shear," *ACI Journal*, March-April 1986, pp. 219-231.

Walraven, J.C. (1978) "Influence of Member Depth on the Shear Strength of Lightweight Concrete Beams without Shear Reinforcement," *Stevin Report 5-78-4*, Delft University of Technology, 1978.

Walraven, J.C. (2002) "Background Document for EC-2," Chapter 6.2 Shear, Delft University of Technology, January 2002.

Weibull, W. (1939) "Phenomenon of Rupture in Solids," *Ingen.-skapsakad. Handl.*, 153, 1–55, 1939.

Zhou, Z. (1994) "Shear Design of Pile Caps and other members without transverse reinforcement," University of British Columbia, January 1994, pp. 263.

Appendix A: Calculation of hexagonal strut cross-sectional area

Calculation of strut cross-sectional area of inclined struts at three dimensional 4C-nodes (2C2T over a pile in this case)

Node geometry

$w := 0.275m$ $\qquad\qquad$ pile width

$a_s := 0.05m$ $\qquad\qquad$ reinforcement level

$u := 2 \cdot a_s$

$\theta_{xy} := 45deg$

$\theta_{xz} := 45deg$

Angle between the inclined strut and the ties

Direction vector of the strut

$$v := \left(\cos(\theta_{xy}) \cdot \cos(\theta_{xz}) \quad \cos(\theta_{xy}) \cdot \sin(\theta_{xz}) \quad \sin(\theta_{xy}) \right)$$

Angle between the strut and the tie along x-axis

$$\theta_1 := acos\left[\frac{(1 \quad 0 \quad 0) \cdot v^T}{\left| v^T \right|} \right] \qquad\qquad \theta_1 = 60 \cdot deg$$

Angle between the strut and the tie along the y-axis

$$\theta_2 := acos\left[\frac{(0 \quad 1 \quad 0) \cdot v^T}{\left| v^T \right|} \right] \qquad\qquad \theta_2 = 60 \cdot deg$$

Calculation using the 3-D method

Coordinates of points A B C D E and F

$A := (0 \quad 0 \quad u)$

$B := (0 \quad w \quad u)$

$C := (0 \quad w \quad 0)$

$D := (w \quad w \quad 0)$

$E := (w \quad 0 \quad 0)$

$F := (w \quad 0 \quad u)$

Distance between the projection of the nodal points in a plane orthogonal to the strut

$$l_{AB} := \left| \left[(B - A) - \left[(B - A) \cdot v^T \right] \cdot v \right]^T \right|$$

$$l_{BC} := \left| \left[(C - B) - \left[(C - B) \cdot v^T \right] \cdot v \right]^T \right|$$

$$l_{CD} := \left| \left[(D - C) - \left[(D - C) \cdot v^T \right] \cdot v \right]^T \right|$$

$$l_{DE} := \left| \left[(E - D) - \left[(E - D) \cdot v^T \right] \cdot v \right]^T \right|$$

$$l_{EF} := \left| \left[(F - E) - \left[(F - E) \cdot v^T \right] \cdot v \right]^T \right|$$

$$l_{FA} := \left| \left[(A - F) - \left[(A - F) \cdot v^T \right] \cdot v \right]^T \right|$$

$$l_{AC} := \left| \left[(C - A) - \left[(C - A) \cdot v^T \right] \cdot v \right]^T \right|$$

$$l_{AD} := \left| \left[(D - A) - \left[(D - A) \cdot v^T \right] \cdot v \right]^T \right|$$

$$l_{AE} := \left| \left[(E - A) - \left[(E - A) \cdot v^T \right] \cdot v \right]^T \right|$$

Area hexagon

$$Area_{ABC} := \frac{1}{4} \sqrt{\left(l_{AB}^2 + l_{BC}^2 + l_{AC}^2 \right)^2 - 2\left(l_{AB}^4 + l_{BC}^4 + l_{AC}^4 \right)}$$

$$Area_{ACD} := \frac{1}{4} \sqrt{\left(l_{AC}^2 + l_{CD}^2 + l_{AD}^2 \right)^2 - 2\left(l_{AC}^4 + l_{CD}^4 + l_{AD}^4 \right)}$$

$$Area_{ADE} := \frac{1}{4} \sqrt{\left(l_{AD}^2 + l_{DE}^2 + l_{AE}^2 \right)^2 - 2\left(l_{AD}^4 + l_{DE}^4 + l_{AE}^4 \right)}$$

$$Area_{AEF} := \frac{1}{4} \sqrt{\left(l_{AE}^2 + l_{EF}^2 + l_{FA}^2 \right)^2 - 2\left(l_{AE}^4 + l_{EF}^4 + l_{FA}^4 \right)}$$

$l_{AB} = 0.238\,m$

$l_{BC} = 0.071\,m$

$l_{CD} = 0.238\,m$

$l_{DE} = 0.238\,m$

$l_{EF} = 0.071\,m$

$l_{FA} = 0.238\,m$

$$Area_{ABCDEF} := Area_{ABC} + Area_{ACD} + Area_{ADE} + Area_{AEF}$$

$$Area_{ABCDEF} = 0.081\,m^2$$

Calculation using the 2-D method with projection in the plane of the strut

$$Area_{strut} := w \cdot \left(w \cdot \sin(\theta_{xy}) + u \cdot \cos(\theta_{xy}) \right)$$

$$Area_{strut} = 0.073 \cdot m^2$$

Appendix B: Main program for the design of a 4-pile cap

```
% ------------------------------------------------------------------------
% Main program
% Strut-and-tie design of a 4-pile cap using FE linear elastic analysis
% ------------------------------------------------------------------------


% --------------------------
% *** Initiate ***
% --------------------------

  clear all
  close all
  clear classes
  dir='M:\Exjobb Pile Caps\FEM3DYN\New Folder\fem3dyn';
  addpath(dir);
  fem3d_setup(dir)
  %cd('M:\Exjobb Pile Caps\FEM3DYN\Model 4 pile cap\Pilecap4general\final 4 pile cap')


% --------------------------
% *** Geometry and loads ***
%          (SI units)
% --------------------------

% Materialdata:

% Steel B500B

  Es=200e9;         % E-modulus
  vs=0.3;           % Poisson's ratio
  fyk=500e6;        % Characteristic yield strength

  fyd=fyk/1.15;     % Design value EC2

  ds=0.016;         % Diameter flexural bars
  dstir=0.012;      % Diameter stirrups
  cover=0.03;       % Concrete cover
  spacing=0.02;     % Minimum spacing

% Concrete C35/40

  Ec=26e9;          % E-modulus
  vc=0.2;           % Poisson's ratio
  fck=35e6;         % Characteristic compressive cylinder strength
  Densc=2500;       % Density

  fcd=fck/1.5;      % Design value EC2

% Piles

  Ep=20e9;          % E-modulus
  wp=0.275;         % Width pile
  Ap=wp^2;          % Area
  Lp=1;             % Length
  kp=Ep*Ap/Lp/100;  % Stiffness
  Epmodif=Ep/10;    % Modified E-modulus for a reduced pile of 4m

% Column
```

```
  wct1=0.6;          % Width column (pile cap x-axis)
  wct2=0.4;          % Width column (pile cap y-axis)

% Pile cap

  h=1;               % Height pile

% First assumption dimension ties
% Number of bars in one layer

  Nb1=ceil(wp/(ds+spacing));    % Number of bars in one layer

% Suppose one layer of steel in first assumption

  as=cover+ds;                % Average as between 2 directions
  us=2*as;                    % Height tie "influence" at node
  As=Nb1*(ds/2)^2*pi;         % Steel area 1st assumption
                              % (useless in determinate problem)
  disp(['as initial  ',num2str(as)])
  Ascolx=As;
  Ascoly=As;
  Aspilex=As;
  Aspiley=As;
  Asstir=As;
  y=As;
  as1=as;
  as2=as;
  as3=as;
  Nl1=1;                      % Initialisation number of layers

% Load

  q=4400e3;                   % Total load

% Load factors

% Strut-and-tie method values

  v=1-fck/(250e6);
  k1=3;                       % Compression node
  k2=0.85*1.1;                % Compression-tension node (one tie)
  k3=0.75*1.1;                % Compression-tension node (more than one tie)

% % --------------------------------------------------------
% % *** Check bearing capacity at load***
% % --------------------------------------------------------

  Acol=(wct1*wct2);
  Nc=q/Acol;
  Na=k1*v*fcd;

% Refinement of nodes at column

  if Nc < Na
     disp('bearing stress ok')
```

```
    Areduced=Acol*Nc/Na;     % Area refinement
    wc1=wct1*sqrt(Nc/Na)/2;  % dimension of one nodal zone in x-direction
    wc2=wct2*sqrt(Nc/Na)/2;  % dimension of one nodal zone in y-direction
    disp(['dimension of one nodal zone in x-direction  ',num2str(wc1)])
    disp(['dimension of one nodal zone in y-direction  ',num2str(wc2)])
    wcn1=wct1/2-wc1/2;       % Node coordinate at column (pile cap x-axis)
    wcn2=wct2/2-wc2/2;       % Node coordinate at column (pile cap y-axis)
  else
     disp('bearing stress not ok')
     break
  end

% No refinement of nodes at column

 wc1=wct1/2;       % Width support one node at column(pile cap x-axis)
 wc2=wct2/2;       % Width support one node at column(pile cap y-axis)
 wcn1=wc1/2;       % Node coordinate at pile (pile cap x-axis)
 wcn2=wc2/2;       % Node coordinate at pile (pile cap y-axis)

% First assumption dimension of struts

 uc=0.04;                % Height horizontal strut
 ac=uc/2;                % Axis horizontal strut
 disp(['ac initial  ',num2str(ac)])
 Achorcolx=uc*wc2;      % Area strut hor(rectangular cross-section) x-axis
 Achorcoly=uc*wc1;      % Area strut hor(rectangular cross-section) y-axis
 Achorpilex=uc*wc2;     % Area strut hor(rectangular cross-section) x-axis
 Achorpiley=uc*wc1;     % Area strut hor(rectangular cross-section) y-axis


% --------------------------------
% *** Load and pile coordinates ***
% --------------------------------

% Geometry:

 iter=1;

 dx=0.675;              % Distance between pile and column faces x-direction
 dy=0.275;              % Distance between pile and column faces y-direction

 coordpilex=dx+wp/2+wct1/2;
 coordpiley=dy+wp/2+wct2/2;

 for iter=1:50
     iter

 coordinterx=(dx+wp/2+wc1/2)/2+wcn1;
 coordintery=(dy+wp/2+wc2/2)/2+wcn2;

 Nodepiles=[1  -coordpilex  -coordpiley  -h+as;
            2   coordpilex  -coordpiley  -h+as;
            3   coordpilex   coordpiley  -h+as;
            4  -coordpilex   coordpiley  -h+as];

 Nodeloads=[5  -wcn1  -wcn2  -ac;
```

```
              6   wcn1  -wcn2  -ac;
              7   wcn1   wcn2  -ac;
              8  -wcn1   wcn2  -ac];

   Nodeinterbottom=[9   -coordinterx  -coordintery  -h+as;
                  10   coordinterx  -coordintery  -h+as;
                  11   coordinterx   coordintery  -h+as;
                  12  -coordinterx   coordintery  -h+as];

   Nodeintertop=[13  -coordinterx  -coordintery  -ac;
               14   coordinterx  -coordintery  -ac;
               15   coordinterx   coordintery  -ac;
               16  -coordinterx   coordintery  -ac];


   Nodepilesdown=[5   -coordpilex  -coordpiley  -2+as-Lp;
                6    coordpilex  -coordpiley  -2+as-Lp;
                7    coordpilex   coordpiley  -2+as-Lp;
                8   -coordpilex   coordpiley  -2+as-Lp];

% Area of diagonal strut

  stironly=0;                      % All the load carried by truss action
  archonly=0;                      % All the load carried by direct arch action

  vstrut1=Nodeintertop(1,2:4)-Nodepiles(1,2:4);% Diagonal strut dir pile
  tetastrut=acos(vstrut1*[0;0;1]/(norm(vstrut1)));% Angle with vertical
  tetastrutdeg=tetastrut*360/(2*pi);
  disp(['strut angle with horizontal plane  ',num2str(90-tetastrutdeg)])
  AreaStrut5C=area5c(vstrut1,uc,wc1,wc2);     % Diagonal strut area column
  AreaStrut2C2T=area2c2t(vstrut1,us,wp);      % Diagonal strut area at pile
  Acdiacol=AreaStrut5C;                       % Average diagonal strut area
  Acdiapile=AreaStrut2C2T;

  varch=Nodeloads(1,2:4)-Nodepiles(1,2:4);       % Vector direction arch
  tetaarch=acos(varch*[0;0;1]/(norm(varch)));    % Angle with vertical
  tetaarchdeg=tetaarch*360/(2*pi);
  disp(['arch angle with horizontal plane  ',num2str(90-tetaarchdeg)])
  aarch=sqrt((Nodepiles(1,2)-Nodeloads(1,2))^2+...
      (Nodepiles(1,3)-Nodeloads(1,3))^2);   % distance centers column-pile
  if aarch < 2*(h-ac-as) & aarch>(h-ac-as)/2 & stironly==0 & archonly==0
     qstir=(1/3)*(2*aarch/(h-ac-as)-1)*(q/4);     % Part force stirrups
  elseif (aarch<(h-ac-as)/2 & stironly==0) | archonly==1
      qstir=1;
  else
     qstir=q/4-1;
  end
  disp(['arch part force stirrups (kN)  ',num2str(qstir/1000)])
  qarchvert=q/4-qstir;                            % Part force arch
  disp(['arch part force arch (kN)  ',num2str(qarchvert/1000)])
  qarch=qarchvert/(cos(tetaarch));                % Applied force at each arch

  plot=0;                                   % No plot until end of iterations

  N=modelanalysis4piles88trussarch(Es,vs,fyd,ds,cover,spacing,...
                  Ec,vc,fcd,Densc,...
```

```
                        Ep,Ap,Lp,kp,Epmodif,...
                        Acdiacol,Acdiapile,Achorcolx,Achorcoly,...
                        Achorpilex,Achorpiley,Ascolx,Ascoly,...
                        Aspilex,Aspiley,Asstir,q,qarch,as,ac,...
                        Nodepiles,Nodeloads,Nodeinterbottom,...
                        Nodeintertop,Nodepilesdown,plot)

% -----------------------------------------------------
% *** Checks and required modification of as and ac ***
% -----------------------------------------------------

  if iter==1
      Fx=N(9);
      Fy=N(11);
      wc1=sqrt((Areduced/4)*(Fy/Fx));
      wc2=sqrt((Areduced/4)*(Fx/Fy));
      wcn1=wct1/2-wc1/2;
      wcn2=wct2/2-wc2/2;
      as=max([as1,as2]);
      us=2*as;
      disp(['as  ',num2str(as)])
      disp(['refined dim of one nodal zone in x-direction  ',num2str(wc1)])
      disp(['refined dim of one nodal zone in y-direction  ',num2str(wc2)])
      Achorcolx=uc*wc2;                  % New horizontal strut area x-axis
      Achorcoly=uc*wc1;                  % New horizontal strut area y-axis

 % Tie reinforcement along x-axis intermediate

  Ascolx=N(13)/fyd;                      % Area of steel required
  Nbcolx=ceil(Ascolx/((ds/2)^2*pi));     % Number of bars required
  disp([num2str(Ascolx), ' m2 (steel area required along x-axis inter)'])
  disp([num2str(Nbcolx), ' bars'])
  disp([num2str(N(13)/1000), ' force member'])

% Tie reinforcement along y-axis intermediate (if differentin 2
% directions)

  Ascoly=N(15)/fyd;                      % Area of steel required
  Nbcoly=ceil(Ascoly/((ds/2)^2*pi));     % Number of bars required
  disp([num2str(Ascoly), ' m2 (steel area required along y-axis inter)'])
  disp([num2str(Nbcoly), ' bars'])
  disp([num2str(N(15)/1000), ' force member'])

  % Tie reinforcement along x-axis at pile

  Aspilex=N(25)/fyd;                     % Area of steel required
  Nbpilex=ceil(Aspilex/((ds/2)^2*pi));   % Number of bars required
  disp([num2str(Aspilex), ' m2 (steel area required along x-axis pile)'])
  disp([num2str(Nbpilex), ' bars'])
  disp([num2str(N(25)/1000), ' force member'])

% Tie reinforcement along y-axis at pile (if different in two directions)

  Aspiley=N(27)/fyd;                       % Area of steel required
  Nbpiley=ceil(Aspiley/((ds/2)^2*pi));     % Number of bars required
  disp([num2str(Aspiley), ' m2 (steel area required along y-axis pile)'])
```

```matlab
    disp([num2str(Nbpiley), ' bars'])
    disp([num2str(N(27)/1000), ' force member'])

% Number of stirrups at each tie

    Asstir=N(17)/fyd;                    % Area of stirrups required
    Nbstir=ceil(Asstir/((dstir/2)^2*pi));   % Number of bars required
    disp(['Area stirrup at each tie (m^2) ',num2str(Asstir)])
    disp(['Number stirrups at each tie  ',num2str(Nbstir)])
    disp(['Force stirrups   ',num2str(N(17)/1000)])

    elseif iter==2

% Tie reinforcement along x-axis intermediate

    Ascolx=N(13)/fyd;                    % Area of steel required
    Nbcolx=ceil(Ascolx/((ds/2)^2*pi));      % Number of bars required

    disp([num2str(Ascolx), ' m2 (steel area required along x-axis inter)'])
    disp([num2str(Nbcolx), ' bars'])
    disp([num2str(N(13)/1000), ' force member'])

% Tie reinforcement along y-axis intermediate (if differentin 2
% directions)

    Ascoly=N(15)/fyd;                    % Area of steel required
    Nbcoly=ceil(Ascoly/((ds/2)^2*pi));       % Number of bars required

    disp([num2str(Ascoly), ' m2 (steel area required along y-axis inter)'])
    disp([num2str(Nbcoly), ' bars'])
    disp([num2str(N(15)/1000), ' force member'])

    % Tie reinforcement along x-axis at pile

    Aspilex=N(25)/fyd;                   % Area of steel required
    Nbpilex=ceil(Aspilex/((ds/2)^2*pi));    % Number of bars required
    Nlpilex=ceil(Nbpilex/Nb1);           % Number of layers required
                                         % Steel area required
                                         % Here steel area could be
                                         % different for each tie.
    if Nlpilex > Nl1
       as1=cover+(Nlpilex*ds+(Nlpilex-1)*spacing/2);%Mean as of 2 directions
       us=2*as1;                         % Height tie "influence" at node
       Nl1=Nlpilex;
       disp([num2str(Nlpilex), 'New number of layers required by tie-pile-x'])
       disp([num2str(Aspilex), ' m2 (steel area required along x-axis pile)'])
       disp([num2str(Nbpilex), ' bars'])
    else
       disp([num2str(Aspilex), ' m2 (steel area required along x-axis pile)'])
       disp([num2str(Nbpilex), ' bars'])
    end
       disp([num2str(N(25)/1000), ' force member'])

% Tie reinforcement along y-axis at pile (if different in two directions)

    Aspiley=N(27)/fyd;                       % Area of steel required
```

```matlab
    Nbpiley=ceil(Aspiley/((ds/2)^2*pi));       % Number of bars required
    Nlpiley=ceil(Nbpiley/Nb1);                 % Number of layers required

    if Nlpiley > Nl1
        as2=cover+(Nlpiley*ds+(Nlpiley-1)*spacing/2);%Mean as of 2 directions
        us=2*as2;                              % Height tie "influence" at node
        Nl1=Nlpiley;
        disp([num2str(Nlpiley), 'New number of layers required by tie-pile-y'])
        disp([num2str(Aspiley), ' m2 (steel area required along y-axis pile)'])
        disp([num2str(Nbpiley), ' bars'])
    else
        disp([num2str(Aspiley), ' m2 (steel area required along y-axis pile)'])
        disp([num2str(Nbpiley), ' bars'])
    end
        disp([num2str(N(27)/1000), ' force member'])

%   Refinement sides of bearing area proportions (paragraph to comment if
%   no node refinement

    Fx=N(9);
    Fy=N(11);
    wc1=sqrt((Areduced/4)*(Fy/Fx));
    wc2=sqrt((Areduced/4)*(Fx/Fy));
    wcn1=wct1/2-wc1/2;
    wcn2=wct2/2-wc2/2;
    as=max([as1,as2]);
    us=2*as;
    disp(['as  ',num2str(as)])
    disp(['refined dim of one nodal zone in x-direction  ',num2str(wc1)])
    disp(['refined dim of one nodal zone in y-direction  ',num2str(wc2)])
    Achorcolx=uc*wc2;                          % New horizontal strut area x-axis
    Achorcoly=uc*wc1;                          % New horizontal strut area y-axis

% Number of stirrups at each tie

    Asstir=N(17)/fyd;                          % Area of stirrups required
    Nbstir=ceil(Asstir/((dstir/2)^2*pi));      % Number of bars required
    disp(['Area stirrup at each tie (m^2) ',num2str(Asstir)])
    disp(['Number stirrups at each tie  ',num2str(Nbstir)])
    disp(['Force stirrups    ',num2str(N(17)/1000)])

    else

    p=0;              % initialisation parameter commanding change of ac & wc
    asprevious=as;
    acprevious=ac;
    wc1previous=wc1;
    wc2previous=wc2;

% Tie reinforcement along x-axis intermediate

    Ascolx=N(13)/fyd;                          % Area of steel required
    Nbcolx=ceil(Ascolx/((ds/2)^2*pi));         % Number of bars required

    disp([num2str(Ascolx), ' m2 (steel area required along x-axis inter)'])
    disp([num2str(Nbcolx), ' bars'])
```

```matlab
    disp([num2str(N(13)/1000), ' force member'])

% Tie reinforcement along y-axis intermediate (if differentin 2
% directions)

    Ascoly=N(15)/fyd;                          % Area of steel required
    Nbcoly=ceil(Ascoly/((ds/2)^2*pi));         % Number of bars required

    disp([num2str(Ascoly), ' m2 (steel area required along y-axis inter)'])
    disp([num2str(Nbcoly), ' bars'])
    disp([num2str(N(15)/1000), ' force member'])

    % Tie reinforcement along x-axis at pile

    Aspilex=N(25)/fyd;                         % Area of steel required
    Nbpilex=ceil(Aspilex/((ds/2)^2*pi));       % Number of bars required
    Nlpilex=ceil(Nbpilex/Nb1);                 % Number of layers required
                                               % Steel area required
                                               % Here steel area could be
                                               % different for each tie.
    if Nlpilex > Nl1
        as1=cover+(Nlpilex*ds+(Nlpilex-1)*spacing/2);%Mean as of 2 directions
        us=2*as1;                              % Height tie "influence" at node
        Nl1=Nlpilex;
        disp([num2str(Nlpilex), 'New number of layers required by tie-pile-x'])
        disp([num2str(Aspilex), ' m2 (steel area required along x-axis pile)'])
        disp([num2str(Nbpilex), ' bars'])
    else
        disp([num2str(Aspilex), ' m2 (steel area required along x-axis pile)'])
        disp([num2str(Nbpilex), ' bars'])
    end
        disp([num2str(N(25)/1000), ' force member'])

% Tie reinforcement along y-axis at pile (if different in two directions)

    Aspiley=N(27)/fyd;                          % Area of steel required
    Nbpiley=ceil(Aspiley/((ds/2)^2*pi));       % Number of bars required
    Nlpiley=ceil(Nbpiley/Nb1);                 % Number of layers required

    if Nlpiley > Nl1
        as2=cover+(Nlpiley*ds+(Nlpiley-1)*spacing/2);%Mean as of 2 directions
        us=2*as2;                              % Height tie "influence" at node
        Nl1=Nlpiley;
        disp([num2str(Nlpiley), 'New number of layers required by tie-pile-y'])
        disp([num2str(Aspiley), ' m2 (steel area required along y-axis pile)'])
        disp([num2str(Nbpiley), ' bars'])
    else
        disp([num2str(Aspiley), ' m2 (steel area required along y-axis pile)'])
        disp([num2str(Nbpiley), ' bars'])
    end
        disp([num2str(N(27)/1000), ' force member'])

% Horizontal strut under column along x-axis

    Acreq1x=abs(N(9))/(k1*v*fcd);       % Required strut area
```

```matlab
  if Acreq1x > Achorcolx
    p=1;
    disp(['Horizontal strut x-axis'])
  end
   disp([num2str(abs(N(9))/1000), ' force horizontal strut x-axis'])
   disp([num2str(100*Acreq1x/Achorcolx),' % horizontal strut x-axis'])

% Horizontal strut under column along y-axis (if different in 2
% directions)

  Acreq1y=abs(N(11))/(k1*v*fcd);       % Required strut area

  if Acreq1y > Achorcoly
    p=1;
    disp(['Horizontal strut y-axis'])
  end
  disp([num2str(abs(N(11))/1000), ' force horizontal strut y-axis'])
  disp([num2str(100*Acreq1y/Achorcoly),' % horizontal strut y-axis'])

% Inclined strut at pile
% Conpression-tension node with one tie (k2)

  resultant=abs(N(5))*vstrut1/norm(vstrut1)+qarch*varch/norm(varch);
  vresultant=resultant/(norm(resultant));
  intensityresultant=norm(resultant);
  tetares=acos(vresultant*[0;0;1]/(norm(vresultant)));% Angle with vertical
  tetaresdeg=tetares*360/(2*pi);
  disp(['resultant angle with horizontal plane  ',num2str(90-tetaresdeg)])
  Acreq2=abs(intensityresultant)/(k3*v*fcd);          % Required strut area
  Acprov2=area2c2t(vresultant,us,wp);                 % Provided strut area

  if Acreq2 > Acprov2
    as3=as+0.005;
    disp(['New as diagonal strut',num2str(as3)])
  end
  disp([num2str(100*Acreq2/Acprov2),' % inclined strut at pile'])

% Inclined strut at column
% Compression node (k1)

  Acreq3=abs(intensityresultant)/(k1*v*fcd);          % Required strut area
  Acprov3=area5c(vresultant,uc,wc1,wc2);

  if Acreq3 > Acprov3
    p=1;
    disp(['Inclined strut at column'])
  end
   disp([num2str(100*Acreq3/Acprov3),' % inclined strut at column'])
   disp([num2str(abs(N(5))/1000), ' force inclined strut truss'])

% Parameter to change

 if p==1;
   if ac <= sqrt(wc1*wc2) | (wc1==wct1/2 & wc2==wct2/2)
      ac=ac+0.005;
      disp(['New ac  ',num2str(ac)])
```

```matlab
  elseif wc1 < wct1/2 & wc2 < wct2/2
      wc1=wc1*1.02;
      wc2=wc2*1.02;
      wcn1=wct1/2-wc1/2;
      wcn2=wct2/2-wc2/2;
      if wc1 > wct1/2
          wc1=wct1/2;
          wcn1=wct1/2-wc1/2;
      end
      if wc2 > wct2/2
          wc2=wct2/2;
          wcn2=wct2/2-wc2/2;
      end
      disp(['New wc1  ',num2str(wc1)])
      disp(['New wc2  ',num2str(wc2)])
      disp(['ac  unchanged  ',num2str(ac)])
  elseif wc2 < wct2/2 & wc1 == wct1/2
      wc2=wc2*1.04;
      wcn2=wct2/2-wc2/2;
      disp(['New wc2  ',num2str(wc2)])
      disp(['ac  unchanged  ',num2str(ac)])
  elseif wc1 < wct1/2 & wc2 == wct2/2
      wc1=wc1*1.04;
      wcn1=wct1/2-wc1/2;
      disp(['New wc1',num2str(wc1)])
      disp(['ac  unchanged  ',num2str(ac)])
  else
      disp(['ERROR WITH WCM'])
  end
 end

 as=max([as1,as2,as3]);
 us=2*as;
 disp(['as  ',num2str(as)])
 uc=2*ac;
 disp(['ac  ',num2str(ac)])
 disp(['dimension of one nodal zone in x-direction  ',num2str(wc1)])
 disp(['dimension of one nodal zone in y-direction  ',num2str(wc2)])
%% Check arch

 AreaArchcol=area5c(varch,uc,wc1,wc2);  % Provided strut area col
 AreaArchpile=area2c2t(varch,us,wp);    % Provided strut area pile
                                        % Provided strut area at middle

%% For the inclined strut kstrut=karch (as defined in the report)
 AreaArchmid=pi/4*(sqrt(AreaArchcol/pi)+sqrt(AreaArchpile/pi))^2;
 DiaArchmid=2*sqrt(AreaArchmid/pi);
 Larch=norm(varch);
 internallevelarm=h-ac-as;
 % Definition of the diameter of the equivalent cylinder the strut is
 % confined in:
 Diacylinder=0.5*(internallevelarm/(sin(tetaarch*pi/180)));
 %% kstrut=kconfinement*kweb, kweb=0,6
 kweb=0.6;

 %kconfinement is calculated as follows:
```

```matlab
    alpha1=0.33*((Diacylinder/DiaArchmid)-1);
    alpha1=max(0,min(1,alpha1));

    beta1=0.33*((Larch/DiaArchmid)-1);
    beta1=max(0,min(1,beta1));

    kconfinement=1+(2*alpha1*beta1);
    %kconfinement=max(1,0.6*kconfinement)

    kstrut=kweb*kconfinement;
    AcreqArch=abs(qarch)/(fcd*kstrut*v);    % % Required strut area

    disp([num2str(100*AcreqArch/AreaArchmid),' % crushing inclined strut'])
    disp([num2str(qarch/1000), ' force inclined strut arch'])


% Number of stirrups at each tie

    Asstir=N(17)/fyd;                        % Area of stirrups required
    Nbstir=ceil(Asstir/((dstir/2)^2*pi));    % Number of bars required
    disp(['Area stirrup at each tie (m^2) ',num2str(Asstir)])
    disp(['Number stirrups at each tie  ',num2str(Nbstir)])
    disp(['Force stirrups   ',num2str(N(17)/1000)])

% New strut dimensions

    Achorcolx=uc*wc2;                        % New horizontal strut area x-axis
    Achorcoly=uc*wc1;                        % New horizontal strut area y-axis

    if as==asprevious & ac==acprevious & wc1==wc1previous & wc2==wc2previous
        disp('################################################################')
        disp('################################################################')
        disp(['Check OK  as= ',num2str(as)])
        disp(['ac=',num2str(ac)])
        plot=1;
        N=modelanalysis4piles88trussarch(Es,vs,fyd,ds,cover,spacing,...
                        Ec,vc,fcd,Densc,...
                        Ep,Ap,Lp,kp,Epmodif,...
                        Acdiacol,Acdiapile,Achorcolx,Achorcoly,...
                        Achorpilex,Achorpiley,Ascolx,Ascoly,...
                        Aspilex,Aspiley,Asstir,q,qarch,as,ac,...
                        Nodepiles,Nodeloads,Nodeinterbottom,...
                        Nodeintertop,Nodepilesdown,plot)
        StressTiecolX=N(13)/Ascolx/(1e6);
        disp(['StressTiecolX',num2str(StressTiecolX)])
        StressTiecolY=N(15)/Ascoly/(1e6);
        disp(['StressTiecolY',num2str(StressTiecolY)])
        StressTiepileX=N(25)/Aspilex/(1e6);
        disp(['StressTiepileX',num2str(StressTiepileX)])
        StressTiepileY=N(27)/Aspiley/(1e6);
        disp(['StressTiepileY',num2str(StressTiepileY)])
        StressStrutDiaPile=N(5)/AreaStrut2C2T/(1e6);
        disp(['StressStrutDiaPile',num2str(StressStrutDiaPile)])
        StressStrutDiaColumn=N(1)/AreaStrut5C/(1e6);
        disp(['StressStrutDiaColumn',num2str(StressStrutDiaColumn)])
        StressStrutHorcolX=N(9)/Achorcolx/(1e6);
```

```matlab
        disp(['StressStrutHorcolX=',num2str(StressStrutHorcolX)])
        StressStrutHorcolY=N(11)/Achorcoly/(1e6);
        disp(['StressStrutHorcolY=',num2str(StressStrutHorcolY)])

        % Number of stirrups at each tie

        disp(['Area stirrup at each tie (m^2) ',num2str(Asstir)])
        disp(['Number stirrups at each tie  ',num2str(Nbstir)])
        break
    end
    end
    end
```

Appendix C: Main program for the analysis of a 4-pile cap

```
% -------------------------------------------------------------------------
% Main program
% Strut-and-tie design of a 4-pile cap using FE linear elastic analysis
% -------------------------------------------------------------------------


% ---------------------------
% *** Initiate ***
% ---------------------------

   clear all
   close all
   clear classes
   dir='M:\Exjobb Pile Caps\FEM3DYN\New Folder\fem3dyn';
   addpath(dir);
   fem3d_setup(dir)
   %cd('M:\Exjobb Pile Caps\FEM3DYN\Model 4 pile cap\Pilecap4general\Gautier')


% -------------------------------------------------------------------------
%                        *** Geometry and loads ***
%                                (SI units)
% -------------------------------------------------------------------------

% Materialdata:

% Steel B500B

  Es=200e9;          % E-modulus
  vs=0.3;            % Poisson's ratio

% Ultimate capacity steel considered in the analysis
% (ultimate load: fym=1,1fyk, design load: fyd=fyk/gamma.s)
  fyd=521.57e6;

  ds=0.0113;         % Diameter bar
  cover=0.03;        % Concrete cover   (50mm-ds pour cover et spacing)
  spacing=0.02;      % Minimum spacing

% Concrete C25/30

  Ec=26e9;           % E-modulus (secant moulus measured)
  vc=0.2;            % Poisson's ratio

% Compressive cylinder strength (28 days) considered in the analysis
% (ultimate load: fcm, design load: fcd=fck/gamma.c)
  fck=20.85e6;
  Densc=2500;        % Density

  fcd=fck/1;      % Design value EC2 (1 should be 1.5)

% Piles

  Ep=27.1e9;         % E-modulus
  wp=0.076;          % Width pile
  Ap=wp^2;           % Area
  Lp=40;             % Length
  kp=Ep*Ap/Lp;       % Stiffness
```

```
  Epmodif=Ep/10;    % Modified E-modulus for a reduced pile of 4m

% Column

  wc1=0.076;
  wc2=0.076;

% Pile cap

  h=0.15;                % Height pile cap

% Struts

  uc=0.05          % Height horizontal strut
  ac=uc/2;                 % Axis horizontal strut

% Ties

  as=0.04014;             % Average as between 2 directions
  us=2*as;             % Height tie "influence" at node

  Aspilex=0.00009095;   % Area tie hor(TC3) x-axis
%   Aspiley=0.0011;    % Area tie hor(TC2) y-axis

% Load

  q=170e3                % Total load

% Load factors


% % ----------------------------------------------------------------------
% %           *** Check bearing capacity at load and support ***
% % ----------------------------------------------------------------------
  Acol=(wc1*wc2);
  Nc=q/Acol;
  Na=3.88*(1-fck/(250e6))*fcd;

  if Nc < Na
      disp('bearing stress ok')
      Areduced=Acol*Nc/Na;
      wc1reduced=sqrt(Areduced)
      wcs1=wc1reduced/2;
      wcs2=wcs1;
      wcn1=wc1/2-wcs1/2;
      wcn2=wcn1;
  else
      disp('bearing stress ok')
      break
  end

      wcs1=wc1reduced/2;
      wcs2=wcs1;
      wcn1=wc1/2-wcs1/2;
      wcn2=wcn1;
```

```
%-------------------------------------------------------------------------
%                     *** Load and pile coordinates ***
% -------------------------------------------------------------------------
% Geometry:

  tolerance=0.02;
  iter=1;

  coordpilex=0.1;
  coordpiley=0.1;


  Nodeloads=[1  -wcn1  -wcn2  -ac;
             2   wcn1  -wcn2  -ac;
             3   wcn1   wcn2  -ac;
             4  -wcn1   wcn2  -ac];

  Nodepiles=[5  -coordpilex  -coordpiley  -h+as;
             6   coordpilex  -coordpiley  -h+as;
             7   coordpilex   coordpiley  -h+as;
             8  -coordpilex   coordpiley  -h+as];

  Nodepilesdown=[9   -coordpilex  -coordpiley  -1+as-h;
                 10   coordpilex  -coordpiley  -1+as-h;
                 11   coordpilex   coordpiley  -1+as-h;
                 12  -coordpilex   coordpiley  -1+as-h];

  Nodes=[Nodeloads;Nodepiles;Nodepilesdown];

% Area of diagonal strut

  Achorcolx=uc*wcs1;     % Area strut hor(rectangular cross-section) x-axis
  Achorcoly=uc*wcs2;     % Area strut hor(rectangular cross-section) y-axis
  % Diagonal strut direction
  vstrut1=Nodeloads(1,2:4)-Nodepiles(1,2:4);

  % Diagonal strut changement de repere
  vstrut11=[vstrut1(2) -vstrut1(1) vstrut1(3)];

  % Diagonal strut area column
  AreaStrut5C=area5c(-vstrut1,uc,wcs1,wcs2);

  % Diagonal strut area at pile
  AreaStrut2C2T=area5c(-vstrut1,us,wp,wp);

  Acdiasidecol=AreaStrut5C;
  Acdiasidepile=AreaStrut2C2T;

  % Average diagonal strut area
  Acstrutmidaverage=pi/4*(sqrt(AreaStrut5C/pi)+sqrt(AreaStrut2C2T/pi))^2;
  Diastrutmidaverage=2*sqrt(Acstrutmidaverage/pi);

  L=norm(Nodeloads(1,2:4)-Nodepiles(1,2:4));
  internallevelarm=h-ac-as;

  % Definition of the diameter of the equivalent cylinder the strut is
```

```
  % confined in:
  teta=acos((vstrut1*[0;0;1])/norm(vstrut1))*180/pi;
  Diacylinder=0.5*(internallevelarm/(sin(teta*pi/180)));




  % No plot until end of iterations
  plot=0;

  Ac=0.0225;

  N=modelanalysis4pilesexperiments(Es,vs,fyd,ds,...
                      Ec,vc,fcd,Densc,...
                      Ep,Ap,Lp,kp,Epmodif,...
                      Ac,q,as,ac,...
                      Nodes,plot)

% -------------------------------------------------------------------------
% ***  Strut-and-tie method coefficient for strength of components ***
% -------------------------------------------------------------------------

  v=1-fck/(250e6); %all concrete strengths are reduced by v

  k1=3.88;            % Compression node
  k3=0.75*1.1;        % Compression-tension node (more than one tie)

  %% For the inclined strut kstrut=karch (as defined in the report)
  %% kstrut=kconfinement*kweb, kweb=0,6
  kweb=0.6;

  %kconfinement is calculated as follows:
  alpha1=0.33*((Diacylinder/Diastrutmidaverage)-1);
  alpha1=max(0,min(1,alpha1));

  beta1=0.33*((L/Diastrutmidaverage)-1);
  beta1=max(0,min(1,beta1));

  kconfinement=1+(2*alpha1*beta1)
  kstrut=kweb*kconfinement;

% -------------------------------------------------------------------------
%                   *** Redifined areas of struts and ties ***
% -------------------------------------------------------------------------

% This step could be done differently and simplified in this case, as the 4
% pile cap studied is a statically determinate system and the internal
% forces in the struts and ties don't depend on their stiffness. The method
% developped here will be used for statically indeterminate systems as
% well.

% -------------------------------------------------------------------------
% *** Checks and required modification of as and ac ***
% -------------------------------------------------------------------------

  asprevious=as;
  acprevious=ac;
```

```
% Tie reinforcement along x-axis at pile

  Aspilexr=N(9)/fyd;                        % Area of steel required

  disp([num2str(Aspilexr), 'm2 (steel area required along x-axis)'])
  disp([num2str(Aspilex), 'm2 (steel area provided along x-axis)',...
      num2str(100*Aspilexr/Aspilex),'%' ])

% Horizontal strut under column along x-axis (k1)

  Acxreq=abs(N(1))/(k1*v*fcd);       % Required strut area

  if Acxreq > Achorcolx
  disp([num2str(Acxreq), 'm2 (column strut area required along x-axis)'])
  disp([num2str(Achorcolx),...
      'm2 (column strut area provided along x-axis)'])
  end

% Inclined strut side at pile
% Conpression-tension node with two ties (k3)

  Acdia1req=abs(N(5))/(k3*v*fcd);      % Required strut area

  if Acdia1req > Acdiasidepile
  disp([num2str(Acdia1req), 'm2 (dia strut side area required at pile)'])
  disp([num2str(Acdiasidepile),...
      'm2 (dia strut side area provided at pile)'])
  end

% Inclined strut side at column
% Compression node (k1)

  Acdia2req=abs(N(5))/(k1*v*fcd);      % Required strut area

  if Acdia2req > Acdiasidecol
  disp([num2str(Acdia2req), 'm2 (dia strut side area required at column)'])
  disp([num2str(Acdiasidecol), ...
      'm2 (dia strut side area provided at column)'])
  end

% % Inclined strut at middle

  Acdiamidreqa=abs(N(5))/(kstrut*v*fcd);      % Required strut area

  if Acdiamidreqa > Acstrutmidaverage
  disp([num2str(Acdiamidreqa),...
      'm2 (dia strut side area required at middle method 1)'])
  disp([num2str(Acstrutmidaverage),...
      'm2 (dia strut side area provided at middle average)'])
  end

% Stresses
  stress1=abs(N(1))/(Achorcolx);
  disp([num2str(stress1/1e6), 'MPa (stress strut hori)'])
  disp([num2str(stress1/fck),'//',...
```

CHALMERS, *Civil and Environmental Engineering*, Master's Thesis 2010:51

```
    num2str(k1*v),'//',num2str(100*stress1/(fcd*k1*v)),'%'])
stress2=abs(N(5))/(Acdiasidecol);
disp([num2str(stress2/1e6), 'MPa (stress strut dia col)'])
disp([num2str(stress2/fck),'//',...
    num2str(k1*v),'//',num2str(100*stress2/(fcd*k1*v)),'%'])
stress3=abs(N(5))/(Acdiasidepile);
disp([num2str(stress3/1e6), 'MPa (stress strut dia pile)'])
disp([num2str(stress3/fck),'//',...
    num2str(k3*v),'//',num2str(100*stress3/(fcd*k3*v)),'%'])
stress4a=abs(N(5))/(Acstrutmidaverage);
disp([num2str(stress4a/1e6), 'MPa (stress strut dia)'])
disp([num2str(stress4a/fck),'//',...
    num2str(kstrut*v),'//',num2str(100*stress4a/(fcd*kstrut*v)),'%'])
stress5=q/((wc1reduced*wc1reduced));
disp([num2str(stress5/1e6), 'MPa (bearing stress at column)'])
disp([num2str(stress5/fck),'//',...
    num2str(k1*v),'//',num2str(100*stress5/(fcd*k1*v)),'%'])
stress6=q/(4*(wp^2));
disp([num2str(stress6/1e6), 'MPa (bearing stress at piles)'])
disp([num2str(stress6/fck),'//',...
    num2str(k3*v),'//',num2str(100*stress6/(fcd*k3*v)),'%'])
```

Appendix D: Calculation of design and ultimate resistance of a square pile cap without shear reinforcement according to EC2 and BBK04

CALCULATION OF DESIGN AND ULTIMATE RESISTANCE OF A SQUARE PILE CAP WITHOUT SHEAR REINFORCEMENT ACCORDING TO EUROCODE 2 AND BBK 04

Length of the pile cap:

$L := 1.2\text{m}$

Height of the pile cap

$h := 0.35\text{m}$

Distance between the centres of the piles:

$e := 0.9\text{m}$

$A_s := 7.85 \cdot 10^{-4}\text{m}^2$

$f_{cck} := 27.2\text{MPa}$

Effective depth:

$d := 0.3\text{m}$

Width of the column

$w_c := .2\text{m}$

Width of the piles (square):

$w_p := 0.177\text{m}$

$f_{yk} := 435\text{MPa}$

Material properties:

CONCRETE:

$$\gamma_c := 1.5$$

The cylinder characteristic strength is given for concrete is most experiments, the value of the mean strength of concrete, used in analysis to find the ultimate resistance is derived using the recommandations for ACI318-08:

$$f_{cck} = 27.2 \cdot MPa \qquad \varepsilon_{cu} := 3.5 \cdot 10^{-3}$$

$$f_{ccm} := \begin{vmatrix} \left(f_{cck} + 6.9MPa\right) & \text{if } f_{cck} \leq 20.7MPa & = 35.5 \cdot MPa \\ \left(f_{cck} + 8.3MPa\right) & \text{if } 20.7MPa < f_{cck} \leq 34.4MPa \\ \left(1.1 f_{cck} + 4.83MPa\right) & \text{otherwise} \end{vmatrix}$$

$$f_{ccd} := \frac{f_{cck}}{\gamma_c} = 18.133 \cdot MPa$$

FLEXURAL REINFORCEMENT:

Steel yielding strength/ultimate strength

$$f_{yk} = 435 \cdot MPa$$

The capacity considered for the steel in order to find the ultimate resistance is the mean steel strength. Indeed, it is supposed that the steel will not be able to reach its ultimate strength as it requires too much deformation. The mean yielding strength of steel is approximated to 1.1 times the charcteristic yield stress.

$$f_{ym} := 1.1 \cdot f_{yk} = 478.5 \cdot MPa \qquad \gamma_s := 1.15$$

$$f_{yd} := \frac{f_{yk}}{\gamma_s} = 378.261 \cdot MPa$$

Steel area, in one direction:

$$A_s = 7.85 \times 10^{-4} \, m^2$$

$$\rho := \frac{A_s}{d \cdot L} = 0.218 \cdot \% \qquad \text{has to be less than 2\%}$$

Yield strain considered in the analysis:

$$E_s := 200GPa$$

$$\varepsilon_{sy} := \frac{f_{ym}}{E_s} = 2.393 \times 10^{-3} \qquad \varepsilon_{syd} := \frac{f_{yd}}{E_s} = 1.891 \times 10^{-3}$$

Flexural capacity, EC2 and BBK04:

Refined analysis with stress blocks. The failure criterion ε.cu=3.5*10^-3 is considered. the stress block factors are taken accordingly. The steel stress is set at f.y and an horizontal top branch without strain limitation is assumed.

$$\alpha_r := 0.81 \qquad \beta_r := 0.416$$

$$x := \frac{f_{ym} \cdot A_s}{\alpha_r \cdot f_{ccm} \cdot L} = 0.011\,m \qquad\qquad x_d := \frac{f_{yd} \cdot A_s}{\alpha_r \cdot f_{ccd} \cdot L} = 0.017\,m$$

$$\varepsilon_s := \frac{d - x}{x} \varepsilon_{cu} = 0.093 \qquad\qquad \varepsilon_{s.d} := \frac{d - x_d}{x_d} \varepsilon_{cu} = 0.059$$

$$0.95d = 0.285\,m$$

$$z := d - \beta_r \cdot x = 0.295\,m \qquad\qquad z_d := d - \beta_r \cdot x_d = 0.293\,m$$

$$M_{fl} := f_{ym} \cdot A_s \cdot z = 110.986 \cdot kN \cdot m \qquad\qquad M_{fl.d} := f_{yd} \cdot A_s \cdot z_d = 86.999 \cdot kN \cdot m$$

Moment level arm considered between the middle of the pile to the face of the column, multiplied by two in order to be expressed as a column load:

$$V_{fl} := \frac{2M_{fl}}{\dfrac{e}{2} - \dfrac{w_c}{2}} = 634.204 \cdot kN \qquad\qquad V_{fl.d} := \frac{2M_{fl.d}}{\dfrac{e}{2} - \dfrac{w_c}{2}} = 497.14 \cdot kN$$

Shear capacity, EC2 and BBK 04:

Load applied close to support:
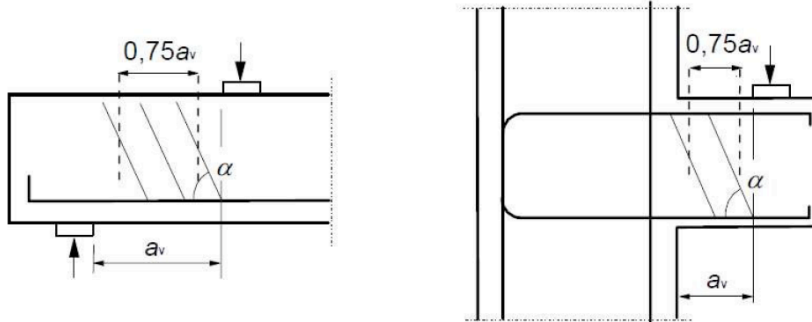
$$a_v := \max\left(\frac{d}{2}, \frac{e - w_p - w_c}{2}\right) = 0.262\,m \qquad \frac{e - w_p - w_c}{2} = 0.262\,m \qquad \frac{d}{2} = 0.15\,m$$

$$\beta := \min\left(1, \frac{a_v}{2 \cdot d}\right) = 0.436$$

Only a ratio β of the load is considered to generate shear

One-way shear capacity of the pile cap, without shear reinforcement

Shear force capacity, after reduction due to direct arch action:

$$f_{cck} = 27.2 \cdot MPa \qquad L = 1.2\,m \qquad d = 0.3\,m \qquad \rho = 0.218 \cdot \% \qquad f_{ccd} = 18.133 \cdot MPa$$

$$\nu := 0.6 \cdot \left(1 - \frac{f_{cck}}{250 MPa}\right) = 0.535 \qquad k := \min\left(2, 1 + \sqrt{\frac{200}{d \cdot \frac{1000}{m}}}\right) = 1.816$$

$$C_{Rd.c} := \frac{0.18}{\gamma_c} = 0.12$$

VRd.c.1 is the classic shear capacity for 1-way flecural elements in Eurocode

$$V_{Rd.c.1} := \left[C_{Rd.c} \cdot k \cdot \left[100 \cdot \rho \cdot \left(\frac{f_{ccm} \cdot 10^{-6}}{Pa} \right) \right]^{\frac{1}{3}} \right] \cdot \left(\frac{L \cdot 1000}{m} \right) \cdot \left(\frac{d \cdot 1000}{m} \right) \cdot N = 155.233 \cdot kN$$

$$V_{Rd.c.1.d} := \left[C_{Rd.c} \cdot k \cdot \left[100 \cdot \rho \cdot \left(\frac{f_{cck} \cdot 10^{-6}}{Pa} \right) \right]^{\frac{1}{3}} \right] \cdot \left(\frac{L \cdot 1000}{m} \right) \cdot \left(\frac{d \cdot 1000}{m} \right) \cdot N = 142.046 \cdot kN$$

V.Rd.c.2 accounts for low flexural reinforcement ratio slabs, this formula often gives higher capacity for pile caps:

$$v_{min} := 0.035 \cdot k^{\frac{3}{2}} \cdot \left(\frac{f_{ccm} \cdot 10^{-6}}{Pa} \right)^{\frac{1}{2}} = 0.511 \qquad v_{min.d} := 0.035 \cdot k^{\frac{3}{2}} \cdot \left(\frac{f_{cck} \cdot 10^{-6}}{Pa} \right)^{\frac{1}{2}} = 0.447$$

$$V_{Rd.c.2} := v_{min} \cdot \left(\frac{L \cdot 1000}{m} \right) \cdot \left(\frac{d \cdot 1000}{m} \right) \cdot N = 183.796 \cdot kN$$

$$V_{Rd.c.2.d} := v_{min.d} \cdot \left(\frac{L \cdot 1000}{m} \right) \cdot \left(\frac{d \cdot 1000}{m} \right) \cdot N = 160.882 \cdot kN$$

Resultant shear capacity

$$V_{Rd.c} := \max \left(V_{Rd.c.1}, V_{Rd.c.2} \right) = 183.796 \cdot kN$$

$$V_{Rd.c.d} := \max \left(V_{Rd.c.1.d}, V_{Rd.c.2.d} \right) = 160.882 \cdot kN$$

The shear capacity is multiplied by 2 so it is expressed as a load at the column

$$V_{Rd.cc} := \frac{2 V_{Rd.c}}{\beta} = 843.424 \cdot kN \qquad\qquad V_{Rd.cc.d} := \frac{2 V_{Rd.c.d}}{\beta} = 738.272 \cdot kN$$

However, the shear capacity of the element cannot be greater than V.Rd,max (crushing control):

$$V_{Rd.max} := 0.5 \cdot L \cdot d \cdot \nu \cdot f_{ccm} = 3.417 \times 10^3 \cdot kN \qquad V_{Rd.max.d} := 0.5 \cdot L \cdot d \cdot \nu \cdot f_{ccd} = 1.745 \times 10^3 \cdot kN$$

In the end:

$$V_{sh} := min\left(2 V_{Rd.max}, V_{Rd.cc}\right) = 843.424 \cdot kN \quad V_{sh.d} := min\left(2 V_{Rd.max.d}, V_{Rd.cc.d}\right) = 738.272 \cdot k$$

Punching capacity at inner column, EC2:

Check at the column face

Figure 7
Recommended standard values for β
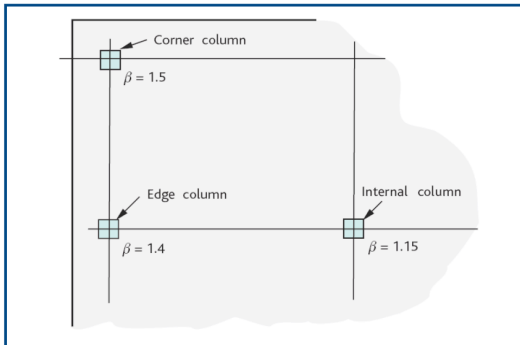
Eurocode factor for inner column, βc:

$$\beta_c := 1.15$$

Capacity determined at the column perimeter:

$$u_i := w_c \cdot 4 = 0.8 \text{ m}$$

$$f_{cck} = 27.2 \cdot MPa$$

$$v_{Rd.max} := 0.5 \nu \cdot f_{ccd} = 4.848 \cdot MPa$$

$$V_{punch.max} := \frac{u_i \cdot d \cdot v_{Rd.max}}{\beta_c} = 1.012 \times 10^3 \cdot kN$$

Check at the control perimeter 2d

Calculation of the shear force taken into consideration, after reduction due to load applied inside the control perimeter considered around the column, square pile caps, square piles:

$$i := 0.1, 0.2 .. 8.1$$

$$a(i) := \frac{i}{4} d$$

$$u_1(i) := 4 \cdot w_c + 2 \cdot \pi \cdot a(i)$$

check will be done at many different control perimeter from the column face up to a distance 2d from the column face:

$$a(1) = 0.075 \, \text{m} \qquad 2d = 0.6 \, \text{m}$$

$$a(2) = 0.15 \, \text{m}$$

Y is the distance from the corner of the column to the corner of the pile

$$Y := \frac{\sqrt{2}}{2} \left(e - w_p - w_c \right) = 0.37 \, \text{m}$$

X is the distance from the corner of the pile to the control perimeter

$$X(i) := a(i) - Y \qquad 2d = 0.6 \, \text{m} \qquad w_p \cdot \sqrt{2} = 0.25 \, \text{m}$$

The reduction factor is equal to 1 when no reduction of load occurs inside the control perimeter (the value 0.01 is set to give a virtual infinite punching capacity):

$$\text{Redfactor}(i) := \begin{cases} 1 & \text{if } X(i) < 0. \\ \max\left(0.001, 1 - \dfrac{X(i)}{w_p \cdot \sqrt{2}} \right) & \text{otherwise} \end{cases}$$
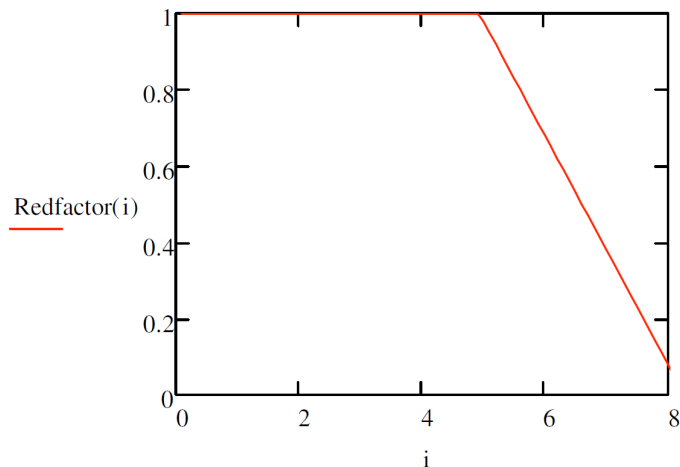
$$X(1) = -0.295 \, \text{m} \qquad \text{Redfactor}(1) = 1 \qquad \text{Redfactor}(5) = 0.979$$

$$X(2) = -0.22 \, \text{m} \qquad \text{Redfactor}(2) = 1 \qquad \text{Redfactor}(6) = 0.68$$

$$\rho = 0.218 \cdot \% \qquad \text{Redfactor}(3) = 1 \qquad \text{Redfactor}(7) = 0.38$$

$$\text{Redfactor}(4) = 1 \qquad \text{Redfactor}(8) = 0.08$$

$$V_{\text{Rd.punch}}(i) := \frac{\max\left[C_{\text{Rd.c}} \cdot k \cdot \left[100 \cdot \rho \cdot \left(\dfrac{f_{\text{ccm}} \cdot 10^{-6}}{\text{Pa}}\right)\right]^{\frac{1}{3}} \cdot 2\,\dfrac{d}{a(i)}\,\text{MPa}, v_{\text{min}} \cdot 2\,\dfrac{d}{a(i)}\,\text{MPa}\right] \cdot u_1(i) \cdot d}{\beta_c \cdot \text{Redfactor}(i)}$$

$$V_{\text{Rd.punch.d}}(i) := \frac{\max\left[C_{\text{Rd.c}} \cdot k \cdot \left[100 \cdot \rho \cdot \left(\dfrac{f_{\text{cck}} \cdot 10^{-6}}{\text{Pa}}\right)\right]^{\frac{1}{3}} \cdot 2\,\dfrac{d}{a(i)}\,\text{MPa}, v_{\text{min.d}} \cdot 2\,\dfrac{d}{a(i)}\,\text{MPa}\right] \cdot u_1(i) \cdot d}{\beta_c \cdot \text{Redfactor}(i)}$$

When i is equal to 8, the control perimeter is equal to its maximum, 2d. The minimum punching capacity is defined when finding the control perimeter that gives the lowest capacity

$$V_{\text{Rd.punch}}(0.1) = 9.026 \times 10^6 \, \text{N} \qquad V_{\text{Rd.punch}}(4) = 7.152 \times 10^5 \, \text{N}$$

$$V_{\text{Rd.punch}}(0.5) = 2.207 \times 10^6 \, \text{N} \qquad V_{\text{Rd.punch}}(5) = 6.868 \times 10^5 \, \text{N}$$

$$V_{\text{Rd.punch}}(1) = 1.354 \times 10^6 \cdot \text{N} \qquad V_{\text{Rd.punch}}(6) = 9.478 \times 10^5 \, \text{N}$$

$$V_{\text{Rd.punch}}(2) = 9.283 \times 10^5 \, \text{N} \qquad V_{\text{Rd.punch}}(7) = 1.642 \times 10^6 \, \text{N}$$

$$V_{\text{Rd.punch}}(3) = 7.862 \times 10^5 \, \text{N} \qquad V_{\text{Rd.punch}}(8) = 7.568 \times 10^6 \, \text{N}$$
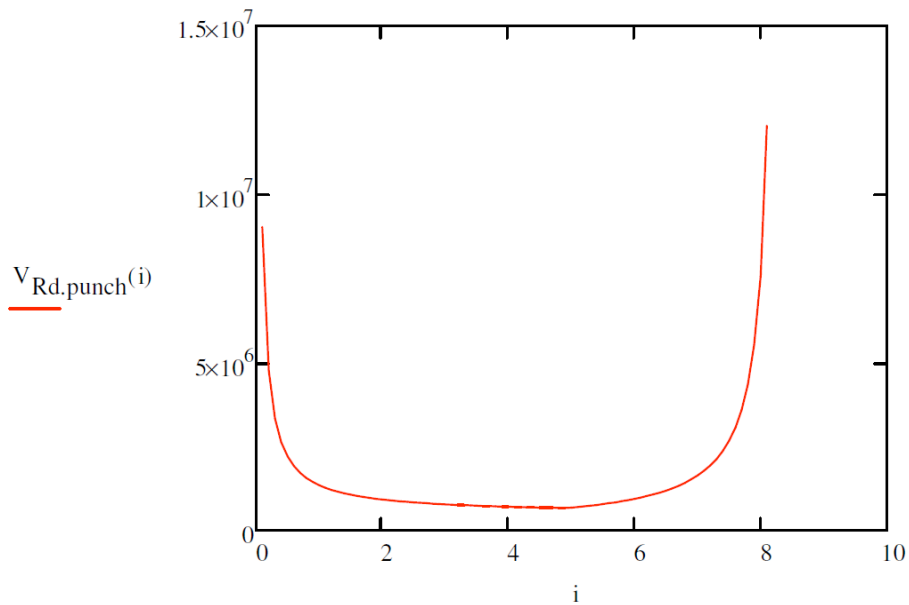
$$p := 1$$

$$\text{sol} := \min\left(\text{Minimize}\left(V_{Rd.punch}, p\right), 8\right) = 4.931$$

$$\text{sol}_d := \min\left(\text{Minimize}\left(V_{Rd.punch.d}, p\right), 8\right) = 4.931$$

The minimum puching capacity is reached at a distance *a.sol* from the column face and the value of the punching capacity is *V.Rd.punch.sol*:

$$a_{sol} := \text{sol} \cdot \frac{d}{4} = 0.37\,\text{m} \qquad\qquad a_{sol.p} := \text{sol}_d \cdot \frac{d}{4} = 0.37\,\text{m} \qquad 2d = 0.6\,\text{m}$$

$$V_{Rd.punch.sol} := V_{Rd.punch}(\text{sol}) = 674.966 \cdot \text{kN}$$

$$V_{Rd.punch.sol.d} := V_{Rd.punch.d}\left(\text{sol}_d\right) = 590.816 \cdot \text{kN}$$

$$V_{punch.col} := \min\left(V_{Rd.punch.sol}, V_{punch.max}\right) = 674.966 \cdot \text{kN}$$

$$V_{punch.col.d} := \min\left(V_{Rd.punch.sol.d}, V_{punch.max}\right) = 590.816 \cdot \text{kN}$$

Punching capacity at the piles, edge columns, EC2:

Check the capacity at the face of the piles:

Factor that accounts for the eccentric loading:

$$\beta_p := 1.5$$

Perimeter of the pile

$$u_{i.p} := 4 \cdot w_p = 0.708 \, m$$

Maximum capacity, the load is multiplied by 4 in order to be expressed at the column:

$$v_{Rd.max} = 4.848 \cdot MPa$$

$$V_{punch.max.pile} := \frac{4 u_{i.p} \cdot d \cdot v_{Rd.max}}{\beta_p} = 2.746 \times 10^3 \cdot kN$$

Check the capacity at the control perimeter:

Figure 6.15: Basic control perimeters for loaded areas close to or at edge or corner
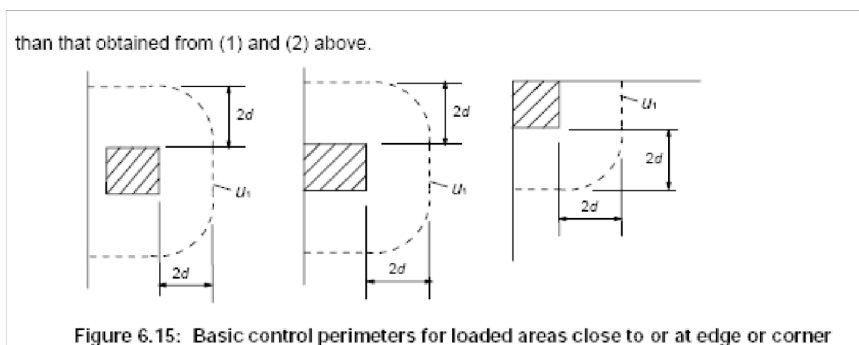
Determine the length of the control perimeter

Z is defined as the distance between the control perimeter and the edge of the pile cap:

$$Z(i) := \frac{L - e - w_p}{2} - a(i) \qquad\qquad 2d = 0.6 \, m$$

control perimeter if Z<0 (as the pile cap is square, the third drawing on figure 6.15 is relevant)

$$u_{1.p.1}(i) := 2 \cdot w_p + 2 \cdot (Z(i) + a(i)) + \pi \frac{a(i)}{2} \qquad\qquad \begin{array}{l}\pi a(i)/2 \text{ is one} \\ \text{forth of the} \\ \text{perimeter of a} \\ a(i) \text{ radius circle}\end{array}$$

control perimeter if Z>0, rectangular shape with rounded angles:

$$u_{1.p.2}(i) := 4 \cdot w_p + 2 \cdot \pi \cdot a(i)$$

Control perimeter:

$$u_{1.p}(i) := \begin{vmatrix} u_{1.p.1}(i) & \text{if } Z(i) < 0 \\ u_{1.p.2}(i) & \text{otherwise} \end{vmatrix}$$

The sudden change in figure u.1.p corresponds to the change of control perimeter
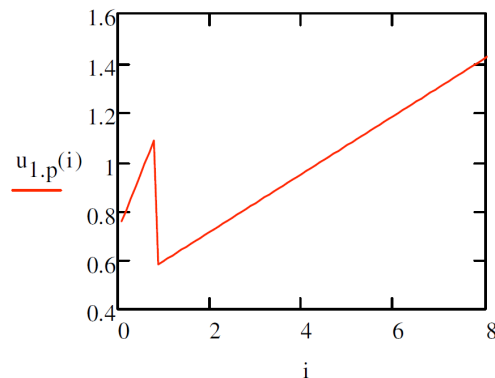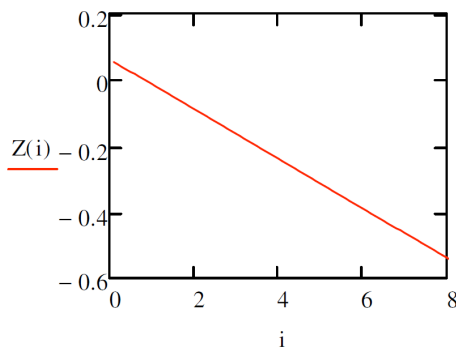
Determine the value of the punching shear capacity at the edge columns, again multiplied by 4 to have the value expressed as a column load:

The reduction factor used is the same for the pile and for the column:

$$V_{Rd.punch.pile}(i) := \frac{4 \cdot \max\left[0.12 \cdot k \cdot \left[100 \cdot \rho \cdot \left(\dfrac{f_{ccm} \cdot 10^{-6}}{Pa}\right)\right]^{\frac{1}{3}} \cdot 2 \dfrac{d}{a(i)} MPa, v_{min} \cdot 2 \dfrac{d}{a(i)} MPa\right] \cdot u_{1.p}(i) \cdot d}{\beta_p \cdot Redfactor(i)}$$

$$V_{Rd.punch.pile.d}(i) := \frac{4 \cdot \max\left[0.12 \cdot k \cdot \left[100 \cdot \rho \cdot \left(\dfrac{f_{cck} \cdot 10^{-6}}{Pa}\right)\right]^{\frac{1}{3}} \cdot 2 \dfrac{d}{a(i)} MPa, v_{min.d} \cdot 2 \dfrac{d}{a(i)} MPa\right] \cdot u_{1.p}(i) \cdot d}{\beta_p \cdot Redfactor(i)}$$

When i is equal to 8, the control perimeter is equal to its maximum, 2d. The minimum punching capacity is defined when finding the control perimeter that gives the lowest capacity:

$$V_{Rd.punch.pile}(0.1) = 2.467 \times 10^7 \, N \qquad V_{Rd.punch.pile}(4) = 7.746 \times 10^5 \, N$$

$$V_{Rd.punch.pile}(0.5) = 6.167 \times 10^6 \, N \qquad V_{Rd.punch.pile}(5) = 7.114 \times 10^5 \, N$$

$$V_{Rd.punch.pile}(1) = 1.944 \times 10^6 \cdot N \qquad V_{Rd.punch.pile}(6) = 9.486 \times 10^5 \, N$$

$$V_{Rd.punch.pile}(2) = 1.164 \times 10^6 \, N \qquad V_{Rd.punch.pile}(7) = 1.599 \times 10^6 \, N$$

$$V_{Rd.punch.pile}(3) = 9.045 \times 10^5 \, N \qquad V_{Rd.punch.pile}(8) = 7.208 \times 10^6 \, N$$
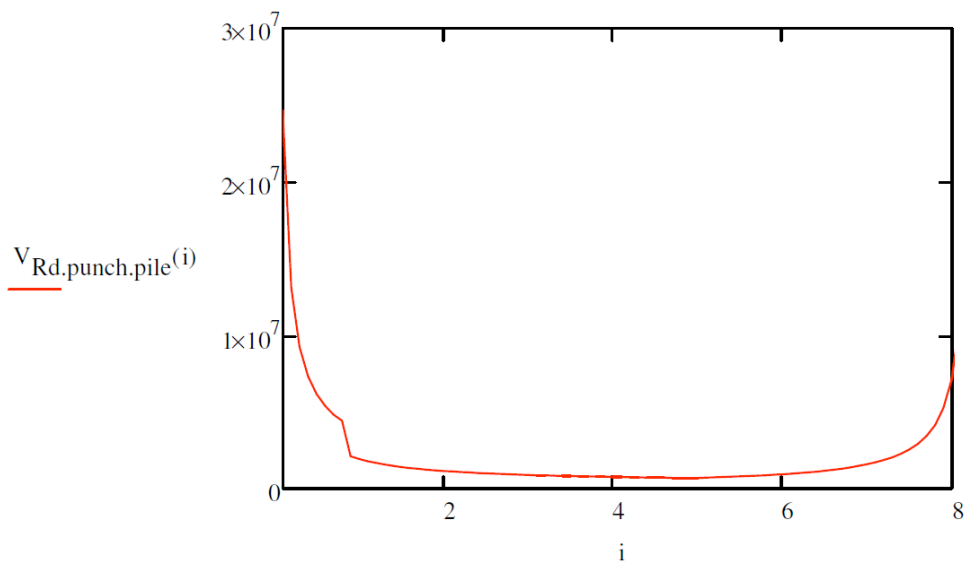
$$sol_{pile} := \min\left(\text{Minimize}\left(V_{Rd.punch.pile}, p\right), 8\right) = 4.931$$

$$sol_{pile.d} := \min\left(\text{Minimize}\left(V_{Rd.punch.pile.d}, p\right), 8\right) = 4.931$$

The minimum puching capacity is reached for a control perimeter at a distance a.sol from the column face and the value of the punching capacity is V.Rd.punch.sol:

distance between pile and edge of the pile cap: $\qquad L - e - w_p = 0.123 \, m$

$$a_{sol.pile} := sol_{pile} \cdot \frac{d}{4} = 0.37 \, m \qquad\qquad d = 0.3 \, m$$

$$a_{sol.pile.d} := sol_{pile.d} \cdot \frac{d}{4} = 0.37 \, m$$

$$V_{Rd.punch.sol.pile} := V_{Rd.punch.pile}(sol_{pile}) = 701.029 \cdot kN$$

$$V_{Rd.punch.sol.pile.d} := V_{Rd.punch.pile.d}(sol_{pile.d}) = 613.63 \cdot kN$$

$$V_{punch.pile} := min(V_{Rd.punch.sol.pile}, V_{punch.max.pile}) = 701.029 \cdot kN$$

$$V_{punch.pile.d} := min(V_{Rd.punch.sol.pile.d}, V_{punch.max.pile}) = 613.63 \cdot kN$$

Punching at the column according to BBK04

The control perimeter is situated at a distance d/2 from the edge of the column:

$$\frac{d}{2} = 0.15\,m$$

the distance between the corner of the column and the corner of the pile is:

$$Y = 0.37\,m$$

Distance between the control perimeter and the face of the pile:

$$l_{bbk} := \frac{d}{2} - Y = -0.22\,m$$

Reduction factor for load applied inside the control perimeter:

The reduction factor $\beta.bbk$ is equal to 1 when no reduction of load occurs inside the control perimeter (the value 0.001 is set to give a virtual infinite punching capacity):

$$\beta_{bbk} := \begin{vmatrix} 1 & \text{if } l_{bbk} < 0 & = 1 \\ max\left(0.001, 1 - \dfrac{l_{bbk}}{w_p \cdot \sqrt{2}}\right) & \text{otherwise} \end{vmatrix}$$

Definition of the control perimeter:

> rectangular shape, rounded at the corner. Total length equal to the perimeter of the column + perimiter of a d/2 radius cirle.

$$u_{bbk.col} := 4 \cdot w_c + \pi\,d = 1.742\,m$$

Effective depth considered in shear calculation in BBK, taking account of size effects:

$$\xi := \begin{vmatrix} 1.4 & \text{if } d \le 0.2m \\ \left(1.6 - \dfrac{d}{m}\right) & \text{if } 0.2m < d \le 0.5m \\ \left(1.3 - 0.4\dfrac{d}{m}\right) & \text{if } 0.5m < d \le 1m \\ 0.9 & \text{otherwise} \end{vmatrix} \qquad = 1.3$$

Definition of the tenisle strength of concrete from the compressive strength:

$$f_{ctm} := 0.3 \cdot \left(\frac{f_{cck}}{MPa}\right)^{\frac{2}{3}} MPa = 2.713 \cdot MPa \qquad f_{ctk} := 0.7 f_{ctm} = 1.899 \cdot MPa$$

$$f_{ctd} := \frac{f_{ctk}}{1.5} = 1.266 \cdot MPa$$

$$\rho_{bbk} := \min(\rho, 1\%) = 2.181 \times 10^{-3}$$

$$f_{v1} := 0.45 \xi \cdot (1 + 50 \rho_{bbk}) f_{ctm} = 1.76 \cdot MPa \qquad f_{v1.d} := 0.45 \xi \cdot (1 + 50 \rho_{bbk}) f_{ctd} = 0.821 \cdot MPa$$

$$V_{punch.col.BBK} := \frac{u_{bbk.col} \cdot d \cdot f_{v1}}{\beta_{bbk}} = 920.211 \cdot kN$$

$$V_{punch.col.BBK.d} := \frac{u_{bbk.col} \cdot d \cdot f_{v1.d}}{\beta_{bbk}} = 429.432 \cdot kN$$

Punching of edge piles according to BBK04

Definition of the length of the control perimeter:

dist is the distance between the edge of the pile cap and the face of the pile:

$$\text{dist} := \frac{L - e - w_p}{2} = 0.061\,\text{m} \qquad \frac{d}{2} = 0.15\,\text{m}$$

one forth of the perimeter of a circle with d/2 as a radius

When dist < h, The control perimeter in 3.12.4 in BBK is used:

$$u_{1.bbk} := 2\left(\text{dist}\sqrt{2} + w_p \cdot \sqrt{2} + \frac{d}{2}\right) = 0.975\,\text{m}$$

When dist > h, the control perimeter for inner column is used:

$$u_{2.bbk} := 4 \cdot w_p + \pi d = 1.65\,\text{m}$$

$$u_{bbk} := \begin{vmatrix} u_{1.bbk} & \text{if dist} < h & = 0.975\,\text{m} \\ u_{2.bbk} & \text{otherwise} \end{vmatrix}$$

$$f_{v2} := 0.33\xi \cdot (1 + 50\rho_{bbk})f_{ctm} = 1.291 \cdot \text{MPa} \qquad f_{v2.d} := 0.33\xi \cdot (1 + 50\rho_{bbk})f_{ctd} = 0.602 \cdot \text{MPa}$$

$$f_{v.pile} := \begin{vmatrix} f_{v1} & \text{if dist} > h & = 1.291 \cdot \text{MPa} \\ f_{v2} & \text{otherwise} \end{vmatrix} \qquad f_{v.pile.d} := \begin{vmatrix} f_{v1.d} & \text{if dist} > h & = 0.602 \cdot \text{MPa} \\ f_{v2.d} & \text{otherwise} \end{vmatrix}$$

Multiplied by a factor 4 so the force is explained as the column force:

$$V_{punch.pile.BBK} := \frac{4 u_{bbk} \cdot d \cdot f_{v.pile}}{\beta_{bbk}} = 1.51 \times 10^3 \cdot \text{kN}$$

$$V_{punch.pile.BBK.d} := \frac{4 u_{bbk} \cdot d \cdot f_{v.pile.d}}{\beta_{bbk}} = 704.54 \cdot \text{kN}$$

Results

Ultimate capacity (no safety factor on material, no safety factor on loads)

$$V_{fl} = 634.204 \cdot kN \quad V_{sh} = 843.424 \cdot kN$$

$$V_{punch.col} = 674.966 \cdot kN \quad V_{punch.pile} = 701.029 \cdot kN$$

$$V_{punch.col.BBK} = 920.211 \cdot kN \quad V_{punch.pile.BBK} = 1.51 \times 10^3 \cdot kN$$

Design capacity (not reduced by partial safety on loads)

$$V_{fl.d} = 497.14 \cdot kN \quad V_{sh.d} = 738.272 \cdot kN$$

$$V_{punch.col.d} = 590.816 \cdot kN \quad V_{punch.pile.d} = 613.63 \cdot kN$$

$$V_{punch.col.BBK.d} = 429.432 \cdot kN \quad V_{punch.pile.BBK.d} = 704.54 \cdot kN$$